THE UNIVERSITY of ADELAIDE

A new flood estimation paradigm for the design of civil infrastructure systems

Phuong Dong Le

Thesis submitted in fulfilment of the requirements for the degree of Doctorate of Philosophy

The University of Adelaide
Faculty of Engineering, Computer and Mathematical Sciences
School of Civil, Environmental and Mining Engineering

July 2018

TABLE OF CONTENTS

Abstract

Methods for quantifying flood risk of civil infrastructure systems such as road and rail networks require considerably more information compared to traditional methods that focus on flood risk at a point. These systems are characterised by multiple interconnected components, whereby a 'failure' of the overall system can arise because of complex combinations of failures in system subcomponents. For example, flooding of a single bridge along a railway may leave the entire railway inoperable, and the interest is often in the probability that one or more bridges along a stretch of railway will be flooded, rather than designing each bridge in isolation. Similarly, the viability of evacuation routes often requires an assessment of the probability that the route is flooded, conditional on an evacuation being necessary as a result of floods elsewhere in the system. Conventional design flood estimation processes are ill-equipped to deal with these complex problems.

Whereas traditional flood estimation approaches focus on estimating flood risk at a single location, this thesis proposes a new estimation paradigm that focuses on estimating system-wide risk. The approach builds on the traditional intensity-duration-frequency (IDF) methods that are commonly used in engineering practice in Australia and internationally; however, this is implemented in such a way at to provide information on the spatial dependence of design storms. A particular innovation in this thesis is to estimate spatial rainfall dependence across multiple storm durations, allowing it to be used to estimate flood risk across multiple catchments with differing times of concentration. This enables the estimation of both conditional probabilities (e.g. probability of one part of a system being flooded conditional on another part of the system being flooded) and joint probabilities (e.g. the probability of multiple parts of a system experiencing floods simultaneously). Finally, whereas traditional IDF approaches consider conversion from point rainfall to spatial rainfall via areal reduction factors as a post-processing step, the approach proposed herein enables this conversion implicitly as part of the method.

The proposed approach is based on two classes of extreme value model: max-stable process models, and inverted max-stable process models. These models differ in their assumption for how spatial dependence scales in the limit, as the rainfall events become increasingly extreme (referred to as "asymptotic dependence"). In particular, max-stable models assume asymptotic dependence (i.e. the spatial dependence converges to a non-zero limit), whereas inverted max-stable models assume asymptotic independence. This assumption has significant implications for very rare events (e.g. the 1% annual exceedance probability event), particularly when the estimates are based on relatively short observational records. Specifically, implementation focuses on the (inverted) Brown-Resnick family of models. This class of model was adjusted by accounting for spatial dependence across multiple storm burst durations. The adjustment used the theoretical pairwise extremal coefficient function as a function of both distance and duration.

The integration of multiple durations into the modelling framework was tested on a 21,400 km^2 spatial domain in the Greater Sydney region, with data on sub-daily rainfall from 25

stations. The updated model shows a reasonable fit between the observed pairwise extremal coefficients and the theoretical pairwise extremal coefficient function across all durations. The asymptotic dependence and comparison with empirically derived areal reduction factors was tested next, and it was shown that the observed data follow the behaviour of an asymptotically independent process, which leads to ARFs that decrease with an increasing return period. This demonstrates that inverted max-stable process models such as the inverted Brown-Resnick model are the most suitable method for simulating spatial rainfall in the study areas that were investigated.

Finally, the outcomes of this research are demonstrated by implementing the spatially dependent IDF approach in a realistic case study that requires information on both conditional and joint dependence. The case study examines a highway upgrade project on the east coast of Australia, containing five bridge crossings with differing contributing catchment areas, and thus differing times of concentration. The results are used to show the differences between conditional-flood and conventional-flood estimates at each bridge, and the relationship between the overall failure of a system and the failure probability of an individual bridge. For example, if one were to design the highway section for a 1% probability of at least one bridge being flooded in any given year, it would be necessary to design each individual bridge to a X% annual exceedance probability design flood. This research therefore is shown to enable a different paradigm for design flood risk estimation, which focuses attention on the risk of the entire system rather than considering individual system elements in isolation.

Statement of originality

I, Phuong Dong Le, certify that this thesis contains no material which has been accepted for the award of any other degree or diploma in my name in any university or other tertiary institution and, to the best of my knowledge and belief, contains no material previously published or written by another person, except where due reference has been made in the text. In addition, I certify that no part of this work will, in the future, be used in a submission in my name for any other degree or diploma in any university or other tertiary institution without the prior approval of the University of Adelaide and, where applicable, any partner institution responsible for the joint award of this degree.

The author acknowledges that copyright of published works contained within this thesis resides with the copyright holder(s) of those works:

Le, PD, Leonard, M & Westra, S 2018, 'Modeling Spatial Dependence of Rainfall Extremes Across Multiple Durations', *Water Resources Research*, vol. 54, no. 3, pp. 2233-2248.

Le, P.D., Davison, A.C., Engelke, S., Leonard, M. and Westra, S., 2018. Dependence properties of spatial rainfall extremes and areal reduction factors. *Journal of Hydrology*.

Le, P. D., Leonard, M., and Westra, S.: Spatially dependent Intensity-Duration-Frequency curves to support the design of civil infrastructure systems, Hydrol. Earth Syst. Sci. Discuss., https://doi.org/10.5194/hess-2018-393, in review, 2018.

I give permission for the digital version of my thesis to be made available on the web, via the University's digital research repository, the Library Search and also through web search engines, unless permission has been granted by the University to restrict access for a period of time.

I acknowledge the support I have received for my research through the provision of an Australian Government Research Training Program Scholarship.

Phuong Dong Le Date

Acknowledgements

I feel honoured and privileged to have been able to undertake this research. My most sincere gratitude goes to my supervisory team, Associate Professor Seth Westra and Dr Michael Leonard, who have believed in my abilities, provided me with great support, inspiration and guidance throughout my candidature, as well as effort and patience in helping me to achieve my goals. Your combined skill, expertise and passion for research have been invaluable to me.

I also express my sincere thanks to Professor Anthony C. Davison (Ecole Polytechnique Fédérale de Lausanne, Switzerland) and Dr Sebastian Engelke (University of Geneva, Switzerland) for their collaborations in the second objective of my research.

I am grateful to the Australia Awards Scholarships (AAS) from the Australian Government for the financial support for my PhD study at the University of Adelaide.

Thanks also to professional editor, Leticia Mooney, who provided copyediting and proofreading services, according to the guidelines laid out in the university-endorsed, national *Guidelines for editing research theses*.

I would like to give many thanks to all my friends in the University of Adelaide, and people of Australia for being such a homely host.

I also give many thanks to my parents, my younger sister and my relatives for the moral support and encouragement dedicated by them during the course of this study.

Finally, thanks go to my wife, Linh, and my daughter, Thuy, for their unwavering encouragement and understanding.

List of Figures

List of Tables

Chapter 1

Flooding due to rainfall extremes is one of the most dangerous natural disasters worldwide. In recent decades, there have been many occurrences of large floods caused by extreme rainfall events. For instance, rainfall extremes together with the failure of dam operation caused series of floods in Queensland in 2010/2011, there were 56,200 claims received by insurers with total payouts of $2.55 billion (van den Honert and McAneney, 2011). In 2011, very large extreme rainfall events together with water discharged from major dams also caused the worst flood in modern Thai history that killed 680 people and caused damages and losses of $46.5 billion (Poapongsakorn and Meethom, 2013). In Australia, the average annual cost of flood damage is estimated to be around $377 million (BITRE, 2008). Besides tangible damages that can be evaluated in term of currency, floods also cause intangible damage such as death, sickness, stress, anxiety, and reduced environmental quality, which cannot be measured in dollar terms (UNDP, 1991).

Flood estimation is important in terms of mitigating flood damages and maintaining public safety. It forms a necessary element of engineering decision making, including (i) the zoning of new land in and around floodplains; (ii) the design and management of infrastructure, such as storm water systems, roads and bridges; (iii) flood protection works; and (iv) management of reservoirs (Pathiraja et al., 2012; Rogger et al., 2012). In many cases, decisions are made using a design flood value, which may be the peak flow, volume, stage or wave-crest elevation of a hypothetical flood event that is associated with a selected probability of exceedance (Pilgrim and Cordery, 1993). While there are many frameworks based directly on estimates of flow (Cunderlik and Ouarda, 2006; Durocher et al., 2016), this thesis is focused on design floods estimated from rainfall – due to the relative abundance of rainfall data. The concept of a design flood, as opposed to an observed (historical) event, enables engineers to use a risk-based decision-making framework, which relies on the relationship between the probability that a flood of a given magnitude will occur and its expected consequences. This kind of framework can then be used to optimize the investment required for flood management (Pathiraja et al., 2012).

The introduction first reviews conventional approaches to estimating design floods and points out their common limitations (Section 1.1). After that, the role of dependence properties of rainfall in design floods is discussed (Section 1.2), which is followed by a new typology for modelling spatial extremes (Section 1.3). Research gaps are identified in Section 1.4, which are then linked to research objectives in Section 1.5. Finally, the structure of this thesis is outlined in Section 1.6.

1.1. Historical approaches to design flood estimates

There are a number of conventional approaches for estimating a design flood. They include frequency analysis of streamflow records, methods in ungauged basins determined by rainfall statistics and catchment properties (e.g. the rational method), event-based modelling, and continuous simulation (Chow et al., 1988). While the first approach uses

streamflow directly to estimate a design flood, the remainder rely on rainfall—whether a specific design storm or the use of continuous rainfall sequences (Beven, 2002; Boughton and Droop, 2003). All of these approaches focus on estimating a design flood for a single location (i.e. the outlet of a catchment), without considering the spatial dependence of flooding (whether flooding at different locations can occur at the same time). The following subsections provide a brief literature review of the conventional approaches for estimating a design flood.

1.1.1. Flood frequency analysis

Flood frequency analysis is used to relate the magnitude of flood events (the peak flow) to the corresponding frequency of flood occurrence. This is achieved by fitting the observed streamflow data to some suitable probability distribution, e.g. a generalised extreme value distribution or a log Pearson Type III distribution (Chow et al., 1988; El Adlouni et al., 2008; Khaliq et al., 2006; Klemes, 1993). A design flood peak can then be obtained for a given exceedance probability.

This approach is relatively simple to implement in engineering design. However, it has several limitations relating to whether observed data is available and representative of future flood potential. The method needs representative flood records, but often data is not available at the majority of locations of interest. Where data is available, short-term records (less than 30 years) can cause large errors in estimating floods for low exceedance probabilities (Katz et al., 2002; Klemes, 1993). Furthermore, the observed streamflow data may be inconsistent because of the non-stationarity of the catchment surface, due to land use change, deforestation, or the construction of flood protection works (such as big dams). Other complications with the direct application of streamflow data for flood risk estimation relate to the ability to relate streamflow to river stage heights, external influences such as tidal boundaries or backwater effects at river confluences, or uncertainty in the raw measurements due to limitations of the observation (e.g. the water level was above the gauge height).

1.1.2. The rational method

The rational method is the oldest rainfall-based approach still in use today (Linsley, 1986; Pilgrim, 1986), and has been a foundational method in hydrological design (Kuichling, 1889; Mulvaney, 1851). This method transforms a quantified design rainfall to a design flow, based on the idea that if the design rainfall happens and continues indefinitely over a catchment, then the flow at the outlet of that catchment will increase until the time of concentration has been reached, i.e. when the flow at the outlet has contributions from all parts of the catchment of interest. This method is very simple and is easy to implement for a rough estimate of flow at the catchment's outlet and is often used in the absence of streamflow data. However, the method is extremely idealistic as it assumes all elements of the rainfall-runoff transformation (e.g. evaporation, infiltration, baseflow) can be represented by a single runoff coefficient and it assumes that rainfall intensity is constant throughout the storm duration and over the region (Chow et al., 1988). Design rainfall information is typically obtained through intensity-duration-frequency (IDF) curves, which are commonly available as part of engineering guidance in Australia (Ball et al., 2016) and

elsewhere. A number of studies have improved upon the method of rational method by using improved techniques and exploiting additional covariates from the catchment (Pegram and Parak, 2004; Pegram, 2003; Rahman et al., 2018).

1.1.3. Event-based modelling

Event-based modelling, which is a more complex rain-based method than the rational method, can simulate a complete flood hydrograph from a single storm event. It conceptually allows for various physical processes involved in the transformation from rainfall to runoff and routes it through catchment streams to the outlet. There are numerous event-based runoff-routing models (Boyd et al., 1996; Laurenson and Mein, 1997). In these event-based models, the IDF curves for rainfall are combined with temporal patterns to develop design rainfall hyetographs. The hyetographs are then input to a runoff-routing model in order to simulate flow in each subcatchment and then convey the flow to the catchment's outlet (Chow et al., 1988). Event-based modelling has been improved and has been used widely in many flooding studies to estimate design floods (Blume et al., 2007; Jain et al., 2004; Talei and Chua, 2012; Talei et al., 2010; Tramblay et al., 2010), but also can be limited in its ability to account for spatial and temporal dependence. For example, the variability of rainfall and infiltration properties over the catchment is often unaccounted for when lumped catchment representations are used, but can be improved by using multiple subcatchments. The selection of initial conditions (or loss parameters) can be complicated since there is often strong dependence between the design burst of rainfall and antecedent rainfall, but this can be improved by calibration to runoff from observed storm events.

1.1.4. Continuous simulation

Continuous simulation is the use of a rainfall-runoff model to account for the cumulative effect of storms on soil moisture. Typically these models simulate runoff from rainfall over long time periods at hourly or daily intervals (Chow et al., 1988; Eagleson, 1972). With improvements in computational techniques, continuous simulation approach now often consists of a continuous rainfall-runoff model using long stochastically generated rainfall sequences to simulate a time-series of flow for estimating a design flood event (Blazkova and Beven, 2002; Blazkova and Beven, 2009; Brath et al., 2002; Faulkner and Wass, 2005; Sivapalan et al., 2005; Srikanthan and Pegram, 2007). A related concept is when stochastic rainfall simulations are conditioned on output from a generalised circulation model, referred to as downscaling (Alaya et al., 2018; Westra et al., 2013). In contrast to event-based modelling, continuous simulation does not need to make any assumptions about the return period of the design rainfall, its duration, or its intensity (Boughton and Droop, 2003; Koutsoyiannis, 1994). Another advantage is its ability to account for the role that antecedent moisture plays in designing flood estimation, because it implicitly incorporates soil moisture within the modelling framework (Pathiraja et al., 2012). Nonetheless, continuous simulation has a number of disadvantages. Continuous simulation models have a heavy computational requirement – simulating very long records of rainfall at a high resolution when the interest is mostly in one value per year (the annual extreme). Secondly, continuous simulation models significantly increase the modelling complexity but may still

retain significant degree of idealisation and error in the simulated rainfall by not always reproducing key statistics of interest (such as the extremes).

1.1.5. Common limitations of conventional approaches to estimating design floods

A common limitation of conventional flood risk estimates is that they often focus on isolated, individual system elements, rather than on the functioning of a spatially connected system (e.g. a road or rail network) as an integrated whole. Because of their inability to estimate the true system risk, they have neglected the element of surprise which may occur in floods. An example of this would be the complex interdependence of rainfall across space and time and how this affects the flood response of a system (Bennett et al., 2016a). One of main sources of surprise in flood risk assessment is the spatial interdependence or rainfall and flood processes, which describes the processes at one location affecting the processes at other locations (Merz et al., 2015). For the example of rainfall over a region, there is the possibility of multiple flood events in space or in time, which amplify an impact (Leonard et al., 2014). There is also the possibility of cascading impact, where the failure of one element leads to the failure of other elements that are associated with the structural complexity of the system being studied.

1.2. The role of spatial and duration dependencies of rainfall in the design flood

While conventional approaches of design floods focus on estimating floods at individual locations, there are many real situations that require an understanding of the spatial dependence of floods at more than two locations. This understanding of a flood's spatial dependence is complicated by the inherent spatial and temporal dependencies of the flood-producing rainfall. The design of civil infrastructure systems, such as a large traffic network, is a good illustration for the need of accounting for a flood's spatial dependence. First, the design of evacuation routes often focuses on understanding the risk of one part of the network failing given that another region is flooded or exceeds the level at which evacuation becomes necessary. Secondly, the failure of any single part of the network (e.g. a river crossing) can lead to the failure of the whole network, but two or more river crossings can fail at the same time. As a result, the overall failure probability of the whole system is difficult to estimate.

The spatial dependence of flooding can be examined directly from observed continuous streamflow; or indirectly from the spatial and temporal dependencies of the flood-producing rainfall by using a rainfall-runoff model. The use of directly observed continuous streamflow considers that the annual maximum stream flows at two locations can be assumed to follow a bivariate generalized extreme value distribution (Favre et al., 2004; Wang, 2001; Wang et al., 2009). However, this approach requires the availability of observed continuous streamflow data, which are not always available for locations of interest. Moreover, the streamflow data may be inconsistent due to the non-stationarity of the catchment surface, as mentioned above. Therefore, using observed continuous streamflow data is restricted, and the focus therefore by necessity is usually on the spatial dependence structure of rainfall to indirectly estimate the spatial dependence of flooding.

Continuous simulation (Boughton and Droop, 2003; Cameron et al., 1999; He et al., 2011; Pathiraja et al., 2012) can be used for analyzing the spatial dependence of flooding if the generated continuous rainfall sequences reflect the spatial dependence structure of flood-producing rainfall. However, continuous models generally do not focus on rainfall extremes in space and time; therefore, the generated continuous rainfall sequences do not necessarily reflect spatial and duration dependencies. Moreover, there are very few models that can simulate spatial rainfall for long periods. Most are designed for simulating the daily timescale (Bennett et al., 2016b), whereas many subcatchments will respond on shorter timescales. Continuous models that are able to simulate subdaily rainfalls are often highly idealised (Leonard et al., 2008) and are difficult to calibrate. Therefore, rain-based methods for continuous simulation are not ideal for analyzing the spatial dependence of flooding.

The dominant rain-based method, which is the event-based method, can characterise the spatial dependence of flooding if the design storm can reflect the dependence characteristics of rainfall extremes. The current method of estimating a design storm relies on an intensity-duration-frequency (IDF) relationship that has been estimated either at a single site, or as a spatial map without presenting the spatial dependence for equivalent durations, or across different durations (Bernard, 1932; Koutsoyiannis et al., 1998). However, there are number of studies have shown that the spatial dependence structure of rainfall extremes can be characterised through modelling for spatial extremes (Nicolet et al., 2017; Padoan et al., 2010; Thibaud et al., 2013; Westra and Sisson, 2011). Therefore, there is a high possibility that a design storm can be estimated by taking into account the spatial dependence characteristics of rainfall extremes. If so, then the event-based method will be able to integrate the dependence structure of rainfall into the spatial dependence of flooding for civil infrastructure systems.

Considering the example of a large traffic network, the problems of spatial dependence in floods requires an understanding not only of the spatial dependence of flood-producing rainfall, but also the dependence across storm-burst durations. This is because different parts of the network may be vulnerable to different critical-duration storm events. Therefore, a model that can account for the dependence characteristics of extreme rainfall across both space and duration is critical in estimating a design storm. This can then be followed by an event-based rainfall-runoff modelling approach to simulate catchment flows at relevant points in the spatial domain.

1.3. Typology for modelling of spatial extremes

Models of spatial extremes have been developed to understand the spatial behaviour of the extremes of natural processes, such as rainfall or temperature (Davison et al., 2012). Previous studies, for example Davison and Gholamrezaee (2012) and Davison et al. (2012), have tried to classify spatial extreme models. In these papers, spatial extremes modelling was classified into three main categories:

1. *latent variable models* — which are based on the underlying latent variables or processes, conditional on which standard extreme models are applied (Casson and

Coles, 1999; Coles and Casson, 1998; Cooley et al., 2006a; Cooley et al., 2007; Fawcett and Walshaw, 2006; Sang and Gelfand, 2009).

2. *copula models* — which transform the observed data's marginal distribution to the probability scale, on which standard multivariate normal or multivariate extreme value distributions may be used.

3. *max-stable models* — which are based on the spectral representations of the extremal processes of so-called max-stable processes proposed by de Haan (1984) and Schlather (2002).

However, this classification seems fragmented, as each category plays a different role in a different step of the spatial extremes modelling process.

Here, a new typology of modelling for spatial extremes is introduced (Figure 1.1), which is based on the functionality of the model at different steps of the modelling process. It includes procedural steps for marginal distributions, the spatial model for marginal parameters, the transformed space, the spatial dependence model, and method of parameter estimation. Each step lists alternative approaches.

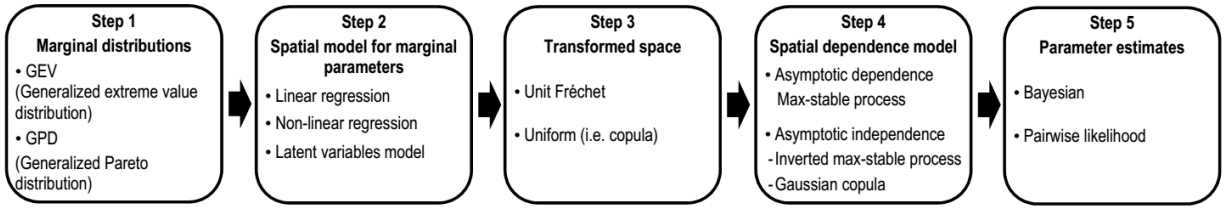

Figure 1.1. Typology for modelling spatial extremes.

The following subsections provide explanations of all approaches in each step, and then provide a summary of previous studies using different combinations of approaches from each step to form different frameworks for modelling spatial extremes.

Step 1: Marginal distributions

In modelling for spatial extremes, the marginal distributions are important. Their parameters are used to transform extreme variables into a different space for convenience (see Section 1.3.3). The generalized extreme value distribution (GEV) (Jenkinson, 1955; von Mises, 1954) was developed for modelling block maxima. For example, it can be used for modelling the annual maximum daily rainfall if the size of the block is equal to 365 days in a year (Coles, 2001; Coles et al., 2003). The generalized Pareto distribution (GPD), which is an alternate marginal distribution of extreme events, was developed for modelling extremes above a threshold (Davison and Smith, 1990; Pickands, 1975; Thibaud et al., 2013) because of the idea that the block maxima model is a wasteful approach if other data on extremes are available; i.e. there are multiple events in the year (Coles, 2001; Davison and Smith, 1990). There are numerous methods for calibrating marginal models such methods based on matching sample moments to theoretical counterparts (including the use of L-moments (Hosking, 1990)), and methods based on the concept of maximum likelihood. This thesis is focused on likelihood-based methods.

Step 2: Spatial model for marginal parameters

To extrapolate the marginal parameters to ungauged locations, spatial models are employed to build a spatial map of marginal parameters over a domain, based on covariates such as longitude, latitude, and elevation. For example, Westra and Sisson (2011) used linear regressions to model the change of the GEV parameters of annual maximum rainfall over a domain. Ribatet (2009) suggested the use of non-linear regression models (such as the semi-parametric regression model) to build the response surfaces for a marginal distribution's parameters. Latent variable models also model the spatial variation in the marginal parameters and so are included in this category. In the latent variable models, the parameters of marginal distribution of extremes – GEV or GPD – are assumed to depend on a latent variable process which follows, for example, a Gaussian process (Diggle and Ribeiro, 2007; Diggle et al., 1998). Consequently, the spatial variations in the marginal distribution's parameters are inferred from the selected latent variable process.

Step 3: Transformed space

In multivariate extreme value distributions, dependence aspects can be isolated from marginal distribution features by implementing a standardization of the marginal distribution (Kotz and Nadarajah, 2000). An example is the transformation from any marginal distribution to unit Fréchet distribution (Coles, 2001; Coles and Tawn, 1994; Kotz and Nadarajah, 2000)—which is a GEV distribution with location value of zero, a scale parameter of one and a shape parameter of one. This transformation is convenient when analysing dependence in extremes (see also, proposition 5.10 in Resnick (1987)).

When modelling spatial extremes, it is convenient to construct a spatial dependence model in a standard marginal distribution, like the unit Fréchet distribution for the max-stable process (de Haan, 1984; de Haan and Ferreira, 2006), or the exponential distribution for the inverted max-stable process (Wadsworth and Tawn, 2012). These transformations can be easily interchanged; for example a unit Fréchet distribution can be converted to a uniform distribution which is known as a copula (Joe, 1997; Nelsen, 2006). The marginal parameters from the GEV or GPD in step 1 are used to transform the marginal distribution of the extreme variables to a more convenient form for dependence analysis.

Step 4: Spatial dependence models

Spatial dependence models have been developed as an approach for capturing the spatial dependence structure of extremes. They can characterize the distribution of extreme rainfall in space, thus they can estimate the conditional and joint probabilities of extreme rainfall for locations of interest.

Dependence models are classified into two groups based on the asymptotic property of extremes. The first group is the asymptotically dependent group of models, where the level of dependence stabilizes to a constant with an increasing return period (Wadsworth and Tawn, 2012). Max-stable processes are asymptotically dependent and represents many families of models, such as the Smith model (Smith, 1990), the Brown-Resnick model (Asadi et al., 2015; Huser and Davison, 2013; Kabluchko et al., 2009; Oesting et al., 2017), and the extremal-t model (Opitz, 2013). Extremal copulas, such as the extremal-t copula

(Demarta and McNeil, 2005), and the Husler-Reiss copula (Hüsler and Reiss, 1989), are also asymptotically dependent models. The second group is the asymptotically independent models, where the level of dependence diminishes with an increasing return period (Wadsworth and Tawn, 2012). An inverted max-stable process, a Gaussian process, and a Gaussian copula, are examples of asymptotically independent models (Thibaud et al., 2013; Wadsworth and Tawn, 2012).

The connections between copula and max-stable models have been noted in literature as needing more investigation (Davison et al., 2012). While the copula approach is intended for a given network of gauge stations, rather than as a spatial analysis (Thibaud et al., 2013), the idea of formulating a max-stable theory in terms of a full spatial process is very attractive (Davison et al., 2012). Davison et al. (2012) also suggested that the difference between copula and max-stable models may be simply a technical matter of using a spatially-defined dependence function, and of extending the copula model to the full spatial domain.

When the interest is spatial dependence in floods, the understanding of the dependence across storm-burst durations is required (see Section 1.2). However, there is no framework in the literature that is able to link rainfall extreme from different duration together within a spatial dependence model, which can also be seen in Table 1.1 below.

Step 5: Parameter estimates

In modelling spatial extremes, parameter estimates are often made using a Bayesian or pairwise likelihood. The Bayesian hierarchical approach has been used for building high precision spatial maps of a marginal distribution's parameters (Bracken et al., 2016; Cooley et al., 2007; Renard, 2011) without accounting for storm-level dependence (i.e. the probability that rainfall extremes at more than two locations come from a common event). The Bayesian hierarchical approach has also been used to estimate parameters for a copula approach (Renard and Lang, 2007; Sang and Gelfand, 2010). The pairwise likelihood approach, which was developed by Padoan et al. (2010) based on the bivariate probability function for the max-stable process, has been used in many papers, including Russell et al. (2016), Westra and Sisson (2011), and Huser and Davison (2014). Smith and Stephenson (2009) and Ribatet et al. (2012) have used Bayes' theorem and pairwise likelihood to fit extremal models to rainfall data.

Table 1.1 provides a framework summary, and highlights the differences and similarities between the papers discussed in this section. It will be used to identify the research gaps for this study in the section that follows.

Table 1.1. Summary of the framework methods of previous papers used for modelling spatial extremes. Step 1 identifies the marginal distribution, Step 2 is the type of spatial model used for the marginal distribution, Step 3 is the type of transformation used to study the dependence structure, Step 4 is the type of dependence structure and Step 5 is the calibration method.

Author	Step 1		Step 2			Step 3		Step 4				Step 5	
								Able to link	Asymp. Dep.	Asymp. Indep.			
	GEV	GPD	Linear regr.	Non-linear	Latent var.	Unit Frechet	Uniform	durations	Max-stab.	In. max-stab.	Gauss. cop.	Pair. Lik.	Bayesian
Padoan et al. (2010)	✓		✓			✓			✓			✓	
Blanchet and Davison (2011)	✓		✓			✓			✓			✓	
Davison and Gholamrezaee (2012)	✓		✓			✓			✓			✓	
Westra & Sisson (2011)	✓		✓			✓			✓			✓	
Davison et al. (2012)	✓		✓			✓			✓			✓	
Thibaud et al. (2013)		✓	✓			✓				✓		✓	
Stephenson et al. (2016)	✓				✓	✓			✓				✓
Ribatet et al. (2012)	✓			✓		✓			✓			✓	✓
Smith and Stephenson (2009)	✓		**NA**	**NA**	**NA**	✓			✓			✓	✓
Cooley et al. (2007)		✓			✓								✓
Gaetan and Grigoletto (2007)	✓				✓								✓
Sang and Gelfand (2009)	✓				✓								✓
Sang and Gelfand (2010)	✓				✓		✓				✓		✓
Coles and Casson (1998)		✓			✓								✓
Casson and Coles (1999)		✓			✓								✓
Bracken et al. (2016)	✓				✓						✓		✓
Renard and Lang (2007)	✓		**NA**	**NA**	**NA**		✓				✓		✓
Reich and Shaby (2011)	✓			✓		✓			✓				✓
This thesis		✓		✓		✓		✓	**May be**	**May be**		✓	

1.4. Identifying research gaps from the literature

Table 1.1 provides a summary of literature for modelling spatial extremes, which helps to identify research gaps that need to be addressed or improved in order to analyse the spatial dependence of flood-producing rainfall across different durations. This section presents research gaps in Step 2 and Step 4 of the framework (as in Table 1.1's columns). There is no research gap in Step 1, Step 3 and Step 5 as these steps are comparatively better developed than the other steps. A framework is proposed that is oriented to the spatial and duration dependencies of rainfall in design floods.

In Step 2, many studies used linear regressions for the spatial model of marginal parameters, and there are few studies that used a non-linear regression model. The reason for this could be the parsimony of the linear regression model even though the non-linear regression model is more flexible. Both approaches have been shown to provide a high precision spatial map of marginal parameters. Latent variable models can also provide high precision spatial maps of marginal parameter by using Bayesian method for parameter estimates; but the spatial structure they attribute to extreme events has been found to be unrealistic (Davison et al., 2012). This research proposes to use a non-linear regression model, specifically a thin plate spline regression model, for building the spatial map of marginal parameters in the framework for modelling of spatial extremes.

The spatial dependence model in Step 4 is the main focus of this research, and is responsible for accounting for the spatial dependence of flood-producing rainfall. There is a significant research gap here: there is currently no spatial dependence model framework for analysing the spatial dependence of rainfall extremes across different durations. The original spatial dependence models have been developed for just one duration of rainfall extremes (see Step 4 in Table 1.1). Two previous papers tried to link rainfall extremes of different durations together, but they did not actually do anything about the spatial dependence across durations. While the first one provided a method for linking together the marginal parameters of GEV for different durations (Koutsoyiannis et al., 1998), the second one developed a max-stable process that fits within a Bayesian hierarchical framework, and did have a marginal GEV distribution across multiple durations (Stephenson et al., 2016), but the storm-level dependence was restricted to extremes of the same duration. A model that can simulate the dependence characteristics of rainfall extremes across both space and duration is critical for analyzing the spatial dependence of flooding (see details in Section 1.2). Therefore, this research gap must be addressed to enable spatial dependence of floods across different durations.

A second gap in Step 4 is that the asymptotic structure of spatial rainfall needs to be diagnosed. Extreme variables can be asymptotically dependent or asymptotically independent, and both of these dependence properties might occur in spatial extremes (Davison et al., 2013; Thibaud et al., 2013; Wadsworth and Tawn, 2012). An asymptotically dependent variable has a level of dependence that stabilizes with an increasing return period, while an asymptotically independent variable has a level of dependence that reduces with an increasing return period (Wadsworth and Tawn, 2012). However, a detailed analysis of the dependence properties of spatial rainfall extremes is

still lacking, because there is a conflict in selecting the spatial dependence model to use for spatial rainfall. While some researchers have used an asymptotically dependent model (e.g., a max-stable process) to simulate spatial extreme rainfall (Nicolet et al., 2017; Padoan et al., 2010; Westra and Sisson, 2011), there are others who have used an asymptotically independent model (e.g., a Gaussian copula or an inverted max-stable process) for spatial extremes rainfall (Bracken et al., 2016; Renard and Lang, 2007; Sang and Gelfand, 2010; Thibaud et al., 2013). Interestingly, only one paper, from Thibaud et al. (2013), provides a detailed analysis to suggest that the spatial rainfall is asymptotically independent. That study was based on only 575 days of record with 58% of the data missing, so it is difficult to assess whether this result generalizes to other locations. Therefore, it is critical to confirm whether spatial rainfall is asymptotically dependent or asymptotically independent. This determination then helps us to select models that are suitable for the spatial dependence studies of extreme rainfall. An analysis of the asymptotic structure of spatial rainfall extremes will also determine the behaviour of areal reduction factors (ARFs), which are necessary for converting an extreme intensity at a point to the average rainfall depth over a catchment in an event-based rainfall-runoff model (Ball et al., 2016).

The research gaps identified and analysis methods used to study them are shown in the last row of Table 1.1. First, the GPD will be used for the marginal distribution, instead of GEV, for more accuracy. Secondly, a thin spline regression model will be used for building a high precision, spatial map of marginal parameters. Thirdly, a new method will be developed to enable spatial dependence models to analyse the dependence of rainfall extremes across different durations. The selection of a max-stable process or an inverted max-stable process instead of copula model is due to the advantage of having a full spatial process formulation of max-stable theory (see Step 4 in Section 1.3). Fourthly, an asymptotically dependent model (max-stable process) and an asymptotically independent model (inverted max-stable process) are analysed to examine the asymptotic structure of spatial rainfall. Finally, all of these steps will be applied to a case study using an event-based model to assess the spatial dependence of flooding for a civil infrastructure system.

1.5. Overall Research Objectives

The overall aim of this research is to develop a new framework that is able to simulate design flood characteristics across civil infrastructure systems, and includes the conditional and joint probability estimates of floods.

Three specific research objectives have been identified, each of which has a number of sub-objectives:

Objective 1 – Spatial dependence of rainfall extremes across multiple durations: To develop an approach for modelling the spatial dependence of rainfall extremes across multiple durations (Paper 1).

Objective 1.1: To develop a method for combining extreme rainfall events across different durations within a spatial extreme value model (max-stable process).

Objective 1.2: To demonstrate the potential application of the new method in developing conditional maps of return periods and return levels of rainfall extremes across different durations.

Objective 2 – Asymptotic behaviour of areal reduction factors (ARFs): To explore the dependence properties of spatial rainfall extremes and the asymptotic behaviour of ARFs (Paper 2).

Objective 2.1: To investigate the behaviour of ARFs for different asymptotic assumptions using synthetic data.

Objective 2.2: To diagnose the asymptotic properties of spatial rainfall and select a suitable dependence model for modelling the rainfall process.

Objective 2.3: To demonstrate the behaviour of ARFs over long return periods.

Objective 3 – Flood probability estimate for complex linear infrastructures: To demonstrate a new framework for simulating design flood characteristics for civil infrastructure systems (Paper 3).

Objective 3.1: To use the results from Objective 2 to select a suitable model, and use the method from Objective 1 to conduct the conditional and joint probability estimates of rainfall extremes for linear infrastructure – a road highway.

Objective 3.2: To use the framework from Objective 2 to calculate areal reduction factors (ARFs), and transform the conditional and joint rainfall extremes into conditional and joint flood flows.

1.6. Thesis Organisation

The thesis contains five chapters, with the main contributions presented in **Chapter 2** to **Chapter 4**. The contents of each of these chapters map directly to each of the three research objectives in Section 1.5, and are presented in the form of a journal paper. The way the papers address the various objectives of the thesis is illustrated in Figure 1.2. The first paper has been published in the *Water Resources Research*; the second has been

published in *Journal of Hydrology*; and the third has been accepted by *Hydrology and Earth System Sciences* for peer review. The focus of these chapters is as follows:

- **Chapter 2** (Objective 1, Paper 1) presents the proposed approach for combining extreme rainfall events across different durations within a spatial extreme value model (max-stable process). This approach is then applied to the development of conditional maps of the return period and return levels across different durations.
- **Chapter 3** (Objective 2, Paper 2) explores tail dependence behaviour for rainfall extremes and its effect on the asymptotic behaviour of areal reduction factors (ARFs).
- **Chapter 4** (Objective 3, Paper 3) demonstrates a new framework for estimating the conditional and joint probabilities of floods for linear infrastructure using the example of a highway.

Although the section figure numbers have been formatted to match the University guidelines, the manuscript material is otherwise unchanged from the submitted papers. A copy of Paper 1 is reproduced in Appendix A as published. Paper 2 and Paper 3 are under review at present.

Conclusions are provided in **Chapter 5**, which includes a discussion of the contributions, limitations and future directions of the research.

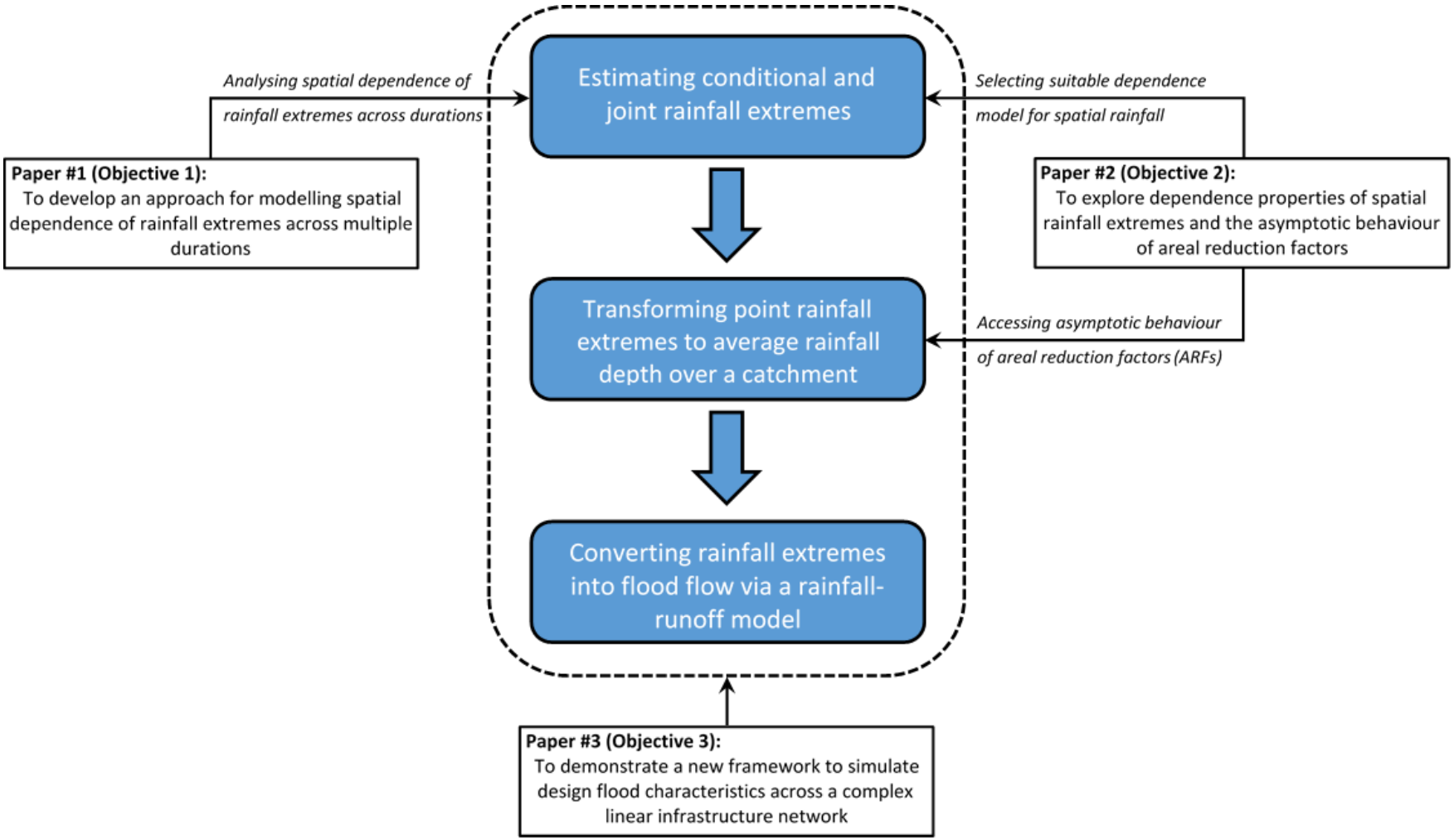

Figure 1.2. The study framework linking the contribution of each of the journal papers to the overall process of flood estimation. Paper #1 and Paper #2 address specific tasks in the analysis of extremes, while Paper #3 helps to demonstrate the use of the proposed framework in the context of a real problem, i.e. to estimate conditional and joint probabilities of flooding for a road highway.

Chapter 2

Modeling Spatial Dependence of Rainfall Extremes Across Multiple Durations (Paper 1)

Phuong Dong Le, Michael Leonard, Seth Westra

Water Resources Research, Volume 54 Issue 3

https://doi.org/10.1002/2017WR022231

Statement of Authorship

Title of Paper	Modeling Spatial Dependence of Rainfall Extremes Across Multiple Durations
Publication Status	☑ Published ☐ Accepted for Publication ☐ Submitted for Publication ☐ Unpublished and Unsubmitted w ork w ritten in manuscript style
Publication Details	Le, P. D., Leonard, M., & Westra, S. (2018). Modeling Spatial dependence of rainfall extremes across multiple durations. Water Resources Research, 54. https://doi.org/10.1002/2017WR022231

Principal Author

Name of Principal Author (Candidate)	Phuong Dong Le
Contribution to the Paper	Implementation and development of approach, visualisation and interpretation of results, preparation of manuscript, preparation of response to reviewers and acted as corresponding author.
Overall percentage (%)	80
Certification:	This paper reports on original research I conducted during the period of my Higher Degree by Research candidature and is not subject to any obligations or contractual agreements with a third party that would constrain its inclusion in this thesis. I am the primary author of this paper.
Signature	Date 16/07/2018

Co-Author Contributions

By signing the Statement of Authorship, each author certifies that:

i. the candidate's stated contribution to the publication is accurate (as detailed above);

ii. permission is granted for the candidate in include the publication in the thesis; and

iii. the sum of all co-author contributions is equal to 100% less the candidate's stated contribution.

Name of Co-Author	Michael Leonard
Contribution to the Paper	Supervised research, helped to evaluate and edit the manuscript.
Signature	Date 16/7/18

Name of Co-Author	Seth Westra
Contribution to the Paper	Supervised research, helped to evaluate and edit the manuscript.
Signature	Date 16/07/2018

Please cut and paste additional co-author panels here as required.

Abstract

Determining the probability of a flood event in a catchment given that another flood has occurred in a nearby catchment is useful in the design of infrastructure such as road networks that have multiple river crossings. These conditional flood probabilities can be estimated by calculating conditional probabilities of extreme rainfall and then transforming rainfall to runoff through a hydrologic model. Each catchment's hydro-logical response times are unlikely to be the same, so in order to estimate these conditional probabilities one must consider the dependence of extreme rainfall both across space and across critical storm durations. To rep-resent these types of dependence, this study proposes a new approach for combining extreme rainfall across different durations within a spatial extreme value model using max-stable process theory. This is achieved in a stepwise manner. The first step defines a set of common parameters for the marginal distributions across multiple durations. The parameters are then spatially interpolated to develop a spatial field. Storm-level dependence is represented through the max-stable process for rainfall extremes across different durations. The dependence model shows a reasonable fit between the observed pairwise extremal coefficients and the theoretical pairwise extremal coefficient function across all durations. The study demonstrates how the approach can be applied to develop conditional maps of the return period and return level across different durations.

2.1. Introduction

For many decades, the rainfall intensity-duration-frequency (IDF) relationship has formed the basis for many extreme rainfall-based flood estimation approaches. For example, the rational method (Mulvaney, 1851) focuses on estimating flow at the catchment outlet, and is based on the rainfall intensity at a duration equal to the catchment's time of concentration. IDF relationships are also used in other flood estimation methods, such as event-based rainfall-runoff models (Boyd et al., 1996; Laurenson and Mein, 1997). In these event-based models, IDF curves are combined with temporal patterns to develop design rainfall hyetographs. The hyetographs are then input to a rainfall-runoff model in order to simulate flood flow at a catchment's outlet (Chow et al., 1988). In almost all cases, these IDFs have been estimated either at a single site or as a spatial map, but without providing parallel information on spatial dependence of rainfall events or the dependence across multiple durations.

A limitation of traditional IDF curves is that they cannot express conditional distributions of extreme rainfall. To be useful for a wide range of flood estimation problems, the conditional relationship should allow for extreme rainfall of different durations, because neighboring catchments are unlikely to be of identical size so that they are likely to respond to extreme rainfall at differing durations. Such a situation is illustrated in Figure 2.1, which describes a hypothetical scenario of designing a route (e.g. road or rail) crossing for a river, which should be designed to operate in the event that a neighboring catchment has flooded. In this case, we may wish to know: What is the probability that a bridge at location x_2 will be flooded, given that the bridge at location x_1 is flooded? Note that for illustration purposes, we assume a one-to-one correspondence between extreme rainfall and flooding; for real-world applications there may be additional factors influencing the magnitude of streamflow extremes that should be taken into account. Assuming that the critical rainfall duration at locations x_1 and x_2 are 24 and 12h, respectively, and that u_1 and u_2 are the depth of rainfall required to flood bridges at these two locations, the question may be rephrased as: What is the probability of having extreme rainfall for 12h exceeding u_2 (mm) at upstream of location x_2, given that extreme rainfall for 24h occurred and exceeds u_1 (mm) at upstream of location x_1? This kind of information is important when designing new infrastructure (e.g. the bridge at location x_2), based on existing infrastructure in the region (i.e. the bridge at location x_1).

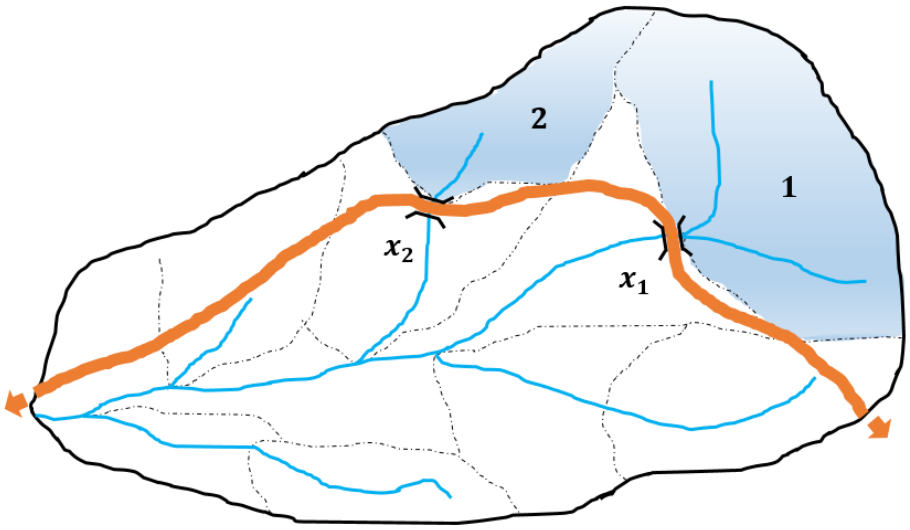

Figure 2.1. Illustrating conditional estimate requirements across multiple durations of extreme rainfall. What is the probability of extreme rainfall for 12h exceeding u_2 (mm) at location x_2, given that extreme rainfall for 24h occurs and exceeds u_1 (mm) at location x_1?

Several approaches have been developed to simulate various spatial features of extreme rainfall. One category is the Bayesian hierarchical approach, which has been developed to explore how the parameters of a marginal distribution (e.g. the generalized extreme value GEV distribution) vary in space. These methods can utilize information from multiple gauges across a region in the estimation process. The Bayesian hierarchical approach is used to infer spatial return levels of extreme rainfall (Bracken et al., 2016; Cooley et al., 2007), as well as deal with difficulties relating to strong hypotheses in regional frequency analysis such as the need to delineate homogenous regions, which may be too restrictive in some cases (Renard, 2011). Although this category of models is useful for building high precision spatial maps of GEV parameters, it does not account for storm level dependence (e.g. the probability that extreme rainfall at two or more locations come from the same event) which is necessary to estimate conditional distributions of extreme rainfall. Another approach is to use multivariate Gaussian processes to provide dependence between multiple locations within a region, whether directly applied to extremes (Renard and Lang, 2007), or as models of the entire rainfall process (Bennett et al., 2016b). These models are able to produce conditional relationships between extremes for the case of asymptotically independent tail dependence.

Max-stable process models have been developed as a method to account for storm-level dependence, and they can characterize the conditional distribution of extreme rainfall in space. Max-stable process has been developed and applied to numerous analyses of the spatial dependence of rainfall extremes (Davison et al., 2012; Padoan et al., 2010; Thibaud et al., 2013; Westra and Sisson, 2011), with Padoan et al. (2010) showing how the application of annual maximum data can provide useful information on conditional rainfall relationships throughout a catchment. This arises because, even though only annual maximum data is used, the generating model used in max-stable process theory assumes that the annual maxima data arise through a set of "storms", such that the dependence can be represented at the storm level. However in all these cases, only one duration of rainfall extremes was considered; thus, the problem of conditional dependence across catchments

with different response durations requires extension of the existing max-stable framework. Stephenson et al. (2016) has developed a max-stable process that fits within a Bayesian hierarchical framework having a marginal GEV distributions across multiple durations, but the storm-level dependence is restricted to extremes of the same duration.

One potential improvement would be developing a max-stable process for more than one variable or alternatively developing a space-time max-stable process (Genton et al., 2015; Huser and Davison, 2014; Oesting et al., 2017). In principle, these models could be used to infer the extremes at different durations. However, they are also very complex and are likely to be difficult to fit for the practical application of a sparse set of rainfall gauges. For example, Huser and Davison (2014) pointed out that some parameters of their model are difficult to estimate, leading to a complex two-stage fitting process; a problem that is likely to be compounded when extending the method to multiple durations. We therefore present an alternative approach that can extend the current max-stable process so that it allows for extreme rainfall across different durations while capturing spatial variation in extreme rainfall as well as storm-level dependencies.

It is important to note that there is a difference between dependence in "time" and "duration" since the former refers to dependence over a sequence of values, whereas the latter refers only to the duration of an event. Thus, for example, a duration-based model is able to parameterize a high dependence between 1 and 2 h extremes and a lesser dependence between 1 and 24 h extremes, without specifying the time-varying structure of the extremes, as implied by space-time dependence.

This paper describes an empirical method that enables the max-stable process to capture the spatial dependence of rainfall extremes across different durations. To achieve this, the method developed by Koutsoyiannis et al. (1998) for linking extreme rainfall across multiple durations is used to fit the marginal model and subsequently transform the extreme rainfall to unit Fréchet scale. A new method is then proposed to fit the max-stable process to extreme rainfall across different durations within the unit Fréchet scale. Finally, the bivariate probability function for the max-stable process (Padoan et al., 2010) is used to estimate the conditional probabilities of rainfall extremes across different durations. This opens up the possibility of using conditional distributions for flood estimation problems that are impacted by rainfall-driven flooding at multiple locations, such as with complex road networks.

This paper demonstrates the model as applied to a case study of the Hawkesbury-Nepean catchment in New South Wales, Australia. In this case study, using annual maximum rainfall from 25 subdaily stations with durations between 1 and 24 h. Section 2.2 outlines the case study and data used. Section 2.3 explains the methodology, including approaches for linking extremes from multiple durations via a marginal model and introducing duration dependence into a spatial model. Results and discussion are provided in Section 2.4 on the performance of the spatial model and the conditional simulation across different durations. Conclusions and recommendations are provided in Section 2.5.

2.2. Hawkesbury-Nepean case study and data

The Hawkesbury-Nepean catchment is located in New South Wales, Australia. It has been chosen as the case study because this area is the focus of ongoing studies for evacuation modelling and requires consideration of the behavior of extreme rainfall across multiple subcatchments (Opper ESM et al., 2010; Ribbons, 2015). An additional reason for choosing this catchment is the relative density of subdaily rainfall data compared to other regions of Australia. The subdaily rainfall records are available in 5 min increments at 25 locations within or near the study catchment.

With an area of 21,400 km^2, the Hawkesbury-Nepean catchment is one of the largest catchments in New South Wales east of the Great Dividing Range. Its rainfall has strong seasonality, particularly for subdaily extreme rainfall durations, with the highest rainfall occurring during the warmer months (December-February) (Zheng et al., 2015). The catchment's average annual rainfall varies from 600 mm inland, to 1000 mm along the coast. Figure 2.2 shows an elevation map of the catchment. The black circles represent the subdaily rain stations used for this study. The sites selected had at least 19 years' record each, and at least 18 years in common with other gauges in the region. Requiring a common period was necessary for conducting a pair-wise calibration, but it restricted the number of sites that could be compared (see Section 2.3.4). The 5 min data were aggregated to 1, 2, 3, 6, 12 and 24h for use in this study. Spatial mapping was performed using latitude and longitude as covariates.

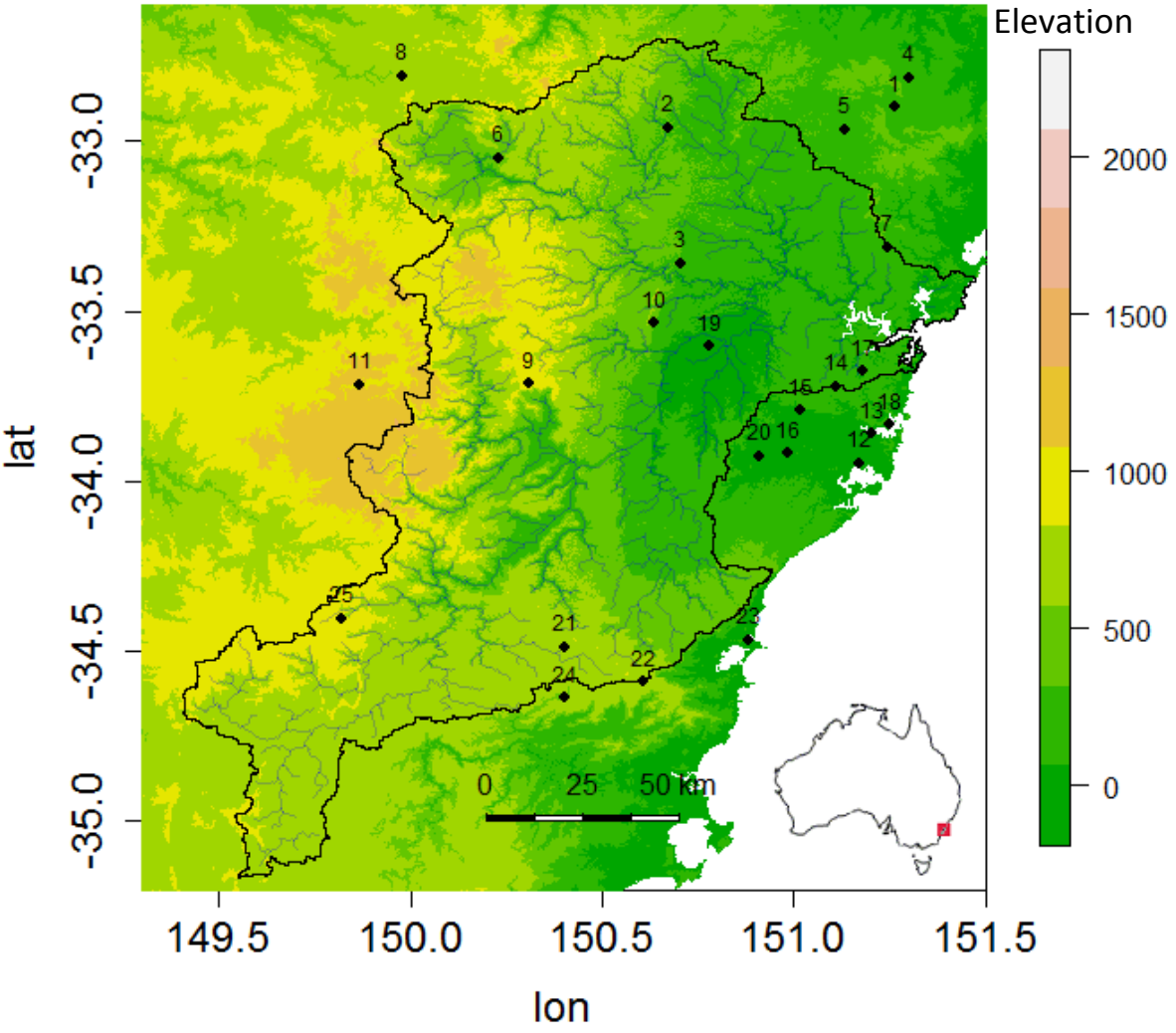

Figure 2.2. The Hawkesbury-Nepean catchment near Sydney, Australia. The catchment is bounded by black lines, and subdaily rainfall gauges are indicated by black dots.

2.3. Methodology

Following a summary of max-stable processes (Section 2.3.1), the proposed method is explained according to the steps shown in Figure 2.3. First, the method of reparameterizing the GEV is explained to allow for convenient representation of marginal distributions across multiple durations (Section 2.3.2). The marginal distribution parameters across multiple sites in the region are then modeled by a thin plate spline regression (Section 2.3.3). At this point there is a complete representation of the marginal model across multiple durations across a region, and this model is use to convert the data to and from the unit Fréchet space. Subsequent steps outline the dependence model, including an empirical method that includes duration in the dependence structure of extremes (Section 2.3.4), and the steps needed to assess conditional probability estimates based on the bivariate max-stable process cumulative distribution function (Section 2.3.5). A subsequent section is provided to summarize the overall methodology.

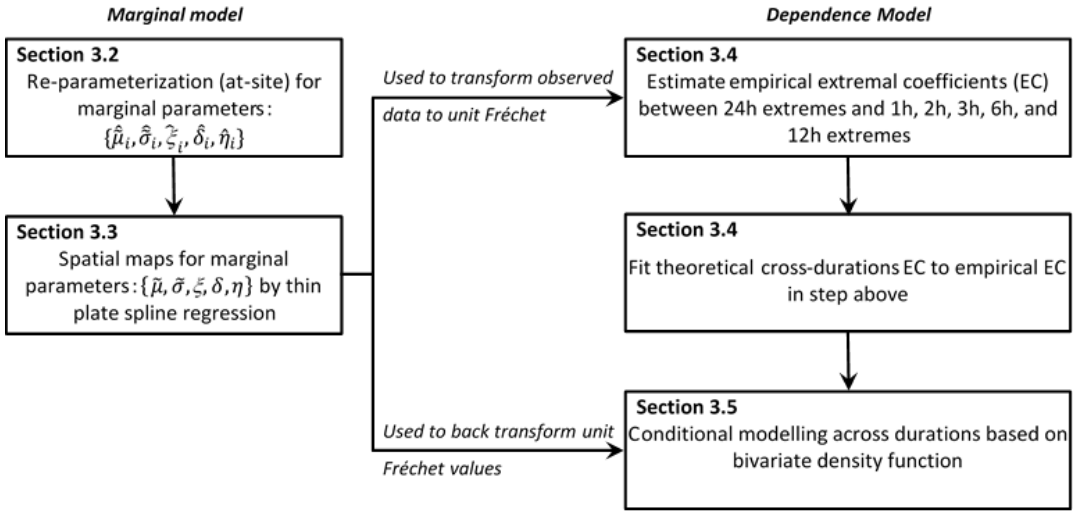

Figure 2.3. The schematic diagram for the overall methodology.

2.3.1. Overview of max-stable process

This study uses a max-stable process as the basis for simulating conditional rainfall extremes. It is used because the model is able to represent storm-level dependence (Davison et al., 2012). The max-stable process extends the generalized extreme value (GEV) distribution into the spatial domain (Davison and Gholamrezaee, 2012; de Haan, 1984; de Haan and Ferreira, 2006). Suppose that $Y_k(x), x \in X$ for $k = 1, \dots, m$ are m independent realizations of a continuous process indexed by location x, where $X \subset R^2$, the set of locations existing in a spatial domain. If the following limit

$$Z(x) = \lim_{m \to +\infty} \frac{\max_{k=1}^{m} Y_k(x) - b_m(x)}{a_m(x)} \tag{2.1}$$

exists jointly for all $x \in X \subset R^2$ and is nondegenerate for some normalizing constants $a_m(x) > 0$ and $b_m(x)$ then $Z(x)$ is a max-stable process (de Haan, 1984). It follows that at a fixed location in space, x, each marginal distribution is the univariate GEV distribution.

It is convenient to construct a simple max-stable process with unit Fréchet margins, and subsequently the marginal distribution can be transformed back to the GEV scale. To construct a simple max-stable process, let $\{(U_i, s_i), U_i > 0, i \geq 1\}$ denote the points of a Poisson process at $s_i \in R^2$ with intensities following $1/U^2$. Then one characterization of a max-stable process with unit Fréchet margins is:

$$Z(x) = \max_i \{U_i f(s_i, x)\}, \qquad x \in X, \tag{2.2}$$

where $f(s, x)$ is a non-negative function that integrates to unity over s for fixed $x \in X$.

The construction above can be interpreted as the rainfall-storm process (e.g., Schlather and Tawn (2003); R. L. Smith, University of Surrey, unpublished manuscript, 1990, http://www.stat.unc.edu/postscript/rs/spatex.pdf). To understand this, consider a continuous domain in R^2 in which n storms occur over this domain with centers at s_i $(i = 1, \dots, n)$ and "intensities" $U_i \in R^+$. The shape of each storm is given by the kernel $f(s_i, x)$. Thus, the storm magnitude at location x is $U_i f(s_i, x)$. Figure 2.4 shows an illustration of

the idea of the max-stable process based on a Gaussian storm profile in R^2 (left panel), and the profile of a max-stable process along a given transect across the catchment (right panel).

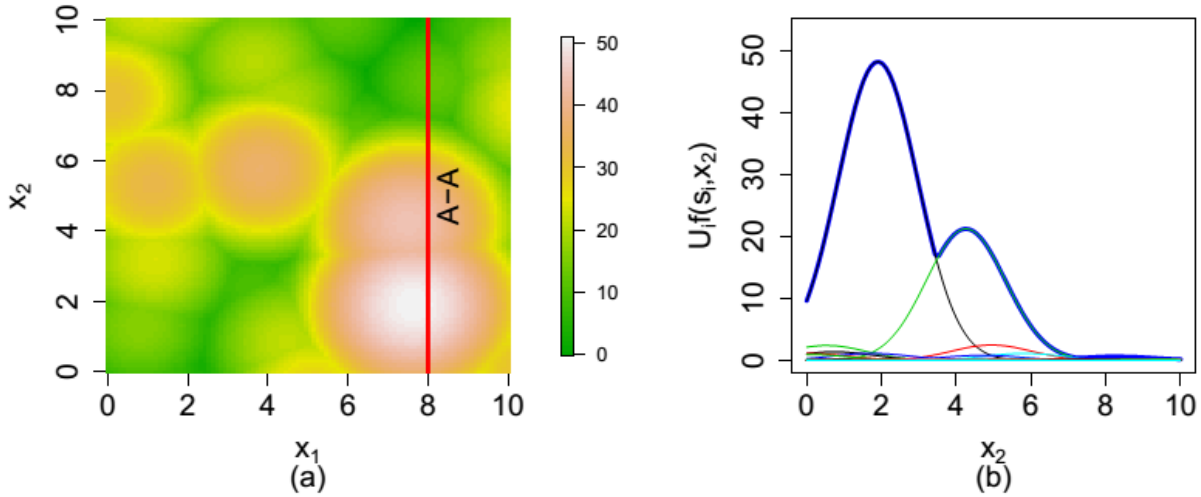

Figure 2.4. Max-stable processes *Z(x)*. (a) Illustrates a max-stable process in two dimensions $X = (x_1, x_2)$ with a positively correlated Gaussian storm profile. The thin colored lines in plot (b) illustrates single storm events $i = 1, \ldots, n$ along transect A-A with specified value of $x_1 = 8$, with magnitude of $U_i f(s_i, x_2)$ and the process maxima $Z(x_2) = max\{U_i f(s_i, x_2)\}$, given as the thick blue line.

2.3.2. Linking multiple durations at each site

The above theory can be generalized to an arbitrary distribution by transforming the marginal distributions. This transformation forms an important step in developing the max-stable process. One challenge in implementing this transformation is that extreme data at each duration has its own marginal distribution, which leads to a large number of parameters that need to be estimated when considering multiple durations. To reduce the number of parameters that need to be estimated, an approach is needed that can link data of multiple durations. This section provides the method of marginal modelling that links the extremes of multiple durations.

Consider the set of annual maximum rainfall depths $r_{i,t,d}$ for a given site $i=1,\ldots,N$, year $t=1,\ldots,T$ and duration $d=1,\ldots,D$. The generalized extreme value (GEV) distribution is used to model the annual maxima $r_{i,t,d} \sim GEV\left(\mu_{i,d}, \sigma_{i,d}, \xi_{i,d}\right)$, with the cumulative distribution function defined as:

$$G\left(r_{i,t,d}\right) = \exp\left\{-\left[1 + \xi_{i,d}\left(\frac{r_{i,t,d} - \mu_{i,d}}{\sigma_{i,d}}\right)\right]^{-1/\xi}\right\}, \qquad (2.3)$$

where for a given site i and duration d, $\mu_{i,d}$ is the location parameter, $\sigma_{i,d} > 0$ is the scale parameter, and $\xi_{i,d}$ is the shape parameter, where $1 + \xi(r - \mu)/\sigma > 0$. The GEV distribution describes the relationship between the frequency and depth of extreme rainfall that occurs in a specified duration and location of interest.

Koutsoyiannis et al. (1998) provided a re-parameterization for the GEV distribution that allows it to be linked across multiple durations. In this re-parameterization, a new parameter, $\tilde{\mu}_i = \mu_{i,d}/\sigma_{i,d}$, is defined and assumed to be constant for all durations of

interest. The shape parameter $\xi_{i,d}$ is also assumed to be constant for all durations, so that the scale parameter can be modified to carry all information relating to rainfall intensities across multiple durations. Koutsoyiannis et al. (1998) proposed the following relationship to express this dependence:

$$\sigma_{i,d} = \frac{\tilde{\sigma}_i d}{(d + \delta_i)^{\eta_i}}, \tag{2.4}$$

where $\sigma_{i,d}$ is the scale parameter corresponding to extreme rainfall for duration d, $\tilde{\sigma}_i$ is a duration-independent parameter, $\delta_i \geq 0$ and $0 \leq \eta_i \leq 1$. This equation represents an empirical formula, encapsulating the experience from several IDF studies (Koutsoyiannis et al., 1998). It should be noted that this equation is used to model the scale parameter when extreme rainfall is measured by depth (mm) rather than intensity (mm/h). By using this equation, the GEV distribution across multiple durations can be modeled at a given location *i* through a single distribution with only two additional parameters: the offset term δ and exponent term η. Regarding the total number of parameters, this approach uses just five parameters to estimate extreme rainfall across all n_d durations, instead of $3n_d$ parameters when using separate GEV distributions for each duration.

As a result of the reparameterization, the rainfall intensities across multiple durations can be represented as $r_{i,t,d} \sim GEV(\tilde{\mu}_i, \tilde{\sigma}_i, \xi_i, \delta_i, \eta_i)$. The log likelihood is then given as:

$$\ell\left(r_{i,t,d} \middle| \tilde{\mu}_i, \tilde{\sigma}_i, \xi_i, \delta_i, \eta_i\right) = \sum_t \sum_d \left(\log\left(GEV\left(\tilde{\mu}_i, \tilde{\sigma}_i, \xi_i, \delta_i, \eta_i\right)\right)\right). \tag{2.5}$$

This is more correctly referred to as a pseudo-likelihood because it assumes that all $r_{i,t,d}$ are independent and while the corresponding estimators from this function are consistent with maximum likelihood estimates, they do not have the same efficiency.

2.3.3. Modelling the re-parameterized at-site GEV parameters across space

The at-site GEV parameters can vary over a region, and practical interest is often in estimating GEV parameters at locations without rain gauges. To be able to provide estimates of extremes at ungauged locations it is necessary to develop a spatial model of the parameters. To maximize the precision in the model's estimates, all five parameters of the modified GEV distribution were modeled spatially.

The parameters were modeled via a thin plate spline regression. In this regression, the employed model is additive $\vartheta = f(x) + e$ where ϑ is a parameter surface of interest, $f(x)$ is the response surface for a given vector x of covariates (here $f(x) = \beta_0 + \beta_{lon} longitude + \beta_{lat} latitude$), and e is an error term. Additional covariates of elevation and distance from coast were tested but did not significantly improve the fit of the parameter surfaces. Additional covariates of elevation and distance from coast were tested but did not significantly improve the fit of the parameter surfaces (see supporting information Figure S2.7). A reason for this is that the longitude covariate provides a surrogate for both these terms since the coastline predominantly runs north-south along the eastern edge of the region and the elevated areas occur along the western edge (visible in Figure 2.2). Each thin plate spline surface is determined by minimizing $\|\vartheta - f\|^2 + \lambda\Delta$,

where Δ is a roughness penalty function determined by a constraint on the dimension of the covariates and λ is a smoothness parameter that is selected by generalized cross-validation. This approach is used to build five response surfaces for the five marginal parameters i.e. $\tilde{\mu}, \tilde{\sigma}, \xi, \delta, \eta$.

2.3.4. Storm-level dependence model

In this study, the Brown-Resnick model (Brown and Resnick, 1977; Kabluchko et al., 2009), is selected for analyzing storm-level dependence. This section describes a detailed method for calibrating the max-stable process, and introduces an empirical approach for linking duration dependence into the dependence model.

To calibrate the max-stable process, it is necessary to calculate the observed pairwise extremal coefficients. It is noted that the dependence model is stationary in unit Fréchet scale, but the final model is nonstationary because of the nonstationary marginal model. First, the rainfall values $r_{i,t,d}$ need to be transformed to a unit Fréchet distribution $z_{i,t,d}$, which is achieved via the following equation:

$$z_{i,t,d} = \left(1 + \xi_{i,d}\frac{r_{i,t,d} - \mu_{i,d}}{\sigma_{i,d}}\right)^{1/\xi_{i,d}}. \tag{2.6}$$

The observed pairwise extremal coefficient $\hat{\theta}$ is then calculated through the *F*-Madogram $\hat{v}_F$ (Cooley et al., 2006b):

$$\hat{v}_F(x_1 - x_2) = \frac{1}{2p}\sum_{t=1}^{p}\left|F\left(z_t(x_1)\right) - F\left(z_t(x_2)\right)\right|, \tag{2.7}$$

where $z_t(x_1)$ and $z_t(x_2)$ are the t-th observations (the annual maximum rainfall in the t-th year) of extremes in the form of unit Fréchet margins at location x_1 and x_2 with p the total number of common observations between the two locations, and $F(z) = exp(-1/z)$. Note that the extreme rainfall at location x_1 and x_2 can be of identical duration (i.e. both 24h) or different durations (e.g. 24 and 1h). The observed pairwise extremal coefficient $\hat{\theta}$ is then estimated by:

$$\hat{\theta}(x_1 - x_2) = \frac{1 + 2\hat{v}_F(x_1 - x_2)}{1 - 2\hat{v}_F(x_1 - x_2)}. \tag{2.8}$$

The max-stable process can be fitted by minimizing the sum of squared errors between the theoretical pairwise extremal coefficient function and the observed pairwise extremal coefficients. The theoretical extremal coefficient function for the Brown-Resnick model is given as:

$$\theta(x_1 - x_2) = 2\Phi\left(\sqrt{\frac{\gamma(h)}{2}}\right), \tag{2.9}$$

where Φ is the standard normal cumulative distribution function, h indicates the Euclidean distance between two locations x_1 and x_2, and $\gamma(h)$ belongs to the class of variograms $\gamma(h) = h^{\beta}/q$ for $q > 0$ and $\beta \in (0,2]$.

In the case that extreme rainfall at locations x_1 and x_2 are of identical duration (i.e. both 24h), then the max-stable process is fitted to the observations by minimizing the sum of squared errors of extremal coefficients numerically. However when the extreme rainfall at location x_1 and x_2 are of different durations (e.g. 24 and 1h), the dependence level of extreme rainfall at these two locations is less than the case of 24 and 24h, including at the distance of $h = 0$ where the rainfall is not "perfectly dependent" as would be the case when using only a single duration. Therefore, an adjustment needs to be made to ensure that the theoretical pairwise extremal coefficient function can capture the observed pairwise extremal coefficients for the case of extreme rainfall of different durations. We propose an approach of adjustment by adding a nugget to the variograms as:

$$\gamma_{ad.}(h) = h^{\beta}/q + c(D-d)/d, \tag{2.10}$$

where h, β, and q are the same as those from Eq. (2.9) above, d is the duration (in hours), $0 < d \leq D$, where D is the maximum duration of interest ($D = 24$ h for the case study described in this paper), and c is a new parameter of the adjustment. This adjustment is intended specifically to condition the behavior of shorter duration extremes on the observation that a D-hour extreme of specified magnitude has occurred. It is constructed to reflect that when compared to a D-hour extreme, the shorter the duration, the lesser the extremal dependence. Cases involving conditioning longer periods on shorter periods (such as a 24 h extreme given a 1 h extreme has occurred) would require a different relationship, and are beyond the scope of this paper.

To fit the max-stable process for all pairs of durations at locations x_1 and x_2 (i.e. 24 and 12h, 24 and 6h, 24 and 3h, 24 and 2h, 24 and 1h), the theoretical pairwise extremal coefficient function in formula (11) is used. That formula is based on $\gamma_{ad.}(h)$ instead of $\gamma(h)$ as:

$$\theta(x_1 - x_2) = 2\Phi\left(\sqrt{\frac{\gamma_{ad.}(h)}{2}}\right). \tag{2.11}$$

The parameters β and q are used from the fitted results of the case of identical 24h durations at location x_1 and x_2. The other parameter c is obtained by least squares fit of the extremal coefficient across all durations.

2.3.5. Conditional probability estimates

The conditional probability $Pr[Z(x_2) > z_2 | Z(x_1) > z_1]$ is obtained from the bivariate max-stable process cumulative distribution function (Padoan et al., 2010), which is given as:

$$Pr[Z(x_1) \leq z_1, Z(x_2) \leq z_2] = \exp\left[-\frac{1}{z_1}\Phi\left(\frac{a}{2} + \frac{1}{a}\log\frac{z_2}{z_1}\right) - \frac{1}{z_2}\Phi\left(\frac{a}{2} + \frac{1}{a}\log\frac{z_1}{z_2}\right)\right], \tag{2.12}$$

where Φ is the standard normal cumulative distribution function, $a = \sqrt{2\gamma_{ad.}(h)}$ with $\gamma_{ad.}(h)$ is variogram which was mentioned in the explanation of Eq. (2.10) above.

Assuming unit Fréchet margins, the relationship between return level z and return period T is given as $z = -1/log(1 - 1/T)$ and the conditional probability for the max-stable process can then be estimated using:

$$Pr[Z(x_2) > z_2 | Z(x_1) > z_1] = T_1 \left[\frac{1}{T_1} - \exp\left(-\frac{1}{z_2}\right) + \exp\left(-\frac{\Phi(\omega)}{z_1} - \frac{\Phi(\nu)}{z_2}\right) \right], \quad (2.13)$$

where $\omega = a/2 + \log(z_2/z_1)/a$, $\nu = a - \omega$, and T_1 is the return period corresponding to return level z_1.

This formula is used to estimate the conditional probability in the form of conditional maps of return periods and return levels across different durations.

2.3.6. Summary of the overall methodology

This section provides an algorithm that summarizes the overall methodology for this study in a stepwise order:

Step 1: Independently fit the univariate GEV at each site across multiple durations

The log-likelihood in Eq. (2.5) is maximized at each site to determine the Koutsoyiannis relationship and GEV marginal parameters for each location $\{\hat{\tilde{\mu}}_i, \hat{\tilde{\sigma}}_i, \hat{\tilde{\xi}}_i, \hat{\delta}_i, \hat{\eta}_i\}$. This yields estimates of five parameters at each site *i=1,...,N*.

Step 2: Perform spatial interpolation on the independently fitted parameter estimates

The marginal parameters estimated in Step 1 are used to perform a preliminary spatial interpolation. Independent application of thin plate spline regression to each parameter surface yields five response surfaces for the five marginal parameters $\{\tilde{\mu}, \tilde{\sigma}, \xi, \delta, \eta\}$.

Step 3: Analyse spatial dependence across different durations

The five response surfaces from Step 2 are used to transform the extreme rainfall for all durations to have a unit Fréchet margin. After that, the observed pairwise extremal coefficients across different durations (e.g., extreme rainfall for 24 and 24h, 24 and 12h, 24 and 6h, 24 and 3h, 24 and 2h, 24 and 1h) are estimated based on the extremal values in the unit Fréchet scale.

Step 4: Fit max-stable process across different durations

The dependence structures of max-stable process across different durations (i.e. extreme rainfall for 24 and 24h, 24 and 12h, 24 and 6h, 24 and 3h, 24 and 2h, 24 and 1h) were fitted to the data by minimizing the sum of squared errors between the theoretical pairwise extremal coefficient function (calculated from Eq. (2.9)–(2.11)) and the observed pairwise extremal coefficients (calculated from Eq. (2.7) and (2.8)).

Step 5: Implement conditional estimates

Conditional estimates are implemented by calculating conditional probabilities for a unit Fréchet max-stable process based on Eq. (2.13) with the dependence parameters from Step 4. The conditional maps of return period and return level are then inferred.

2.4. Results and discussion

This section provides results in a stepwise manner that parallels the steps used in the methodology. First, the approach is evaluated for its ability to link extreme rainfall data across multiple durations at individual stations. The spatial patterns of the at-site parameters are then explored. Subsequently, the results of the calibration of the max-stable process across different durations are presented. The final section demonstrates maps of the conditional return periods and return levels.

2.4.1. Linking extreme rainfall for multiple durations at each site

To evaluate the performance of the re-parameterization, we checked the quantile-quantile plots (QQ plots) to see if the fits are reasonable. Figure 2.5 provides the QQ plots for the marginal model for one representative station for extreme rainfall of all durations. The QQ plots for all durations indicate that the fitted results for station 20 are reasonable. Similar QQ plots for other stations can be found in the supporting information (supporting information Figure S2.1–S2.6), showing that the marginal estimates by using the re-parameterization are reasonable for all stations.

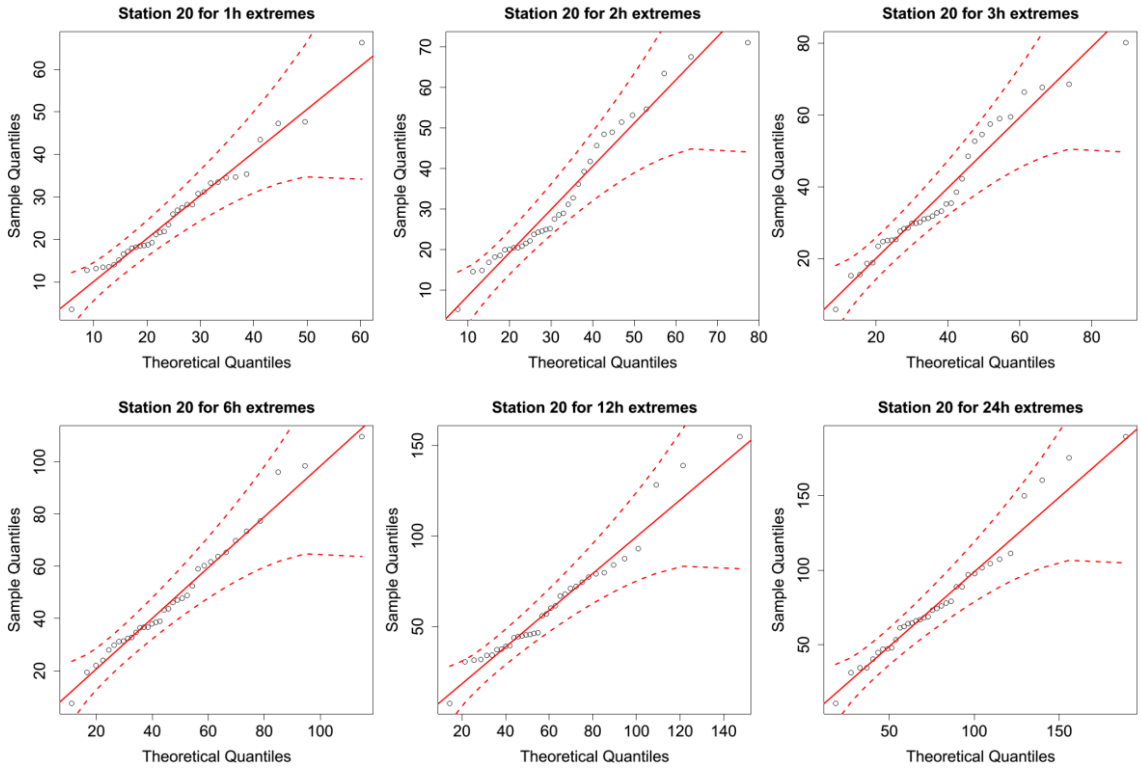

Figure 2.5. QQ plots for the marginal model based on the reparameterization approach to fit GEV at rain station 20 in the case study. The solid diagonal line indicates a perfect fit, and the dotted lines indicate a 95% confidence interval.

2.4.2. Building the response surface for the re-parameterization model parameters

The second step in the modeling approach is the development of the spatial model for marginal distribution parameters, which is important for predicting extreme rainfall at unobserved locations. As mentioned in Section 2.3.4, applying the max-stable process requires transforming extreme data to a unit Fréchet distribution. Marginal distribution parameters are needed to complete this transformation. This section provides the spatial

model for the re-parameterization of marginal parameters, which can then be used to predict the re-parameterized marginal parameters at ungauged locations.

To allow the marginal parameters to vary spatially, the thin plate splines are employed to build the response surface for parameters $\tilde{\mu}$, $\tilde{\sigma}$, ξ, δ, and η based on covariates of longitude and latitude. For this case study, the parameter δ for all stations was found to be in a small range from 0 to 0.03, with $\delta = 0$ for most sites. A simplification was therefore made to set δ constant at 0 for the whole domain. Figure 2.6 shows both the at-site estimates (as colors within each circle) and the response surfaces for $\tilde{\mu}$ and $\tilde{\sigma}$ (on the top) and for ξ and η (on the bottom).

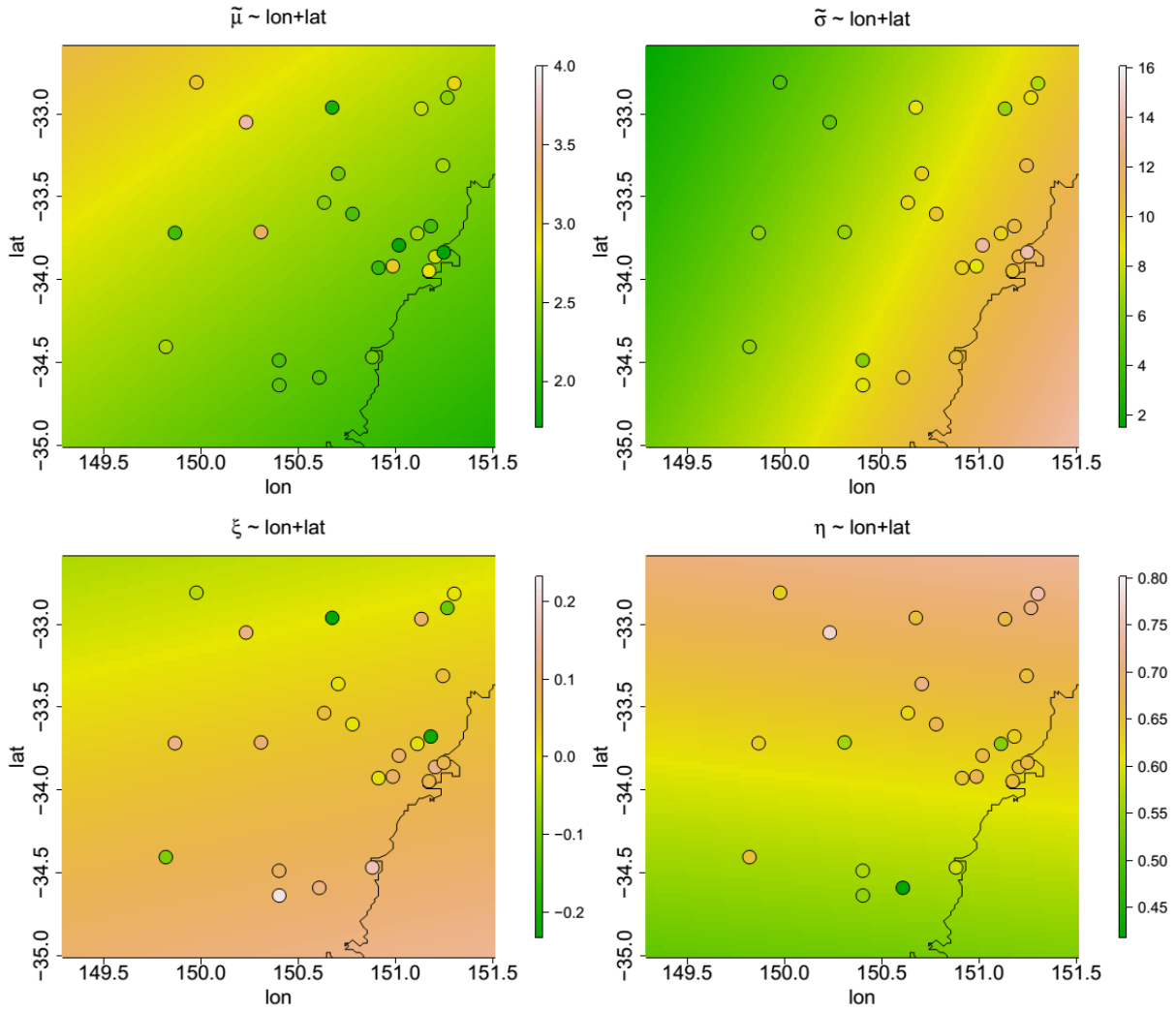

Figure 2.6. Response surfaces for (top) $\tilde{\mu}$ and $\tilde{\sigma}$ and for (bottom) ξ and η. The circles are at-site parameter estimates of subdaily extremes, matching the domain in Figure 2.2.

The top-left panel in Figure 2.6 shows that the range of magnitude for $\tilde{\mu}$ varies from 2.2 to 3.0, with lower magnitude values of $\tilde{\mu}$ at the bottom right of the domain, and higher values at the top left of the domain. The top-right panel shows that the magnitude of $\tilde{\sigma}$ tends to vary from left to right across the domain, with a range from 5 to 11. The modelled surfaces can have discrepancies with some of the at-site estimates due to a large nugget effect.

The response surface for ξ in the bottom-left panel in Figure 2.6 shows considerable variation over the region, though the range of magnitude is very small, only from −0.05 to 0.1. However, these small variations in values of ξ have a noticeable effect on the shape of the marginal extremal distribution, which then impacts on the predictions, particularly under extrapolation to long recurrence-interval values. The magnitude for ξ is generally higher for the lower portion of the region.

The response surface for η in the bottom-right panel is the most variable surface among the four parameters. This parameter is the power term for the location parameter μ and the scale parameter σ across durations, which affects the function's shape. Spatially, it fluctuates with local highs and lows across the region, ranging from 0.45 to 0.75, which indicates that the shape of the relationships between the location parameter μ and durations and between the scale parameter σ and durations are different over the domain.

2.4.3. Calibration of the max-stable process across different durations

The max-stable process across different durations was calibrated to determine the spatial dependence parameters for extreme rainfall. To do this, the theoretical pairwise extremal coefficient function was estimated and compared with the observed pairwise extremal coefficients. The theoretical pairwise extremal coefficient function between two locations (x_1 and x_2) was calculated based on Eq. (2.9)–(2.11), and the observed pairwise extremal coefficient $\hat{\theta}$ was calculated using Eq. (2.7) and (2.8) in Section 2.3.4.

Figure 2.7 provides the pairwise extremal coefficient estimates for the Brown-Resnick model vs. distance *h* (in km). To reduce the uncertainty of the observed pairwise extremal coefficients, pairs of rain gauges were grouped into distance classes. The black points are observed pairwise extremal coefficients while the red lines are the fitted extremal coefficient functions. A coefficient equal to 1 indicates complete spatial dependence, and a value of 2 indicates complete spatial independence. The top-left panel shows the dependence between 24h extremes across space, with the distance $h = 0$ corresponding to "complete dependence", and with the dependence decreasing for increasing distance.

The remaining panels of Figure 2.7 show the 24 vs. 12h extremes, 24 vs. 6h extremes, and 24 vs. 3h extremes. As can be seen, the dependence levels are weaker compared with 24h vs. 24h extremes at the same distance, especially at the distance of 0. This is expected, as the dependence at the same site between annual maxima at different durations will be lower than between annual maxima at the same duration. This is because the annual maxima of different durations may arise from different storm events (Zheng et al., 2015). Even though events giving rise to the maxima may be different, there can still be a level of dependence as they can arise from the same generating process (e.g. low pressure system or a wetter than average season).

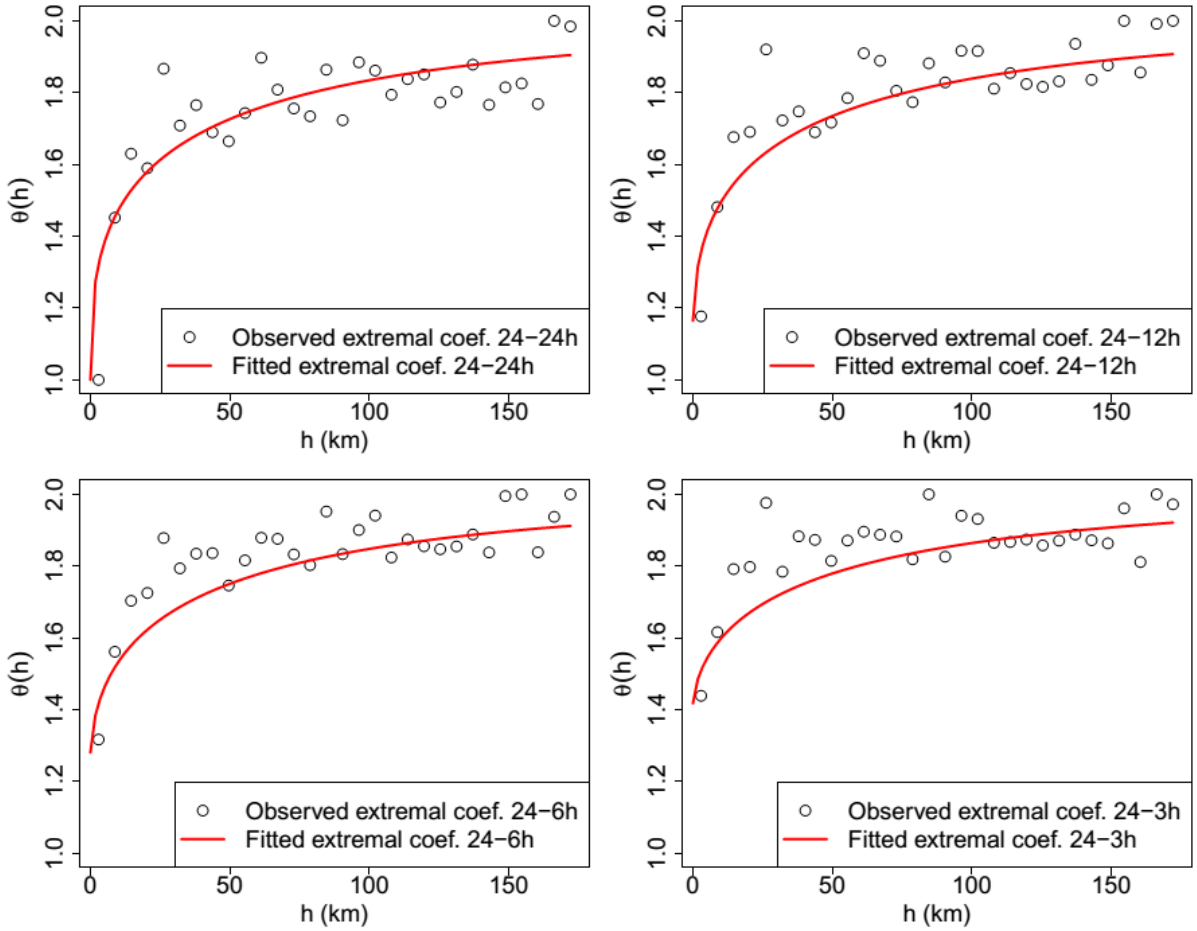

Figure 2.7. Plot of pairwise extremal coefficient against distance. Pairwise extremal coefficient estimates for Brown-Resnick model between: (top left) 24 h extremes and 24 h extremes; (top right) 24 h extremes and 12 h extremes; (bottom left) 24 h extremes and 6 h extremes; and (bottom right) 24 h extremes and 3 h extremes. The black points are observed extremal coefficients for pairs of subdaily stations grouped into distance classes, and the red lines are fitted extremal coefficient function.

2.4.4. Conditional modelling across durations

The previous sections outlined how to link extremes across multiple durations and how to extend the dependence structure of the extremes to encompass space and duration. Having defined and calibrated this model it is now possible to use it for estimating conditional extremes over a spatial domain. While the model is noticeably idealized when compared to real observations (Figures 2.5–2.7), the approach opens up new possibilities for addressing design problems that are not otherwise achievable with the use of typical IDF curves.

Consider the situation where a house at location i has been designed to a 20% annual exceedance probability (AEP; corresponding to a 5 year return period). In other words, this exceedance probability has been used to set the building level for the house. Assuming a one-to-one correspondence between extreme rainfall intensity and flood magnitude, the probability of the house getting flooded is given as:

$$Pr(r_i > u_i) = 0.2, \tag{2.14}$$

where u_i mm is the minimum water level at which the house would be considered "flooded". Assuming that the residents of the house will need to evacuate to higher ground

upon the house flooding, it is desirable to design a route at some other location *j* with its own corresponding probability of failure. Given that the evacuation route is only needed if location *i* is flooded, we might specify a design criterion that we are only willing to tolerate a 10% risk of the evacuation route being flooded conditional on it being required. To specify this problem, we can write the conditional probability as follows:

$$Pr(r_j > u_j | r_i > u_i) = 0.1. \tag{2.15}$$

To calculate the conditional distribution, it is necessary to account for the spatial dependence of flooding at the two locations. Hence, we use spatial dependence of the flood-producing rainfall (assuming a one-to-one correspondence). There are two extreme situations in this scenario:

(1) **Very strong spatial dependence between locations *i* and *j*.** This situation might arise if locations *i* and *j* are very close together, such that if there is a rainfall event of a given exceedance probability at location *i*, one can expect a rainfall event of identical exceedance probability at location *j*. To preserve the conditional probability in Eq. (2.15) we would have to design the evacuation route at location *j* to have marginal probability $Pr(r_j > u_j) = 0.2 * 0.1 = 0.02$, so that the evacuation route can only be flooded once every 50 years on average. In other words, designing the evacuation route to a 2% annual failure probability will ensure that its average failure rate is one in every 10 times that location *i* is flooded.

(2) **Very weak spatial dependence between locations *i* and *j*.** This situation might arise if locations *i* and *j* are very far apart, so that a rainfall event at location *i* provides no information on the likely magnitude of a rainfall event at location *j*. We would design the evacuation route at location *j* to have a marginal probability equivalent to the conditional probability, so that $Pr(r_j > u_j)$ = 0.1. This is because a flood at location *i* will have no influence on whether the evacuation route at location *j* is flooded.

In reality, the marginal probability at location *j* needed to achieve the conditional probability given in Eq. (2.15) will be somewhere between the two extremes specified above. The max-stable process described in the previous sections is capable of providing information to estimate these conditional probabilities, so that it is possible to calculate the appropriate marginal probabilities $Pr(r_i > u_i)$ to be used for design. This is illustrated in Figure 2.8, which is specified to provide marginal probabilities $Pr(r_j > u_j)$, such that the conditional probability in Eq. (2.15) is preserved, assuming the marginal probability at location *i* given in Eq. (2.14).

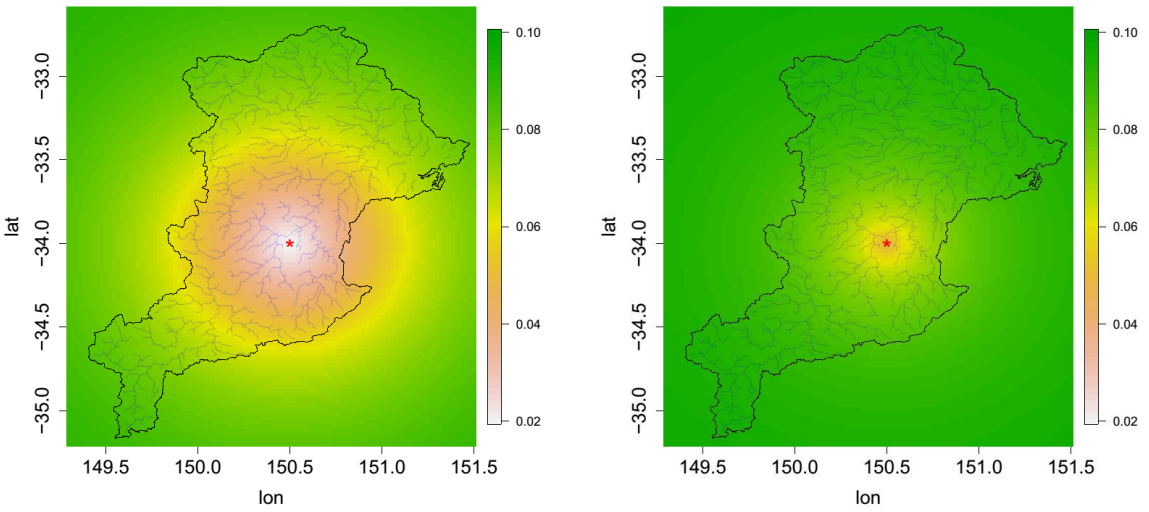

Figure 2.8. Map of marginal probabilities $Pr(r_j > u_j)$ corresponding to a conditional probabilities $Pr(r_j > u_j | r_i > u_i) = 0.1$, assuming a house at location *i* (indicated in the centre of the domain by the red star) floods with probability $Pr(r_i > u_i) = 0.2$. Plots are presented for (left) 24 h extremes and (right) 1 h extremes at locations *j*, conditional on a 24h extreme event at location *i*. The color scales are the same for comparison.

Figure 2.8 (left panel) illustrates the situation where the critical storm durations for locations *i* and *j* are the same (i.e. both 24h). Here, the range of annual exceedance probabilities varies from 0.02 when locations *i* and *j* are close together, to 0.1 when locations *i* and *j* are far apart. The shape of the decay is determined by the function $f(s_i, x)$ mentioned in Section 2.3.1. These results show that the design criteria of the evacuation route (in terms of marginal failure criteria) needs to be stronger as the evacuation route is increasingly close to location *i*, as expected from the spatial nature of the storm.

The situation where critical durations at locations *i* and *j* are different (Figure 2.8, right panel) shows a similar decaying behavior away from the storm, but with lower annual exceedance probabilities required for the evacuation route design close to location *i*. Such a situation might arise in practice if a house is located near a larger river system, but where the evacuation route needs to cross over a smaller tributary into that river system. The lowered dependence can be explained by the fact that a large 24 h storm event does not imply an equally large (in terms of exceedance probabilities) 1 h storm event. This is consistent with *Zheng et al.* (2015) who showed that annual maximum 24h events in Sydney often occur in different seasons from the annual maximum 1h events.

The above results are expressed as exceedance probabilities, but it is also possible to illustrate the results as a return level. The left hand panel of Figure 2.9 shows the unconditional return level map for u_j corresponding to $Pr(r_j > u_j) = 0.1$. As can be seen, there is a gradient of rainfall intensity from relatively less intense in the top left of the domain to higher intensity in the bottom right of the domain. This feature is a result of the coastal effects that are well-known in the Sydney region, with higher extreme rainfall typically occurring closer to the coastline. These results are presented for both the 24 h rainfall event (top left panel) and 1 h event (bottom left panel). They are obtained from the multi-duration surface of the fitted max stable model developed in the previous section.

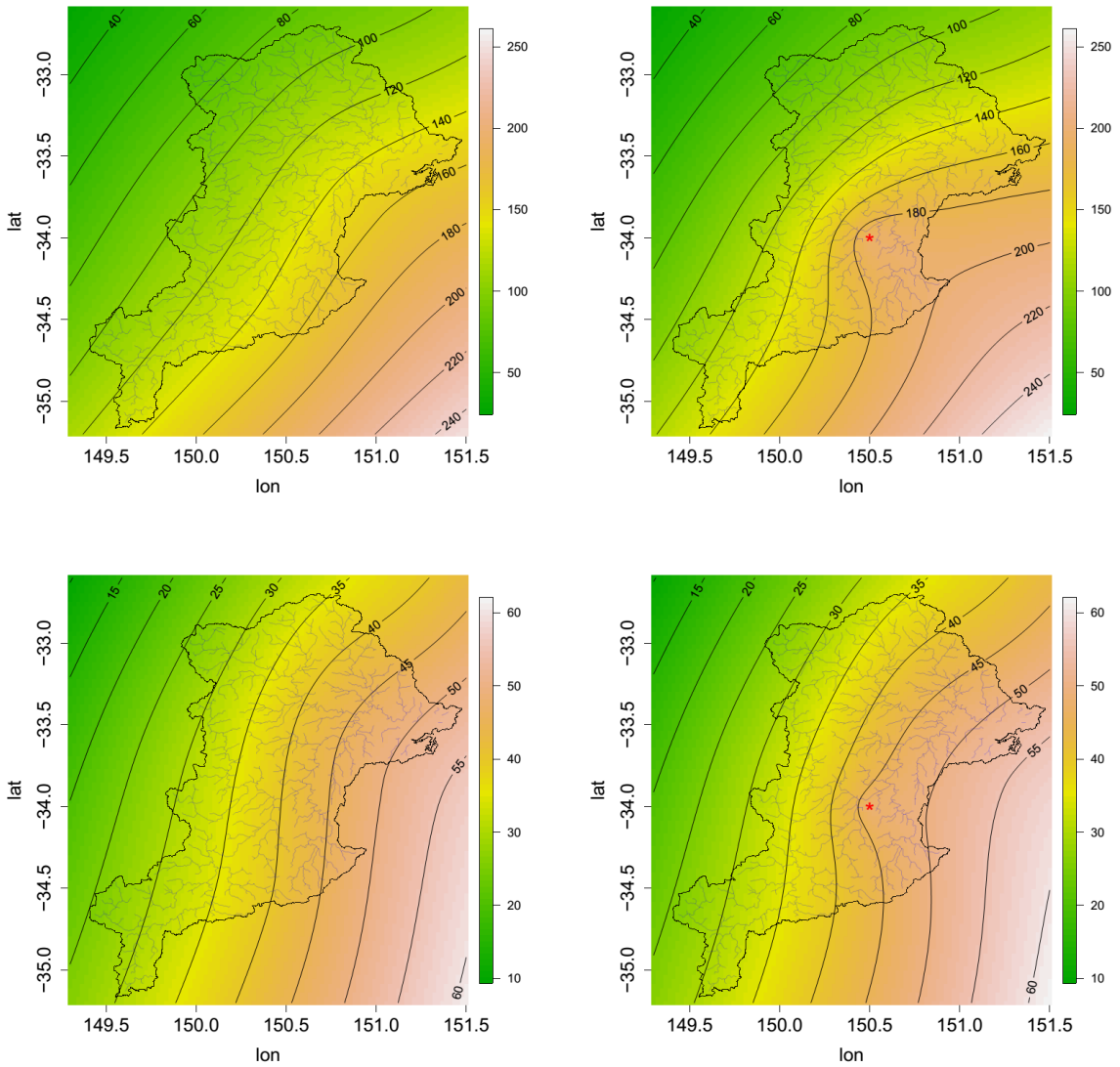

Figure 2.9. Pointwise 10 year unconditional return level map (mm), and pointwise 10-year conditional return level map (mm) given a 5 year event for 24h extremes happen at location *i* (the red star). (top) Pointwise unconditional return level map for (left) 24 h extremes, and (right) pointwise conditional return level map for 24 h extremes. (bottom) Pointwise unconditional return level map for (left) 1 h extremes, and (right) pointwise conditional return level map for 1h extremes.

We now consider the return level given that an event equal to the return periods given in Figure 2.8 for the 24h rainfall (Figure 2.9 upper right panel) and 1h rainfall (Figure 2.9 lower right panel). The return levels are higher close to the conditional point (i) and decrease away from this point, until they become equivalent to the unconditional plots. All the plots in Figure 2.9 are produced using the same model, thus providing a unifying framework for generating both conditional and unconditional IDF maps.

This above analysis highlights the potential of the spatial max-stable process approach. Not only is it possible to develop spatial maps of return periods and return levels at both gauged and ungauged locations, but it is also possible to use a single model to estimate return periods and levels at all durations from 1h through to 24h. Furthermore, it is possible to estimate the conditional return periods given that an extreme rainfall event has occurred at a given location. There are some assumptions using the analysis of extreme

rainfall to infer the properties of a flood, which include that there is a one-to-one correspondence between the extreme rainfall and the streamflow derived from a hydrological model of that rainfall, and that the spatial dependence structure of the rainfall is the same as the streamflow. These assumptions are common to most methods that rely on IDF curves.

The substantial differences in return levels for the conditional and unconditional plots highlight the potential for under-designing infrastructure if conditional dependencies are not taken into account. This figure shows that the neighboring region of the location i would likely be under-designed if considering only the unconditional extremes. In particular, it is extremely common for infrastructure and engineered systems to fail in multiple places during a single extreme event, because of the substantial conditional storm-level dependencies associated with extremes. Conditional probabilities are not just an issue in spatial extreme rainfall; they can also be found in a wider range of extreme events, such as extreme rainfall together with storm surge in coastal areas (Zheng et al., 2014; Zheng et al., 2013). To ensure that critical emergency infrastructure does not fail during a hazardous event, it is necessary to use much higher return levels than if one is merely designing to the marginal distribution of key decision variables such as rainfall or floods.

2.5. Conclusions

With increasing exposure of the built environment to floods, improving frameworks used to model extreme rainfall is an active and important domain of research. Conditional estimates of extremes such as those described in this paper are useful for the design of complex civil engineering systems, such as road and rail networks, as well as for emergency evacuation planning. Such estimates need to account for the dependence between extreme rainfall not only in space, but also across different durations.

This challenge has been addressed here by exploring the ability to link the max-stable process of extreme rainfall across multiple durations using the reparameterization of Koutsoyiannis et al. (1998). Subdaily rainfall from 25 sites, having at least 19 years of record, were taken from the Hawkesbury-Nepean catchment of New South Wales, Australia. Six durations spanning from 1 to 24 h were considered. Assuming each duration is estimated separately, this would require 450 parameters (i.e. 25 sites × 6 durations × 3 parameters) in order to represent the marginal distributions at all locations. Due to the linking of durations, the number of parameters needed to estimate the marginal distribution is significantly lower than if independent estimates of the GEV distribution were made (125 parameters, i.e. 25 sites × 5 parameters) followed by spatial interpolation (20 parameters, i.e. 5 parameter surfaces × 4 interpolation parameters per surface). It would be possible to further reduce the number of parameters by implementing a method of jointly fitting the sites so that the 125 at-site parameters did not need to be determined prior to fitting the spatial surface. It is possible that joint fitting of the marginal and dependence components of the model may lead to different outcomes regarding the significance of the covariate terms. Two additional parameters are required for the max-stable dependence structure at a 24h duration along with one additional parameter that extends the dependence structure across durations (i.e. from 24h to shorter durations). Given the large

number of parameters across the marginal, spatial and dependence structures of the model it would be useful to further explore the uncertainty contribution of each component (Stephenson et al., 2016).

The reparameterization used in this study, to link together the extremes for multiple durations when fitting the marginal model, works well for the locations analyzed. The proposed adjustment for the variograms helps the max-stable process capture the spatial dependence of rainfall extremes across different durations. A key reason for this proposed method is that it accounts for the dependence between durations, which arises because in some situations long-duration extreme rainfall events will have shorter-duration extremes embedded inside them, but in other situations the extremes at different durations will occur at different times. This is addressed by the pairwise extremal coefficient, which shows complete dependence at a distance of zero for the 24–24 h duration, but shows lesser dependence for other pairs of durations, such as the 24h extreme event and a 6h extreme event at the same location. While this paper focused on subdaily durations, application to large catchments may require durations longer than 1 day or take into account the influence of daily rainfall accumulations (Lehmann et al., 2016).

The additional complexity involved in fitting a max-stable process to rainfall extremes across different durations may not be warranted in all cases. For example, where the interest is in developing conditional estimates of rainfall in two neighboring gauges with sufficient at-site rainfall data, it may be sufficient to represent the bivariate dependence in catchment-average rainfall at the relevant critical durations of both catchments, for example using a bivariate extreme value model. However, frameworks of extremes offer numerous advantages over traditional approaches that only have point-wise estimates of extremes; for example by providing consistency between both unconditional and conditional IDF estimates. The development of spatiotemporal models of rainfall is also important for the potential to merge multiple data sources and further improve estimates of extremes, whether conditional or unconditional. For example, the use of ground-based and satellite-based remote sensed data to characterize spatial and spatio-temporal features of storms merged with daily and subdaily gauges across a region that have longer periods of observation. The proposed adjustment in this paper for pairwise distances with three additional parameters enables the model to infer the conditional estimate for any shorter duration extreme given the 24h extreme. Understanding the storm-level dependence structure of rainfall is important for achieving more realistic representations of flood-generating mechanisms and their role in flood impacts. This allows results to be presented in conditional maps that show exceedance probabilities and return levels across different durations. These maps can then be used to better communicate and account for the complex dependences associated with extreme rainfall for use in a range of planning and engineering design contexts.

Acknowledgments

The lead author was supported by the Australia Awards Scholarships (AAS) from Australia Government. A/Prof Westra was supported by ARC Discovery project DP150100411. We are grateful to the three anonymous reviewers for their detailed

constructive comments and helpful insights to improve the paper. We would like to thank Leticia Mooney (editor at the School of Civil, Environmental and Mining Engineering at Adelaide University) for her help in improving this manuscript. The extracted data set used for this study can be directly accessed here https://figshare.com/articles/Data_zip/5923789.

References

Bennett, B., M. Thyer, M. Leonard, M. Lambert, and B. Bates (2016), A comprehensive and systematic evaluation framework for a parsimonious daily rainfall field model, *Journal of Hydrology*.

Boyd, M. J., E. H. Rigby, and R. VanDrie (1996), WBNM — a computer software package for flood hydrograph studies, *Environmental Software*, *11*(1), 167-172.

Bracken, C., B. Rajagopalan, L. Cheng, W. Kleiber, and S. Gangopadhyay (2016), Spatial Bayesian hierarchical modeling of precipitation extremes over a large domain, *Water Resources Research*, *52*(8), 6643-6655.

Brown, B. M., and S. I. Resnick (1977), Extreme Values of Independent Stochastic Processes, *Journal of Applied Probability*, *14*(4), 732-739.

Chow, V. T., D. R. Maidment, and L. W. Mays (1988), *Applied Hydrology*, McGraw-Hill, c1988, New York.

Cooley, D., P. Naveau, and P. Poncet (2006), Variograms for spatial max-stable random fields, in *Dependence in Probability and Statistics*, edited by P. Bertail, P. Soulier and P. Doukhan, pp. 373-390, Springer New York, New York, NY.

Cooley, D., D. Nychka, and P. Naveau (2007), Bayesian Spatial Modeling of Extreme Precipitation Return Levels, *Journal of the American Statistical Association*, *102*(479), 824-840.

Davison, A. C., and M. M. Gholamrezaee (2012), Geostatistics of extremes, *Proceedings of the Royal Society A: Mathematical, Physical and Engineering Science*, *468*(2138), 581-608.

Davison, A. C., S. A. Padoan, and M. Ribatet (2012), Statistical Modeling of Spatial Extremes, *Statistical Science*, 161-186.

de Haan, L. (1984), A Spectral Representation for Max-stable Processes, *The Annals of Probability*, *12*(4), 1194-1204.

de Haan, L., and A. Ferreira (2006), *Extreme Value Theory An Introduction*, Springer New York.

Genton, M. G., S. A. Padoan, and H. Sang (2015), Multivariate max-stable spatial processes, *Biometrika*, *102*(1), 215-230.

Huser, R., and A. C. Davison (2014), Space–time modelling of extreme events, *Journal of the Royal Statistical Society: Series B (Statistical Methodology)*, *76*(2), 439-461.

Kabluchko, Z., M. Schlather, and L. de Haan (2009), Stationary Max-Stable Fields Associated to Negative Definite Functions, *The Annals of Probability*, *37*(5), 2042-2065.

Koutsoyiannis, D., D. Kozonis, and A. Manetas (1998), A mathematical framework for studying rainfall intensity-duration-frequency relationships, *Journal of Hydrology*, *206*(1–2), 118-135.

Laurenson, E. M., and R. G. Mein (1997), *RORB Version 4 Runoff Routing Program User Manual*, Monash University Department of Civil Engineering.

Lehmann, E. A., A. Phatak, A. Stephenson, and R. Lau (2016), Spatial modelling framework for the characterisation of rainfall extremes at different durations and under climate change, *Environmetrics*, *27*(4), 239-251.

Mulvaney, T. J. (1851), On the use of self-registering rain and flood gauges in making observation of the relation of rainfall and floods discharges in a given catchment, *Proc. Civ. Eng. Ireland*, *4*, 18–31.

Oesting, M., M. Schlather, and P. Friederichs (2017), Statistical post-processing of forecasts for extremes using bivariate Brown-Resnick processes with an application to wind gusts, *Extremes*, *20*(2), 309-332.

Opper ESM, S., P. Cinque OAM, and B. Davies (2010), Timeline modelling of flood evacuation operations, *1st Conference on Evacuation Modeling and Management, Procedia Engineering*, *3*, 175-187.

Padoan, S. A., M. Ribatet, and S. A. Sisson (2010), Likelihood-Based Inference for Max-Stable Processes, *Journal of the American Statistical Association*, *105*(489), 263-277.

Renard, B. (2011), A Bayesian hierarchical approach to regional frequency analysis, *Water Resources Research*, *47*(11), W11513.

Renard, B., and M. Lang (2007), Use of a Gaussian copula for multivariate extreme value analysis: Some case studies in hydrology, *Advances in Water Resources*, *30*(4), 897-912.

Ribbons, S. (2015), Hawkesbury-nepean valley flood management review - developing a strategy where flood depth can be nine metres above flood planning level, in *2015 Floodplain Management Association National Conference*, edited, Australia.

Schlather, M., and J. A. Tawn (2003), A Dependence Measure for Multivariate and Spatial Extreme Values: Properties and Inference, *Biometrika*, *90*(1), 139-156.

Smith, R. L. (1990), Max-stable processes and spatial extremes, edited, Unpublished manuscript.

Stephenson, A. G., E. A. Lehmann, and A. Phatak (2016), A max-stable process model for rainfall extremes at different accumulation durations, *Weather and Climate Extremes*, *13*(Supplement C), 44-53.

Thibaud, E., R. Mutzner, and A. C. Davison (2013), Threshold modeling of extreme spatial rainfall, *Water Resources Research*, *49*(8), 4633-4644.

Westra, S., and S. A. Sisson (2011), Detection of non-stationarity in precipitation extremes using a max-stable process model, *Journal of Hydrology*, *406*(1–2), 119-128.

Zheng, F., S. Westra, and S. A. Sisson (2013), Quantifying the dependence between extreme rainfall and storm surge in the coastal zone, *Journal of Hydrology*, *505*, 172-187.

Zheng, F., S. Westra, and M. Leonard (2015), Opposing local precipitation extremes, *Nature Clim. Change*, *5*(5), 389-390.

Zheng, F., S. Westra, M. Leonard, and S. A. Sisson (2014), Modeling dependence between extreme rainfall and storm surge to estimate coastal flooding risk, Water Resources Research, 50(3), 2050-2071.

Supplementary material

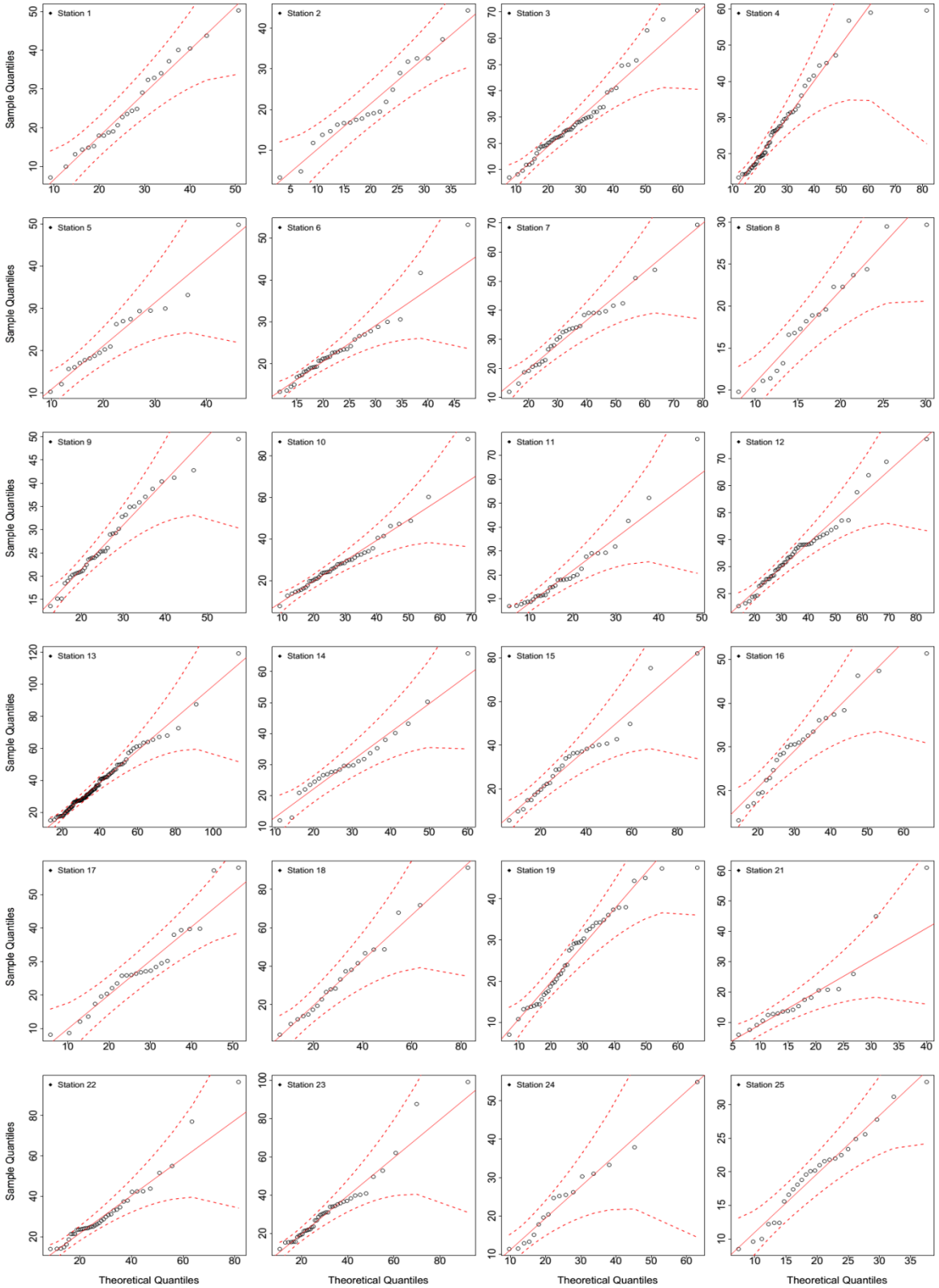

Figure S2.1. QQ plots for the marginal model based on the re-parameterization approach to fit GEV for 1h rainfall extremes for all stations. The solid diagonal line indicates a perfect fit, and the dotted lines indicate a 95% confidence interval.

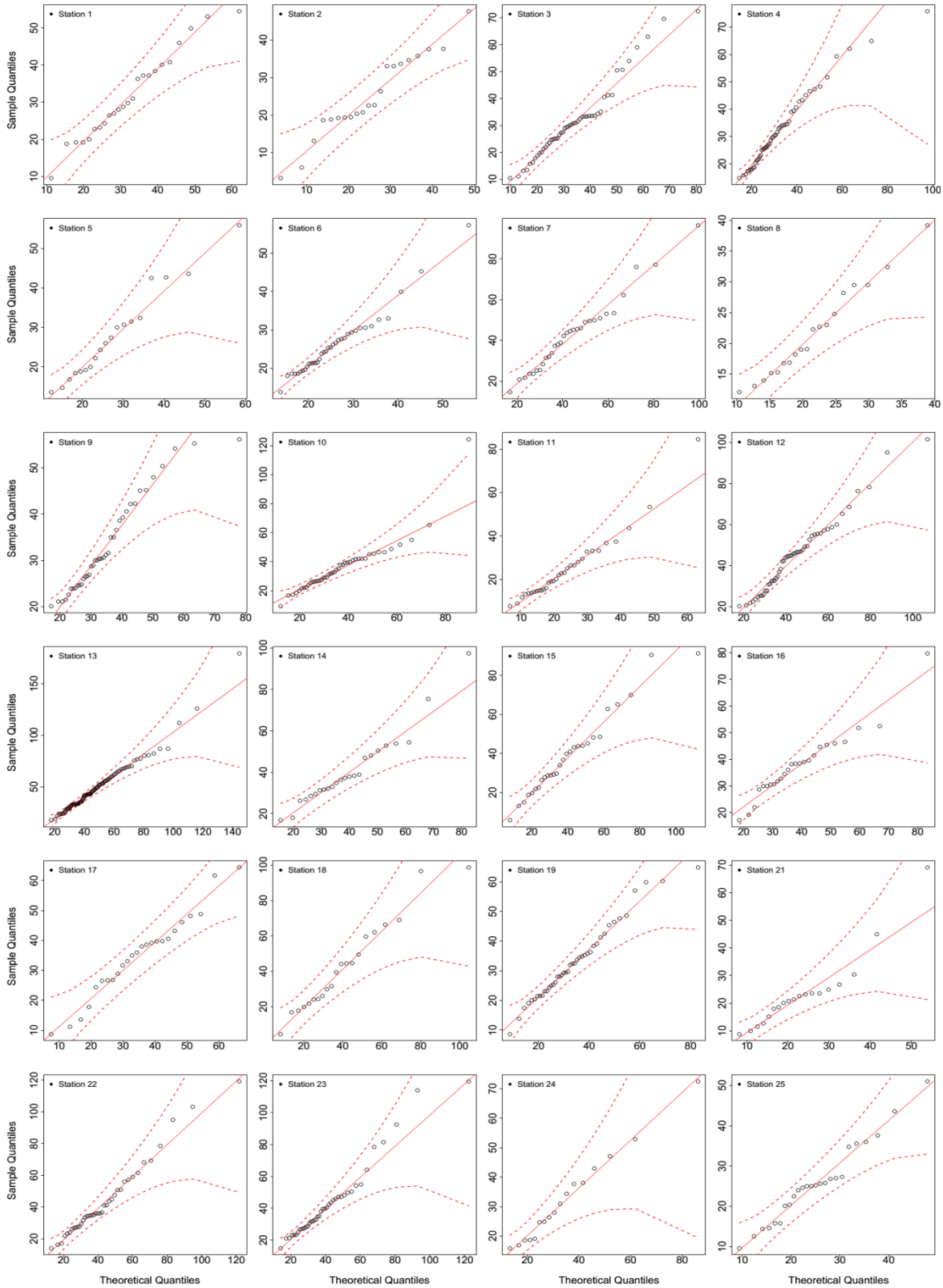

Figure S2.2. QQ plots for the marginal model based on the re-parameterization approach to fit GEV for 2h rainfall extremes for all stations. The solid diagonal line indicates a perfect fit, and the dotted lines indicate a 95% confidence interval.

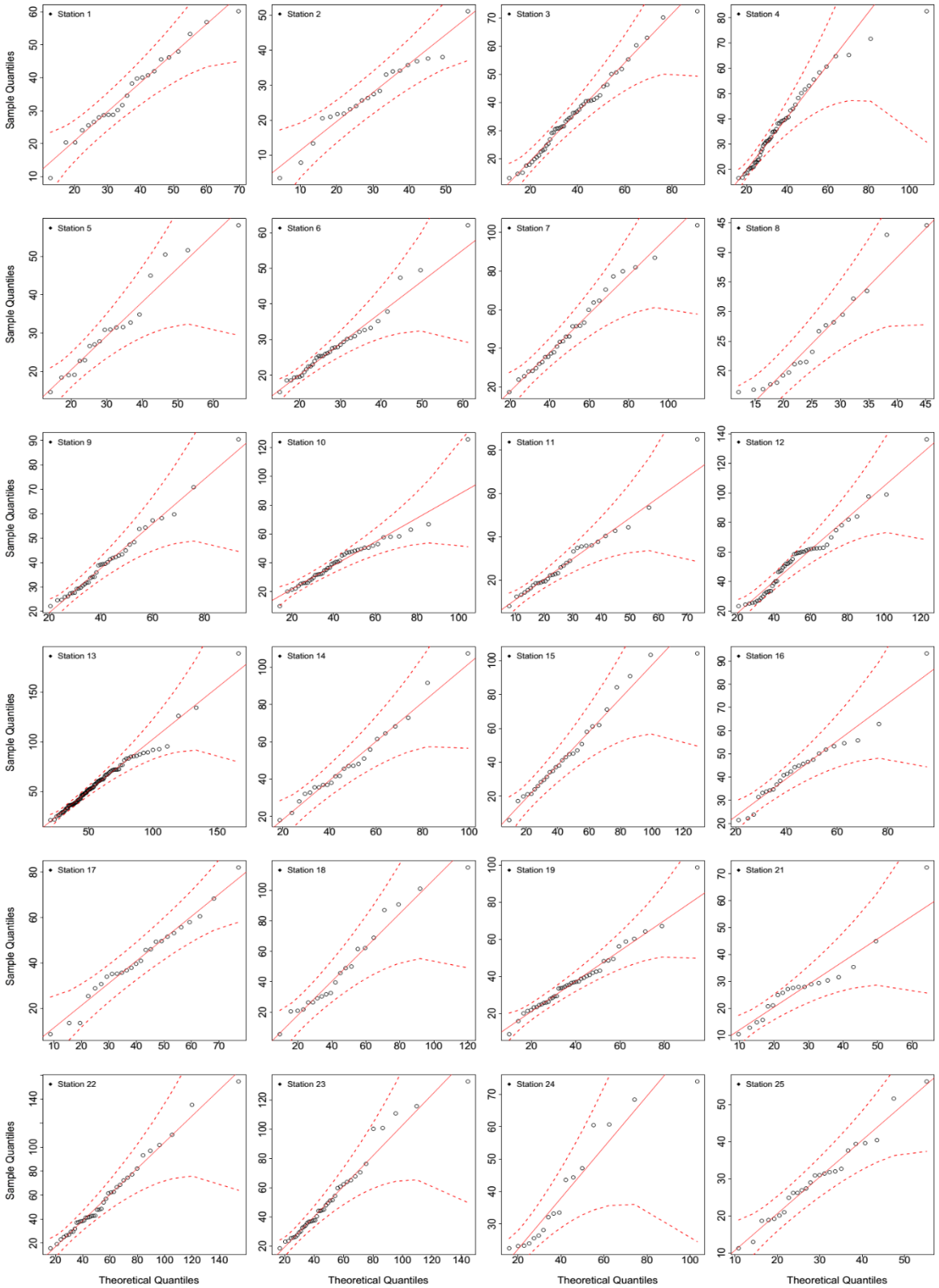

Figure S2.3. QQ plots for the marginal model based on the re-parameterization approach to fit GEV for 3h rainfall extremes for all stations. The solid diagonal line indicates a perfect fit, and the dotted lines indicate a 95% confidence interval.

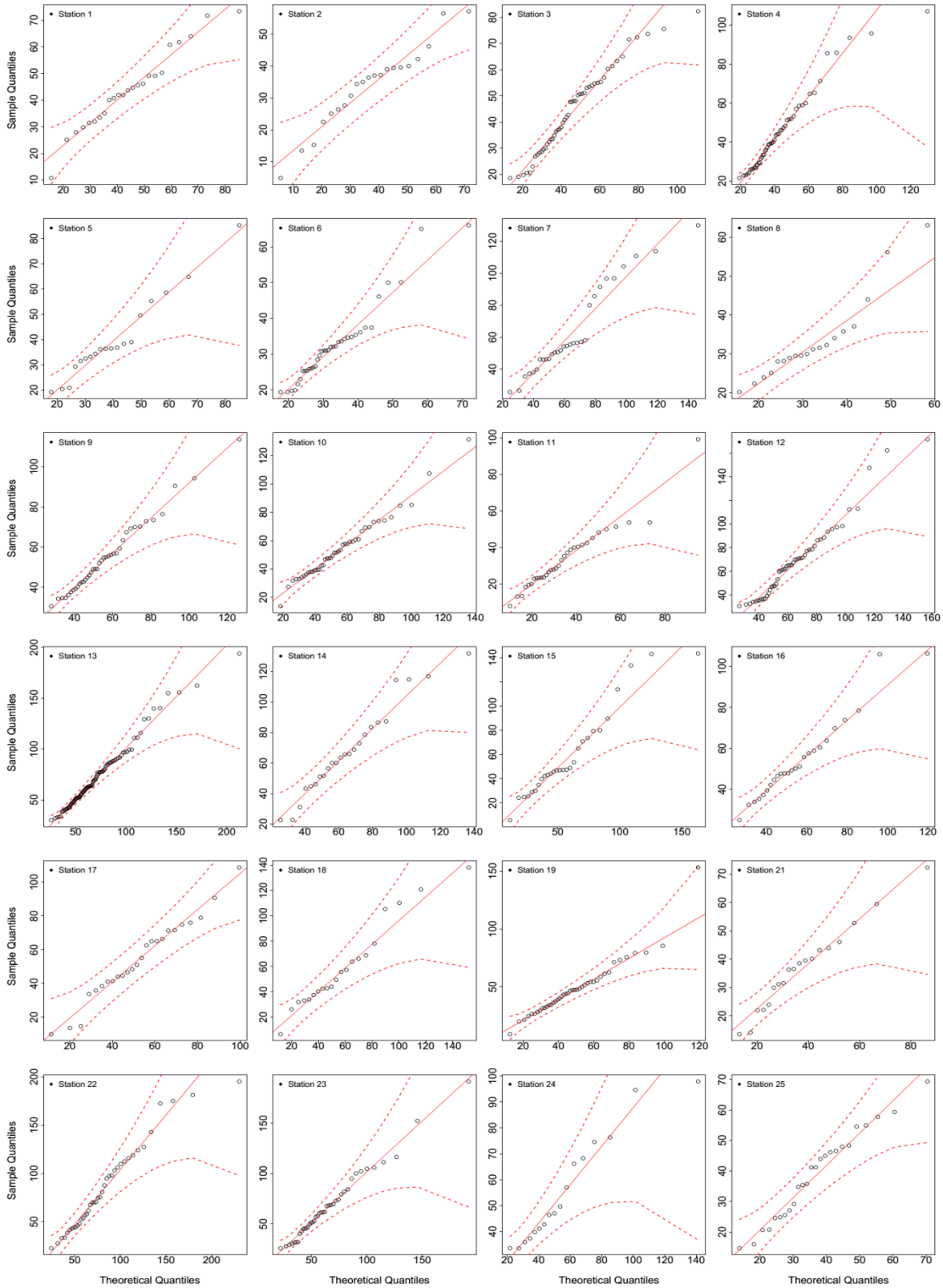

Figure S2.4. QQ plots for the marginal model based on the re-parameterization approach to fit GEV for 6h rainfall extremes for all stations. The solid diagonal line indicates a perfect fit, and the dotted lines indicate a 95% confidence interval.

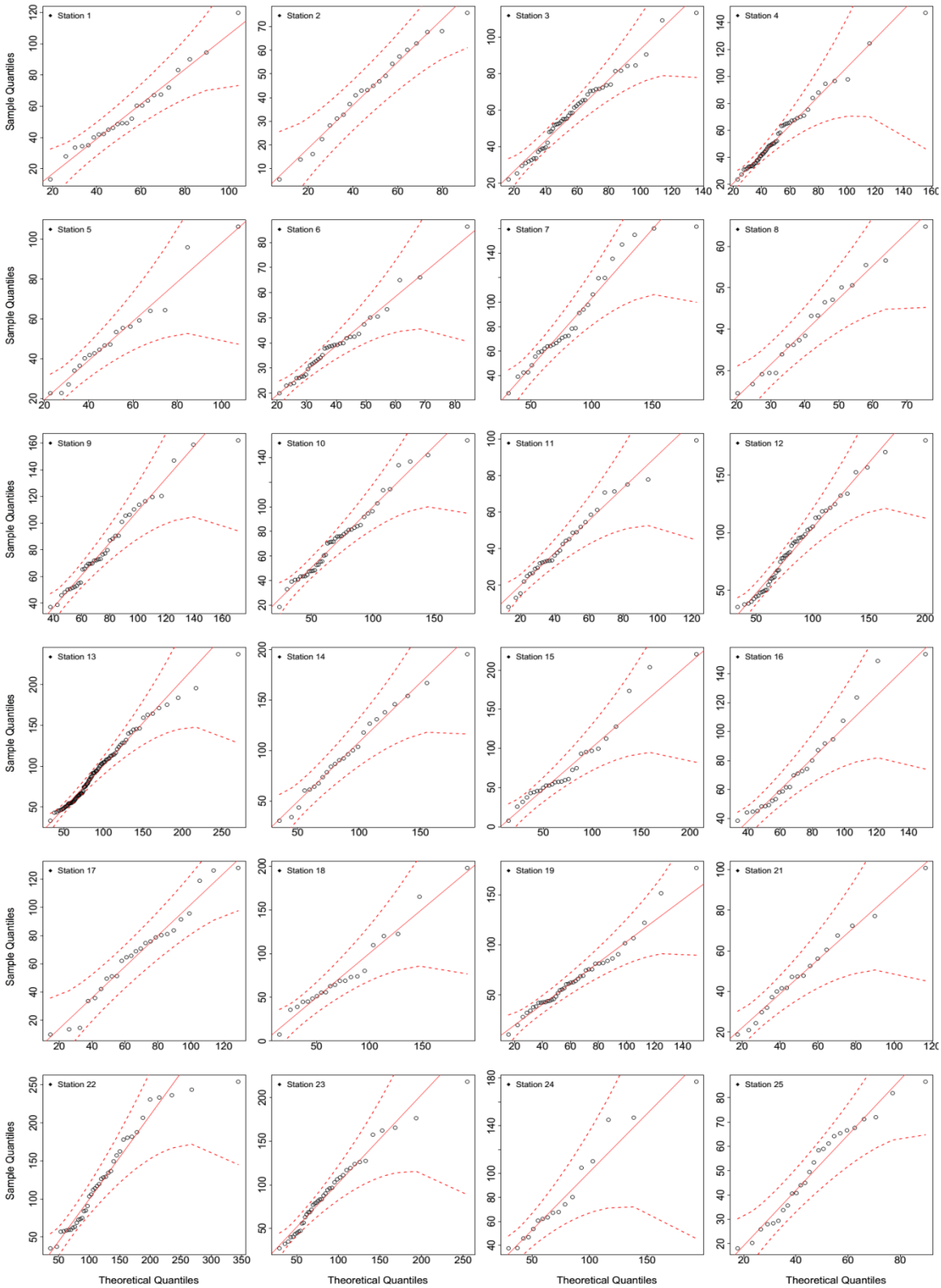

Figure S2.5. QQ plots for the marginal model based on the re-parameterization approach to fit GEV for 12h rainfall extremes for all stations. The solid diagonal line indicates a perfect fit, and the dotted lines indicate a 95% confidence interval.

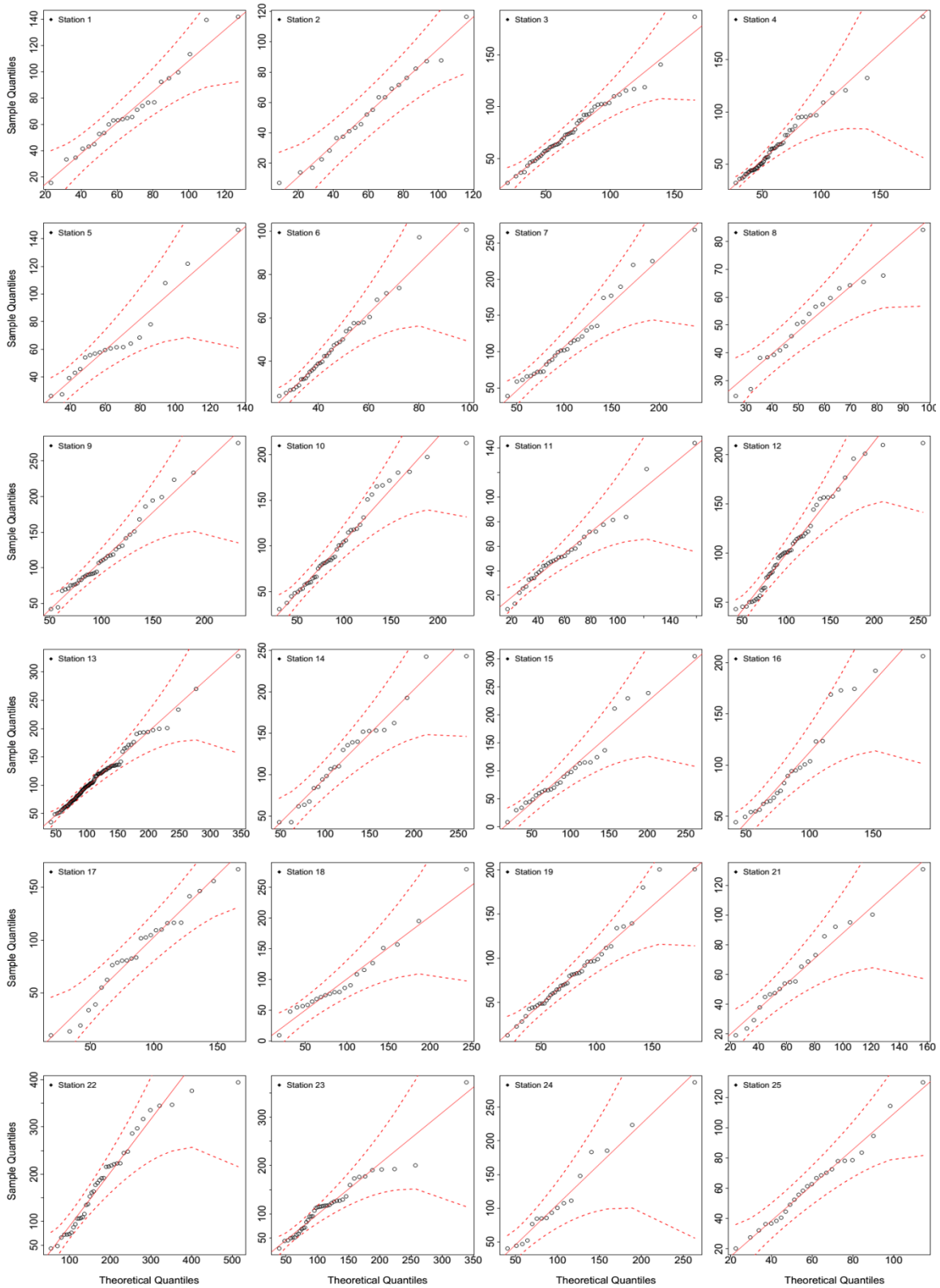

Figure S2.6. QQ plots for the marginal model based on the re-parameterization approach to fit GEV for 24h rainfall extremes for all stations. The solid diagonal line indicates a perfect fit, and the dotted lines indicate a 95% confidence interval.

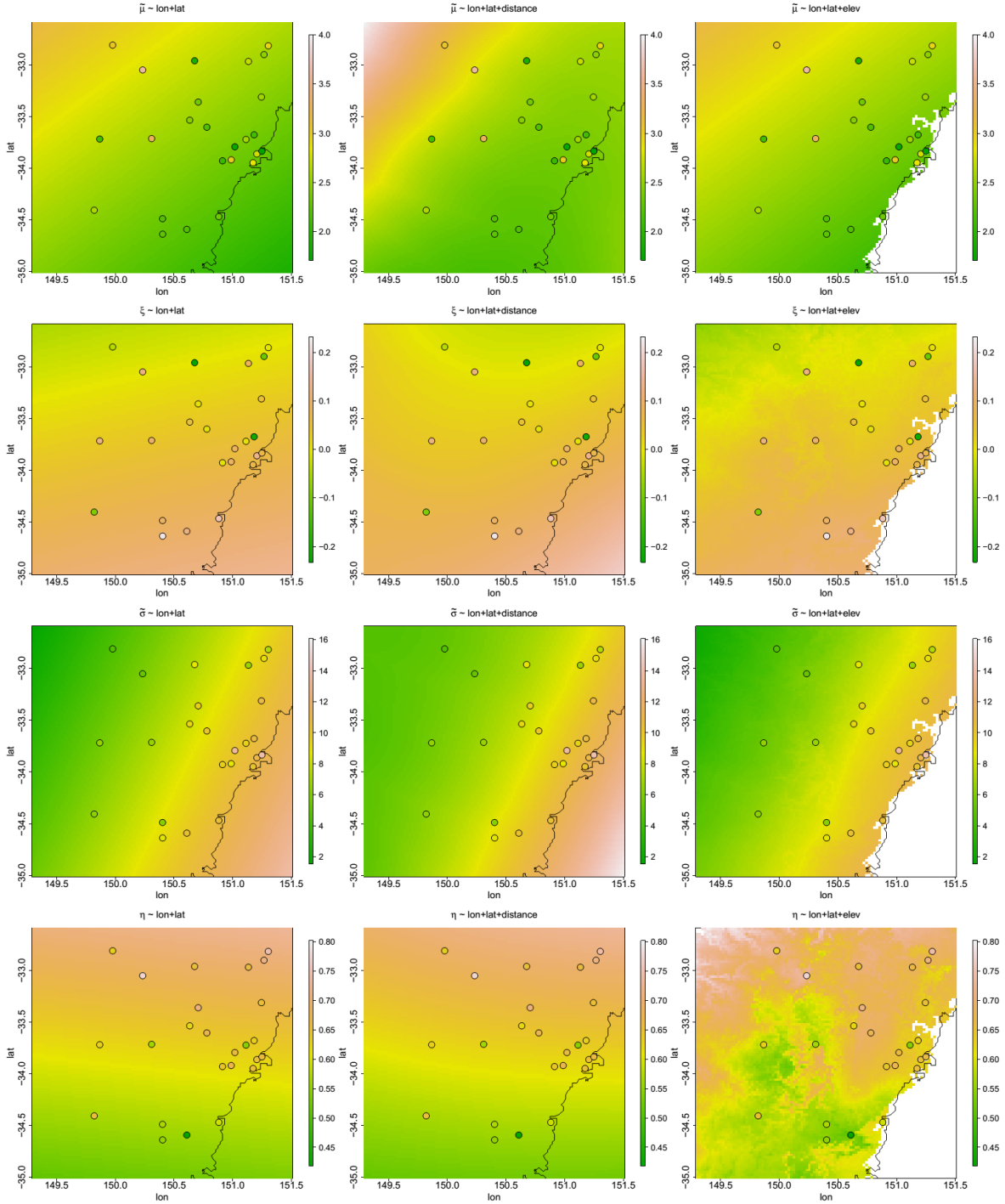

Figure S2.7. Comparison of spatial regression models: left column par~lat+lon, middle column par~lat+lon+distance-to-coast, right column par~lat+lon+elevation.

Chapter 3

Dependence Properties of Spatial Rainfall Extremes and Areal Reduction Factors (Paper 2)

Phuong Dong Le, Anthony C. Davison, Sebastian Engelke, Michael Leonard, Seth Westra

Journal of Hydrology, Volume 565, October 2018, Pages 711-719

https://doi.org/10.1016/j.jhydrol.2018.08.061

Statement of Authorship

Title of Paper	Dependence properties of spatial rainfall extremes and areal reduction factors
Publication Status	☐ Published ☐ Accepted for Publication ☑ Submitted for Publication ☐ Unpublished and Unsubmitted work written in manuscript style
Publication Details	Le, P.D., Davison, A.C., Engelke, S., Leonard, M., Westra, S., 2018. Dependence properties of spatial rainfall extremes and areal reduction factors. Journal of Hydrology, (submitted).

Principal Author

Name of Principal Author (Candidate)	Phuong Dong Le
Contribution to the Paper	Implementation and development of approach, visualisation and interpretation of results, preparation of manuscript, preparation of response to reviewers and acted as corresponding author.
Overall percentage (%)	70
Certification:	This paper reports on original research I conducted during the period of my Higher Degree by Research candidature and is not subject to any obligations or contractual agreements with a third party that would constrain its inclusion in this thesis. I am the primary author of this paper.
Signature	Date 16/07/2018

Co-Author Contributions

By signing the Statement of Authorship, each author certifies that:

i. the candidate's stated contribution to the publication is accurate (as detailed above);

ii. permission is granted for the candidate in include the publication in the thesis; and

iii. the sum of all co-author contributions is equal to 100% less the candidate's stated contribution.

Name of Co-Author	Anthony C. Davison
Contribution to the Paper	Supervised research, helped to evaluate and edit the manuscript.
Signature	Date 16/7/2018

Name of Co-Author	Sebastian Engelke
Contribution to the Paper	Supervised research, helped to evaluate and edit the manuscript.
Signature	Date 18/7/2018

Name of Co-Author	Michael Leonard		
Contribution to the Paper	Supervised research, helped to evaluate and edit the manuscript.		
Signature		Date	16/7/18

Name of Co-Author	Seth Westra		
Contribution to the Paper	Supervised research, helped to evaluate and edit the manuscript.		
Signature		Date	16-07-2018

Please cut and paste additional co-author panels here as required.

Abstract

Areal reduction factors (ARFs) transform an estimate of extreme rainfall at a point to an estimate of extreme rainfall over a spatial domain, and are commonly used in flood risk estimation. For applications such as the design of large infrastructure, dam safety and land use planning, ARFs are needed to estimate flood risk for very rare events that are often larger than the biggest historical events. The nature of the relationship between ARFs and frequency for long return periods is unclear as it depends on the asymptotic dependence structure of rainfall over a region, i.e., the extent to which rainfall from a surrounding region is extreme as rainfall at a point becomes more extreme. Miscalculating this for very rare events could lead to poor design of infrastructure. To investigate this, spatial rainfall processes are simulated using asymptotically dependent and independent models, and the implications for ARFs of the asymptotic assumptions are explored in a synthetic study. The models are then applied to a case study in Victoria, Australia, using 88 daily rainfall gauges with 50 years of data. The analysis shows that the observed data follow the behaviour of an asymptotically independent process, leading to ARFs that decrease with increasing return period. The study demonstrates that the use of inverted max-stable process models to simulate ARFs can provide a rigorous alternative to empirical approaches, particularly for long return periods requiring significant extrapolation from the data.

3.1. Introduction

Areal reduction factors (ARFs) are commonly employed to convert point-based estimates of extreme rainfall—usually in the form of intensity-frequency-duration (IFD) relationships—to a catchment-wide rainfall intensity of equivalent exceedance probability (Ball et al., 2016). ARFs account for the spatial dependence of rainfall, and generally have a value of unity for very small catchment areas (where catchment-average rainfall is almost equivalent to point rainfall) and decrease as the area increases. In addition to understanding how ARFs scale with area, it is important to understand how they scale with the exceedance probability of the extreme rainfall event, especially for very rare but high-consequence events for which observations are scarce. The scaling of ARFs with geographic area and frequency is often provided as part of engineering design guidance (Ball et al., 2016), and when combined with IFD maps can be used as an input to flood models.

Approaches to estimating ARFs can be classified as empirical or analytic. Empirical methods describe the observed relationship between distributions of point rainfall extremes and areal extremes for a range of frequencies and areal extents. They assume homogeneity of the distribution after rescaling for all points in a region, but make no parametric assumptions on the dependence structure of the rainfall process (Svensson and Jones, 2010). The implementation depends on whether the method is storm-centred or fixed-area. In the storm-centred approach, the areal extent is not fixed and the central location, the point having maximum rainfall, changes with each storm. The ARF is then calculated based on the concurrent maximal point and areal estimates of rainfall. This approach is difficult to implement for multi-centre storms, and has not seen widespread application (Asquith and Famiglietti, 2000). In contrast, the fixed-area approach (Myers, 1980; Omolayo, 1993; Shaw et al., 2011; Siriwardena and Weinmann, 1996) takes an area, such as a catchment, and constructs the ratio of areal average rainfall and point rainfall at a representative location, with both extremes having the same exceedance probability; the point and the area extremes may not come from the same event. The storm-centred approach is sometimes used with Probable Maximum Precipitation storms, whereas the fixed-area approach is used widely in design methods that by construction preserve a specified event frequency, such as the design of drainage systems and hydraulic structures for flood control (Srikanthan, 1995).

Unlike empirical methods, analytic methods are based on statistical models for the spatial dependence of rainfall over a region (Svensson and Jones, 2010). An early method used the pairwise correlation between gauges (Rodriguez-Iturbe and Mejía, 1974), assuming various decaying isotropic correlation functions (e.g., exponential, Bessel), and a Gaussian process for areal average rainfall. Another early method involves consideration of partial coverage of catchments, where an analytic representation of a storm having specified extent and speed is assumed to cross over the catchment (Bengtsson and Niemczynowicz, 1986). More elaborate statistical models have been used as the basis of ARFs to better reflect the properties of spatial rainfall, including Poisson-distributed threshold exceedances (Bacchi and Ranzi, 1996), multi-fractal models that use a scale-invariance

assumption (Veneziano and Langousis, 2005), and max-stable models (Buishand et al., 2008).

Whether empirical or analytical approaches are used to estimate ARFs, a key question is how ARFs scale with rainfall frequency or what is the asymptotic behaviour of ARFs? where the term "asymptotic" indicates limiting properties as events become increasingly rare. Several papers, using a variety of methods, suggest that ARFs decrease with rarer events. They include (i) a fixed-area empirical approach applied to a 46-year dataset (Allen and DeGaetano, 2005); (ii) an annual-maxima centred empirical approach applied to 9-year and 24-year datasets (Asquith and Famiglietti, 2000); and (iii) an analytical approach based on an assumed spatial correlation structure of rainfall estimated from a 4-year dataset (Sivapalan and Blöschl, 1998). However, a detailed analysis of the tail dependence of spatial rainfall extremes, which would assist in understanding the asymptotic behaviour of ARFs, is still lacking. This is particularly critical when extrapolating to rare events, given that data availability is typically on the order of several decades but interest often focuses on longer return periods (e.g., 100 or 1000 years).

Tail dependence behaviour for extremes can be classified as asymptotically dependent or asymptotically independent, and both can occur in spatial extremes (Davison et al., 2013; Thibaud et al., 2013; Wadsworth and Tawn, 2012). For asymptotically dependent models, the level of dependence stabilizes with increasing return period, indicating that the "areal coefficient" or "reduction factor", which is equivalent to ARFs in hydrology, should theoretically be stable above certain high levels (Coles and Tawn, 1996; Engelke et al., 2017; Ferreira et al., 2012). Some papers have used an asymptotically dependent model (e.g., a max-stable process) to simulate spatial extreme rainfall (Nicolet et al., 2017; Padoan et al., 2010; Westra and Sisson, 2011). However, Thibaud et al. (2013) suggest that extreme rainfall may be asymptotically independent, although their study concerned a mountain catchment with only 575 days of record with 58% missing data, making it difficult to assess whether their tentative conclusion can be generalized. For asymptotically independent models (Wadsworth and Tawn, 2012), the level of dependence declines with increasing return period, and intuitively, the corresponding ARFs should decrease. In order to select models suitable for spatial dependence of extreme rainfall and use them to calculate ARFs for rare events, it is thus critical to confirm whether rainfall is asymptotically dependent or independent.

To directly explore the relationship between the ARFs and return period, we perform a simulation study to investigate tail dependence, followed by a real case study. To simulate the rainfall process, models of both asymptotically dependent and independent spatial extremes are introduced and used with the fixed-area method to estimate ARFs (Section 3.2). Section 3.3 describes the data used and the case study, which shows how these assumptions change the ARFs with return period (Section 3.4.1). A diagnostic procedure is used to indicate whether the observed rainfall data are asymptotically dependent or independent, before fitting the models and simulating the rainfall process for the case study (Section 3.4.2.1). The modelled ARFs, together with the diagnostic results and the fitted results, help to determine the asymptotic dependence structure of the observed rainfall,

which then suggests the likely behaviour of ARFs for long return periods (Section 3.4.2.2). Our results and their potential implications are discussed in Section 3.5.

3.2. Methodology

3.2.1. Modelling for rainfall extremes at a single location

For reasons of mathematical simplicity, models for spatial extremes have unit Fréchet marginal distributions, but this is not the case for real rainfall data, so marginal modelling is needed so that data simulated on the unit Fréchet scale can be transformed to the rainfall scale. This study considers the behaviour of extremes that exceed a high threshold u. For large u, the distribution of Y conditional on $Y > u$ may be approximated by the generalized Pareto distribution (GPD) (Davison and Smith, 1990; Pickands, 1975; Thibaud et al., 2013), which has distribution function

$$G(y) = 1 - \left(1 + \frac{\xi(y-u)}{\sigma_u}\right)^{-1/\xi}, \quad y > u, \tag{3.1}$$

defined on $\{y: 1 + \xi(y-u)/\sigma_u > 0\}$ where $\sigma_u > 0$ and $-\infty < \xi < +\infty$ are scale and shape parameters, respectively. The probability that a level y is exceeded is then $\Phi_u\{1 - G(y)\}$, where $\Phi_u = \Pr(Y > u)$.

The selection of the appropriate threshold u involves a trade-off between bias and variance. Too low a threshold will lead to bias due to a poor GPD approximation, whereas too high a threshold will lead to high variance due to a small number of excesses. Two approaches commonly used to determine the appropriate threshold u are the mean residual life and parameter estimate plots (Coles, 2001; Davison and Smith, 1990), which rely on a stability property: if a GPD is valid for all excesses above u, then those of any threshold greater than u should also follow a GPD.

3.2.2. Dependence modelling for spatial rainfall extremes

Consider a spatial domain X, with a stationary stochastic process $\{Y(x): x \in X \subset R^2\}$ that represents spatial rainfall. We say that $Y(x)$ is asymptotically dependent if $\lim_{y\to\infty} P\{Y(x_1) > y | Y(x_2) > y\} > 0$ for all x_1, x_2; the dependence structure stabilizes at high thresholds. On the other hand, if $\lim_{y\to\infty} P\{Y(x_1) > y | Y(x_2) > y\} = 0$ for all $x_1 \neq x_2$, then we say that $Y(x)$ is asymptotically independent: its dependence structure becomes weaker when the threshold increases, so that the spatial extent of an extreme event can be expected to diminish as its rarity increases.

Max-stable processes are the non-degenerate limits for linearly rescaled maxima of random processes and are asymptotically dependent. In simplified terms, as the maxima become more extreme, their distribution retains the same shape after linear rescaling, as represented in Eq. (3.2). Suppose that $Y_k(x), x \in X \subset R^2$ $(k = 1, \ldots, m)$ represent m independent realisations of a continuous process indexed by x in a spatial domain X. If the limit

$$Z(x) = \lim_{m\to+\infty} \frac{\max_{k=1}^{m} Y_k(x) - b_m(x)}{a_m(x)} \tag{3.2}$$

exists jointly for all $x \in X \subset R^2$ and is non-degenerate for some normalising constants $a_m(x) > 0$ and $b_m(x)$ then $Z(x)$ is a max-stable process (de Haan, 1984).

As mentioned above, it is mathematically convenient to consider so-called simple max-stable processes, which have unit Fréchet margins; the marginal distributions can easily be transformed to the GPD scale. All simple max-stable processes on X may be represented in the form

$$Z(x) = \max_{i \geq 1} W_i(x)/U_i\,, \quad x \in X, \tag{3.3}$$

where the U_i are points of a unit rate Poisson process on $(0, \infty)$ and the $W_i(x)$ are independent replicas of a continuous, non-negative stochastic process $W(x)$ defined on X, with $E[W(x)] = 1$ for all $x \in X$. Eq. (3.3) can be interpreted as a rainfall-storm process in which $W_i(x)$ represent the storm shapes, and $1/U_i$ represents the magnitude at the centre of each storm.

The inverted max-stable process is an example of an asymptotically independent model (Wadsworth and Tawn, 2012). Let $Z(x)$ be a max-stable process as in Eq. (3.3), and define

$$\widetilde{\Omega}(x) = 1/Z(x) = \min_{i \geq 1} U_i/W_i\,, \quad x \in X. \tag{3.4}$$

Then $\widetilde{\Omega}$ is an asymptotically independent process with standard exponential margins. To transform $\widetilde{\Omega}$ to unit Fréchet margins, the following transformation is used:

$$\Omega(x) = -\frac{1}{\log\left(1 - e^{-\widetilde{\Omega}(x)}\right)}, \quad x \in X, \tag{3.5}$$

then $\Omega(x)$ is an asymptotically independent process with unit Fréchet margins.

From Eq. (3.3) and Eq. (3.4), different models for W give different max-stable and inverted max-stable processes. This study focuses on two popular and easily-simulated classes of max-stable processes: Brown-Resnick processes, where W is a log-Gaussian process (Asadi et al., 2015; Huser and Davison, 2013; Kabluchko et al., 2009; Oesting et al., 2017), and extremal-t processes, where W is a transformed stationary Gaussian process (Opitz, 2013). The next section will provide details of their dependence structures.

3.2.3. Fitting of dependence models

The dependence structure of the max-stable process is encapsulated by the pairwise extremal coefficient $\theta \in [1,2]$, while that of the inverted max-stable process is encapsulated by the pairwise residual tail dependence coefficient $\eta \in (0,1]$ (Ledford and Tawn, 1996).

With $Y(x)$ a continuous process, the empirical pairwise extremal coefficient θ and the empirical pairwise residual tail dependence coefficient η for each pair of locations $x_1, x_2 \in X$ are calculated using the formulae

$$\theta(x_1, x_2) = 2 - \lim_{y \to \infty} P\{Y(x_1) > y | Y(x_2) > y\} \tag{3.6}$$

and

$$\eta(x_1, x_2) = \lim_{y\to\infty} \frac{\log P\{Y(x_2) > y\}}{\log P\{Y(x_1) > y, Y(x_2) > y\}}, \tag{3.7}$$

with the probabilities replaced by their empirical counterparts for suitably high values of *y*, typically above the 0.8-quantile of the corresponding distribution. The interpretations of θ and η are:

- if $\theta < 2$, then $Y(x_1)$ and $Y(x_2)$ are asymptotically dependent, and necessarily $\eta = 1$. In this case, θ indicates the level of extremal dependence between $Y(x_1)$ and $Y(x_2)$;
- if $\theta = 2$, then $Y(x_1)$ and $Y(x_2)$ are asymptotically independent, and $\eta \leq 1$ indicates the level of extremal dependence between $Y(x_1)$ and $Y(x_2)$ (Coles et al., 1999), with lower values indicating lower dependence.

To estimate the dependence structure of the max-stable and inverted max-stable models, the theoretical extremal coefficient and residual tail dependence coefficient functions are usually fitted to their empirical counterparts. If the process is stationary and isotropic then they depend only on the Euclidean distance $h = \|x_1 - x_2\|$ between two locations. The theoretical extremal coefficient function for the extremal-t model is

$$\theta(h) = 2T_{\alpha+1}\left(\sqrt{\frac{(\alpha+1)\big(1-\rho(h)\big)}{1+\rho(h)}}\right), \tag{3.8}$$

where $T_{\alpha+1}(.)$ is a standard univariate Student-t CDF with $\alpha + 1$ degrees of freedom and $\rho(h)$ is the correlation function of the stationary Gaussian process used to construct the extremal-t process. For this analysis, the powered exponential correlation

$$\rho(h) = \exp\left[-\left(\frac{h}{c}\right)^{\nu}\right], \quad c > 0, 0 < \nu \leq 2, \tag{3.9}$$

is used. The theoretical extremal coefficient function for the Brown-Resnick model is

$$\theta(h) = 2\Phi\left(\sqrt{\frac{\gamma(h)}{2}}\right), \tag{3.10}$$

where Φ is the standard normal cumulative distribution function and the variogram $\gamma(h) = \|h\|^{\beta}/q$ for $q > 0$ and $\beta \in (0,2)$.

These two models are fitted to the empirical extremal coefficients by choosing parameters α, c, and ν, or parameters q and β, to minimize the sum of squared errors. A similar fitting process is used for the inverted extremal-t and inverted Brown-Resnick models. The theoretical residual tail dependence coefficient functions for the inverted extremal-t and the inverted Brown-Resnick models are

$$\eta(h) = \frac{1}{2T_{\alpha+1}\left(\sqrt{\frac{(\alpha+1)\left(1-\rho(h)\right)}{1+\rho(h)}}\right)}, \tag{3.11}$$

and

$$\eta(h) = \frac{1}{2\Phi\left(\sqrt{\frac{\gamma(h)}{2}}\right)}. \tag{3.12}$$

The dependence structures could be fitted more efficiently using likelihood methods, both for max-stable (Engelke et al., 2015; Thibaud and Opitz, 2015; Wadsworth and Tawn, 2014) and for inverted max-stable models (Wadsworth and Tawn, 2012), but here we use least squares for simplicity.

3.2.4. Estimating ARFs using the fixed-area approach

Bell's method (Siriwardena and Weinmann, 1996), a fixed-area approach to calculating ARFs, treats them as ratios of spatial rainfall to representative point rainfall at equal recurrence intervals. We use this method because it accounts for spatial rainfall patterns and has been used in recent studies (Bennett et al., 2016a; Jordan et al., 2013; Li et al., 2015). To calculate ARFs for the spatial domain X with area A, frequency F, and duration d, we write

$$ARF_{(A,F,d)} = \frac{C(A,d)_F}{R(d)_F}, \tag{3.13}$$

where $C(A,d)_F$ is the spatial rainfall depth for the catchment, and $R(d)_F$ is the representative extreme point rainfall calculated as the spatial average of the extreme point rainfall values within the catchment.

The following steps are needed to calculate ARFs using Eq. (3.13).

Step 1: Calculate spatial rainfall depth

Let R denote the set of point rainfall depths for a given duration d for all points x in a spatial domain X and all time intervals t in the data record of length Θ with time increment equal to the rainfall duration d, such that $R = \{R(x,t): x \in X, t = 1, \dots, \Theta/d\}$. For the t-th time interval, the spatial rainfall depth for a catchment is defined as

$$C_t(A,d) = \frac{1}{A}\int_X R(x,t)dx. \tag{3.14}$$

Frequency analysis is then applied to $C(A,d) = \{C_1(A,d), \dots, C_{\Theta/d}(A,d)\}$ to calculate $C(A,d)_F$.

Step 2: Estimate representative extreme point rainfall for a catchment

The representative point rainfall of a certain frequency, denoted by $R(d)_F$, is the spatial average of the extreme point rainfall values within the catchment domain,

$$R(d)_F = \frac{1}{A}\int_X R(x,d)_F dx, \tag{3.15}$$

where $R(x,d)_F$ denotes the rainfall depth corresponding to duration d for a particular location x and frequency F.

3.3. Case study and data

The case study for this paper uses a relatively densely-gauged region in Victoria, Australia (Fig. 3.1a), bounded by longitudes from 142.0 to 144.1 and latitudes from –38.7 to –36.6. Only those gauges with daily data available over a common period from 1960 to 2009 are selected. Given the length of instrumental records, it is difficult to extrapolate ARFs for long return periods, whereas simulation can achieve this for a model that provides a good match to the marginal distributions. The simulation of rainfall is performed for each site within the region (Fig. 3.1) so that the marginal distribution of each site can be directly compared to observations and so that the results are not confounded by the introduction of a spatial model. If the gauges are unrepresentative of the region then bias may be introduced into calculated statistics such as the ARF, but the region for our case study is relatively homogeneous with evenly-spaced gauges. If a reliable spatial model of rainfall extremes was available it would be possible to construct the ARF based on simulations on a regular grid or specific to a given catchment.

The source of the daily rainfall data was the Australian Bureau of Meteorology. To provide a "complete" dataset, the Bureau of Meteorology used an algorithm that used the neighbouring rainfall gauges to infill any missing data, and to disaggregate accumulated data. This study only includes the 88 gauges that had less than 20% of their data filled in.

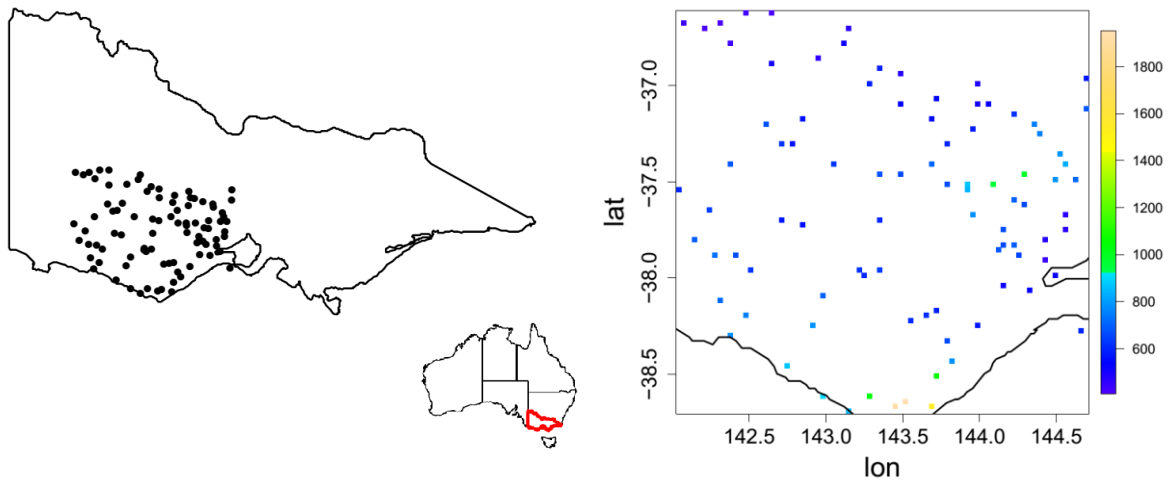

(a) **(b)**

Fig. 3.1. Map of the case study area in Victoria, Australia. (a) The black dots indicate the rainfall gauges. (b) Average annual rainfall (mm) in the period 1960-2009.

Most of the region receives between 410mm and 1200mm of rainfall per year (Fig. 3.1b). The highest rainfall is in the southernmost part of the domain, with two gauges having average annual rainfall above 1900mm. Rainfall is higher in winter and spring and lower in summer and autumn. Although the winter and spring averages are higher than in the other seasons, annual maximum daily rainfall events can occur in any season. Owing to the seasonality, only the wetter period, from May to October, is used to analyse the behaviour of ARFs.

3.4. Results

3.4.1. Effects of asymptotic dependence structures on the behaviour of ARFs with return periods

We now present a synthetic study to demonstrate how the asymptotic dependence structure affects the behaviour of ARFs for increasing return periods. To eliminate the effect of marginal variability, we used synthetic constant scale and shape parameters for all locations, comparable with those from the real data, over a synthetic study domain that is identical with that of the real case study. Sets of data with unit Fréchet margins, simulated from the Brown-Resnick and inverted Brown-Resnick models over a spatial domain were transformed to the rainfall scale using these synthetic constant marginal parameters, and then areal reduction factors were calculated based on these two sets of simulations. As the dependence properties do not depend on the marginal distributions, pairwise extremal coefficients and residual tail dependence coefficients can be calculated directly from sets of data with unit Fréchet margins. On the contrary, since the ARFs integration on the rainfall scale, they are not only affected by the dependence properties but also by the marginal distributions. Since the focus of the synthetic study is on the behaviour in terms of ARFs and the dependence measures $\theta(h)$ and $\eta(h)$, rather than on the parametric properties of the models, the two sets of simulations need not have identical parameters.

The pairwise extremal coefficients and residual tail dependence coefficients for different thresholds for each simulation are given in Fig. 3.2 and Fig. 3.3. Fig. 3.2 indicates that for

increasing thresholds the extremal coefficients for asymptotically dependent models stabilize, while the residual tail dependence coefficients increase. Fig. 3.3 shows that for increasing thresholds, the asymptotically independent model's extremal coefficients increase, while its residual tail dependence coefficients stabilize. This behaviour can be used to distinguish asymptotically dependent from asymptotically independent data.

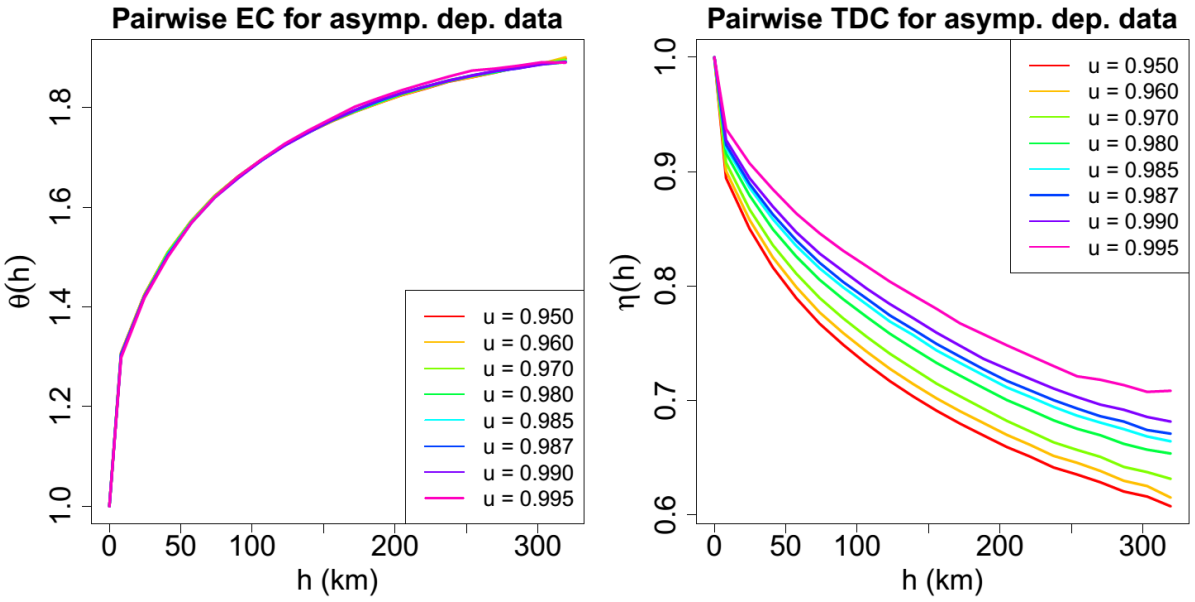

Fig. 3.2. Pairwise extremal coefficients (EC) and pairwise residual tail dependence coefficients (TDC), for thresholds corresponding to different quantiles u, calculated from data simulated from an asymptotically dependent model.

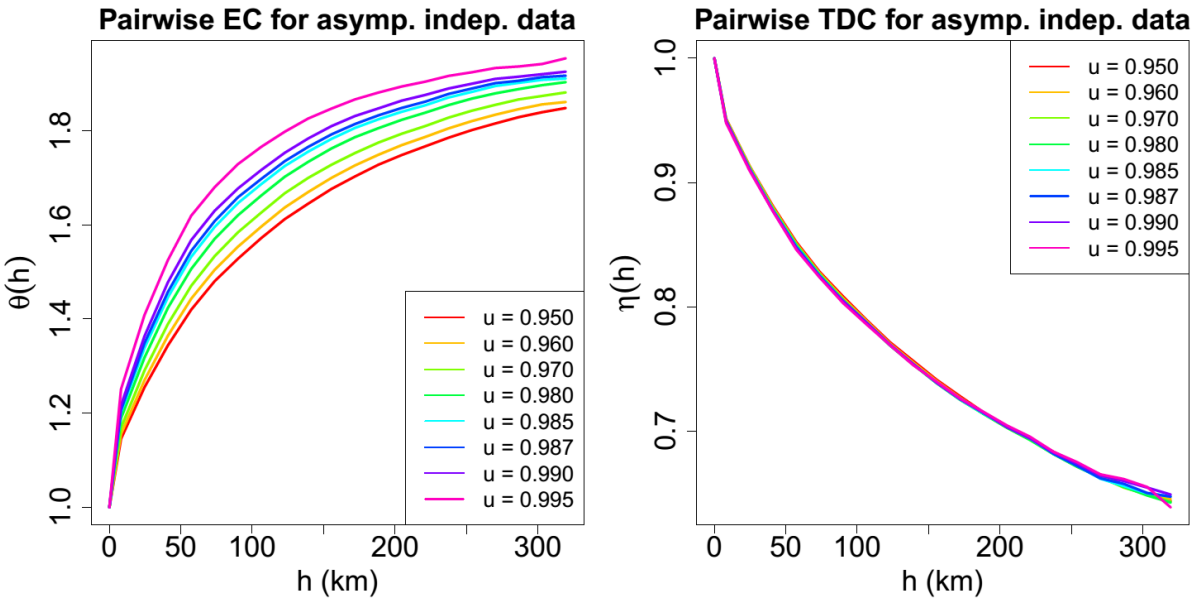

Fig. 3.3. Pairwise extremal coefficients (EC) and pairwise residual tail dependence coefficients (TDC), for thresholds corresponding to different quantiles u, calculated from data simulated from an asymptotically independent model.

Fig. 3.4 indicates how the behaviour of the corresponding ARFs depends on the return period: as the return period increases, the ARFs increase for the asymptotically dependent model and decrease for the asymptotically independent model. The ARFs from both models seem to converge at very high return periods (e.g., 500-year and 1000-year),

suggesting that ARF behaviour at shorter return periods is pre-asymptotic, though a limit is reached for long enough return periods. As the ARFs are sensitive to the asymptotic behaviour, it is important to identify the latter correctly.

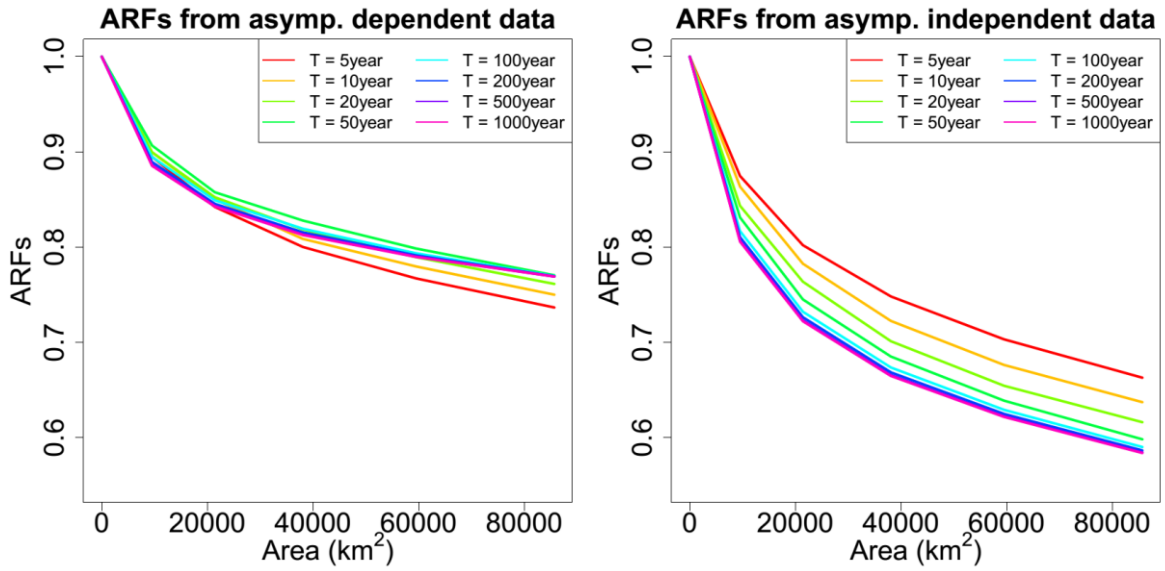

Fig. 3.4. Illustration of how the asymptotic dependence structure affects the behaviour of ARFs for different return periods. The left is for ARFs from the asymptotically dependent model, and the right is for ARFs from the asymptotically independent model.

3.4.2. Case study results

3.4.2.1. Modelling the rainfall process

To model the rainfall for the case study, we first fitted the GPD with appropriate thresholds to the observed daily rainfall data. Then the extremal-t and Brown-Resnick max-stable and inverted max-stable processes were calibrated as described above. Each daily record was treated as an independent replicate of the spatial rainfall process.

By applying standard methods (Coles, 2001) to a subset of the rain stations, thresholds at the 0.99 quantile of all daily rainfall values at each site were found to be reasonable. The marginal estimates were obtained by fitting the GPD to the excesses above the selected thresholds, with the shape parameter taken to be an unknown constant throughout the catchment, as in previous studies (Davison et al., 2012; Thibaud et al., 2013; Westra and Sisson, 2011); the GPD was fitted jointly at all stations via one likelihood function with different scale parameters. QQ plots, which can be found in the supplementary material (Fig. S3.1 to Fig. S3.4), show that the marginal estimates are reasonable.

We implemented a diagnostic procedure to assess tail dependence behaviour for the observed data, calculating the empirical pairwise extremal and residual tail dependence coefficients for a range of thresholds. For higher thresholds the extremal coefficients increase and the residual tail dependence coefficients stabilize (Fig. 3.5), so the observed data match the characteristics of the asymptotically independent data discussed in Section 3.4.1. This suggests that we use inverted max-stable models to calculate ARFs.

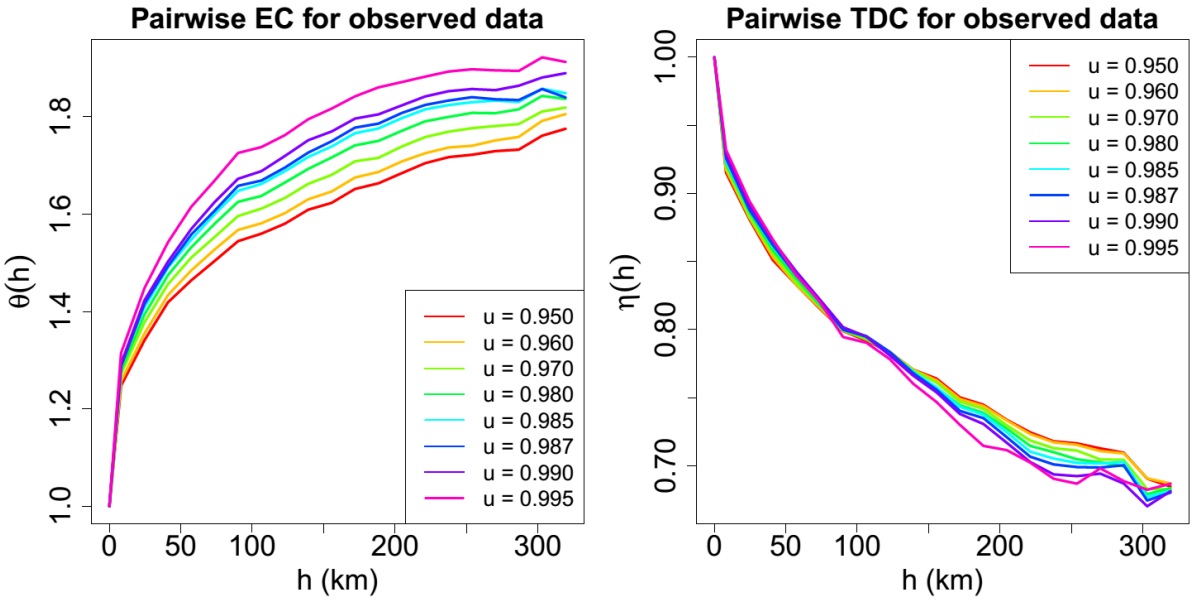

Fig. 3.5. Pairwise extremal coefficients (EC) and pairwise residual tail dependence coefficients (TDC), for thresholds corresponding to different quantiles u, calculated from observed rainfall data.

Fits of the extremal coefficient function for the max-stable processes and the residual tail dependence coefficient function for the inverted max-stable processes to their empirical counterparts are shown in Fig. 3.6 for two thresholds. Both asymptotically dependent and independent models fit the observed data well for both thresholds. The extremal and tail dependence coefficients fitted at the 0.99 threshold are also presented in the right panel of Fig. 3.6. The fitted extremal coefficient functions differ significantly for the two thresholds, but the fitted residual tail dependence coefficient functions barely change, strongly suggesting that the asymptotically dependent models cannot capture the empirical dependence structure, but that the asymptotically independent models can.

Fig. 3.6 shows generally reasonable performance for both asymptotically independent models, suggesting that both inverted Brown-Resnick and inverted extremal-t models are sufficiently flexible to match the empirical residual tail dependence coefficients, although the former appears to perform better for distances over 150 km. Both models are used to simulate the rainfall process for the case study.

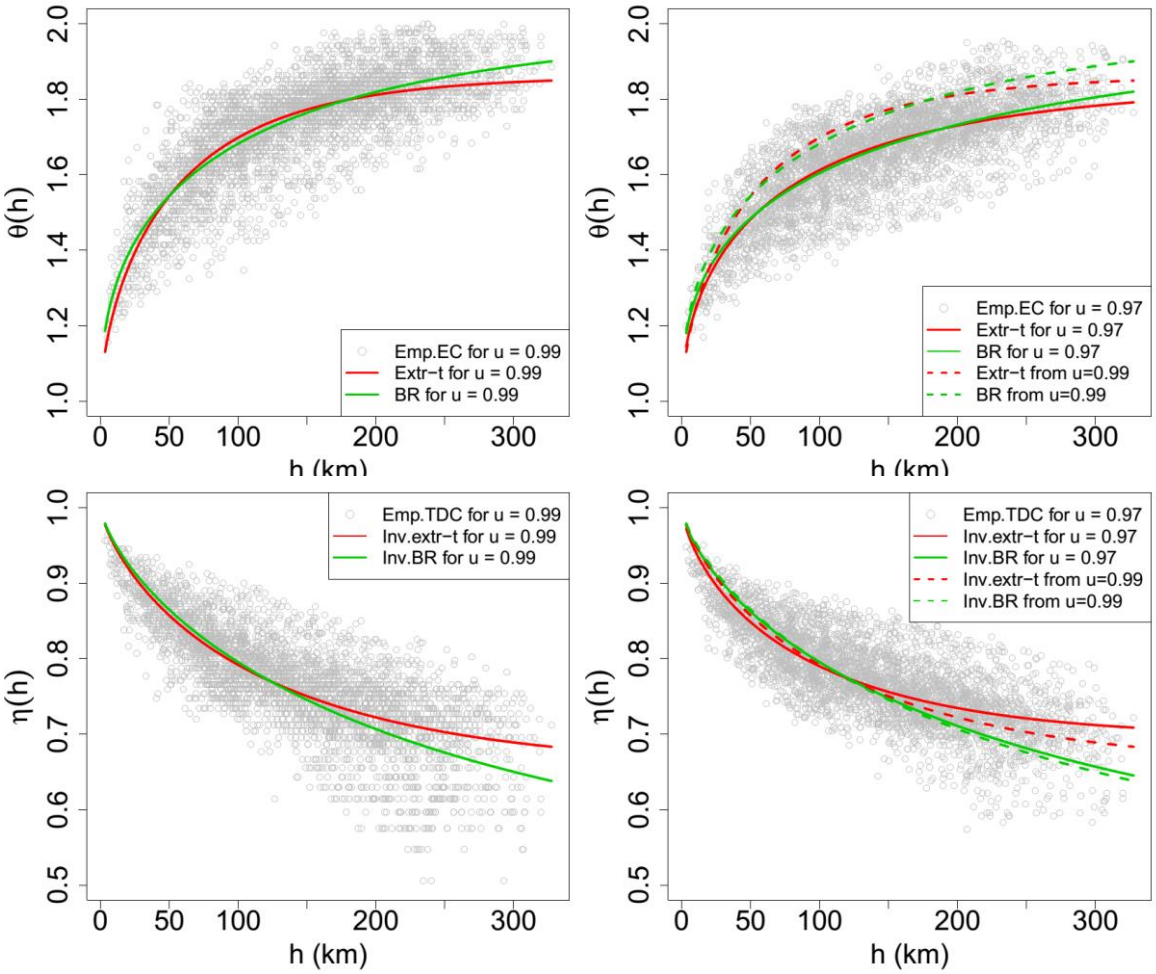

Fig. 3.6. Top panel: Empirical and fitted extremal coefficient function (EC) for the asymptotically dependent models at thresholds of 0.99 (left) and 0.97 quantiles (right). Bottom panel: Empirical and fitted residual tail dependence coefficient function (TDC) for the asymptotically independent models at thresholds of 0.99 (left) and 0.97 quantiles (right). To aid comparison, the dashed lines in the right column show the fitted results based on the 0.99 threshold from the left column.

The max-stable processes were simulated using the algorithm of Dombry et al. (2016), and the inverted max-stable processes were obtained via Eqs. (3.4) and (3.5). Spatial rainfall processes are obtained by transforming the simulations, which have unit Fréchet marginal distributions, to the scale of the original data using the distribution in Eq. (3.1) above the threshold, and the empirical distribution of the original data below it. This ensures that the simulated rainfall contains zero values (dry days), thereby mirroring the zeroes in the empirical distribution (Thibaud et al., 2013). This also forces the rainfall simulated below the threshold to have the same fitted extremal dependence structure as rainfall above the threshold, which may be inappropriate. However, the dependence structure for rainfall below the threshold contributes 'insignificantly' to extreme events (Thibaud et al., 2013), and thus is unlikely to influence our results. Moreover, the transformation ensures that the simulated marginal distributions match the observed marginal distributions below the threshold.

3.4.2.2. Comparison of analytic ARFs to empirical observations for different return periods

ARFs were calculated using both the observed data and simulated data, for different areas and different return periods. The asymptotically independent simulated data come from the inverted extremal-t and inverted Brown-Resnick models. The results, in Fig. 3.7, show that ARFs from both the inverted extremal-t and inverted Brown-Resnick models decrease when return periods increase, consistent with the observed data. For the inverted extremal-t model, the ARFs for 5- and 10-year return periods are significantly under-estimated, while those for longer return periods are closer to those for the observed data. By contrast, ARFs from the inverted Brown-Resnick model for a 5-year return period almost match that from observed data, while ARFs for longer return periods give slight overestimates.

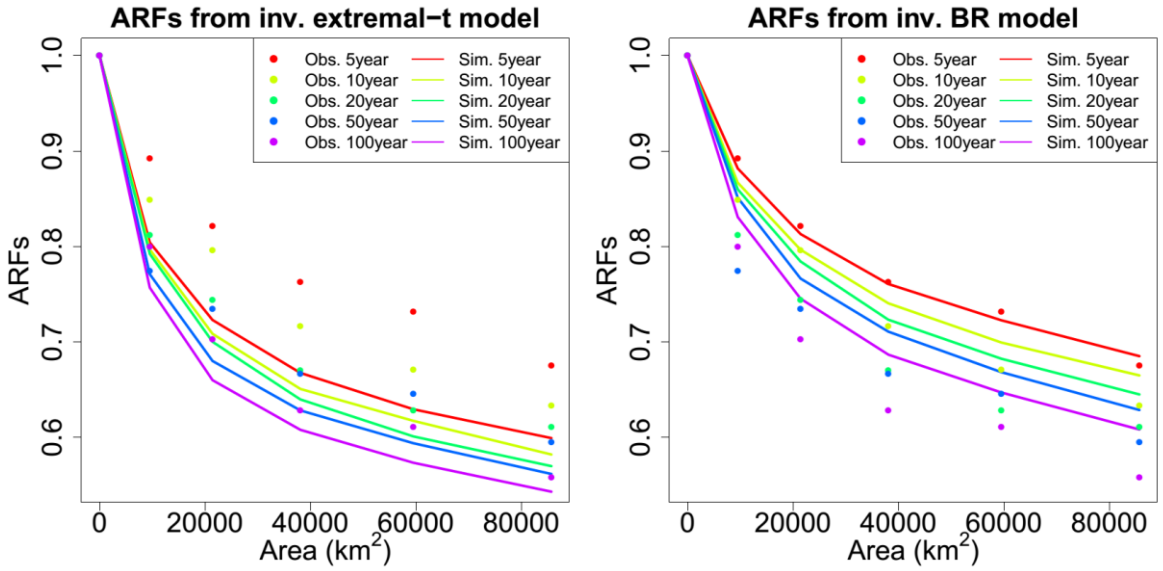

Fig. 3.7. ARFs from observed data (circles) and from simulated data (lines) for different areas and at different return periods. Left is for inverted extremal-t model, and right is for inverted Brown-Resnick model.

To further evaluate the performance of the inverted extremal-t and Brown-Resnick models, the ARFs from the observed and the simulated data are plotted for different areas at the same return period. Bootstrapped 95% confidence intervals are estimated for the ARFs from observed data, by resampling with replacement the observed data from all 88 gauges simultaneously. Fig. 3.8 shows the results for the inverted extremal-t and Brown-Resnick models.

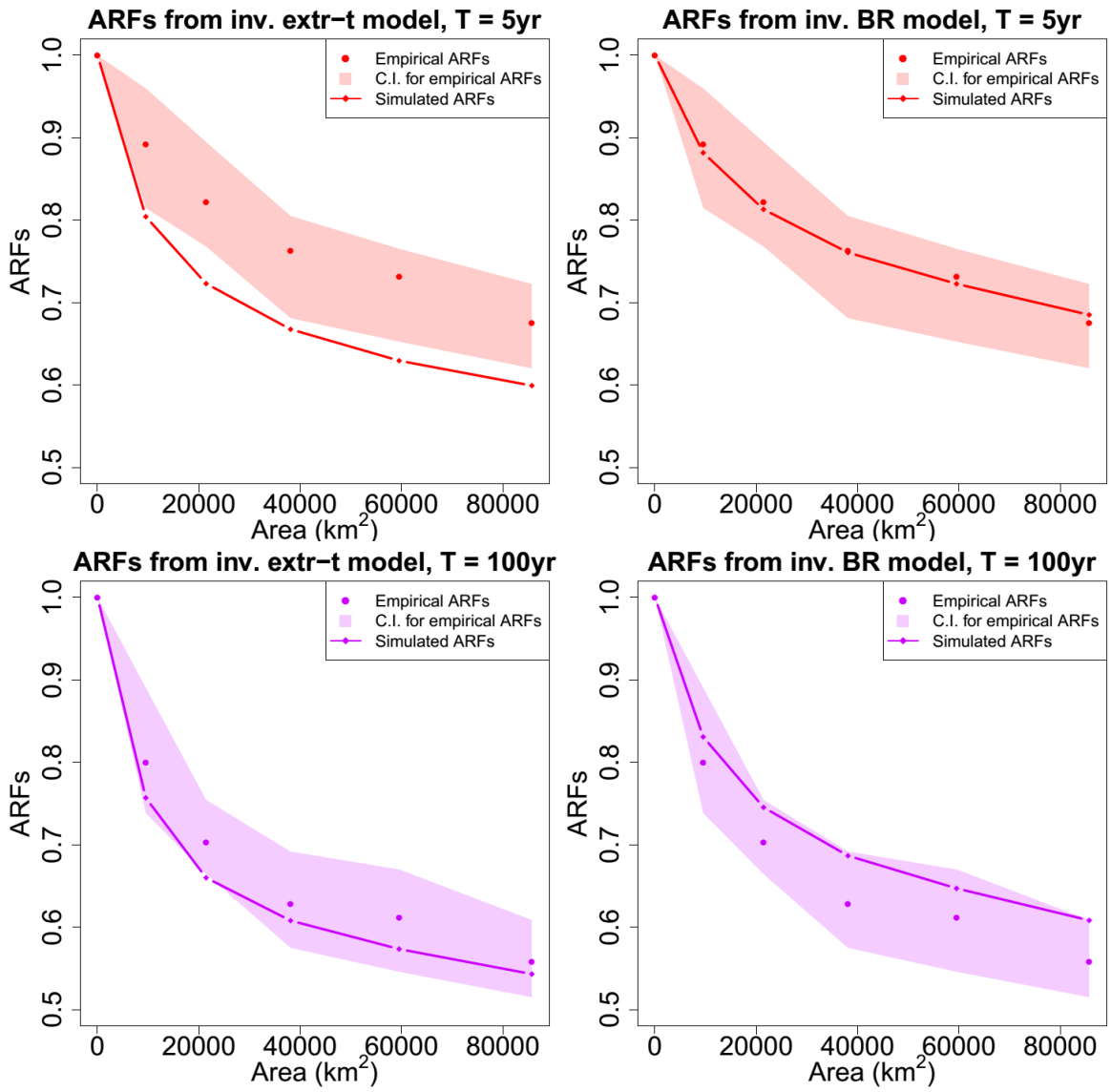

Fig. 3.8. ARFs from simulated data (lines) of asymptotically independent models, and ARFs from observed data (circular points) with 95% confidence interval (shadows) at the same return periods of 5 years and 100 years. Left panel is for inverted extremal-t model, and right panel is for inverted Brown-Resnick model. The colour of the ARFs for each return period is consistent with that in Fig. 3.7.

Fig. 3.8 indicates that the performance of the inverted extremal-t model is poor, as the ARFs from simulations at a 5-year return period are significantly too low, being outside the 95% confidence band. The same is true for the 10-year return period (not shown). The ARFs from simulation of the inverted Brown-Resnick model for both 5-year and 100-year return periods are close to those from observed data, and the same is true for 10-year and 50-year return periods, not shown here. This suggests that the inverted Brown-Resnick model gives better simulated spatial rainfall for the case study.

Fig. 3.8 also shows that the inverted Brown-Resnick model provides smooth ARFs at the 100-year return period, so it should also be useful when extrapolating to rarer frequencies.

3.5. Discussion and conclusions

The use of design events with long return periods is common in hydrology, e.g., for large scale infrastructure such as dams or for design along built-up water courses in urban environments. Translating extreme point rainfall to an area leads to significant uncertainty in ARFs, but there has been limited research into ARFs and their underlying assumptions, relative to other aspects of the design process. Moreover, ARFs are typically based on empirical studies that do not account for analytic tail dependence properties and are limited under extrapolation to rare events.

We designed a synthetic study to see how different asymptotic assumptions affect the behaviour of ARFs with respect to return period, using two dependence models to simulate spatial rainfall. This indicates that ARFs from asymptotically dependent data increase for longer return periods and converge to a limiting state (Fig. 3.4), appearing stable at 200-, 500-, and 1000-year return periods. In contrast, ARFs from asymptotically independent data decrease for longer return periods.

The synthetic study also shows that pairwise extremal coefficients for asymptotically dependent data stabilize for increasing thresholds, while the pairwise residual tail dependence coefficients increase. By contrast, as thresholds increase for asymptotically independent data the pairwise extremal coefficients increase but the pairwise residual tail dependence coefficients stabilize. These features can be used to assess the asymptotic behaviour of observed data.

A diagnostic procedure, which estimates the pairwise extremal coefficients and pairwise tail dependence coefficients at different thresholds, was employed before fitting models to observed data. It indicates that the observed data are asymptotically independent (Fig. 3.5). When fitting the max-stable and inverted max-stable models to observed rainfall data at different thresholds, the results also confirm that only asymptotically independent models can represent the dependence structure of the observed data. Together with Thibaud et al. (2013), this suggests that max-stable processes may not be suitable for modelling rainfall extremes, although this would need to be confirmed by further work. Future studies about spatial rainfall extremes should take this into consideration.

This paper has shown that observed ARFs follow the behaviour of an asymptotically independent process and that inverted max-stable process models are able to reproduce this behaviour. To date, a significant amount of engineering design has been conducted by decoupling statistics of extremal rainfall at a point from (as in intensity-duration-frequency maps) from estimates of rainfall over a region (ARFs). One possibility suggested by our work is to use simulation studies, such as in this paper, to supplement the derivation of empirical ARFs for different regions – providing smooth extrapolations of ARFs and the ability to calculate localised ARFs for individual catchments. As with empirical studies, we can anticipate significant differences in ARFs for different regions. Another possibility is the direct use of spatiotemporal models of rainfall in the design of infrastructure requiring very rare events (as with large dams and water-related infrastructure in major urban centres that have high-consequence impacts). Spatiotemporal rainfall models have become increasingly used for hydrologic analysis and design, including multi-scaling models (Over

and Gupta, 1996), Poisson cluster models (Leonard et al., 2008), and Gaussian latent-variable models (Bennett et al., 2016b). However, the development and calibration of these models is typically based on all the data, with the extremal properties evaluated as an emergent feature. While there has also been increasing attention given to the dependence structure of spatiotemporal extremes, including Gaussian dependence of multisite extreme rainfall (Evin et al., 2018; Renard and Lang, 2007) and multi-scaling frameworks of spatial rainfall (Panthou et al., 2014; Veneziano and Langousis, 2005), there is an ongoing need to provide a rigorous framework for extremes over a region that is also linked to more frequent rainfall.

Our analysis suggests that the rainfall process is asymptotically independent, so the ARFs decrease for longer return periods. The smoothness of the modelled ARFs is useful when extrapolating to rare events. Our findings provide a rigorous foundation for the development of ARF curves against both area and frequency as the basis for engineering design.

Acknowledgments

The lead author was supported by the Australia Awards Scholarships (AAS) from Australia Government. Seth Westra was supported by Australian Research Council Discovery grant DP150100411. Anthony C. Davison and Sebastian Engelke were supported by the Swiss National Science Foundation; the paper was completed while ACD was a visitor at the Institute for Mathematical Sciences, National University of Singapore, and SE was a visitor at the Department of Statistical Sciences, University of Toronto. We thank Leticia Mooney for her help in improving this manuscript. The rainfall data used in this study were provided by the Australian Bureau of Meteorology, and can be obtained from the corresponding author.

References

Allen, R.J., DeGaetano, A.T., 2005. Areal Reduction Factors for Two Eastern United StatesRegions with High Rain-Gauge Density. Journal of hydrologic engineering: 327-335. DOI:10.1061/(ASCE)1084-0699(2005)10:4(327)

Asadi, P., Davison, A.C., Engelke, S., 2015. Extremes on river networks. Ann. Appl. Stat., 9(4): 2023-2050. DOI:10.1214/15-AOAS863

Asquith, W.H., Famiglietti, J.S., 2000. Precipitation areal-reduction factor estimation using an annual-maxima centered approach. Journal of Hydrology, 230(1–2): 55-69. DOI:http://dx.doi.org/10.1016/S0022-1694(00)00170-0

Bacchi, B., Ranzi, R., 1996. On the derivation of the areal reduction factor of storms. Atmospheric Research, 42(1): 123-135. DOI:http://dx.doi.org/10.1016/0169-8095(95)00058-5

Ball, J. et al., 2016. Australian Rainfall and Runoff: A Guide to Flood Estimation. © Commonwealth of Australia (Geoscience Australia).

Bengtsson, L., Niemczynowicz, J., 1986. Areal Reduction Factors from Rain Movement. Hydrology Research, 17(2): 65-82.

Bennett, B., Lambert, M., Thyer, M., Bates, B.C., Leonard, M., 2016. Estimating Extreme Spatial Rainfall Intensities. Journal of Hydrologic Engineering, 21(3): 04015074. DOI:doi:10.1061/(ASCE)HE.1943-5584.0001316

Coles, S., 2001. An Introduction to Statistical Modeling of Extreme Values. Springer Series in Statistics. Springer.

Coles, S., Heffernan, J., Tawn, J., 1999. Dependence Measures for Extreme Value Analyses. Extremes, 2(4): 339-365. DOI:10.1023/a:1009963131610

Coles, S., Tawn, J., 1996. Modelling Extremes of the Areal Rainfall Process. Journal of the Royal Statistical Society. Series B (Methodological), 58(2): 329-347. DOI:10.2307/2345980

Davison, A.C., Huser, R., Thibaud, E., 2013. Geostatistics of Dependent and Asymptotically Independent Extremes. Mathematical Geosciences, 45(5): 511-529. DOI:10.1007/s11004-013-9469-y

Davison, A.C., Padoan, S.A., Ribatet, M., 2012. Statistical Modeling of Spatial Extremes. Statistical Science: 161-186. DOI:10.1214/11-STS376

Davison, A.C., Smith, R.L., 1990. Models for exceedances over high thresholds. Journal of the Royal Statistical Society. Series B (Methodological): 393-442.

de Haan, L., 1984. A Spectral Representation for Max-stable Processes. The Annals of Probability, 12(4): 1194-1204. DOI:10.2307/2243357

Dombry, C., Engelke, S., Oesting, M., 2016. Exact simulation of max-stable processes. Biometrika, 103(2): 303-317.

Engelke, S., de Fondeville, R., Oesting, M., 2017. Extremal behavior of aggregated data with an application to downscaling. DOI:https://arxiv.org/abs/1712.09816

Engelke, S., Malinowski, A., Kabluchko, Z., Schlather, M., 2015. Estimation of Hüsler–Reiss distributions and Brown–Resnick processes. Journal of the Royal Statistical Society: Series B (Statistical Methodology), 77(1): 239-265. DOI:10.1111/rssb.12074

Ferreira, A., de Haan, L., Zhou, C., 2012. Exceedance probability of the integral of a stochastic process. Journal of Multivariate Analysis, 105(1): 241-257. DOI:http://dx.doi.org/10.1016/j.jmva.2011.08.020

Huser, R., Davison, A.C., 2013. Composite likelihood estimation for the Brown–Resnick process. Biometrika, 100(2): 511-518. DOI:10.1093/biomet/ass089

Jordan, P., Weinmann, E., Hill, P., Wiesenfeld, C., 2013. Australian Rainfall & Runoff Revision Project: Project 2-Collation and Review of Areal Reduction Factors from Applications of the CRC-FORGE Method in Australia.

Kabluchko, Z., Schlather, M., de Haan, L., 2009. Stationary Max-Stable Fields Associated to Negative Definite Functions. The Annals of Probability, 37(5): 2042-2065.

Ledford, A.W., Tawn, J.A., 1996. Statistics for Near Independence in Multivariate Extreme Values. Biometrika, 83(1): 169-187.

Li, J., Sharma, A., Johnson, F., Evans, J., 2015. Evaluating the effect of climate change on areal reduction factors using regional climate model projections. Journal of

Hydrology, 528(Supplement C): 419-434. DOI:https://doi.org/10.1016/j.jhydrol.2015.06.067

Myers, V.A., 1980. A methodology for point-to-area rainfall frequency ratios. In: Zehr, R.M. (Ed.). Dept. of Commerce, National Oceanic and Atmospheric Administration, National Weather Service, [Silver Spring, Md.] :.

Nicolet, G., Eckert, N., Morin, S., Blanchet, J., 2017. A multi-criteria leave-two-out cross-validation procedure for max-stable process selection. Spatial Statistics, 22(Part 1): 107-128. DOI:https://doi.org/10.1016/j.spasta.2017.09.004

Oesting, M., Schlather, M., Friederichs, P., 2017. Statistical post-processing of forecasts for extremes using bivariate Brown-Resnick processes with an application to wind gusts. Extremes, 20(2): 309-332. DOI:10.1007/s10687-016-0277-x

Omolayo, A.S., 1993. On the transposition of areal reduction factors for rainfall frequency estimation. Journal of Hydrology, 145(1): 191-205. DOI:http://dx.doi.org/10.1016/0022-1694(93)90227-Z

Opitz, T., 2013. Extremal t processes: Elliptical domain of attraction and a spectral representation. Journal of Multivariate Analysis, 122: 409-413. DOI:https://doi.org/10.1016/j.jmva.2013.08.008

Padoan, S.A., Ribatet, M., Sisson, S.A., 2010. Likelihood-Based Inference for Max-Stable Processes. Journal of the American Statistical Association, 105(489): 263-277. DOI:10.1198/jasa.2009.tm08577

Pickands, J., 1975. Statistical Inference Using Extreme Order Statistics. The Annals of Statistics, 3(1): 119-131. DOI:10.2307/2958083

Rodriguez-Iturbe, I., Mejía, J.M., 1974. On the transformation of point rainfall to areal rainfall. Water Resources Research, 10(4): 729-735. DOI:10.1029/WR010i004p00729

Shaw, S.B., Royem, A.A., Riha, S.J., 2011. The Relationship between Extreme Hourly Precipitation and Surface Temperature in Different Hydroclimatic Regions of the United States. Journal of Hydrometeorology, 12(2): 319-325. DOI:10.1175/2011jhm1364.1

Siriwardena, L., Weinmann, P., 1996. Derivation of areal reduction factors for design rainfalls in Victoria for Rainfall Durations 18–120 hours. Report, 96(4): 60.

Sivapalan, M., Blöschl, G., 1998. Transformation of point rainfall to areal rainfall: Intensity-duration-frequency curves. Journal of Hydrology, 204(1): 150-167. DOI:http://dx.doi.org/10.1016/S0022-1694(97)00117-0

Srikanthan, R., 1995. A review of the methods for estimating areal reduction factors for design rainfalls / R. Srikanthan. Report (Cooperative Research Centre for Catchment Hydrology) ; 95/3. Cooperative Research Centre for Catchment Hydrology, Clayton, Vic.

Svensson, C., Jones, D.A., 2010. Review of methods for deriving areal reduction factors. Journal of Flood Risk Management, 3(3): 232-245. DOI:10.1111/j.1753-318X.2010.01075.x

Thibaud, E., Mutzner, R., Davison, A.C., 2013. Threshold modeling of extreme spatial rainfall. Water Resources Research, 49(8): 4633-4644. DOI:10.1002/wrcr.20329

Thibaud, E., Opitz, T., 2015. Efficient inference and simulation for elliptical Pareto processes. Biometrika, 102(4): 855-870. DOI:10.1093/biomet/asv045

Veneziano, D., Langousis, A., 2005. The areal reduction factor: A multifractal analysis. Water Resources Research, 41(7): n/a-n/a. DOI:10.1029/2004WR003765

Wadsworth, J.L., Tawn, J.A., 2012. Dependence modelling for spatial extremes. Biometrika, 99(2): 253-272. DOI:10.1093/biomet/asr080

Wadsworth, J.L., Tawn, J.A., 2014. Efficient inference for spatial extreme value processes associated to log-Gaussian random functions. Biometrika, 101(1): 1-15. DOI:10.1093/biomet/ast042

Westra, S., Sisson, S.A., 2011. Detection of non-stationarity in precipitation extremes using a max-stable process model. Journal of Hydrology, 406(1–2): 119-128. DOI:http://dx.doi.org/10.1016/j.jhydrol.2011.06.014

Supplementary material

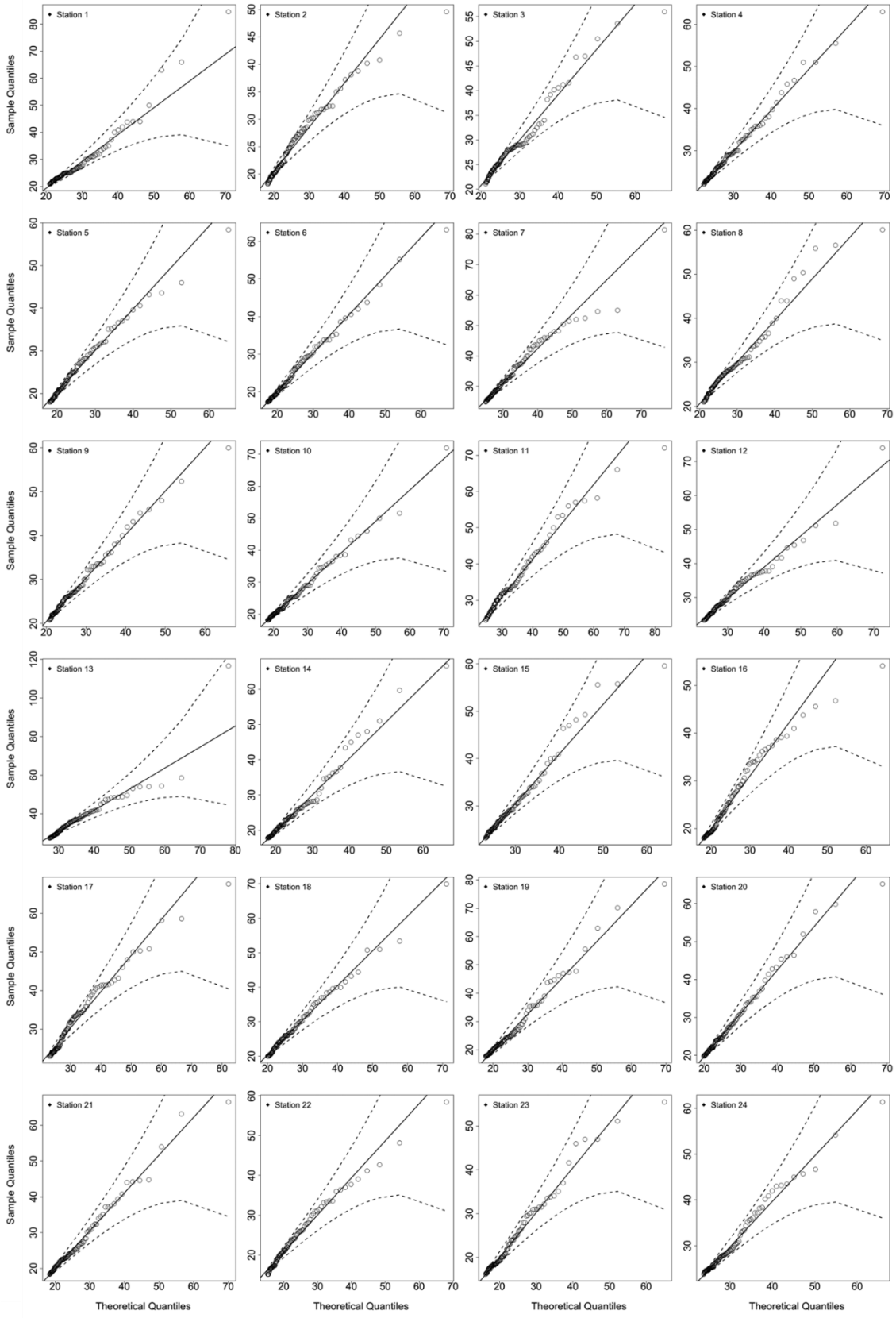

Fig. S3.1. QQ plots for the estimate of marginal distribution GPD for rain gauges from 1 to 24. The solid diagonal line indicates a perfect fit, and the dotted lines indicate a 95% confidence interval.

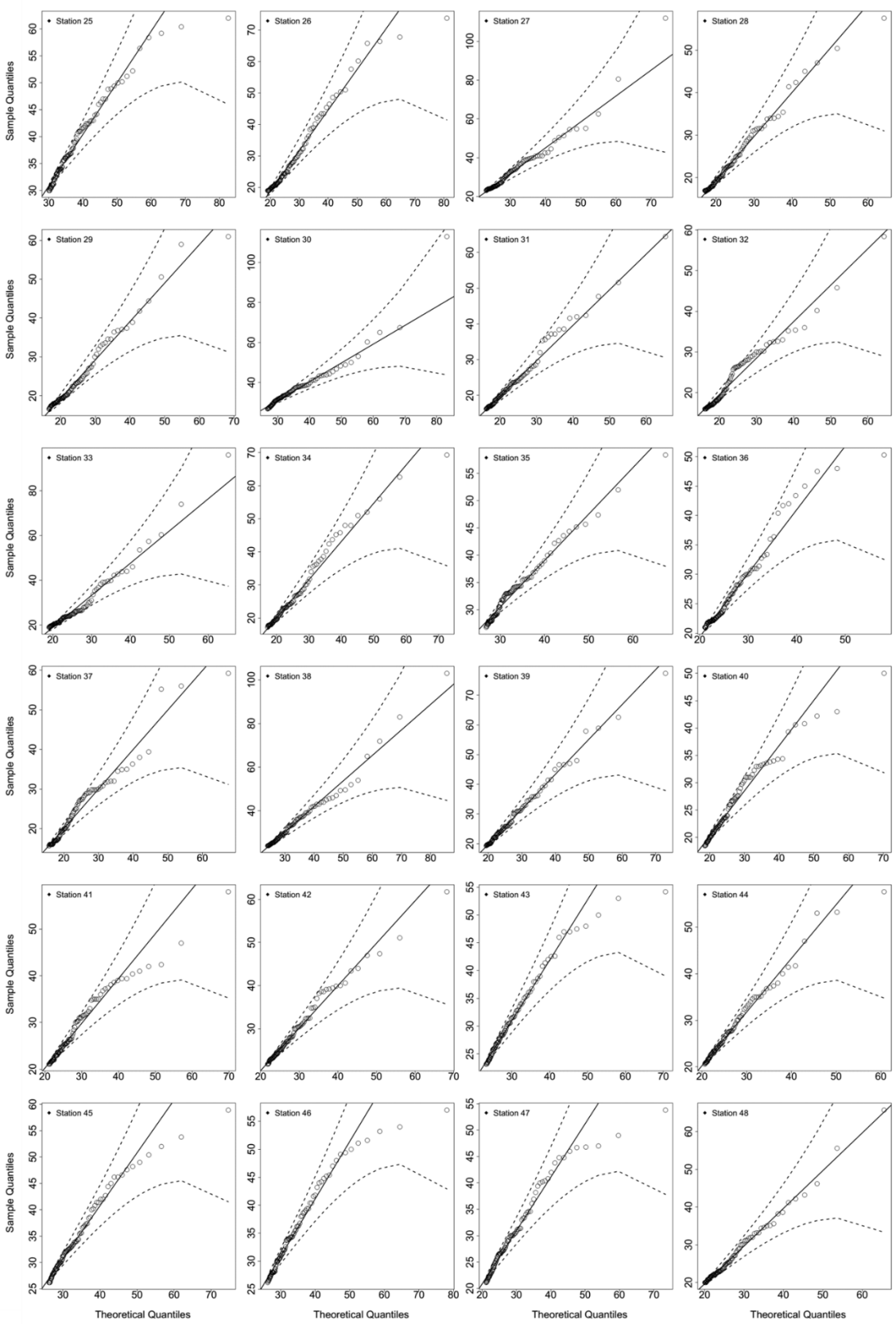

Fig. S3.2. QQ plots for the estimate of marginal distribution GPD for rain gauges from 25 to 48. The solid diagonal line indicates a perfect fit, and the dotted lines indicate a 95% confidence interval.

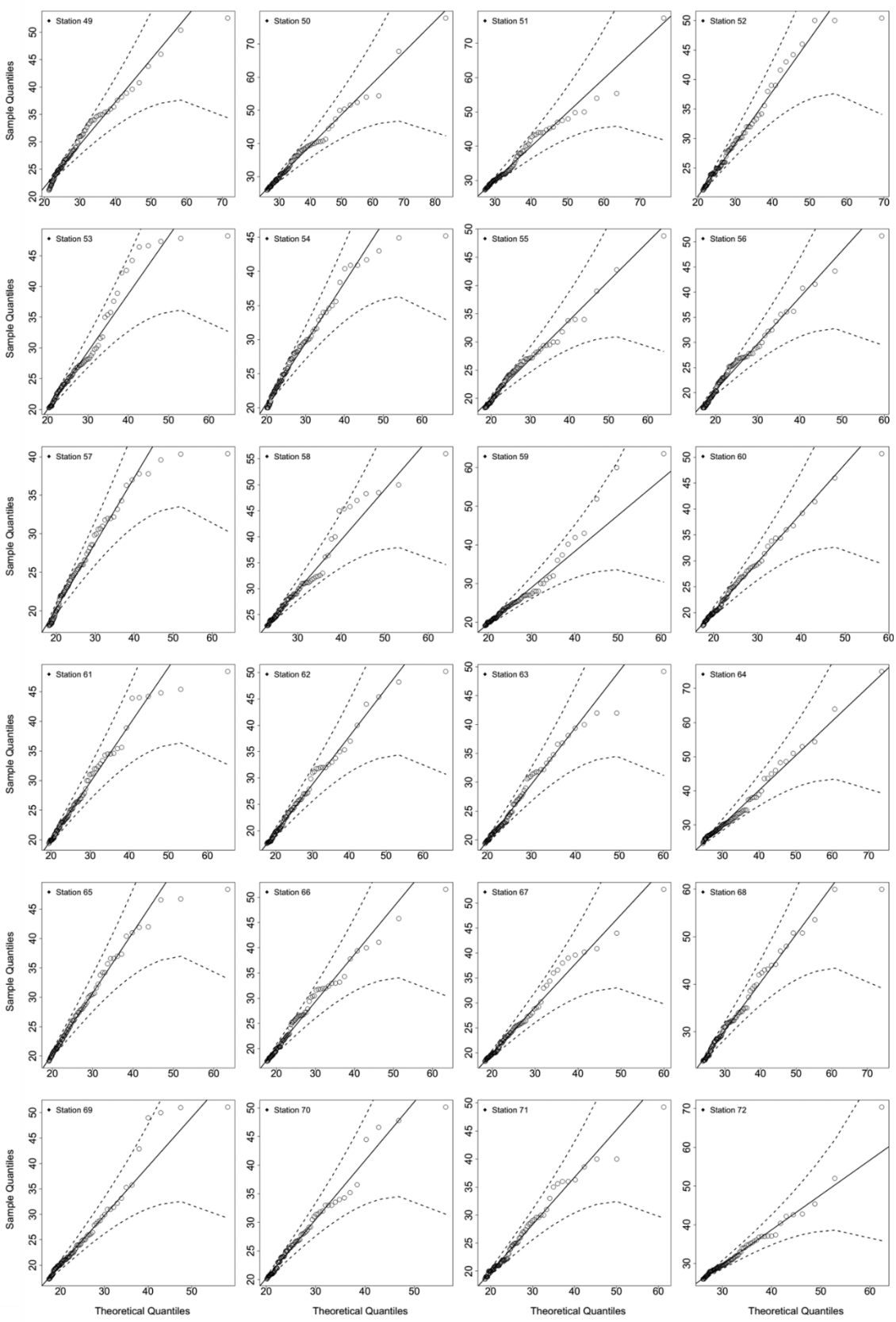

Fig. S3.3. QQ plots for the estimate of marginal distribution GPD for rain gauges from 49 to 72. The solid diagonal line indicates a perfect fit, and the dotted lines indicate a 95% confidence interval.

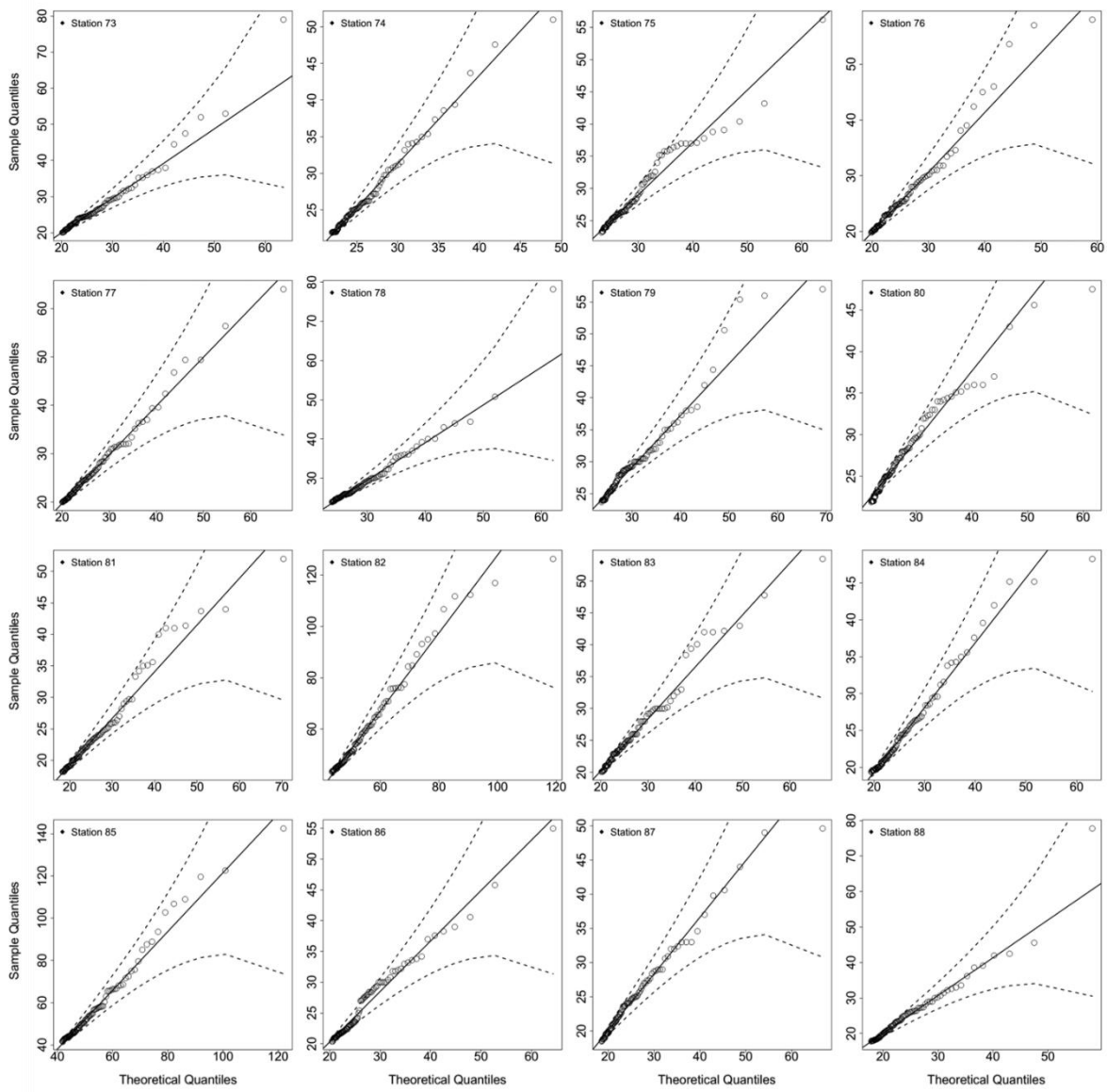

Fig. S3.4. QQ plots for the estimate of marginal distribution GPD for rain gauges from 73 to 88. The solid diagonal line indicates a perfect fit, and the dotted lines indicate a 95% confidence interval.

Chapter 4

Spatially dependent Intensity-Duration-Frequency curves to support the design of civil infrastructure systems (Paper 3)

Phuong Dong Le, Michael Leonard, Seth Westra

Hydrology and Earth System Sciences, accepted for review 27/08/2018

https://doi.org/10.5194/hess-2018-393, in review, 2018

Statement of Authorship

Title of Paper	Spatially dependent Intensity-Duration-Frequency curves to support the design of civil infrastructure systems
Publication Status	☐ Published ☐ Accepted for Publication ☑ Submitted for Publication ☐ Unpublished and Unsubmitted work written in manuscript style
Publication Details	Le, P.D., Leonard, M., Westra, S., 2018. Spatially dependent Intensity-Duration-Frequency curves to support the design of civil infrastructure systems. Hydrology and Earth System Sciences, (submitted).

Principal Author

Name of Principal Author (Candidate)	Phuong Dong Le
Contribution to the Paper	Implementation and development of approach, visualisation and interpretation of results, preparation of manuscript, preparation of response to reviewers and acted as corresponding author.
Overall percentage (%)	80
Certification:	This paper reports on original research I conducted during the period of my Higher Degree by Research candidature and is not subject to any obligations or contractual agreements with a third party that would constrain its inclusion in this thesis. I am the primary author of this paper.
Signature	Date 19/07/2018

Co-Author Contributions

By signing the Statement of Authorship, each author certifies that:

i. the candidate's stated contribution to the publication is accurate (as detailed above);

ii. permission is granted for the candidate in include the publication in the thesis; and

iii. the sum of all co-author contributions is equal to 100% less the candidate's stated contribution.

Name of Co-Author	Michael Leonard
Contribution to the Paper	Supervised research, helped to evaluate and edit the manuscript.
Signature	Date 19/7/18

Name of Co-Author	Seth Westra
Contribution to the Paper	Supervised research, helped to evaluate and edit the manuscript.
Signature	Date 19/07/2018.

Please cut and paste additional co-author panels here as required.

Abstract

Conventional flood risk methods typically focus on estimation at a single location, which is inadequate for civil infrastructure systems such as road or railway infrastructure. This is because rainfall extremes are spatially dependent, so that to understand overall system risk it is necessary to assess the interconnected elements of the system jointly. For example, when designing evacuation routes it is necessary to understand the risk of one part of the system failing given that another region is flooded or exceeds the level at which evacuation becomes necessary. Similarly, failure of any single part of a road section (e.g., a flooded river crossing) may lead to the wider system's failure (i.e. the entire road becomes inoperable). This study demonstrates a spatially dependent Intensity-Duration-Frequency curve framework that can be used to estimate flood risk across multiple catchments, accounting for dependence both in space and across different critical storm durations. The framework is demonstrated via a case study of a highway upgrade, comprising five bridge crossings where the upstream contributing catchments each have different times of concentration. The results show that conditional and unconditional design flows can differ by a factor of two, highlighting the importance of taking an integrated approach. There is also a reduction in the failure probability of the overall system compared with the case of no spatial dependence between storms. The results demonstrate the potential uses of spatially dependent Intensity-Duration-Frequency curves and suggest the need for more conservative design estimates to take into account conditional risks.

4.1. Introduction

Methods for quantifying flood risk of civil infrastructure systems such as road and rail networks require considerably more information compared to traditional methods that focus on flood risk at a point. For example, the design of evacuation routes requires the quantification of the risk that one part of the system will fail at the same time that another region is flooded or exceeds the level at which evacuation becomes necessary. Similarly, a railway route may become impassable if any of a number of bridges are submerged, such that the 'failure probability' of that route becomes some aggregation of the failure probabilities of each individual section. Successful estimation of flood risk in these systems therefore requires recognition both of the networked nature of the civil infrastructure system across a spatial domain, as well as the spatial and temporal structure of flood-producing mechanisms (e.g. storms and extreme rainfall) that can lead to system failure (e.g., Leonard et al. (2014), Seneviratne et al. (2012), Zscheischler et al. (2018)).

One way to estimate such flood probabilities is to directly use information contained in historical streamflow data. For example, annual maximum streamflow at two locations might be assumed to follow a bivariate generalized extreme value distribution (Favre et al., 2004; Wang, 2001; Wang et al., 2009), which can then be used to estimate both conditional probabilities (e.g. the probability that one river is flooded given that the other river level exceeds a specified threshold) and joint probabilities (e.g. the probability that one or both rivers are flooded). However, continuous streamflow data are often not available at the locations most relevant to the civil infrastructure system in question, or the catchment conditions have changed to a degree that reflects historical streamflow records as unrepresentative of likely future risk. Thus, direct application of streamflow data for flood risk quantification in civil infrastructure systems does not represent a viable approach for the majority of situations.

To deal with these difficulties, two alternative rainfall-based approaches are commonly used. The first uses continuous rainfall data (either historical or generated) to compute continuous streamflow data using a rainfall-runoff model (Boughton and Droop, 2003; Cameron et al., 1999; He et al., 2011; Pathiraja et al., 2012), with flood risk then estimated based on the simulated streamflow time series. This method is computationally burdensome, and can often fail to take into account the dependence structure of the extremes. Furthermore, although this approach can implicitly account for spatial dependence in rainfall when using historical rainfall data at multiple locations, there are not many models that simulate rainfall in space and time for long periods when this historical data is unavailable (e.g., Baxevani and Lennartsson (2015), Kleiber et al. (2012), Rasmussen (2013)). Furthermore, most rainfall models operate at the daily timescale (Bennett et al., 2016b), whereas many sub-catchments will respond on shorter timescales, and the capacity of space-time rainfall models to simulate the statistics of sub-daily rainfall remains a challenging research problem (Leonard et al., 2008), particularly for data-sparse regions. Therefore, available rain-based methods for continuous simulation are also often unviable for most practical situations.

The second rainfall-based approach proceeds by conducting the probability calculations on rainfall, to construct 'Intensity-Duration-Frequency' (IDF) curves, which are then translated to a runoff event of equivalent probability via either empirical models such as the Rational method (Kuichling, 1889; Mulvaney, 1851) to estimate peak flow rate, or via event-based rainfall-runoff models that are able to simulate the full flood hydrograph (Boyd et al., 1996; Chow et al., 1988; Laurenson and Mein, 1997). Currently IDF curves are estimated either at a point location, or are estimated over a spatial domain by multiplication with an areal reduction factor (ARF) to convert point rainfall to spatially averaged rainfall of an equivalent exceedance probability (Ball et al., 2016); this information then can be used to estimate either peak flow or the flood hydrograph at any point location within a catchment. However, such methods do not account for information on the spatial dependence of extreme rainfall—whether for single storm duration across a region, or for the more complex case of different durations across a region (Bernard, 1932; Koutsoyiannis et al., 1998). This prevents these approaches from being applied to estimate conditional or joint flood risk at multiple points in a catchment or across several catchments as would be required for a civil infrastructure system.

Although tailored multivariate approaches can be applied to estimate conditional and joint probabilities of extreme rainfall for specific situations (e.g., Kao and Govindaraju (2008), Wang et al. (2010), Zhang and Singh (2007)), the development of a unified methodology that integrates with existing IDF-based flood estimation approaches remains elusive. This is particularly challenging given that it is not only necessary to preserve dependence of rainfall across space, but also to account for dependence across storm burst durations, as different parts of the system may be vulnerable to different critical duration storm events. To this end, arguably the most promising recent research direction has been the application of max-stable process theory that is able to represent storm-level dependence (de Haan, 1984; Schlather, 2002). This has been applied on a spatial domain by Padoan et al. (2010), who calculated conditional probabilities for a spatial domain located in United States. However, to ensure that this general approach can be applied for practical flood estimation problems, two further problems need to be overcome:

1. The approach needs to not only account for spatial dependence for rainfall 'events' of a single duration (e.g. the field of annual maximum daily rainfall data), but must also account for dependence across multiple durations. This was addressed by Le et al. (2018b), who linked the max-stable model of Brown and Resnick (1977) and Kabluchko et al. (2009) with the duration-dependent model of Koutsoyiannis et al. (1998), in order to create a model that could be used to reflect dependencies between nearby catchments of different sizes.

2. Given that often the interest is in rare flood events, the model needs to capture appropriate asymptotic properties of spatial dependence as the events become increasingly extreme. Recent evidence is emerging that rainfall has an asymptotically independent characteristic (Le et al., 2018a; Thibaud et al., 2013), which means that the level of the rainfall's dependence reduces with an increasing return period (Wadsworth and Tawn, 2012). This implies that inverted max-stable models, which are asymptotically independent, are likely to be preferable as an

approach for representing spatially dependent IDF information. An added benefit of correctly representing asymptotic dependence is that information on areal reduction factors can be obtained directly from the model, rather than estimating ARF information independently from the computation of the IDF curves.

This study addresses both these issues by demonstrating the application of the inverted max-stable process to estimate joint and conditional probabilities of flood-producing rainfall in the form of spatially dependent IDF curves. This approach adapts the methods developed by (Le et al., 2018b) to inverted max-stable models, and then uses the derived spatially-dependent IDF curves combined with the extracted information on AFRs as the basis for transforming the rainfall into flood flows. The approach is demonstrated on a highway system spanning 20 km with five separate bridge crossings, and with the contributing catchment at each crossing having a different time of concentration.

The case study is designed to address two related questions: (i) "What flood flow needs to be used to design a bridge that will fail only once on average every M times (e.g., $M = 10$ for a 10-year event) that a neighbouring catchment is flooded?"; and (ii) "What is the probability that the overall system fails given that each bridge is designed to a specific exceedance probability event (e.g., the 1% annual exceedance probability event)?" The method for resolving these questions represents a new paradigm in which to estimate flood risk for engineering design, by focusing attention on the risk of the entire system, rather than the risk of individual system elements in isolation.

In the remainder of the paper, Section 4.2 emphasises the need for spatially dependent IDF curves in flood risk design, followed by Section 4.3 which outlines the case study and data used. Section 4.4 explains the methodology of the framework, including a method for analysing the spatial dependence of extreme rainfall across different durations. It also includes an algorithm with which to use that information in estimating the conditional and joint probabilities of floods. The results, and a discussion on the behaviour of flood due to the spatial and duration dependence of rainfall extremes, are provided in Section 4.5. Conclusions and recommendations follow in Section 4.6.

4.2. The need for spatially dependent IDF curves in flood risk estimation

The main limitation of conventional methods of flood risk estimation is that they isolate bursts of rainfall and break the dependence structure of extreme rainfall. Figure 4.1 demonstrates a traditional process of estimating at-site extreme rainfall for two locations (gauge 1, gauge 2) and three durations (1, 3, and 5 hr) (Stedinger et al., 1993). The process first involves extracting the extreme burst of rainfall for each site, duration and year from the continuous rainfall data, and then fitting a probability distribution (such as the Generalised Extreme Value (GEV) distribution) to the extracted data. Figure 4.1 demonstrates that, through the process of converting the continuous rainfall data to a series of discrete rainfall 'bursts', this process breaks both the dependence with respect to duration and space. Firstly, the duration dependence is broken by extracting each duration separately, whereas for the hypothetical storm in Fig. 4.1 it is clear that the annual maxima from some of the extreme bursts come from the same storm. Secondly, the spatial dependence is broken because each site is analysed independently. Again, for the

hypothetical storm of Fig. 4.1 it can be seen that the 5 hr storm has occurred at the same time across the two catchments, and this information is lost in the subsequent probability distribution curves. Lastly, there is cross-dependence in space and duration. For example, the 1 hr extreme from gauge 2 occurs at the same time as the 5 hr extreme from gauge 1. This may be relevant if there are two catchments with times of concentration matching 1 hr and 5 hr respectively, where catchments are neighbouring or nested.

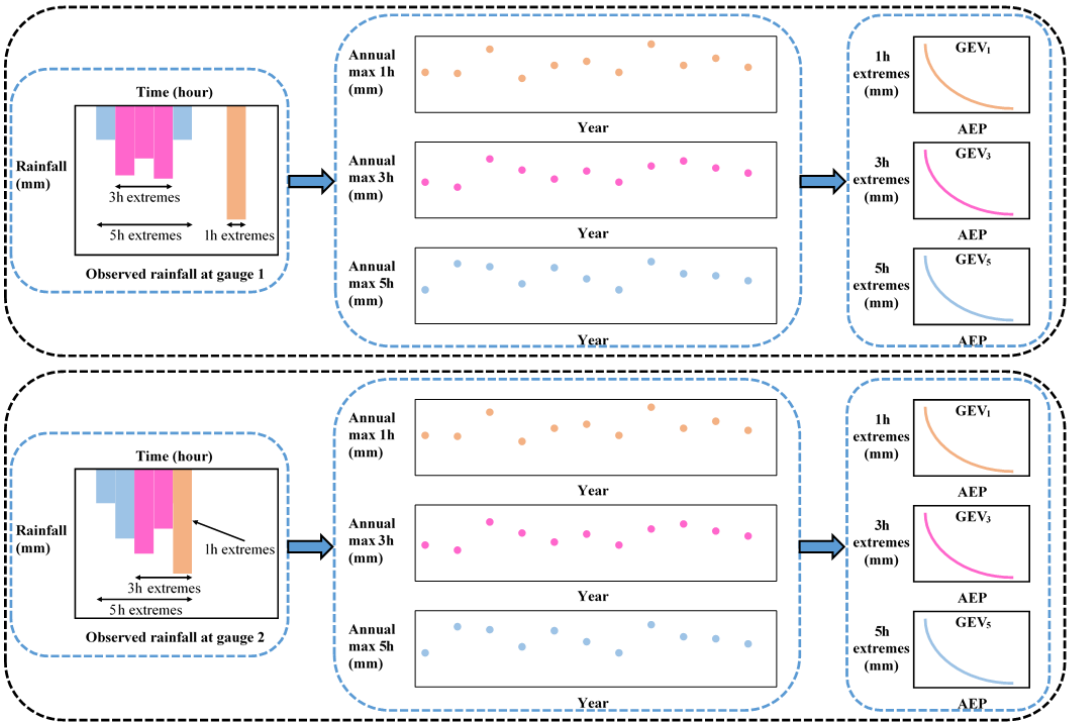

Figure 4.1. Illustration of process to estimate rainfall extremes for each individual location in conventional flood risk approach, the upper panel is for gauge 1 and the lower panel is for gauge 2.

Having obtained the IDF curves for individual locations in Fig. 4.1, the next step is commonly to convert this to spatial IDF maps by interpolating results between gauged locations. Figure 4.2 shows hypothetical IDF curves from individual sites, with a separate spatial contour map usually provided for each storm burst duration. In a conventional application the respective maps are used to estimate the magnitude of extreme rainfall over catchments for a specified time of concentration. The IDF curves are combined with an areal reduction factor (ARF) to determine the volume of rainfall over a region (since rainfall is not simultaneously extreme at all locations over the region). However, because the spatial dependence was broken in the analysis of IDF curves, the ARFs come from a separate analysis and are an attempt to correct for the broken spatial relationship within a catchment (Bennett et al., 2016a). Lastly, the rainfall volume over the catchment is combined with a temporal pattern and input to a runoff model to simulate flood-flow at a catchment's outlet. Where catchment flows can be considered independently this process has been acceptable for conventional design, but because this process does not account for dependence across durations and across a region, it is not possible to address problems that span multiple catchments, as with civil infrastructure systems.

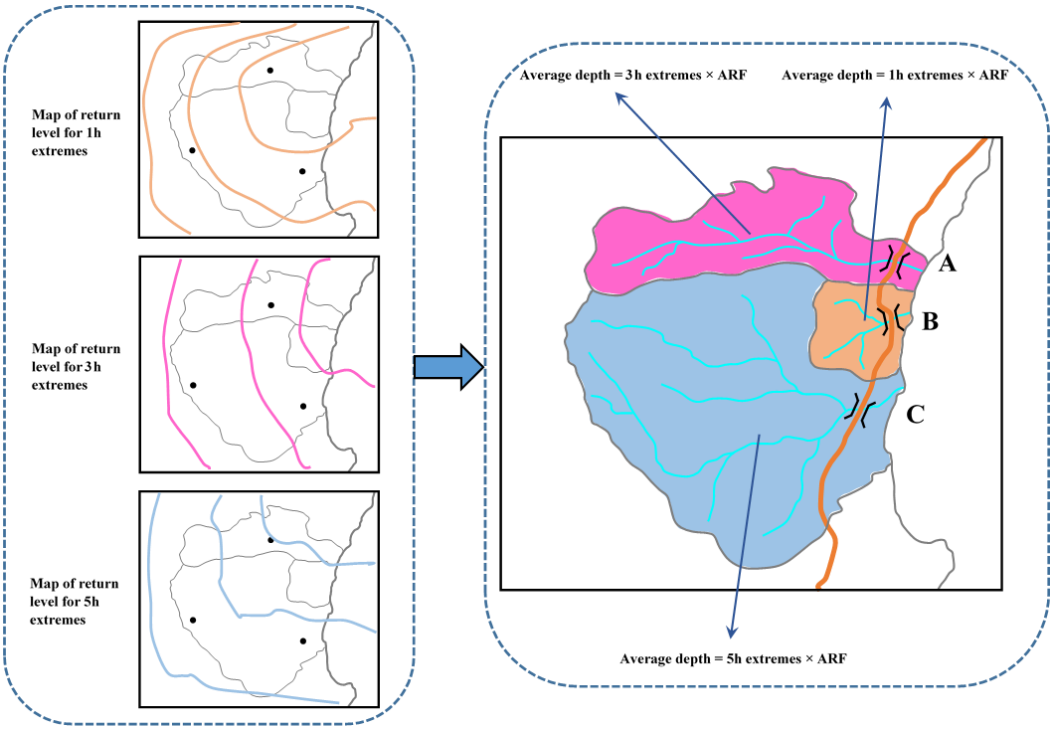

Figure 4.2. Illustration of map of return level and how to use it in estimating flood flow in conventional flood risk estimates approach.

The process in Fig. 4.1 breaks out the dependence of the observed rainfall, which makes the conventional approach unable to analyse the dependence of flooding at two or more separate locations. Instead, this paper advocates for spatially dependent IDF curves which are developed by retaining the dependence of observed rainfall in the estimation of extremal rainfall. By applying spatially dependent IDF curves to a rainfall-runoff model, the dependence of flooding between separate locations can be achieved.

4.3. Case study and data

The region chosen for the case study is in the mid north coast region of New South Wales, Australia. This region has been the focus of a highway upgrade project and has an annual average daily traffic volume on the order of 15,000 vehicles along the existing highway. The upgrade traverses a series of coastal foothills and floodplains for a total length of approximately 20 km. The project's major river crossings consist of extensive floodplains with some marsh areas.

The case study has five main catchments that are numbered in sequence in Fig. 4.3: (1) Bellinger, (2) Kalang River, (3) Deep Creek, (4) Nambucca and (5) Warrell Creek. The area and time of concentration of these catchments is summarised in Table 4.1, with the latter estimated using the ratio of the flow path length and average flow velocity (SKM, 2011). The Deep Creek catchment has a time of concentration of 8.3 hr, while the other four catchments have much longer times of concentration, ranging from 27.8 to 38.9 hr. These require the estimates of spatial dependence across different durations of rainfall extremes. Although the spatial dependence across rainfall durations would be expected to be lower than across a single duration, since short- and long-rain events are often driven by different meteorological mechanisms (Zheng et al., 2015), it is nonetheless likely that some

level of spatial dependence would exist and need to be integrated into the risk calculations. This is particularly of relevance given extremal rainfall in this region is strongly associated with ‘east coast low’ systems off the eastern coastline, whereby extreme hourly rainfall bursts are often embedded in heavy multi-day rainfall events.

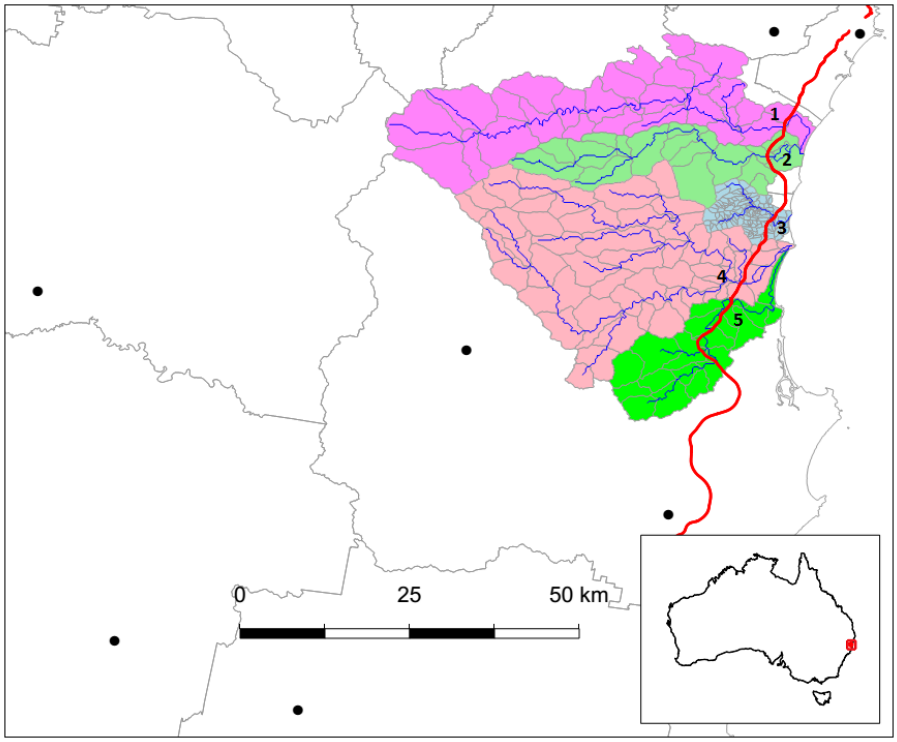

Figure 4.3. Map of the case study in New South Wales, Australia. The black dots indicate the rainfall gauges, the red line indicates the Pacific Highway upgrade project, and the blue lines indicate the main river network. The numbers from one to five indicate the locations of the main river crossings.

Table 4.1. Summary of properties for catchments in the case study.

No.	Catchment	Area (ha)	Raw time of concentration (hour)
1	Bellinger	77150	37
2	Kalang River	34140	33
3	Deep Creek	9180	8
4	Nambucca (upper)	102015	38
5	Warrell Creek	29440	27

The black circles in Fig. 4.3 represent the sub-daily rain stations used for this study. There were 7 sub-daily stations selected, with 35 years of record in common for the whole region. The data was available at a 5 minute interval and aggregated to longer durations. For convenience in comparing the times of concentration between the catchments, this study assumes a time of concentration of 9 hr for the Deep Creek catchment, while identical times of concentration of 36 hr are assumed for the other four catchments.

4.4. Methodology

This section provides the method used to estimate the conditional and joint probabilities of flood for civil infrastructure systems based on rainfall extremes, which is explained according to the steps shown in Fig. 4.4. First, the generalized Pareto distribution (GPD) is used as marginal distribution to fit to observed rainfall for all duration at each locations (Section 4.4.1). After that, an inverted max-stable process is introduced and then fitted to rainfall extremes of identical or different durations (Sections 4.4.2 & 4.4.3). The conditional and joint probabilities of rainfall are then estimated in Section 4.4.4, which is followed by the simulation to calculate areal reduction factor (ARF) in Section 4.4.5. An event-based rainfall-runoff model is employed in Section 4.4.6 to transform conditional rainfall to conditional flows. With an assumption that there is a one-to-one correspondence between rainfall intensity and flow rate, the joint flood probability for the case study is equal to the joint probability of rainfall. An analysis for the independent model (the case of complete independence) is also implemented for comparison.

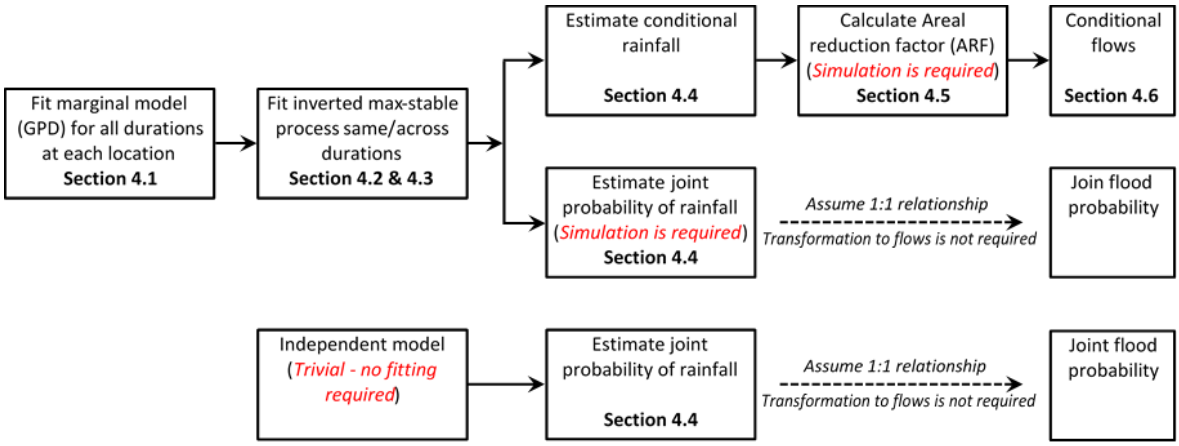

Figure 4.4. The flow chart for the overall methodology.

4.4.1. Marginal model for rainfall

This study defines extremes as those greater than some threshold u. For large u, the distribution of Y conditional on $Y > u$ may be approximated by the generalized Pareto distribution (GPD) (Davison and Smith, 1990; Pickands, 1975; Thibaud et al., 2013):

$$G(y) = 1 - \left\{1 + \frac{\xi(y-u)}{\sigma_u}\right\}^{-1/\xi}, \quad y > u, \tag{4.1}$$

defined on $\{y: 1 + \xi(y-u)/\sigma_u > 0\}$ where $\sigma_u > 0$ and $-\infty < \xi < +\infty$ are scale and shape parameters, respectively. The probability that a level y is exceeded is then $\Phi_u\{1 - G(y)\}$, where $\Phi_u = \Pr(Y > u)$.

The selection of the appropriate threshold u involves a trade-off between bias and variance. A threshold that is too low leads to bias because the GPD approximation is poor. A threshold too high leads to high variance because of a small number of excesses. Two diagnostic tests are used to determine the appropriate threshold u: the mean residual life plot and the parameter estimate plot (Coles, 2001; Davison and Smith, 1990). These methods use the stability property of a GPD, so that if a GPD is valid for all excesses

above u, then excesses of a threshold greater than u should also follow a GPD. Detailed guidance of these methods can be found in Coles (2001).

4.4.2. Dependence model for spatial rainfall

Consider rainfall as a stationary stochastic process Z_i associated with a location x_i in a region of interest. Models for spatial extremes often use the convention of transforming marginal values to a unit Fréchet distribution. An important property of dependence in the extremes is whether or not two variables are likely/unlikely to co-occur as the extremes become rarer, as this can significantly influence the estimate of frequency for flood events of large magnitude. This is referred to as asymptotic dependence/independence, respectively. For the case of asymptotic independence, the dependence structure becomes weaker as the extremal threshold increases, which is formally defined as $\lim_{z\to\infty} P\{Z_1 > z | Z_2 > z\} = 0$ for all $x_1 \neq x_2$. The spatial extent of a rainfall event with asymptotically independent extremes will diminish as its rarity increases.

An example of an asymptotically independent model is the inverted max-stable process (Wadsworth and Tawn, 2012). This study uses the Brown-Resnick form of equations from the family of an inverted max-stable process, and has been widely studied elsewhere (Asadi et al., 2015; Huser and Davison, 2013; Kabluchko et al., 2009; Oesting et al., 2017).

4.4.3. Fitting the dependence model

One simple way to calibrate dependence models is to fit them to data by matching a suitable statistic. The dependence structure of the inverted max-stable process is represented by the pairwise residual tail dependence coefficient (Ledford and Tawn, 1996).

For a generic continuous process Z_i associated with a specific location x_i the empirical pairwise residual tail dependence coefficient η for each pair of locations (x_1, x_2) is

$$\eta(x_1, x_2) = \lim_{y\to\infty} \frac{\log P\{Z_2 > z\}}{\log P\{Z_1 > z, Z_2 > z\}}. \tag{4.2}$$

The value of $\eta \in (0,1]$ indicates the level of extremal dependence between Z_1 and Z_2 (Coles et al., 1999), with lower values indicating lower dependence. An example of how to calculate the residual tail dependence coefficient is provided in Appendix 4A for a sample dataset.

To estimate the dependence structure of an inverted max-stable model, the theoretical residual tail dependence coefficient function is usually fitted to its empirical counterpart. Here the residual tail dependence coefficient function is assumed to only depend on the Euclidean distance between two locations $h = \|x_1 - x_2\|$. The theoretical residual tail dependence coefficient function for the inverted Brown-Resnick model is given as:

$$\eta(h) = \frac{1}{2\Phi\left\{\sqrt{\frac{\gamma(h)}{2}}\right\}}, \tag{4.3}$$

where Φ is the standard normal cumulative distribution function, h is the distance between two locations, and $\gamma(h)$ belongs to the class of variograms $\gamma(h) = \|h\|^{\beta}/q$ for $q > 0$ and

$\beta \in (0,2)$. The models are then fitted to the empirical residual tail dependence coefficients by modifying parameters q and β until the sum of squared errors is minimized.

In the case that extreme rainfall at locations x_1 and x_2 are of identical duration (i.e. both 36 hr), then the inverted max-stable process is fitted to the observations by minimizing the sum of the squared errors of the residual tail dependence coefficients. This information can be directly applied to the case where two catchments have a similar time of concentration owing to their similar shape and size. However, there are many instances when two catchments of interest will have differing times of concentration; in particular, when the extreme rainfall at location x_1 and x_2 are of different durations (e.g., 36 hr and 9 hr), the dependence is less than the case of 36 hr and 36 hr. This observation is evident when considering the special case of a single location, i.e. the same point is considered twice, at a distance of $h = 0$. For the case where the duration is the same, the rainfall values are identical and have perfect dependence, but when the duration of extremes are different the values are not identical and the dependence is less. Therefore, an adjustment needs to be made to ensure that the theoretical pairwise residual tail dependence coefficient function suitably represents the observed pairwise residual tail dependence coefficients for the case of extreme rainfalls of different durations.

Following Le et al. (2018b), an adjusted approach is used by adding a nugget to the variograms as:

$$\gamma_{ad.}(h) = h^{\beta}/q + c(D - d)/d, \tag{4.4}$$

where h, β, and q are the same as those in Eq. (4.3); d is the duration (in hours); $0 < d \leq D$, where D is the maximum duration of interest (e.g. $D = 36$ hr for the case study described in this paper); and c is a parameters to adjust dependence according to duration. This adjustment is intended to condition the behaviour of shorter duration extremes on a D-hour extreme of a specified magnitude. It is constructed to reflect the fact that when compared to a D-hour extreme, a shorter duration results in less extremal dependence. Cases involving conditioning of longer periods on shorter periods (such as a 36 hr extreme given a 9 hr extreme has occurred) would require a different relationship.

To fit the inverted max-stable process for all pairs of durations at locations x_1 and x_2 (i.e. 36 hr and 12 hr, 36 hr and 9 hr, 36 hr and 6 hr, 36 hr and 2 hr, 36 hr and 1 hr), the theoretical pairwise residual tail dependence coefficient function in Eq. (4.3) is used with the adjusted variogram from Eq. (4.4) where the parameters β and q are first obtained from the fitted results of the case of identical 36 hr durations at location x_1 and x_2. The parameter c is obtained by a least square fit of the residual tail dependence coefficient across all durations.

4.4.4. Estimate of conditional and joint probabilities of rainfall extremes

This section introduces general concepts for evaluating a conditional probability and a joint probability for a bivariate case. A detailed method is then presented for estimating the conditional probability and the joint probability for the realistic case of rainfall extremes.

Figure 4.5 illustrates a bivariate case for two locations x_1 and x_2 as a scatterplot of events (extremes and non-extremes) at two locations. The extremes are delineated for each location according to a specified threshold (e.g. $u = 0.98$ percentile) and to distinguish them, colour coding and different symbols have been used. The four regions have been labelled for ease of reference: (A) only Z_2 extreme events but not Z_1, (B) both Z_1 and Z_2 extreme, (C) only Z_1 extreme events but not Z_2, and (D) non-extreme events.

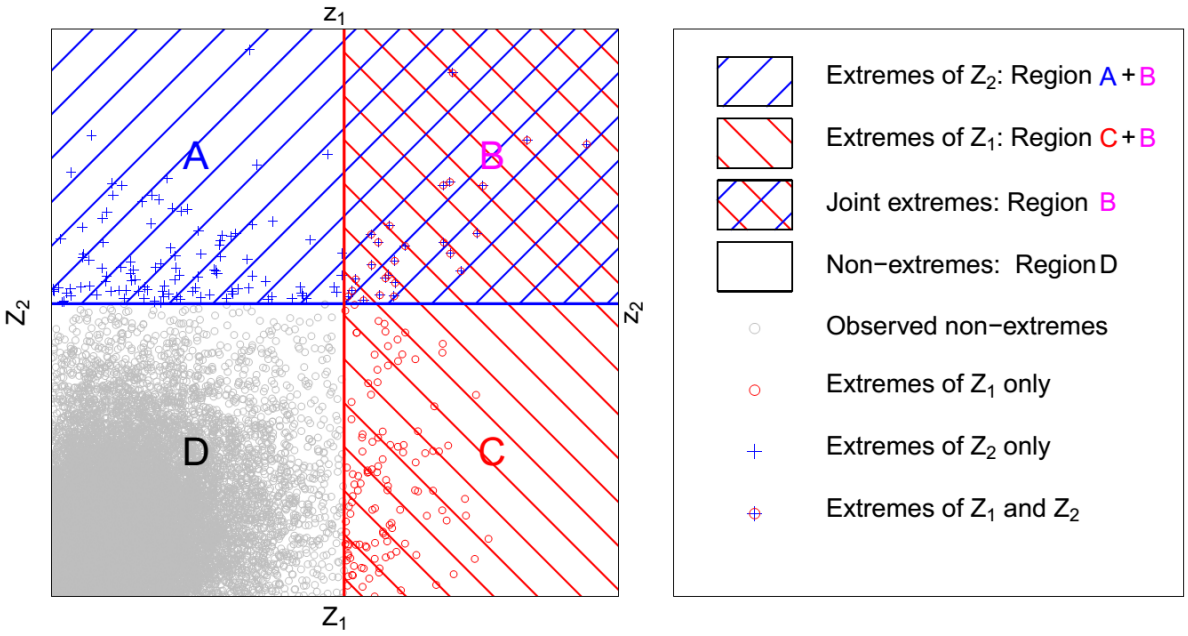

Figure 4.5. Illustration of general concept of probabilities for a bivariate case. Z_1 and z_1 indicate stochastic process Z and a threshold at location x_1; Z_2 and z_2 indicate stochastic process Z and a threshold at location x_2. Z_1 and Z_2 are in their original scales.

To explain how the joint and conditional probabilities are calculated, their definitions are provided in Table 4.2 with reference to the regions of Fig. 4.5. Rather than consider the specific case of a theoretical model of extremal rain (e.g. inverted max-stable), Table 4.2 presents these concepts more simply using only two variables and with generic probability estimates. Equations for both dependence and independence are provided in Table 4.2.

Table 4.2. Definition of joint and conditional probabilities and how to calculate them for the case of bivariate independent and dependent variables.

Case	Definition	Calculation
1. Conditional prob. dependent	$P\{Z_2 > z_2 \mid Z_1 > z_1\}$	$= P(B)/\{P(B) + P(C)\}$
2. Conditional prob. independent	$P\{Z_2 > z_2 \mid Z_1 > z_1\} = P\{Z_2 > z_2\}$	$= P(A) + P(B)$
3. Joint prob. dependent	$P\{Z_1 > z_1, Z_2 > z_2\}$	$= P(B)$
4. Joint prob. independent	$P\{Z_1 > z_1, Z_2 > z_2\} = P\{Z_1 > z_1\} \times P\{Z_2 > z_2\}$	$= \{P(B) + P(C)\}\{P(A) + P(B)\}$

Case 1: Conditional probability can be defined as the joint probability divided by the marginal probability $P\{Z_2 > z_2 \mid Z_1 > z_1\} = P\{Z_1 > z_1, Z_2 > z_2\}/P\{Z_1 > z_1\}$. For the

dependent case, the relationship is $P(B)/\{P(B)+P(C)\}$. Using these concepts, equations for the conditional probability of the inverted max-stable process have been derived in literature and are summarised in Appendix 4B. The detailed formulae are of the same nature as those in Table 4.2, and are used in this study to estimate conditional maps for return periods once the model has been fitted to all durations.

Case 2: Using the definition of $P\{Z_2 > z_2 | Z_1 > z_1\} = P\{Z_1 > z_1, Z_2 > z_2\}/P\{Z_1 > z_1\}$ for the independent case results in the exceedance probability for Z_2, which is $P(A) + P(B)$ (since intuitively Z_1 has no effect on exceedances of Z_2).

Case 3: For the case of dependent variables the joint exceedance is defined by $P(B)$. For the case of only two locations, the probability that there is at least one location that has an extreme event exceeding a given threshold is calculated as $P\{Z_1 > z_1 \text{ or } Z_2 > z_2\} = P\{Z_1 > z_1\} + P\{Z_2 > z_2\} - P\{Z_1 > z_1, Z_2 > z_2\}$. Here, $P\{Z_1 > z_1, Z_2 > z_2\}$ can be easily obtained from the bivariate CDF for inverted max-stable process in Eq. (B.1). However, for the case of multiple locations (five different locations for this paper), it is difficult to derive the formula for this probability because there are dependences between extreme events at all locations. So this probability is empirically calculated from a large number of simulations of the dependent model (see the description of the simulation procedure for an inverted max-stable process in Section 4.4.5). It is also noted that the case study contains five catchments, which have approximate times of concentration of either 36 hr or 9 hrs.

Case 4: Joint probability for independent variables is broken down as the product of the marginals. The exceedance probability for Z_1 is $P(B) + P(C)$ and the exceedance probability for Z_2 is $P(A) + P(B)$, and by definition their independent product will result in the joint probability. In order to compare with a situation of no spatial dependence of rainfall extremes, the probability that there is at least one location that has an extreme event exceeding a given threshold for the case that all of events are independent can be calculated based on the addition rule for the union of probabilities, as:

$$P(Z_1 > z_1 \text{ or } \dots \text{ or } Z_N > z_N) = \sum_{i=1}^{N} P(Z_i > z_i) - \sum_{i<j} P\left(Z_i > z_i, Z_j > z_j\right) + \cdots$$
$$+(-1)^{N-1} P(Z_1 > z_1, \dots, Z_N > z_N), \quad (4.5)$$

where N is the number of locations, and $P(Z_1 > z_1, \dots, Z_N > z_N) = P(Z_1 > z_1) \dots P(Z_N > z_N)$, because all of the events are independent.

4.4.5. Areal reduction factor estimation and simulation procedure for spatial rainfall

Before being transformed to flood flow through an event-based model, the point rainfall extremal estimates need to be converted to the average spatial rainfall using an areal reduction factor (ARF) (Ball et al., 2016). ARFs can be estimated from observed point rainfall data, but it is difficult to extrapolate ARFs for long return periods from observations with just 35 years of record for this study. To deal with this difficulty and to analyse the asymptotic behaviour of ARFs, Le et al. (2018a) proposed a framework to simulate ARFs for long return periods by using an inverted max-stable process, which is applied here for durations of 36 and 9 hrs.

The simulation procedure for spatial rainfall is implemented in two steps. In the first step, the Brown-Resnick process with unit Fréchet margins is simulated using the algorithm of Dombry et al. (2016) over a spatial domain (whether specific locations of interest or grid points), and then the inverted Brown-Resnick process with unit Fréchet margins is obtained through Eq. (4) and Eq. (5) in Le et al. (2018a). In the second step, the spatial rainfall processes are obtained by transforming the simulation of the inverted Brown-Resnick process in step 1 from unit Fréchet margins to the rainfall scaled margins using the GP distribution in Eq. (4.1) for rainfall magnitude above the threshold, and the empirical distribution for rainfall magnitude below the threshold. An advantage of this approach is that it can reflect the proportion of dry days in the empirical distribution by making the simulated rainfall contain zero values (Thibaud et al., 2013). Another advantage is that this approach guarantees that the marginal distributions of simulated rainfall below the threshold matches the observed marginal distributions. There may be a drawback of this approach by forcing the simulated rainfall to have the same extremal dependence structure for both parts below and above the threshold, which may not be true for non-extreme rainfall. However, the dependence structure of non-extreme rainfall contributes insignificantly to extreme events (Thibaud et al., 2013) and is unlikely to affect the results.

For calculating ARFs, the simulation is implemented separately for spatial rainfall of 36 and 9 hrs duration. After the simulated spatial rainfall for 36 and 9 hrs are respectively obtained, ARFs are calculated for each duration and different return periods, which can be found in the supplementary material (Fig. S4.1 and S4.2). When the interest is in the joint probability of rainfall extremes of different durations (see Case 3 in Section 4.4.4), the simulation of spatial rainfall should be implemented across multiple durations. In this case, each term of the covariance matrix is calculated from the dependence structure of the corresponding pair of locations.

4.4.6. Transforming rainfall extremes to flood flow

To estimate flood flow from rainfall extremes, the Watershed Bounded Network Model (WBNM) (Boyd et al., 1996), is employed in this study. WBNM calculates flood runoff from rainfall hyetographs. It divides the catchment into subcatchments, allowing hydrographs to be calculated at various points within the catchment, and allowing the spatial variability of rainfall and rainfall losses to be modelled. It separates overland flow routing from channel routing, allowing changes to either or both of these processes, for example in urbanised catchments. The rainfall extremes are estimated at the centroid of the catchment, and are converted to average spatial rainfall using the simulated ARFs described in Section 4.4.5 before estimation of the rainfall hyetographs.

Hydrological models for the case study area were developed and calibrated by engineering consultants (WMAWater, 2011). As an example, Fig. 4.6 provides details of the hydrological models for the Bellinger catchment and Kalang River catchment in the North. The plots for details of the hydrological models for the Nambucca basin in the South and the Deep Creek catchment in the East can be found in the supplementary material (Fig. S4.3 and S4.4).

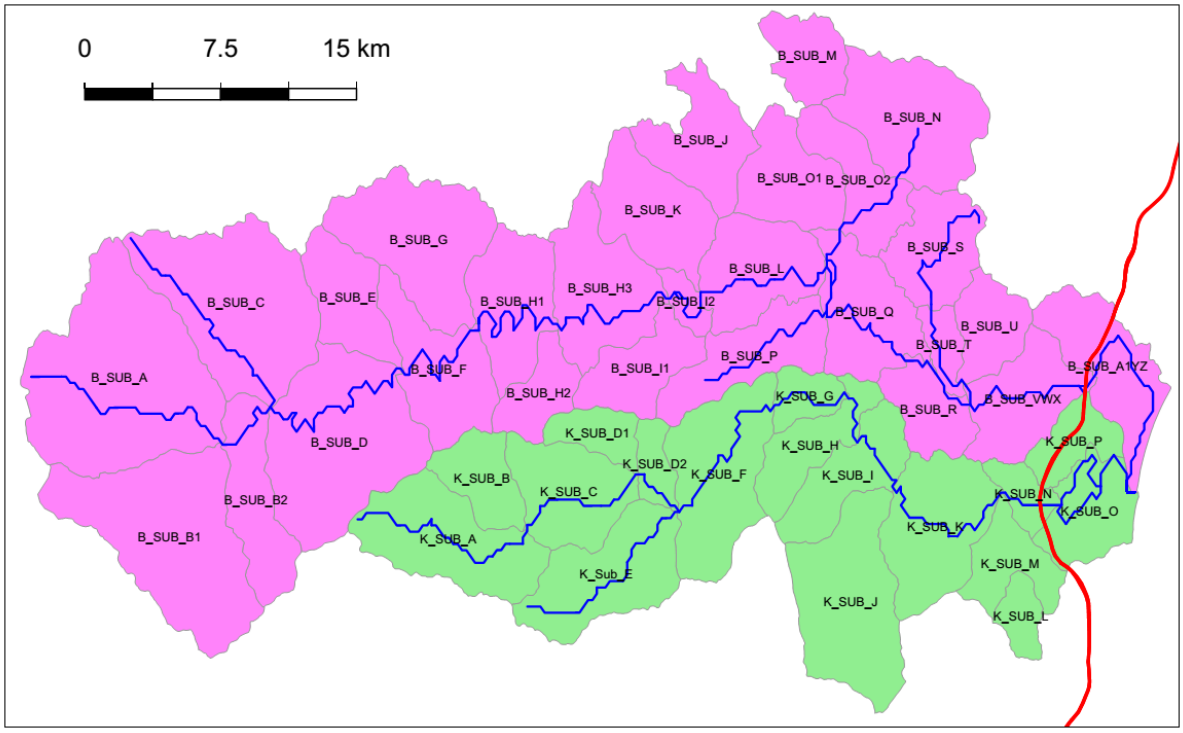

Figure 4.6. Hydrological model layout for Bellinger catchment and Kalang River catchment. The blue lines are the river network, and the red line is the Pacific Highway upgrade project.

4.5. Results and discussion

4.5.1. Evaluation of model for space-duration rainfall process

A GPD with an appropriate threshold was fitted to the observed rainfall data for 36 hr and 9 hr durations, and the Brown-Resnick inverted max-stable process model was calibrated to determine the spatial dependence.

Analysis of the rainfall records led to the selection of a threshold of 0.98 for all records as reasonable across the spatial domain and the GPD was fitted to data above the selected threshold. Figure 4.7 shows QQ plots of the marginal estimates for a representative station for two durations 36 and 9 hr. Overall the quality of fitted distributions is good and plots for all other stations can be found in the supplementary material (Fig. S4.5 and S4.6).

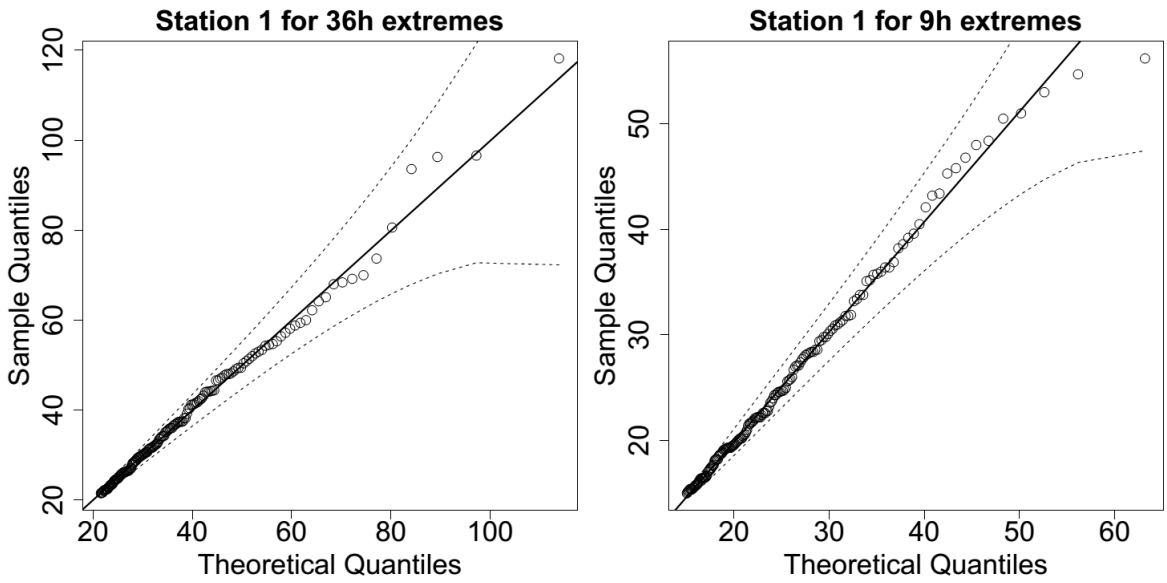

Figure 4.7. QQ plots for the fitted GPD at one representative station, dotted lines are the 95% confidence bounds, and the solid diagonal line indicates a perfect fit.

The inverted max-stable process across different durations was calibrated to determine dependence parameters. The theoretical pairwise residual tail dependence coefficient function between two locations (x_1 and x_2) was calculated based on Eq. (4.3) and Eq. (4.4), and the observed pairwise residual tail dependence coefficient η was calculated using Eq. (4.2). The model has a reasonable fit to the observed data given the small number of dependence parameters. Figure 4.8 shows the pairwise residual tail dependence coefficients for the Brown-Resnick inverted max-stable process versus distance. The black points are the observed pairwise residual tail dependence coefficients, while the red lines are the fitted pairwise residual tail dependence coefficient functions. A coefficient equal to 1 indicates complete spatial dependence, and a value of 0.5 indicates complete spatial independence. The top-left panel shows the dependence between 36 hr extremes across space, with the distance $h = 0$ corresponding to "complete dependence". It also shows the dependence decreasing with increasing distance.

The remaining panels of Fig. 4.8 show the dependence of 36 vs. 9 hr extremes, 36 vs. 6 hr extremes, and 36 vs. 3 hr extremes, with the latter two duration combinations not being used directly in the study but nonetheless showing the model performance across several durations. As expected, the dependence levels are weaker compared with 36 vs. 36 hr extremes at the same distance, especially at the distance of 0. This is expected, as the dependence at the same site between annual maxima at different durations will be lower than between annual maxima at the same duration. This is because the annual maxima of different durations may arise from different storm events (Zheng et al., 2015).

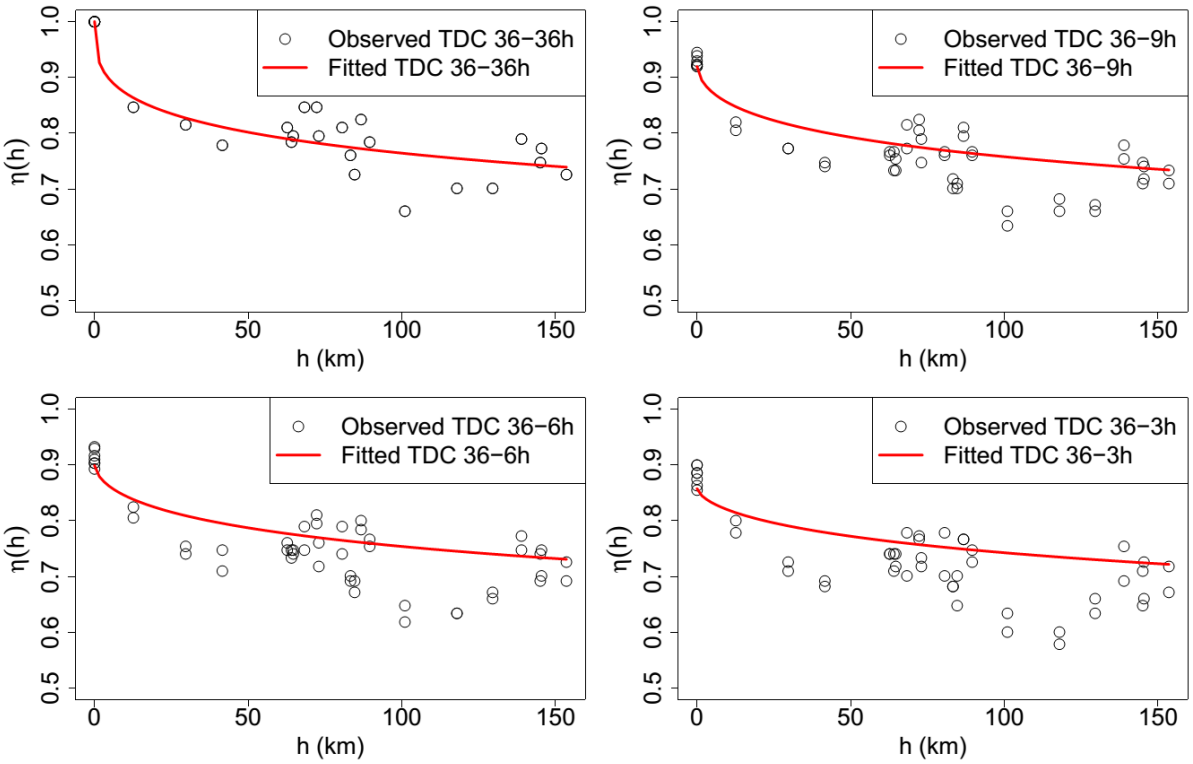

Figure 4.8. Plots of pairwise residual tail dependence coefficient (TDC) against distance for 36 hr extremes and 36 hr extremes (top left), for 36 hr extremes and 9 hr extremes (top right), for 36 hr extremes and 6 hr extremes (bottom left), and for 36 hr extremes and 3 hr extremes (bottom right). The black points are estimated residual tail dependence coefficients (TDC) for pairs of sub-daily stations, and the red lines are theoretical residual tail dependence coefficient (TDC) function.

4.5.2. Estimating conditional rainfall extremes and corresponding conditional flows for evacuation route design

The recommended approach for estimating conditional rainfall extremes is demonstrated by considering a hypothetical evacuation route across location x_2, given a flood occurs at location x_1, evaluated using Eq. (4B.3). This approach is applied to a case study of the Pacific Highway upgrade project that contains five main river crossings (from Fig. 4.3). For evacuation purposes, we need to know "what is the probability that a bridge fails only once on average every M times (e.g., $M = 10$ for a 10-year event) that its neighbouring bridge is flooded?" This section provides the conditional estimates for two pairs of neighbouring bridges in the case study that have the shortest Euclidean distances, i.e. pairs (x_1, x_2) and (x_2, x_3). The comparisons of unconditional and conditional maps are given in Fig. 4.9 and Fig. 4.10, and the corresponding unconditional and conditional flows are given in Fig. 4.11.

The left panel of Fig. 4.9 provides the pointwise 10-year unconditional return level map over the case study area for 36 hr rainfall extremes. The value at the location of interest—the blue star (the centroid of Bellinger catchment)—is around 260 mm. The right panel of Fig. 4.9 indicates that when accounting for the effect of a 20-year event for 36 hr rainfall extremes happening at the location of the red star (the centroid of Kalang River catchment), the pointwise 10-year conditional return level at the blue star rises to around 453 mm (i.e., 1.74 times the unconditional value).

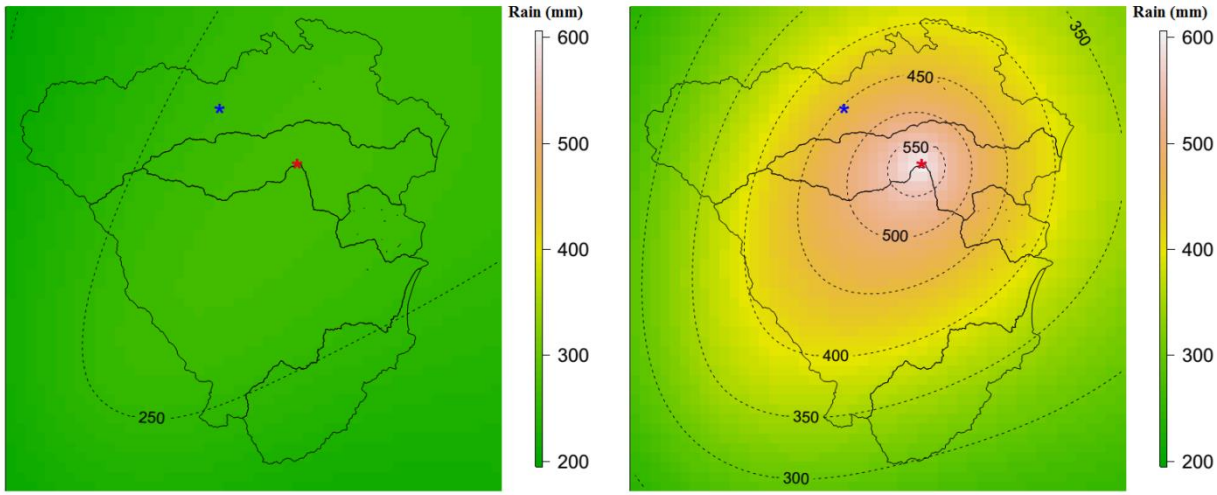

Figure 4.9. Pointwise 10-year unconditional return level map (mm) for 36 hr extremes (left), and pointwise 10-year conditional return level map (mm) for 36 hr extremes given a 20-year event for 36 hr extremes happen at location of the red star for the centroid of Kalang River catchment (right). The colour scales are the same for comparison.

Figure 4.10 provides similar plots to Fig. 4.9 for another pair of locations having different durations of rainfall extremes due to different times of concentration in each catchment. Here, the location of interest is the centroid of the Deep Creek catchment (the blue star in Fig. 4.10) and the conditional point is the centroid of the Kalang River catchment (the red star in Fig. 4.10). The pointwise 10-year unconditional and conditional return levels at the location of the blue star are 134 mm and 194 mm, respectively. The relative difference between the conditional and unconditional return levels is only 1.45 times, compared with 1.74 times for the case in Fig. 4.9. This is because the pair of locations in Fig. 4.10 has a longer distance than those in Fig. 4.9, so that the dependence level is weaker. Moreover, the location pair in Fig. 4.10 was analysed for different durations (between 36 and 9 hr extremes), which has weaker dependence than the case of the equivalent durations in Fig. 4.9 (between 36 and 36 hr), based on Fig. 4.8.

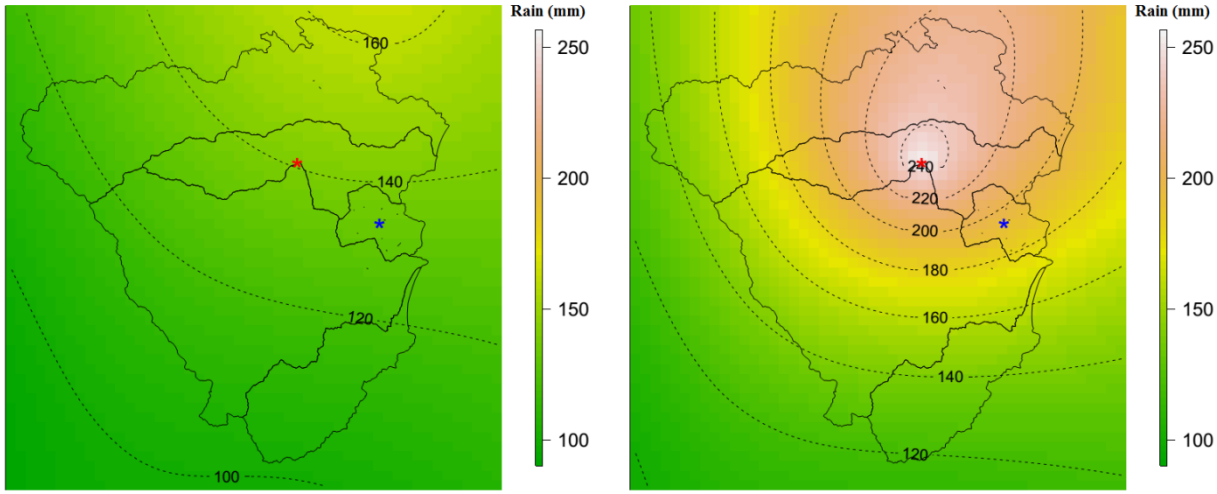

Figure 4.10. Pointwise 10-year unconditional return level map (mm) for 9 hr extremes (left), and pointwise 10-year conditional return level map (mm) for 9 hr extremes, given a 20-year event for 36 hr extremes

happens at location of the red star for the centroid of the Kalang River catchment (right). The colour scales are the same for comparison.

The unconditional and conditional return levels are transformed to flood flows via the hydrological model WBNM previously calibrated to each catchment (WMAWater, 2011). The unconditional and conditional return levels were extracted at the centroid of each main catchment, which were then converted to the average spatial rainfall using an areal reduction factor (ARF). The corresponding unconditional and conditional flood flows at the river crossing in the Bellinger catchment (corresponding to the unconditional and conditional rainfall extremes in Fig. 4.9) are given in Fig. 4.11 (left panel). Similar plots for the river crossing in the Deep Creek catchment (corresponding to the unconditional and conditional rainfall extremes in Fig. 4.10) are given in Fig. 4.11 (right panel).

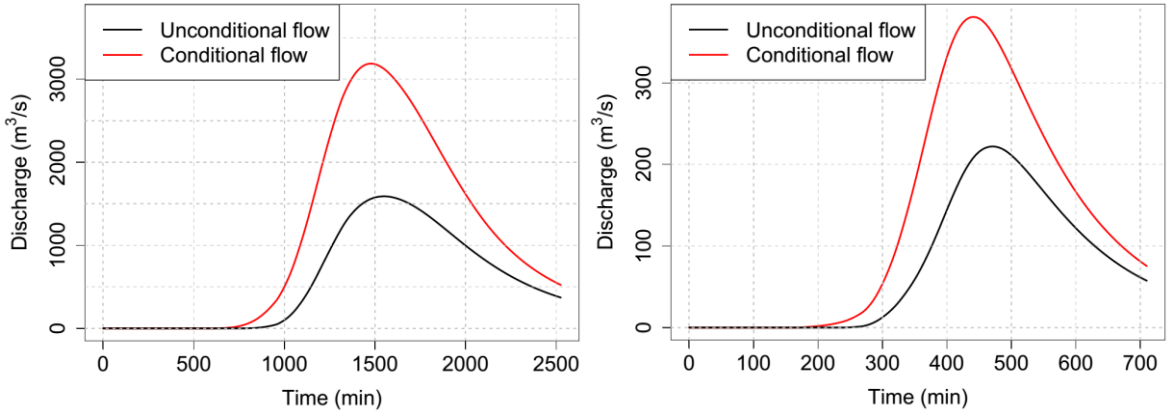

Figure 4.11. Comparison between conditional flows (red line) and unconditional flows (black line). (left) At the river crossing in the Bellinger catchment: conditional flow caused by a 10 year conditional event for 36 hr rainfall in considering the effect of a 20 year event for 36 hr rainfall occurring at the river crossing in the Kalang River catchment, and unconditional flow caused by a 10 year unconditional event for 36 hr. (right) At the river crossing in the Deep Creek catchment: conditional flow caused by a 10 year conditional event for 9 hr rainfall in considering the effect of a 20 year event for 36 hr rainfall occurring at the river crossing in the Kalang River catchment, and unconditional flow caused by a 10 year unconditional event for 9 hr rainfall.

The left panel of Fig. 4.11 indicates that the peak conditional flow at the river crossing in the Bellinger catchment is almost 2.0 times higher than that for unconditional flow. The time taken to reach to the peaks is the same for both cases. This is because this river crossing is affected by a large region with a long time of concentration (36 hr); the impact of rainfall losses on the hydrograph is insignificant. This difference is a direct result of the conditional relationship being more stringent than the unconditional relationship. Given that there is an existing extreme event nearby, it is more likely for an extreme event to occur at another location of interest in the region. If a bridge design were to take into account this extra criterion for the purposes of evacuation planning it would require the design to be at a higher level.

Shown in the right panel in Fig. 4.11, the peak of the conditional flow at the river crossing in the Deep Creek catchment occurred earlier, and is around 1.7 times higher than that for the unconditional flow. This is due to the fact that the river crossing in Deep Creek covers a small region with a short time of concentration (9 hr) and the impact of rainfall losses on the hydrograph is significant.

Although Fig. 4.11 shows a difference in terms of the time taken to reach the peak flows, the two design hydrographs are separate and this is not a physical timing difference. The relevant feature of the conditional design hydrograph is the peak, and timing information is not a part of the method.

The difference between the maximum discharge of conditional and unconditional flows at the river crossing in the Bellinger catchment is shown in Fig. 4.12 for the case of a 20-year event occurring in the Kalang River catchment nearby. The relationship with annual exceedance probability AEP indicates that the difference between the maximum discharge of conditional and unconditional flows decreases when AEP increases, and that the difference approaches zero when the AEP increases to above 50% (i.e. a 2-year return period).

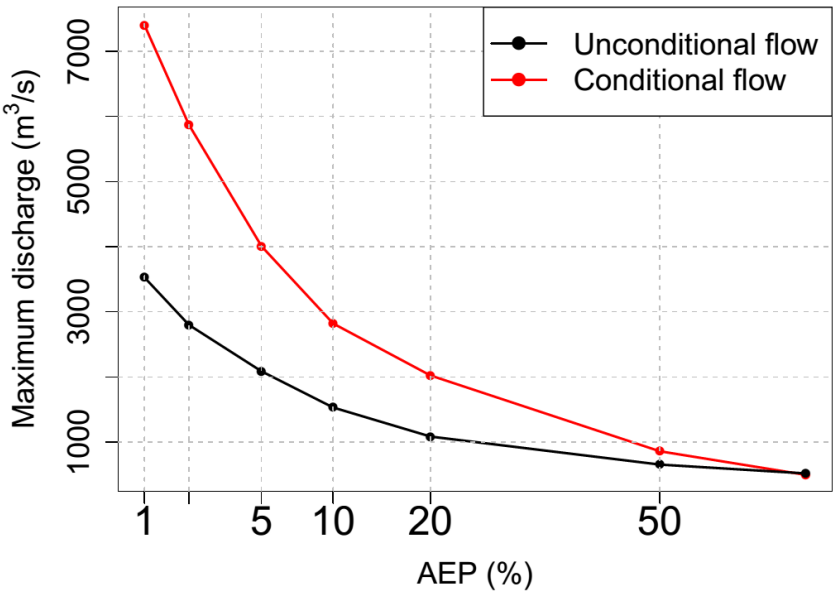

Figure 4.12. Plot for peak of conditional flow (red points) caused by conditional flood-producing rainfall and peak of unconditional flow (black points) for different annual exceedance probabilities (AEP) at the river crossing in the Bellinger catchment. This plot considers the effect of a 20-year event occurring at the river crossing in the Kalang River catchment. The horizontal axis is constructed at a double log scale for viewing purposes.

4.5.3. Estimating the failure probability of the highway section based on the joint probability of rainfall extremes

The recommended approach for estimating the overall failure probability of a system is demonstrated by considering a hypothetical traffic system with multiple river crossings at locations $x_1, \ldots, x_N$. If there is a one-to-one correspondence between extreme rainfall intensity and flood magnitude, the overall failure probability will be approximately equal to the probability that there is at least one river crossing whose contributing catchment has rainfall extremes exceeding the design level, which can be estimated using a large number of simulations from the spatial rainfall model. This approach is applied to the Pacific Highway upgrade project containing five river crossings. A set of 10,000 year simulated rainfall (Section 4.4.5) is generated from the fitted model (Section 4.5.1) to calculate the overall failure probability of the highway section. This process is repeated 100 times to

estimate the average failure probability, under the assumption that all river crossings are designed to the same individual failure probability.

Figure 4.13 is a plot of the overall failure probability of the highway and the failure probability of each individual river crossing (black). Similar relationships for the cases of complete dependence (blue) and complete independence (red) are also provided for comparison. For the case of complete dependence, when the whole region is extreme at the same time, the overall failure probability of the highway is equal to the individual river crossing failure probability and it represents the best case (the lowest overall failure probability). The worst case is complete independence where extremes do not happen together unless by random chance; this means the failure probability of the highway is much higher than that for individual river crossings. Taking into account the real dependence, there are some extremes that align and it seems from the Fig. 4.13 that this is a relatively weak effect. As an example from Fig. 4.13, to design the highway with a failure probability of 1% annual exceedance probability (AEP), we would have to design each individual river crossing to a much rarer AEP of 0.25% (see green lines in Fig. 4.13).

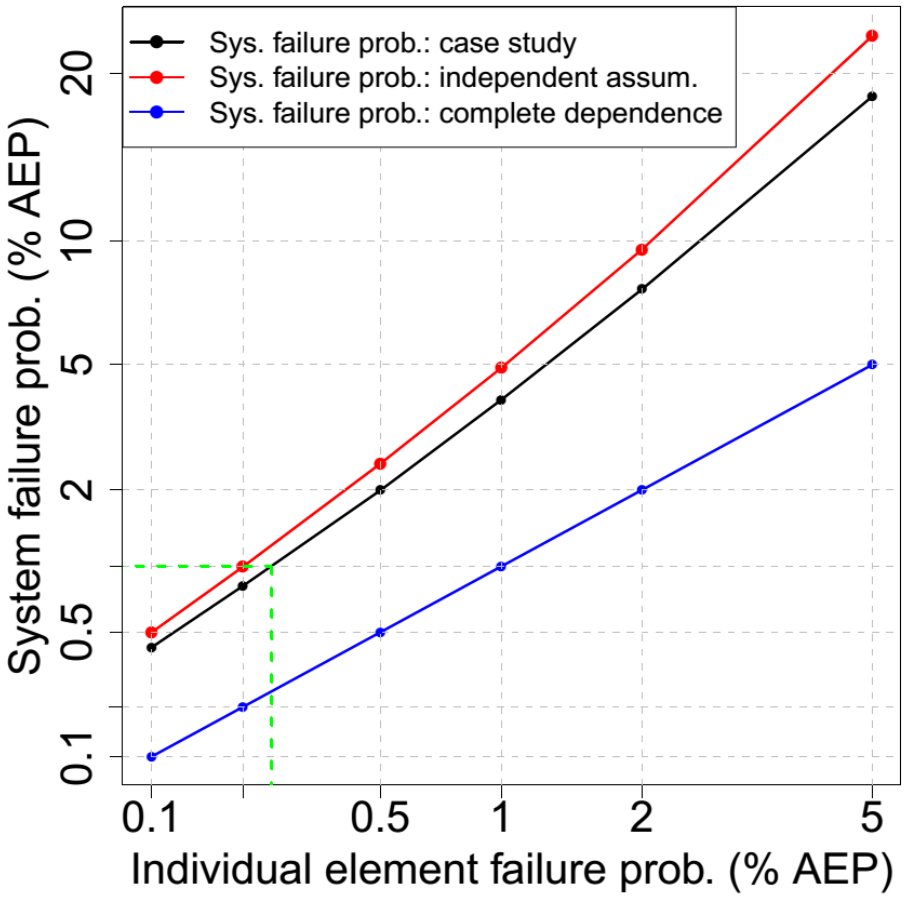

Figure 4.13. Relationship between system failure probability and individual element failure probability in % annual exceedance probability (% AEP). The black colour is for the case study, the red colour is for the case of complete independence, and the blue is for the case of complete dependence. The green lines help to interpolate the individual element failure probability from a given system failure probability of 1%. Both horizontal axis and vertical axis are constructed at a double log scale for viewing purposes.

4.6. Discussion and Conclusions

Hydrological design has conventionally focussed on individual catchments and individual extremes. Such an approach can lead to an underestimation of wider system risk of flooding since weather systems exhibit dependence in space and time, which can lead to the coincidence of extremes. A number of methods have been developed to address the problem of antecedent moisture within a single catchment, by accounting for the temporal dependence of rainfall at locations of interest through loss parameters or sampling rainfall patterns (Rahman et al., 2002). However, there have been fewer methods that account for the spatial dependence of rainfall across multiple catchments, due in part to the complexity of representing the effects of spatial dependence in risk calculations. Different catchments can have different times of concentration, so spatial dependence may also imply the need to consider dependence across different durations of extreme rainfall bursts.

Recent and ongoing advances in modelling spatial rainfall extremes provide an opportunity to revisit the scope of hydrological design. Such models include a max-stable model fitted using a Bayesian hierarchical approach (Stephenson et al., 2016), max-stable and inverted max-stable models (Nicolet et al., 2017; Padoan et al., 2010; Russell et al., 2016; Thibaud et al., 2013; Westra and Sisson, 2011) and latent-variable Gaussian models (Bennett et al., 2016b). The ability to simulate rainfall over a region means that hydrological problems need not be confined to individual catchments, but may cover multiple catchments. Civil infrastructure systems such as highways, railways or levees are such examples, since the failure of any one element may lead to overall failure of the system. Alternatively, where there is a network, the failure of one element may have implications for the overall system to accommodate the loss, by considering alternative routes. With models of spatial dependence and duration dependence of extremes there is a new and improved ability to address these problems explicitly as part of the design methodology.

This paper demonstrated an application for evaluating conditional and joint probabilities of flood at different locations. This was achieved with two examples: (i) the design of a river crossing that will fail once on average every M times given that its neighbouring river crossing is flooded; and (ii) estimating the probability that a highway section, which contains multiple river crossings, will fail based on the failure probability of each individual river crossing. Due to the lack of continuous streamflow data and subdaily limitations of rain-based continuous simulation, this study used an event-based method of conditional and joint rainfall extremes to estimate the corresponding conditional and joint flood flows. The spatial rainfall was simulated using an asymptotically independent model, which was then used to estimate conditional and joint rainfall extremes. An empirical method was obtained from the framework of Le et al. (2018b) to make an asymptotically independent model—the inverted max-stable process—able to capture the spatial dependence of rainfall extremes across different durations. The fitted residual tail dependence coefficient function showed that the model can capture the dependence for different pairs of durations. For our example, the highest ratio of conditional to unconditional extremes was 1.74, for the two catchments having the strongest dependence (Fig. 4.9). The corresponding conditional flows were then estimated using a hydrological

model WBNM and shown to be strongly related to the ratio of conditional and unconditional rainfall extremes (Fig. 4.11).

The joint probability of rainfall extremes for all catchments and for all possible pairs of catchments in the case study area was estimated empirically from a set of 10,000 years of simulated rainfall extremes, repeated 100 times to estimate the average value. The results showed that there were differences in the failure probability of the highway after taking into account the rainfall dependence, but the effect was not as emphatic as with the case of conditional probabilities. The difference in the failure probability became weaker as the return period increased, which is consistent with the characteristic of asymptotically independent data (Ledford and Tawn, 1996; Wadsworth and Tawn, 2012). A relationship was demonstrated (Fig. 4.13) to show how the design of the overall system to a given failure probability requires the design of each individual river crossing to a rarer extremal level than when each crossing is considered in isolation. For the case study example, it would be necessary to design each bridge to a 0.25% AEP event in order to obtain a system failure probability of 1%.

There is a need to reimagine the role of intensity-duration-frequency curves. Conventionally they have been developed as maps of the marginal rainfall in a point-wise manner for all locations and for a range of frequencies and durations. The increasing sophistication of mathematical models for extremes, computational power and interactive graphics abilities of online mapping platforms means that analysis of hydrological extremes could significantly expand in scope. With an underlying model of spatial and duration dependence between the extremes, it is not difficult to conceive of digital maps that dynamically transform from the marginal representation of extremes to the corresponding representation conditional extremes after any number of conditions are applied. This transformation is exemplified by the differences between left and right panels in Fig. 4.9 and Fig. 4.10. Enhanced IDF maps would enable a very different paradigm of design flood risk estimation, breaking away from analysing individual system elements in isolation to emphasize the behaviour of entire system.

Appendix 4A. Calculation of empirical tail dependence coefficient

To illustrate how Eq. (4.2) in the manuscript is calculated, consider a set of $n = 10$ observed values at the two locations: Z_1 and Z_2 (see Table 4A.1). First, Z_1 and Z_2 are converted to empirical cumulative probability estimates via the Weibull plotting position formula $P = j/(n+1)$ where j is ranked index of a data point giving P_1 and P_2 (see Table 4A.1).

Table 4A.1. Observed data Z_1 and Z_2 and corresponding empirical cumulative probabilities P_1 and P_2.

Z_1	Z_2	P_1	P_2
5	10	0.455	0.909
9	1	0.818	0.091
1	7	0.091	0.636
2	6	0.182	0.545
10	4	0.909	0.364
3	3	0.273	0.273
8	9	0.727	0.818
6	2	0.545	0.182
4	8	0.364	0.727
7	5	0.636	0.455

Assume that interest is in values above a threshold $u = 0.5$, in other words, $P\{Z_2 > z\} = P\{P_2 > u\} = 0.5$. In this case we have only one pair, at the index of 7, that satisfy both P_1 and P_2 are greater than $u = 0.5$, thus $P\{Z_1 > z, Z_2 > z\} = P\{P_1 > u, P_2 > u\} = 1/10 = 0.1$. The calculation of the empirical tail dependence coefficient is then

$$\eta(x_1, x_2) = \frac{\log P\{Z_2 > z\}}{\log P\{Z_1 > z, Z_2 > z\}} = \frac{\log P\{P_2 > u\}}{\log P\{P_1 > u, P_2 > u\}} = \frac{\log(0.5)}{\log(0.1)} = 0.301. \quad (4A.1)$$

Appendix 4B. Equations for bivariate conditional and joint probabilities for inverted max-stable

In the context of this study, the conditional probability $P\{Z_2 > z_2 | Z_1 > z_1\}$ is obtained from the bivariate inverted max-stable process cumulative distribution function (CDF) in unit Fréchet margins (Thibaud et al., 2013), which is given as:

$$P\{Z_1 \le z_1, Z_2 \le z_2\} = 1 - \exp\left\{-\frac{1}{g_1}\right\} - \exp\left\{-\frac{1}{g_2}\right\} + \exp[-V\{g_1, g_2\}], \quad (4B.1)$$

where $g_1 = -1/\log\{1 - \exp(-1/z_1)\}$, $g_2 = -1/\log\{1 - \exp(-1/z_2)\}$, and the exponent measure V (Padoan et al., 2010) is defined as:

$$V\{g_1, g_2\} = -\frac{1}{g_1}\Phi\left\{\frac{a}{2} + \frac{1}{a}log\frac{g_2}{g_1}\right\} - \frac{1}{g_2}\Phi\left\{\frac{a}{2} + \frac{1}{a}log\frac{g_1}{g_2}\right\}. \quad (4B.2)$$

In Eq. (4B.2), Φ is the standard normal cumulative distribution function, $a = \sqrt{2\gamma_{ad.}(h)}$ with $\gamma_{ad.}(h)$ is the variograms that was mentioned in the explanation of Eq. (4.4) in the manuscript.

In unit Fréchet margins, the relationship between the return level z and the return period T is given as $z = -1/log(1 - 1/T)$, and the conditional probability for the max-stable process can then be estimated using:

$$P\{Z_2 > z_2 | Z_1 > z_1\} = T_1 \left[\frac{1}{T_1} - \exp\left(-\frac{1}{z_2}\right) + P\{Z_1 \leq z_1, Z_2 \leq z_2\}\right], \quad (4B.3)$$

where T_1 is the return period corresponding to the return level z_1.

Acknowledgments

The lead author was supported by the Australia Awards Scholarships (AAS) from Australia Government. A/Prof Westra was supported by Australian Research Council Discovery grant DP150100411. We thank Mark Babister and Isabelle Testoni of WMA Water for providing the hydrologic models for the case study; and Leticia Mooney for her editorial help in improving this manuscript. The rainfall data used in this study were provided by the Australian Bureau of Meteorology, and can be obtained from the corresponding author.

References

Asadi, P., Davison, A. C., and Engelke, S.: Extremes on river networks, Ann. Appl. Stat., 9, 2023-2050, 2015.

Ball, J., Babister, M., Nathan, R., Weeks, W., Weinmann, E., Retallick, M., and Testoni, I.: Australian Rainfall and Runoff: A Guide to Flood Estimation, © Commonwealth of Australia (Geoscience Australia), 2016.

Baxevani, A. and Lennartsson, J.: A spatiotemporal precipitation generator based on a censored latent Gaussian field, Water Resources Research, 51, 4338-4358, 2015.

Bennett, B., Lambert, M., Thyer, M., Bates, B. C., and Leonard, M.: Estimating Extreme Spatial Rainfall Intensities, Journal of Hydrologic Engineering, 21, 04015074, 2016a.

Bennett, B., Thyer, M., Leonard, M., Lambert, M., and Bates, B.: A comprehensive and systematic evaluation framework for a parsimonious daily rainfall field model, Journal of Hydrology, doi: https://doi.org/10.1016/j.jhydrol.2016.12.043, 2016b. 2016b.

Bernard, M. M.: Formulas for rainfall intensities of long duration, Transactions of the American Society of Civil Engineers, 96, 592-606, 1932.

Boughton, W. and Droop, O.: Continuous simulation for design flood estimation—a review, Environmental Modelling & Software, 18, 309-318, 2003.

Boyd, M. J., Rigby, E. H., and VanDrie, R.: WBNM — a computer software package for flood hydrograph studies, Environmental Software, 11, 167-172, 1996.

Brown, B. M. and Resnick, S. I.: Extreme Values of Independent Stochastic Processes, Journal of Applied Probability, 14, 732-739, 1977.

Cameron, D. S., Beven, K. J., Tawn, J., Blazkova, S., and Naden, P.: Flood frequency estimation by continuous simulation for a gauged upland catchment (with uncertainty), Journal of Hydrology, 219, 169-187, 1999.

Chow, V. T., Maidment, D. R., and Mays, L. W.: Applied Hydrology, McGraw-Hill, c1988, New York, 1988.

Coles, S.: An Introduction to Statistical Modeling of Extreme Values, Springer, 2001.

Coles, S., Heffernan, J., and Tawn, J.: Dependence Measures for Extreme Value Analyses, Extremes, 2, 339-365, 1999.

Davison, A. C. and Smith, R. L.: Models for exceedances over high thresholds, Journal of the Royal Statistical Society. Series B (Methodological), 1990. 393-442, 1990.

de Haan, L.: A Spectral Representation for Max-stable Processes, The Annals of Probability, 12, 1194-1204, 1984.

Dombry, C., Engelke, S., and Oesting, M.: Exact simulation of max-stable processes, Biometrika, 103, 303-317, 2016.

Favre, A. C., Adlouni, S. E., Perreault, L., Thiémonge, N., and Bobée, B.: Multivariate hydrological frequency analysis using copulas, Water Resources Research, 40, 2004.

He, Y., Bárdossy, A., and Zehe, E.: A review of regionalisation for continuous streamflow simulation, Hydrology and Earth System Sciences, 15, 3539, 2011.

Huser, R. and Davison, A. C.: Composite likelihood estimation for the Brown–Resnick process, Biometrika, 100, 511-518, 2013.

Kabluchko, Z., Schlather, M., and de Haan, L.: Stationary Max-Stable Fields Associated to Negative Definite Functions, The Annals of Probability, 37, 2042-2065, 2009.

Kao, S.-C. and Govindaraju, R. S.: Trivariate statistical analysis of extreme rainfall events via the Plackett family of copulas, Water Resources Research, 44, 2008.

Kleiber, W., Katz, R. W., and Rajagopalan, B.: Daily spatiotemporal precipitation simulation using latent and transformed Gaussian processes, Water Resources Research, 48, 2012.

Koutsoyiannis, D., Kozonis, D., and Manetas, A.: A mathematical framework for studying rainfall intensity-duration-frequency relationships, Journal of Hydrology, 206, 118-135, 1998.

Kuichling, E.: The relation between the rainfall and the discharge of sewers in populous districts, Transactions of the American Society of Civil Engineers, 20, 1-56, 1889.

Laurenson, E. M. and Mein, R. G.: RORB Version 4 Runoff Routing Program User Manual, Monash University Department of Civil Engineering, 1997.

Le, P. D., Davison, A. C., Engelke, S., Leonard, M., and Westra, S.: Dependence properties of spatial rainfall extremes and areal reduction factors, Journal of Hydrology, Submitted, 2018a.

Le, P. D., Leonard, M., and Westra, S.: Modeling Spatial Dependence of Rainfall Extremes Across Multiple Durations, Water Resources Research, 54, 2233-2248, 2018b.

Ledford, A. W. and Tawn, J. A.: Statistics for Near Independence in Multivariate Extreme Values, Biometrika, 83, 169-187, 1996.

Leonard, M., Lambert, M. F., Metcalfe, A. V., and Cowpertwait, P. S. P.: A space-time Neyman–Scott rainfall model with defined storm extent, Water Resources Research, 44, 2008.

Leonard, M., Westra, S., Phatak, A., Lambert, M., Hurk, B. v. d., McInnes, K., Risbey, J., Schuster, S., Jakob, D., and Stafford-Smith, M.: A compound event framework for understanding extreme impacts, Wiley Interdisciplinary Reviews: Climate Change, 5, 113-128, 2014.

Mulvaney, T. J.: On the use of self-registering rain and flood gauges in making observation of the relation of rainfall and floods discharges in a given catchment, Proc. Civ. Eng. Ireland, 4, 18–31, 1851.

Nicolet, G., Eckert, N., Morin, S., and Blanchet, J.: A multi-criteria leave-two-out cross-validation procedure for max-stable process selection, Spatial Statistics, 22, 107-128, 2017.

Oesting, M., Schlather, M., and Friederichs, P.: Statistical post-processing of forecasts for extremes using bivariate Brown-Resnick processes with an application to wind gusts, Extremes, 20, 309-332, 2017.

Padoan, S. A., Ribatet, M., and Sisson, S. A.: Likelihood-Based Inference for Max-Stable Processes, Journal of the American Statistical Association, 105, 263-277, 2010.

Pathiraja, S., Westra, S., and Sharma, A.: Why continuous simulation? The role of antecedent moisture in design flood estimation, Water Resources Research, 48, 2012.

Pickands, J.: Statistical Inference Using Extreme Order Statistics, The Annals of Statistics, 3, 119-131, 1975.

Rahman, A., Weinmann, P. E., Hoang, T. M. T., and Laurenson, E. M.: Monte Carlo simulation of flood frequency curves from rainfall, Journal of Hydrology, 256, 196-210, 2002.

Rasmussen, P. F.: Multisite precipitation generation using a latent autoregressive model, Water Resources Research, 49, 1845-1857, 2013.

Russell, B. T., Cooley, D. S., Porter, W. C., and Heald, C. L.: Modeling the spatial behavior of the meteorological drivers' effects on extreme ozone, Environmetrics, 27, 334-344, 2016.

Schlather, M.: Models for Stationary Max-Stable Random Fields, Extremes, 5, 33-44, 2002.

Seneviratne, S. I., Nicholls, N., Easterling, D., Goodess, C. M., Kanae, S., Kossin, J., Luo, Y., Marengo, J., McInnes, K., and Rahimi, M.: Managing the Risks of Extreme Events and Disasters to Advance Climate Change Adaptation: Changes in Climate Extremes and their Impacts on the Natural Physical Environment, 2012.

SKM:
http://www.nambucca.nsw.gov.au/cp_content/resources/16152_2011__Nambucca_Heads_Flood_Study_Final_Draft_Chapter_6a.pdf, 2011.

Stedinger, J., Vogel, R., and Foufoula-Georgiou, E.: Frequency Analysis of Extreme Events. In: Handbook of Hydrology, Maidment, D. R. (Ed.), McGraw-Hill, New York, 1993.

Stephenson, A. G., Lehmann, E. A., and Phatak, A.: A max-stable process model for rainfall extremes at different accumulation durations, Weather and Climate Extremes, 13, 44-53, 2016.

Thibaud, E., Mutzner, R., and Davison, A. C.: Threshold modeling of extreme spatial rainfall, Water Resources Research, 49, 4633-4644, 2013.

Wadsworth, J. L. and Tawn, J. A.: Dependence modelling for spatial extremes, Biometrika, 99, 253-272, 2012.

Wang, Q. J.: A Bayesian Joint Probability Approach for flood record augmentation, Water Resources Research, 37, 1707-1712, 2001.

Wang, Q. J., Robertson, D. E., and Chiew, F. H. S.: A Bayesian joint probability modeling approach for seasonal forecasting of streamflows at multiple sites, Water Resources Research, 45, 2009.

Wang, X., Gebremichael, M., and Yan, J.: Weighted likelihood copula modeling of extreme rainfall events in Connecticut, Journal of Hydrology, 390, 108-115, 2010.

Westra, S. and Sisson, S. A.: Detection of non-stationarity in precipitation extremes using a max-stable process model, Journal of Hydrology, 406, 119-128, 2011.

WMAWater: Review of Bellinger, Kalang and Nambucca River Catchments Hydrology, Bellingen Shire Council, Nambucca Shire Council, New South Wales Government, 2011.

Zhang, L. and Singh, V. P.: Gumbel–Hougaard Copula for Trivariate Rainfall Frequency Analysis, Journal of Hydrologic Engineering, 12, 409-419, 2007.

Zheng, F., Westra, S., and Leonard, M.: Opposing local precipitation extremes, Nature Clim. Change, 5, 389-390, 2015.

Zscheischler, J., Westra, S., van den Hurk, B. J. J. M., Seneviratne, S. I., Ward, P. J., Pitman, A., AghaKouchak, A., Bresch, D. N., Leonard, M., Wahl, T., and Zhang, X.: Future climate risk from compound events, Nature Climate Change, 8, 469-477, 2018.

Supplementary material

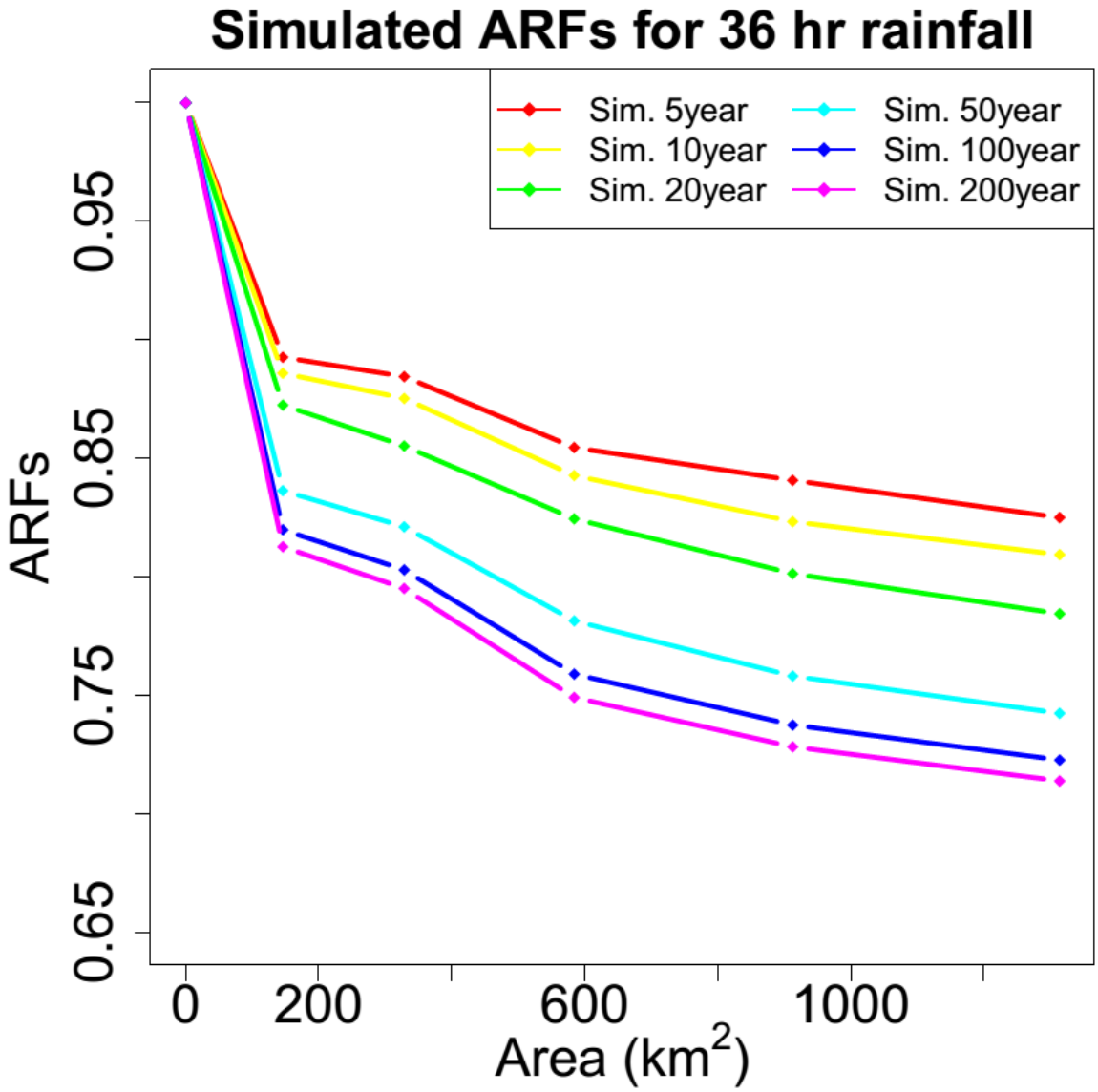

Fig. S4.1. Simulated ARFs for spatial rainfall of 36 hr duration for different return periods in the Bellinger catchment.

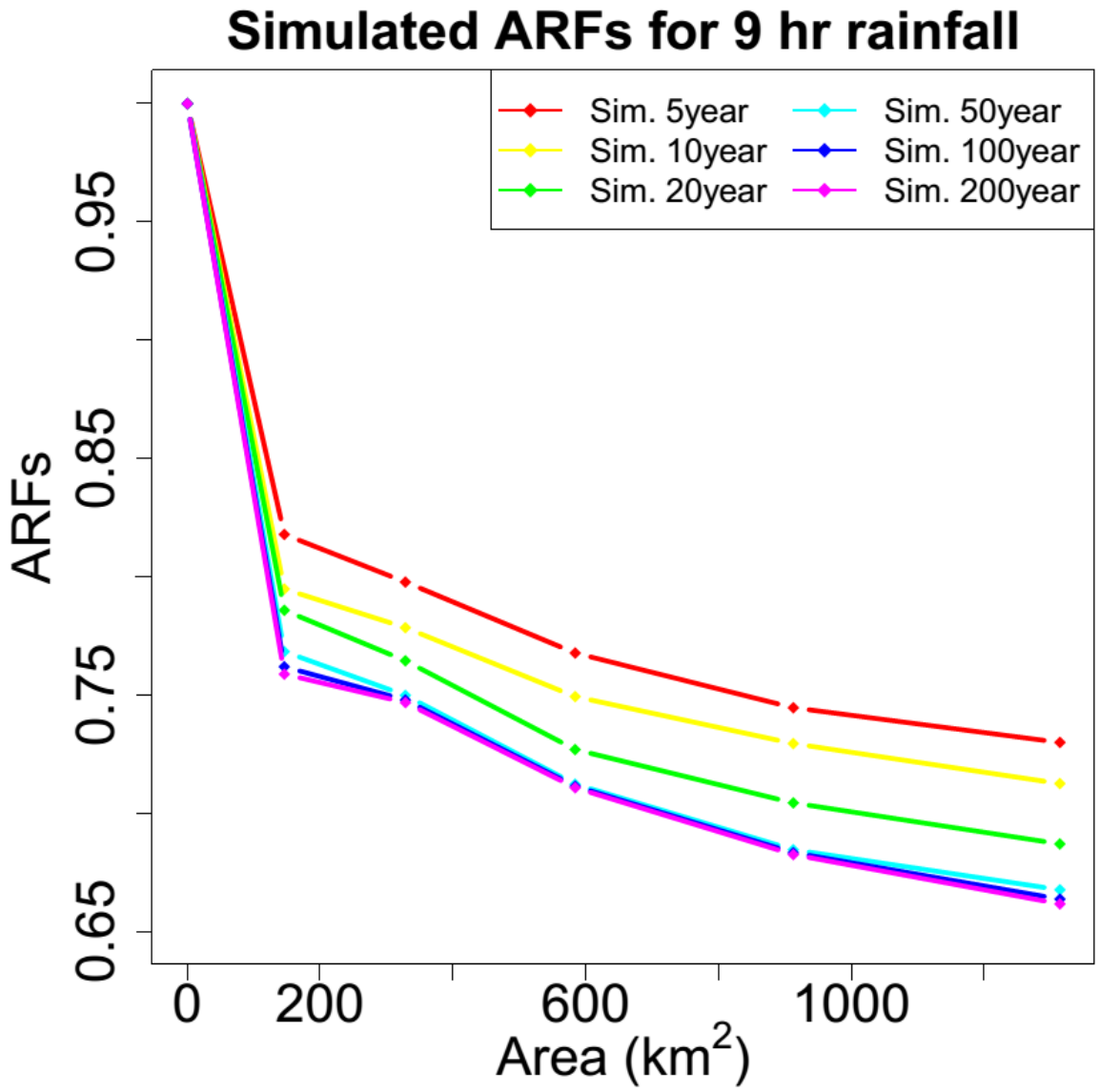

Fig. S4.2. Simulated ARFs for spatial rainfall of 9 hr duration for different return periods in the Deep Creek catchment.

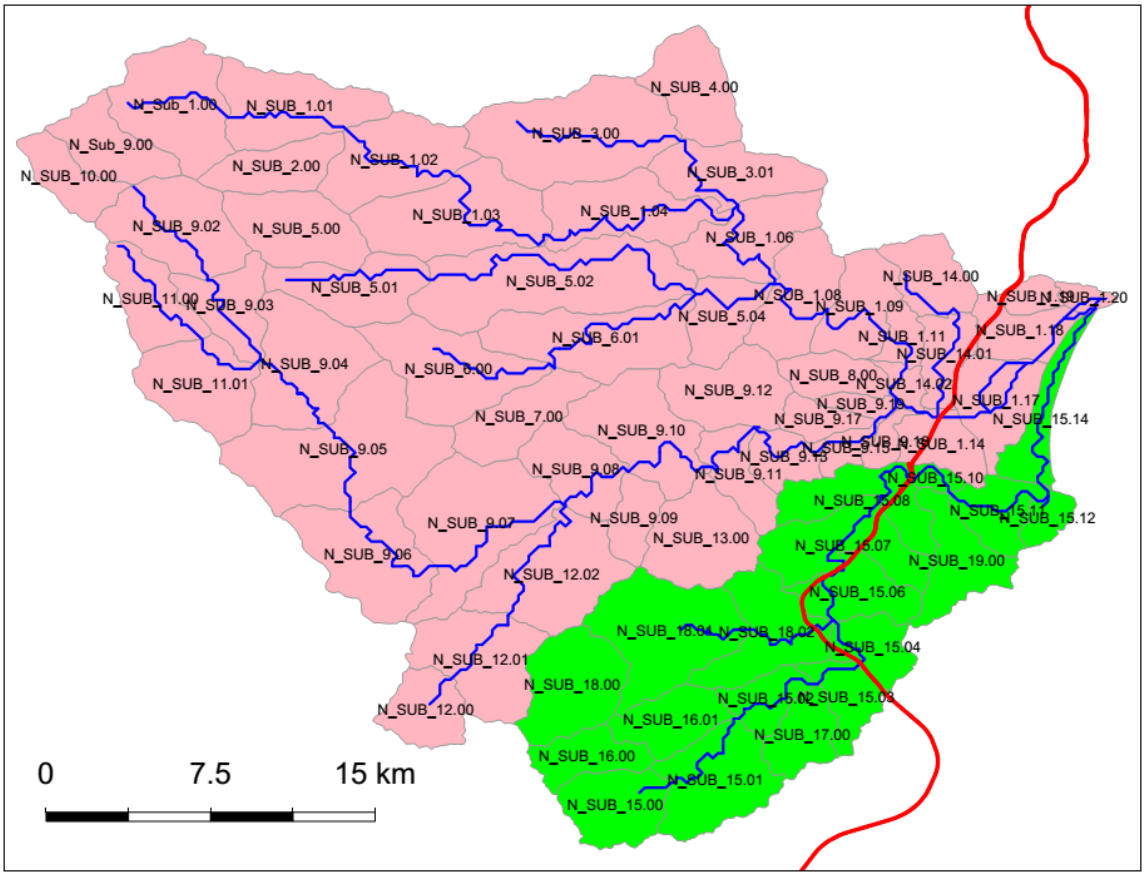

Fig. S4.3. Hydrological model layout for Nambucca (upper) catchment and Warrell Creek catchment. The blue lines are the river network, and the red line is the Pacific Highway upgrade project.

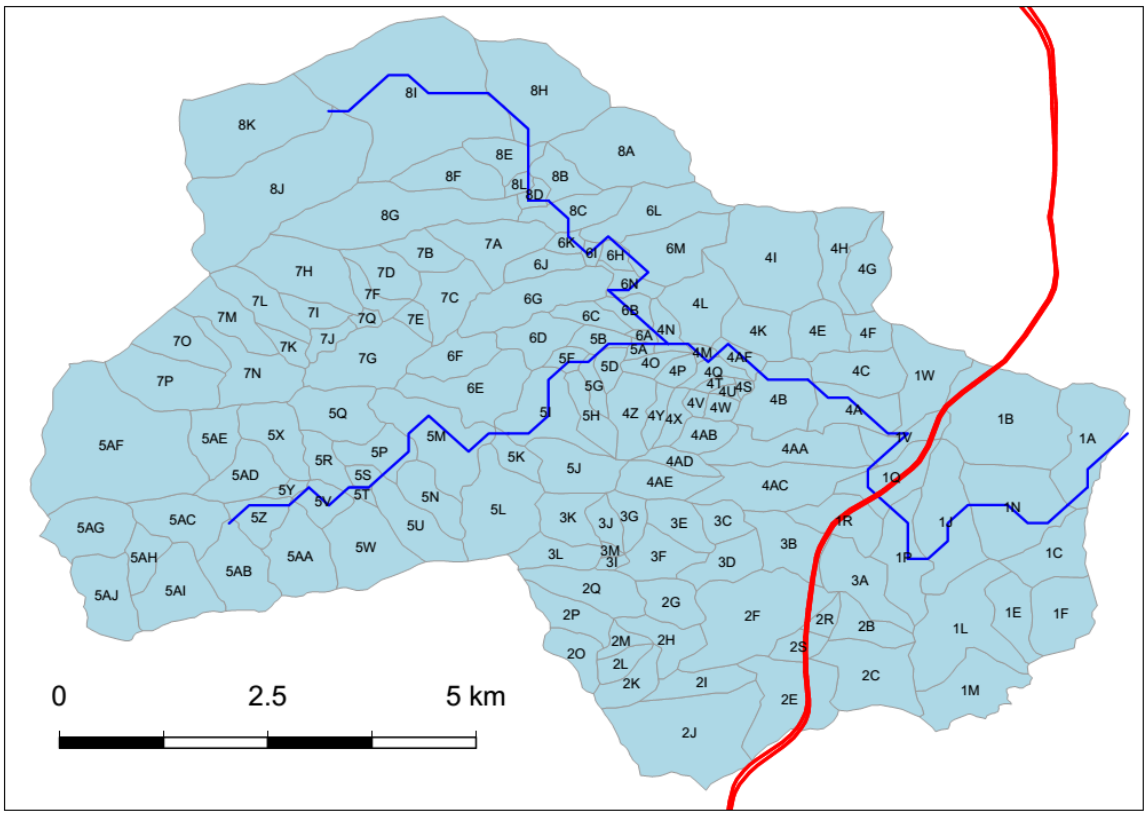

Fig. S4.4. Hydrological model layout for Deep Creek catchment. The blue lines are the river network, and the red line is the Pacific Highway upgrade project.

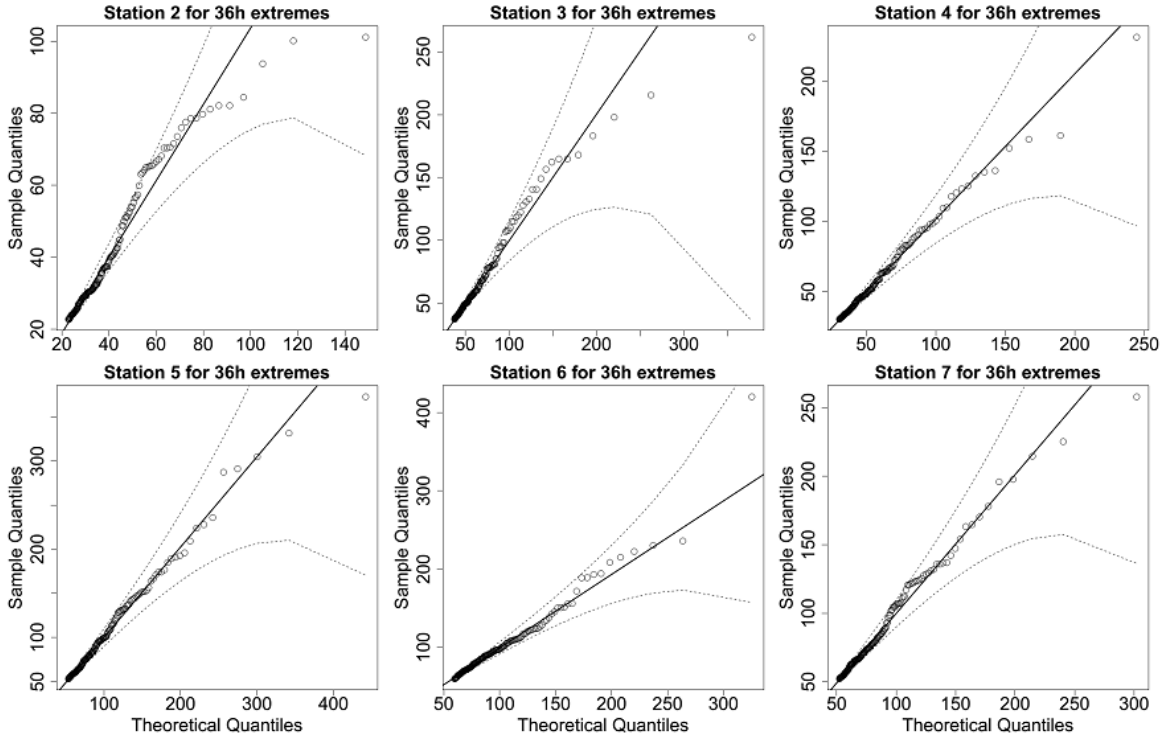

Fig. S4.5. QQ plots for the estimate of marginal distribution GPD for 36 hr rainfall extremes for rain gauges from 2 to 7. The solid diagonal line indicates a perfect fit, and the dotted lines indicate a 95% confidence interval.

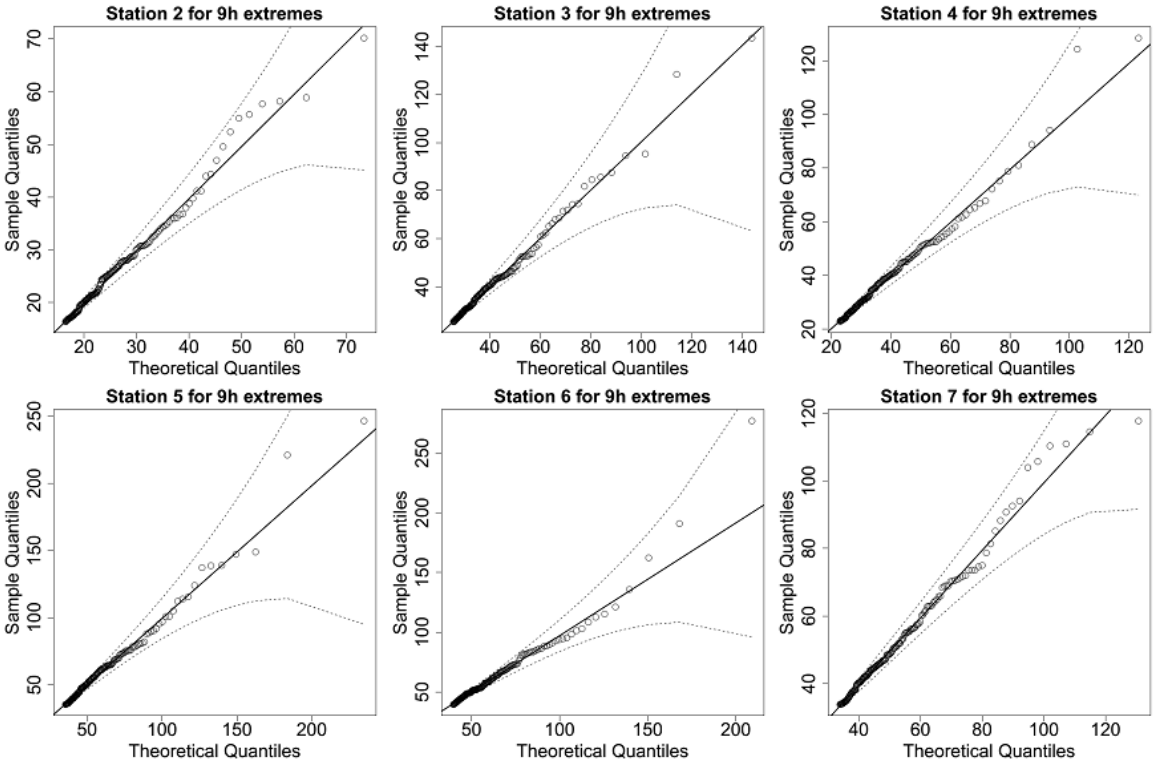

Fig. S4.6. QQ plots for the estimate of marginal distribution GPD for 9 hr rainfall extremes for rain gauges from 2 to 7. The solid diagonal line indicates a perfect fit, and the dotted lines indicate a 95% confidence interval.

Chapter 5

5.1. Research contribution

This thesis has focused on developing a framework for simulating flood characteristics for civil infrastructure systems, which can deal with the complexity of the interdependencies of rainfall extremes, both in space and between elements of the system. The framework uses an event-based method to estimate the conditional and joint probabilities of flooding. It is based on IDF curves estimated dependently over space and across different durations.

To achieve the research objectives, a new approach was developed for combining rainfall extremes across different durations within a spatial extreme value model (max-stable process) in Objective 1. An analysis was conducted to investigate the asymptotic properties of rainfall and its effect on the asymptotic behaviour of areal reduction factors (ARFs) in Objective 2. The diagnostic results indicated that spatial rainfall has asymptotically independent properties, which indicated that inverted max-stable process models were preferable for achieving realistic spatial rainfall fields. However, the general approach proposed in Objective 1 is still valid: It can be adopted for an asymptotically independent model (inverted max-stable process). Objective 3 takes this approach, combining rainfall extremes across different durations within an inverted max-stable process. It demonstrates how to estimate conditional and joint probabilities of flooding for a civil infrastructure system.

Objective 1 – Spatial dependence of rainfall extremes across multiple durations: Traditionally rainfall intensity-duration-frequency (IDF) curves have been estimated without providing parallel information on the spatial dependence of rainfall events, or on their dependence across multiple durations. As a result, traditional IDF curves cannot express conditional or joint distributions of rainfall extremes, which are required in a wide range of flood estimation problems, such as in designing a road network with multiple river crossings, or whenever there is interest in determining the probability of a flood event in a catchment given that another flood has occurred nearby.

The new approach, developed in Chapter 2, enables the max-stable process (and by proxy, other dependence models including asymptotically independent models) to capture the spatial dependence of rainfall extremes across different durations. A method proposed by Koutsoyiannis et al. (1998) was used to link the marginal parameters of rainfall extremes across different durations, and to reduce the number of parameters that need to be estimated. In the dependence model, storm-level dependence across different durations was represented through the max-stable process. An improvement was made to the dependence structure to deal with the fact that the dependence levels across different durations (e.g., 24h and 1h) at short distances, or even at the same location, are less than those of identical durations (e.g. 24h and 24h). It was proposed that a nugget term (which is a function of the two durations) is added into the original variograms to match this characteristic. This approach allows the storm-level dependence structure of rainfall to be presented in

conditional maps that show exceedance probabilities and return levels across different durations. This can then be used to better account for, and communicate, the complex dependences associated with extreme rainfall, and can be used in a range of planning and engineering design contexts.

Objective 2 – Asymptotic behaviour of areal reduction factors (ARFs): In the event-based method of estimating floods, areal reduction factors (ARFs) are commonly employed to convert point-based estimates of extreme rainfall—usually in the form of intensity-frequency-duration (IFD) relationships—to a catchment-wide rainfall intensity of equivalent exceedance probability. The key question here is 'how do ARFs scale with rainfall frequency?' In the literature, there is evidence that ARFs decrease with rarer events. However, a detailed analysis of the tail dependence of spatial rainfall extremes, which helps us to understand the asymptotic behaviour of ARFs, is still lacking. This is particularly critical when extrapolating to rare events, given that data availability is typically in the order of several decades but interest focuses on longer return periods (e.g. 100 or 1000 years).

The analysis in Chapter 3 has shown that the observed data follow the behaviour of an asymptotically independent process, leading to ARFs that decrease with an increasing return period. The study demonstrated that the use of inverted max-stable process models to simulate ARFs can provide a rigorous alternative to empirical approaches, particularly for long return periods that require significant extrapolation from the data. A secondary contribution of Chapter 3 was to confirm that only asymptotically independent models can represent the dependence structure of the observed data. Together with Thibaud et al. (2013), this suggests that max-stable processes may not be suitable for modelling rainfall extremes, although this would need to be confirmed by further case studies. It implies that the use of an asymptotically dependent model (e.g. a max-stable process) to simulate spatial extreme rainfall in a number of previous studies (Nicolet et al., 2017; Padoan et al., 2010; Westra and Sisson, 2011) is not suitable in the limit for the rainfall fields analysed in this study. Future studies about spatial rainfall extremes need to take this into consideration.

Objective 3 – Flood probability estimate for linear infrastructure: The proposed framework in Chapter 2, and the results of the analysis in Chapter 3, were adopted in a framework in Chapter 4 for simulating flood characteristics across a network, which is illustrated in a case study of a highway section containing five river crossings. The proposed framework in Chapter 2 was adopted in Chapter 4 to enable an asymptotically independent model (inverted max-stable process) to capture the dependence structure of spatial rainfall across different durations.

Chapter 4 points out the main limitation of the conventional methods for estimating flood risk that is they isolate bursts of rainfall and break the nature of spatial dependences of extreme rainfall for identical duration, or across different durations. This makes the conventional methods unable to analyse spatial dependences of flooding. Spatially dependent IDF curves that integrate the dependence structure of observed rainfall with marginal estimates of extreme rainfall (i.e. traditional IDF curves) are an elegant solution

to this problem. Chapter 4 demonstrates the method of estimating the conditional probability that an element of a civil infrastructure system is flooded, considering the effects when a flood event occurs at a neighbouring element. This method is useful in evacuation route design. Chapter 4 also illustrates how to estimate the overall failure probability of a system given that each element of the system was designed to a specific annual exceedance probability event. Typically, this overall failure probability is not easy to estimate, because it has previously been difficult to determine the chance that two or more elements fail at the same time.

5.2. Limitations

This thesis is the first to estimate flood probabilities in civil infrastructure systems by formally taking into account the spatial dependence of flood-producing rainfall for identical durations and across different durations. Although it provides a complete framework, this thesis still has some limitations relating to data availability, fitting the model to observed data, and implementing simulations of the proposed models. These limitations are discussed below, with respect to each research objective.

Objective 1 – Spatial dependence of rainfall extremes across multiple durations: The block maxima model has been used in many previous studies of spatial rainfall modelling in the form of annual maximum rainfall. However, this approach may be inappropriate for analyzing the spatial dependence structure of rainfall because the annual maximum rainfall in a given year at different locations can occur at different times (e.g., at different date in a month, or at different month).

Another limitation in Objective 1 is that the marginal model and the dependence model were fitted separately because of the complexity of the overall model. Consequently, the standard errors relating to the spatial dependence parameters were underestimated, because the data was transformed into unit Fréchet before fitting the dependence structure. It would also be possible to further reduce the number of parameters by implementing a method of jointly fitting the sites. Then, the at-site parameters would not need to be determined prior to fitting the spatial surface. It is possible that jointly fitting the marginal and dependence components of the model may lead to different outcomes regarding the significance of the covariate terms.

Objective 2 – Asymptotic behaviour of areal reduction factors (ARFs): The behaviour of ARFs was analysed for daily rainfall data in an area in which rain gauges were not dense and were not distributed equally in space. The ARFs cannot be estimated for relatively small areas. The behaviour of ARFs for subdaily and longer time scales, which are critical for urban flooding or flooding in big regions, cannot be estimated from daily data.

Objective 3 – Flood probability estimates for linear infrastructure: There is a limitation of scaling marginal parameters in the framework for estimating flood probabilities for civil infrastructure systems. This limitation relates to the peak over threshold model (POT) for estimating the marginal distribution. The POT model is used for marginal modelling because it is more accurate, but there is not any method for linking

GPD parameters for different durations, like the Koutsoyiannis et al. (1998) method for GEV distribution in a block maxima model. This prevents the proposed framework from extrapolating the spatially dependent IDF curve for rainfall of any duration.

5.3. Future work

The limitations of this research present opportunities for future developments:

- *Duration scaling of IFDs:* A method of linking the marginal parameters for the POT model – GP distribution – is required so that the conditional probability between rainfall of any duration vs. rainfall of a base duration (e.g. d hours rainfall vs. 36 hours rainfall) can be extrapolated from the method in Objective 1 and Objective 3.
- *Behaviour of ARFs for subdaily and longer time scales:* Analyzing the behaviour of ARFs is required for subdaily rainfall, and for rainfall of longer durations (e.g. 36 h or 48 h) because the time of concentration for catchments is often less than 24 h. This requires subdaily rainfall data, which will then be aggregated into longer durations. The framework from Objective 2 would be applied to rainfall of subdaily and longer time scales to analyse the behaviour of ARFs.
- *Joint probability estimates across different time scales:* This thesis estimates joint probabilities of flooding for civil infrastructure systems (Objective 3) by simulating spatial rainfall across different time scales. Alternatively, these probabilities may be calculated indirectly from the pairwise dependence between rainfalls for a given pair of time scales.
- *Linking properties of extremes to models of regular rainfall:* There is an ever expanding number of models available for simulating spatial rainfall across a wide range of timescales and region sizes. These models include the well-known class of cascade models that embed properties of power-law scaling and have efficient schemes of parameterisation. It would be useful to have a class of rainfall models that in addition to simulating the full distribution of rain events, are able to conform to theoretical properties of extreme rainfall as represented in IDF curves of extremes. In other words, current models are compared to IDF curves to see how well they compare, but it would be useful to have these properties derived for classes of models so they can be used in calibration of model parameters.

Addressing these recommendations will significantly improve the ability to develop and dynamically apply IDF curves that include spatial dependence. The framework proposed by this research leads to a very different paradigm of design flood risk estimation, because it focuses attention on the risk of the entire system, rather of individual system elements in isolation. This is particularly important given there is more and more evidence that extreme events frequently together with other extreme events, known as a *compound event* (Leonard et al., 2014). Compound events are due to spatial dependence between extremes. This spatial dependence is not just an issue of rainfall extremes, it can also be found in different extreme events, such as storm surges together with rainfall extremes in coastal areas (Wahl et al., 2015; Zheng et al., 2014; Zheng et al., 2013), which is challenging for

conventional methods of flood risk estimation. Taking the long view, the following works could be implemented and updated into guidelines for estimating design floods (e.g. the Australian Rainfall and Runoff guidelines) for applications in industry:

- Build IDF maps for the "Spatially Dependent-IDF" for all regions where sufficient spatial rainfall data is available. These web-based maps could represent the conditional IDF for a whole region of a city, given an extreme event is occurring at a particular location within that region, which would be helpful for engineers and managers in estimating design floods. The interactivity of an online platform would allow for flexibility in specifying any number of conditions on the properties of the extremes.
- Re-derive ARFs for different rainfall durations in guidance documents such as Australian Rainfall and Runoff by using the framework proposed in Objective 2. These ARFs, with the awareness of the asymptotically independent properties of spatial rainfall, combined with the advantage of computer simulation, would help to estimate correctly the relationship between point extremes and areal rainfall for long return periods.

There is still important development work required before the contribution of this research can be implemented and applied widely in industry. However, there are two final recommendations that could be implemented immediately by future researchers:

- The asymptotically dependent model (e.g. max-stable process) may not be suitable for simulating spatial rainfall. Future studies about rainfall extremes should use a diagnostic that calculates the pairwise extremal coefficient, and the tail dependence coefficient for multiple thresholds to check which kind of tail dependence occurs. It is likely that spatial rainfall is asymptotically independent and that an asymptotically independent model (e.g. inverted max-stable process) is suitable for simulating spatial rainfall.
- For analyzing conditional and joint probabilities extremes (not just rainfall extremes), the peak over a threshold (POT) model should be used for more accurate results.

Appendix A

Copy of paper from Chapter 2:

Phuong Dong Le, Michael Leonard, Seth Westra

Water Resources Research, Volume 54 Issue 3

AGU100 ADVANCING EARTH AND SPACE SCIENCE

Water Resources Research

RESEARCH ARTICLE
10.1002/2017WR022231

Modeling Spatial Dependence of Rainfall Extremes Across Multiple Durations

Phuong Dong Le[1], Michael Leonard[1], and Seth Westra[1]

[1]School of Civil, Environmental and Mining Engineering, University of Adelaide, Adelaide, SA, Australia

Key Points:
- A method is proposed to account for duration dependence into the spatial model for extreme rainfall
- The method uses max-stable process theory with extremal coefficients calculated across durations
- Conditional maps of return period/level across different durations can be developed to support engineering planning, design, and management

Supporting Information:
- Supporting Information S1

Correspondence to:
P. D. Le,
phuongdong.le@adelaide.edu.au

Citation:
Le, P. D., Leonard, M., & Westra, S. (2018). Modeling Spatial dependence of rainfall extremes across multiple durations. *Water Resources Research*, *54*. https://doi.org/10.1002/2017WR022231

Received 15 NOV 2017
Accepted 2 MAR 2018
Accepted article online 8 MAR 2018

Abstract Determining the probability of a flood event in a catchment given that another flood has occurred in a nearby catchment is useful in the design of infrastructure such as road networks that have multiple river crossings. These conditional flood probabilities can be estimated by calculating conditional probabilities of extreme rainfall and then transforming rainfall to runoff through a hydrologic model. Each catchment's hydrological response times are unlikely to be the same, so in order to estimate these conditional probabilities one must consider the dependence of extreme rainfall both across space and across critical storm durations. To represent these types of dependence, this study proposes a new approach for combining extreme rainfall across different durations within a spatial extreme value model using max-stable process theory. This is achieved in a stepwise manner. The first step defines a set of common parameters for the marginal distributions across multiple durations. The parameters are then spatially interpolated to develop a spatial field. Storm-level dependence is represented through the max-stable process for rainfall extremes across different durations. The dependence model shows a reasonable fit between the observed pairwise extremal coefficients and the theoretical pairwise extremal coefficient function across all durations. The study demonstrates how the approach can be applied to develop conditional maps of the return period and return level across different durations.

1. Introduction

For many decades, the rainfall intensity-duration-frequency (IDF) relationship has formed the basis for many extreme rainfall-based flood estimation approaches. For example, the rational method (Mulvaney, 1851) focuses on estimating flow at the catchment outlet, and is based on the rainfall intensity at a duration equal to the catchment's time of concentration. IDF relationships are also used in other flood estimation methods, such as event-based rainfall-runoff models (Boyd et al., 1996; Laurenson & Mein, 1997). In these event-based models, IDF curves are combined with temporal patterns to develop design rainfall hyetographs. The hyetographs are then input to a rainfall-runoff model in order to simulate flood flow at a catchment's outlet (Chow et al., 1988). In almost all cases, these IDFs have been estimated either at a single site or as a spatial map, but without providing parallel information on spatial dependence of rainfall events or the dependence across multiple durations.

A limitation of traditional IDF curves is that they cannot express conditional distributions of extreme rainfall. To be useful for a wide range of flood estimation problems, the conditional relationship should allow for extreme rainfall of different durations, because neighboring catchments are unlikely to be of identical size so that they are likely to respond to extreme rainfall at differing durations. Such a situation is illustrated in Figure 1, which describes a hypothetical scenario of designing a route (e.g. road or rail) crossing for a river, which should be designed to operate in the event that a neighbouring catchment has flooded. In this case, we may wish to know: What is the probability that a bridge at location x_2 will be flooded, given that the bridge at location x_1 is flooded? Note that for illustration purposes, we assume a one-to-one correspondence between extreme rainfall and flooding; for real-world applications, there may be additional factors influencing the magnitude of streamflow extremes that should be taken into account. Assuming that the critical rainfall duration at locations x_1 and x_2 are 24 and 12 h, respectively, and that u_1 and u_2 are the depth of rainfall required to flood bridges at these two locations, the question may be rephrased as: What is the probability of having extreme rainfall for 12 h exceeding u_2 (mm) at upstream of location x_2, given that extreme rainfall for 24 h occurred and exceeds u_1 (mm) at upstream of location x_1? This kind of information is important when designing new infrastructure (e.g., the bridge at location x_2), based on existing infrastructure in the region (i.e., the bridge at location x_1).

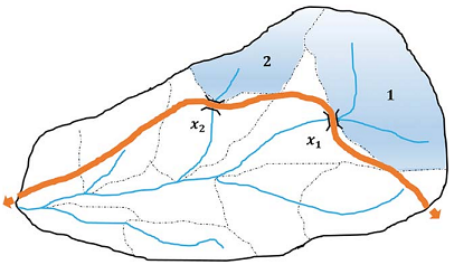

Figure 1. Illustrating conditional estimate requirements across multiple durations of extreme rainfall. What is the probability of extreme rainfall for 12 h exceeding u_2 (mm) at location x_2, given that extreme rainfall for 24 h occurs and exceeds u_1 (mm) at location x_1?

Several approaches have been developed to simulate various spatial features of extreme rainfall. One category is the Bayesian hierarchical approach, which has been developed to explore how the parameters of a marginal distribution (e.g., the generalized extreme value GEV distribution) vary in space. These methods can utilize information from multiple gauges across a region in the estimation process. The Bayesian hierarchical approach is used to infer spatial return levels of extreme rainfall (Bracken et al., 2016; Cooley et al., 2007), as well as deal with difficulties relating to strong hypotheses in regional frequency analysis such as the need to delineate homogenous regions, which may be too restrictive in some cases (Renard, 2011). Although this category of models is useful for building high precision spatial maps of GEV parameters, it does not account for storm level dependence (e.g., the probability that extreme rainfall at two or more locations comes from the same event) which is necessary to estimate conditional distributions of extreme rainfall. Another approach is to use multivariate Gaussian processes to provide dependence between multiple locations within a region, whether directly applied to extremes (Renard & Lang, 2007), or as models of the entire rainfall process (Bennett et al., 2016). These models are able to produce conditional relationships between extremes for the case of asymptotically independent tail dependence.

Max-stable process models have been developed as a method to account for storm-level dependence, and they can characterize the conditional distribution of extreme rainfall in space. Max-stable process has been developed and applied to numerous analyses of the spatial dependence of rainfall extremes (Davison et al., 2012; Padoan et al., 2010; Thibaud et al., 2013; Westra & Sisson, 2011), with Padoan et al. (2010) showing how the application of annual maximum data can provide useful information on conditional rainfall relationships throughout a catchment. This arises because, even though only annual maximum data is used, the generating model used in max-stable process theory assumes that the annual maxima data arise through a set of "storms," such that the dependence can be represented at the storm level. However in all these cases, only one duration of rainfall extremes was considered; thus, the problem of conditional dependence across catchments with different response durations requires extension of the existing max-stable framework. Stephenson et al. (2016) has developed a max-stable process that fits within a Bayesian hierarchical framework having a marginal GEV distributions across multiple durations, but the storm-level dependence is restricted to extremes of the same duration.

One potential improvement would be developing a max-stable process for more than one variable or alternatively developing a space-time max-stable process (Genton et al., 2015; Huser & Davison, 2014; Oesting et al., 2017). In principle, these models could be used to infer the extremes at different durations. However, they are also very complex and are likely to be difficult to fit for the practical application of a sparse set of rainfall gauges. For example, Huser and Davison (2014) pointed out that some parameters of their model are difficult to estimate, leading to a complex two-stage fitting process; a problem that is likely to be compounded when extending the method to multiple durations. We therefore present an alternative approach that can extend the current max-stable process so that it allows for extreme rainfall across different durations while capturing spatial variation in extreme rainfall as well as storm-level dependencies.

It is important to note that there is a difference between dependence in "time" and "duration" since the former refers to dependence over a sequence of values, whereas the latter refers only to the duration of an event. Thus, for example, a duration-based model is able to parameterize a high dependence between 1 and 2 h extremes and a lesser dependence between 1 and 24 h extremes, without specifying the time-varying structure of the extremes, as implied by space-time dependence.

This paper describes an empirical method that enables the max-stable process to capture the spatial dependence of rainfall extremes across different durations. To achieve this, the method developed by Koutsoyiannis et al. (1998) for linking extreme rainfall across multiple durations is used to fit the marginal model and subsequently transform the extreme rainfall to unit Fréchet scale. A new method is then proposed to fit the max-stable process to extreme rainfall across different durations within the unit Fréchet scale. Finally, the bivariate probability function for the max-stable process (Padoan et al., 2010) is used to estimate the

conditional probabilities of rainfall extremes across different durations. This opens up the possibility of using conditional distributions for flood estimation problems that are impacted by rainfall-driven flooding at multiple locations, such as with complex road networks.

This paper demonstrates the model as applied to a case study of the Hawkesbury-Nepean catchment in New South Wales, Australia. In this case study, using annual maximum rainfall from 25 subdaily stations with durations between 1 and 24 h. Section 2 outlines the case study and data used. Section 3 explains the methodology, including approaches for linking extremes from multiple durations via a marginal model and introducing duration dependence into a spatial model. Results and discussion are provided in section 4 on the performance of the spatial model and the conditional simulation across different durations. Conclusions and recommendations are provided in section 5.

2. Hawkesbury-Nepean Case Study and Data

The Hawkesbury-Nepean catchment is located in New South Wales, Australia. It has been chosen as the case study because this area is the focus of ongoing studies for evacuation modeling and requires consideration of the behavior of extreme rainfall across multiple subcatchments (Opper ESM et al., 2010; Ribbons, 2015). An additional reason for choosing this catchment is the relative density of subdaily rainfall data compared to other regions of Australia. The subdaily rainfall records are available in 5 min increments at 25 locations within or near the study catchment.

With an area of 21,400 km^2, the Hawkesbury-Nepean catchment is one of the largest catchments in New South Wales east of the Great Dividing Range. Its rainfall has strong seasonality, particularly for subdaily extreme rainfall durations, with the highest rainfall occurring during the warmer months (December–February) (Zheng et al., 2015). The catchment's average annual rainfall varies from 600 mm inland, to 1,000 mm along the coast. Figure 2 shows an elevation map of the catchment. The black circles represent the subdaily rain stations used for this study. The sites selected had at least 19 years' record each, and at least 18 years in common with other gauges in the region. Requiring a common period was necessary for conducting a pairwise calibration, but it restricted the number of sites that could be compared (see section 3.4). The 5 min data were aggregated to 1, 2, 3, 6, 12, and 24 h for use in this study. Spatial mapping was performed using latitude and longitude as covariates.

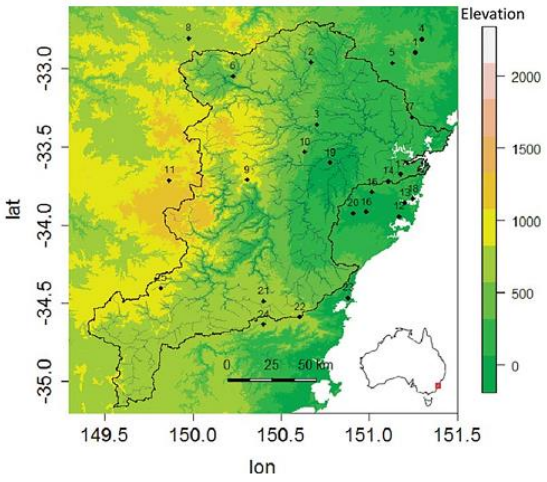

Figure 2. The Hawkesbury-Nepean catchment near Sydney, Australia. The catchment is bounded by black lines, and subdaily rainfall gauges are indicated by black dots.

3. Methodology

Following a summary of max-stable processes (section 3.1), the proposed method is explained according to the steps shown in Figure 3. First, the method of reparameterizing the GEV is explained to allow for convenient representation of marginal distributions across multiple durations (section 3.2). The marginal distribution parameters across multiple sites in the region are then modeled by a thin plate spline regression (Section 3.3). At this point there is a complete representation of the marginal model across multiple durations across a region, and this model is use to convert the data to and from the unit Fréchet space. Subsequent steps outline the dependence model, including an empirical method that includes duration in the dependence structure of extremes (section 3.4), and the steps needed to assess conditional probability estimates based on the bivariate max-stable process cumulative distribution function (section 3.5). A subsequent section is provided to summarize the overall methodology.

3.1. Overview of Max-Stable Process

This study uses a max-stable process as the basis for simulating conditional rainfall extremes. It is used because the model is able to represent storm-level dependence (Davison et al., 2012). The max-stable process extends the generalized extreme value (GEV) distribution into the spatial domain (Davison & Gholamrezaee, 2012; de Haan, 1984; de Haan & Ferreira, 2006). Suppose that $Y_k(x), x \in X$ for $k=1,\ldots,m$ are m independent realizations of a continuous process indexed by location x, where $X \subset R^2$, the set of locations existing in a spatial domain. If the following limit

$$Z(x)=\lim_{m\to+\infty}\frac{\max_{k=1}^{m}Y_k(x)-b_m(x)}{a_m(x)} \tag{1}$$

exists jointly for all $x \in X \subset R^2$ and is nondegenerate for some normalizing constants $a_m(x) > 0$ and $b_m(x)$ then $Z(x)$ is a max-stable process (de Haan, 1984). It follows that at a fixed location in space, x, each marginal distribution is the univariate GEV distribution.

It is convenient to construct a simple max-stable process with unit Fréchet margins, and subsequently the marginal distribution can be transformed back to the GEV scale. To construct a simple max-stable process, let $\{(U_i, s_i),\ U_i > 0, i \geq 1\}$ denote the points of a Poisson process at $s_i \in R^2$ with intensities following $1/U^2$. Then one characterization of a max-stable process with unit Fréchet margins is:

$$Z(x)=\max_i\ \{U_i f(s_i,x)\},\ x \in X \tag{2}$$

where $f(s,x)$ is a non-negative function that integrates to unity over s for fixed $x \in X$.

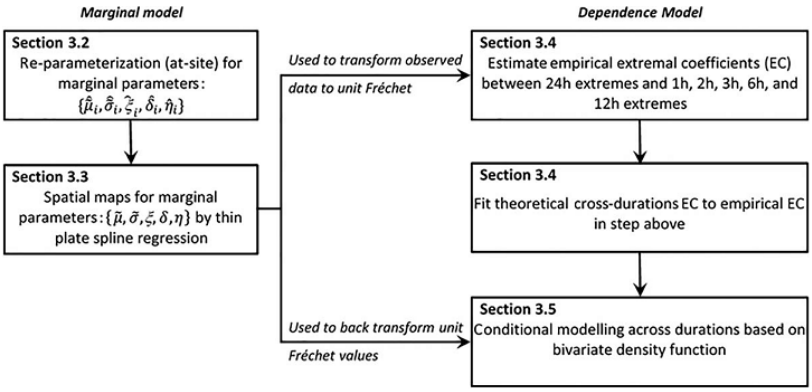

Figure 3. The schematic diagram for the overall methodology.

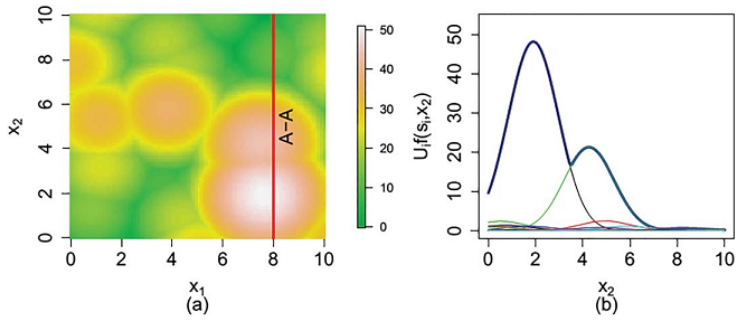

Figure 4. Max-stable processes $Z(x)$. (a) Illustrates a max-stable process in two dimensions $X = (x_1, x_2)$ with a positively correlated Gaussian storm profile. The thin colored lines in plot (b) illustrates single storm events $i = 1, \ldots, n$ along transect A-A with specified value of $x_1 = 8$, with magnitude of $U_i f(s_i, x_2)$ and the process maxima $Z(x_2) = \max\{U_i f(s_i, x_2)\}$, given as the thick blue line.

The construction above can be interpreted as the rainfall-storm process (Schlather & Tawn, 2003; Smith, 1990, http://www.stat.unc.edu/postscript/rs/spatex.pdf). To understand this, consider a continuous domain in R^2 in which n storms occur over this domain with centers at s_i $(i = 1, \ldots, n)$ and "intensities" $U_i \in R^+$. The shape of each storm is given by the kernel $f(s_i, x)$. Thus, the storm magnitude at location x is $U_i f(s_i, x)$. Figure 4 shows an illustration of the idea of the max-stable process based on a Gaussian storm profile in R^2 (left panel), and the profile of a max-stable process along a given transect across the catchment (right panel).

3.2. Linking Multiple Durations at Each Site

The above theory can be generalized to an arbitrary distribution by transforming the marginal distributions. This transformation forms an important step in developing the max-stable process. One challenge in implementing this transformation is that extreme data at each duration has its own marginal distribution, which leads to a large number of parameters that need to be estimated when considering multiple durations. To reduce the number of parameters that need to be estimated, an approach is needed that can link data of multiple durations. This section provides the method of marginal modelling that links the extremes of multiple durations.

Consider the set of annual maximum rainfall depths $r_{i,t,d}$ for a given site $i = 1, \ldots, N$, year $t = 1, \ldots, T$ and duration $d = 1, \ldots, D$. The generalized extreme value (GEV) distribution is used to model the annual maxima $r_{i,t,d} \sim GEV(\mu_{i,d}, \sigma_{i,d}, \xi_{i,d})$, with the cumulative distribution function defined as:

$$G(r_{i,t,d}) = \exp\left\{-\left[1 + \xi_{i,d}\left(\frac{r_{i,t,d} - \mu_{i,d}}{\sigma_{i,d}}\right)\right]^{-1/\xi}\right\} \tag{3}$$

where for a given site i and duration d, $\mu_{i,d}$ is the location parameter, $\sigma_{i,d} > 0$ is the scale parameter, and $\xi_{i,d}$ is the shape parameter, where $1 + \xi(r - \mu)/\sigma > 0$. The GEV distribution describes the relationship between the frequency and depth of extreme rainfall that occurs in a specified duration and location of interest.

Koutsoyiannis et al. (1998) provided a re-parameterization for the GEV distribution that allows it to be linked across multiple durations. In this reparameterization, a new parameter, $\tilde{\mu}_i = \mu_{i,d}/\sigma_{i,d}$, is defined and assumed to be constant for all durations of interest. The shape parameter $\xi_{i,d}$ is also assumed to be constant for all durations, so that the scale parameter can be modified to carry all information relating to rainfall intensities across multiple durations. Koutsoyiannis et al. (1998) proposed the following relationship to express this dependence:

$$\sigma_{i,d} = \frac{\tilde{\sigma}_i d}{(d + \delta_i)^{\eta_i}} \tag{4}$$

where $\sigma_{i,d}$ is the scale parameter corresponding to extreme rainfall for duration d, $\tilde{\sigma}_i$ is a duration-independent parameter, $\delta_i \geq 0$ and $0 \leq \eta_i \leq 1$. This equation represents an empirical formula,

encapsulating the experience from several IDF studies (Koutsoyiannis et al., 1998). It should be noted that this equation is used to model the scale parameter when extreme rainfall is measured by depth (mm) rather than intensity (mm/h). By using this equation, the GEV distribution across multiple durations can be modeled at a given location i through a single distribution with only two additional parameters: the offset term δ and exponent term η. Regarding the total number of parameters, this approach uses five parameters to estimate extreme rainfall across all n_d durations, instead of $3n_d$ parameters when using separate GEV distributions for each duration.

As a result of the reparameterization, the rainfall intensities across multiple durations can be represented as $r_{i,t,d} \sim GEV(\tilde{\mu}_i, \tilde{\sigma}_i, \xi_i, \delta_i, \eta_i)$. The log likelihood is then given as:

$$\ell\left(r_{i,t,d}|\tilde{\mu}_i, \tilde{\sigma}_i, \xi_i, \delta_i, \eta_i\right) = \sum_t \sum_d \left(\log\left(GEV(\tilde{\mu}_i, \tilde{\sigma}_i, \xi_i, \delta_i, \eta_i)\right)\right) \tag{5}$$

This is more correctly referred to as a pseudo-likelihood because it assumes that all $r_{i,t,d}$ are independent and while the corresponding estimators from this function are consistent with maximum likelihood estimates, they do not have the same efficiency.

3.3. Modeling the Reparameterized At-Site GEV Parameters Across Space

The at-site GEV parameters can vary over a region, and practical interest is often in estimating GEV parameters at locations without rain gauges. To be able to provide estimates of extremes at ungauged locations it is necessary to develop a spatial model of the parameters. To maximize the precision in the model's estimates, all five parameters of the modified GEV distribution were modeled spatially.

The parameters were modeled via a thin plate spline regression. In this regression, the employed model is additive $\vartheta = f(x) + e$ where ϑ is a parameter surface of interest, $f(x)$ is the response surface for a given vector x of covariates (here $f(x) = \beta_0 + \beta_{lon} longitude + \beta_{lat} latitude$), and e is an error term. Additional covariates of elevation and distance from coast were tested but did not significantly improve the fit of the parameter surfaces. Additional covariates of elevation and distance from coast were tested but did not significantly improve the fit of the parameter surfaces (see supporting information Figure S7). A reason for this is that the longitude covariate provides a surrogate for both these terms since the coastline predominantly runs north-south along the eastern edge of the region and the elevated areas occur along the western edge (visible in Figure 2). Each thin plate spline surface is determined by minimizing $\|\vartheta - f\|^2 + \lambda\Delta$, where Δ is a roughness penalty function determined by a constraint on the dimension of the covariates and λ is a smoothness parameter that is selected by generalized cross-validation. This approach is used to build five response surfaces for the five marginal parameters i.e., $\tilde{\mu}, \tilde{\sigma}, \xi, \delta, \eta$.

3.4. Storm-Level Dependence Model

In this study, the Brown-Resnick model (Brown & Resnick, 1977; Kabluchko et al., 2009) is selected for analyzing storm-level dependence. This section describes a detailed method for calibrating the max-stable process, and introduces an empirical approach for linking duration dependence into the dependence model.

To calibrate the max-stable process, it is necessary to calculate the observed pairwise extremal coefficients. It is noted that the dependence model is stationary in unit Fréchet scale, but the final model is nonstationary because of the nonstationary marginal model. First, the rainfall values $r_{i,t,d}$ need to be transformed to a unit Fréchet distribution $z_{i,t,d}$, which is achieved via the following equation:

$$z_{i,t,d} = \left(1 + \xi_{i,d} \frac{r_{i,t,d} - \mu_{i,d}}{\sigma_{i,d}}\right)^{1/\xi_{i,d}} \tag{6}$$

The observed pairwise extremal coefficient $\hat{\theta}$ is then calculated through the F-Madogram $\hat{v}_F$ (Cooley et al., 2006):

$$\hat{v}_F(x_1 - x_2) = \frac{1}{2p} \sum_{t=1}^{p} \left|F(z_t(x_1)) - F(z_t(x_2))\right| \tag{7}$$

where $z_t(x_1)$ and $z_t(x_2)$ are the tth observations (the annual maximum rainfall in the tth year) of extremes in the form of unit Fréchet margins at location x_1 and x_2 with p the total number of common observations between the two locations, and $F(z) = \exp(-1/z)$. Note that the extreme rainfall at location x_1 and x_2 can

be of identical duration (i.e., both 24 h) or different durations (e.g., 24 and 1 h). The observed pairwise extremal coefficient $\hat{\theta}$ is then estimated by:

$$\hat{\theta}(x_1-x_2)=\frac{1+2\hat{\nu}_F(x_1-x_2)}{1-2\hat{\nu}_F(x_1-x_2)} \tag{8}$$

The max-stable process can be fitted by minimizing the sum of squared errors between the theoretical pairwise extremal coefficient function and the observed pairwise extremal coefficients. The theoretical extremal coefficient function for the Brown-Resnick model is given as:

$$\theta(x_1-x_2)=2\Phi\left(\frac{\sqrt{\gamma(h)}}{2}\right) \tag{9}$$

where Φ is the standard normal cumulative distribution function, h indicates the Euclidean distance between two locations x_1 and x_2, and $\gamma(h)$ belongs to the class of variograms $\gamma(h)=h^\beta/q$ for $q>0$ and $\beta\in(0,2]$.

In the case that extreme rainfall at locations x_1 and x_2 are of identical duration (i.e., both 24 h), then the max-stable process is fitted to the observations by minimizing the sum of squared errors of extremal coefficients numerically. However when the extreme rainfall at location x_1 and x_2 are of different durations (e.g., 24 and 1 h), the dependence level of extreme rainfall at these two locations is less than the case of 24 and 24 h, including at the distance of $h=0$ where the rainfall is not "perfectly dependent" as would be the case when using only a single duration. Therefore, an adjustment needs to be made to ensure that the theoretical pairwise extremal coefficient function can capture the observed pairwise extremal coefficients for the case of extreme rainfall of different durations. We propose an approach of adjustment by adding a nugget to the variograms as:

$$\gamma_{ad.}(h)=h^\beta/q+c(D-d)/d \tag{10}$$

where h, β, and q are the same as those from equation (9) above, d is the duration (in hours), $0<d\leq D$, where D is the maximum duration of interest ($D=24$ h for the case study described in this paper), and c is a new parameter of the adjustment. This adjustment is intended specifically to condition the behavior of shorter duration extremes on the observation that a D-hour extreme of specified magnitude has occurred. It is constructed to reflect that when compared to a D-hour extreme, the shorter the duration, the lesser the extremal dependence. Cases involving conditioning longer periods on shorter periods (such as a 24 h extreme given a 1 h extreme has occurred) would require a different relationship, and are beyond the scope of this paper.

To fit the max-stable process for all pairs of durations at locations x_1 and x_2 (i.e., 24 and 12 h, 24 and 6 h, 24 and 3 h, 24 and 2 h, 24 and 1 h), the theoretical pairwise extremal coefficient function in formula (11) is used. That formula is based on $\gamma_{ad.}(h)$ instead of $\gamma(h)$ as:

$$\theta(x_1-x_2)=2\Phi\left(\frac{\sqrt{\gamma_{ad.}(h)}}{2}\right) \tag{11}$$

The parameters β and q are used from the fitted results of the case of identical 24 h durations at location x_1 and x_2. The other parameter c is obtained by least squares fit of the extremal coefficient across all durations.

3.5. Conditional Probability Estimates

The conditional probability $Pr[Z(x_2)>z_2|Z(x_1)>z_1]$ is obtained from the bivariate max-stable process cumulative distribution function (Padoan et al., 2010), which is given as:

$$Pr[Z(x_1)\leq z_1, Z(x_2)\leq z_2]=\exp\left[-\frac{1}{z_1}\Phi\left(\frac{a}{2}+\frac{1}{a}log\frac{z_2}{z_1}\right)-\frac{1}{z_2}\Phi\left(\frac{a}{2}+\frac{1}{a}log\frac{z_1}{z_2}\right)\right] \tag{12}$$

where Φ is the standard normal cumulative distribution function, $a=\sqrt{2\gamma_{ad.}(h)}$ with $\gamma_{ad.}(h)$ is variogram which was mentioned in the explanation of equation (10) above.

Assuming unit Fréchet margins, the relationship between return level z and return period T is given as $z=-1/log(1-1/T)$ and the conditional probability for the max-stable process can then be estimated using:

$$Pr\left[Z(x_2) > z_2 | Z(x_1) > z_1\right] = T_1\left[\frac{1}{T_1} - \exp\left(-\frac{1}{z_2}\right) + \exp\left(-\frac{\Phi(\omega)}{z_1} - \frac{\Phi(v)}{z_2}\right)\right] \quad (13)$$

where $\omega = a/2 + log(z_2/z_1)/a$, $v = a - \omega$, and T_1 is the return period corresponding to return level z_1.

This formula is used to estimate the conditional probability in the form of conditional maps of return periods and return levels across different durations.

3.6. Summary of the Overall Methodology

This section provides an algorithm that summarizes the overall methodology for this study in a stepwise order:

Step 1: Independently fit the univariate GEV at each site across multiple durations

The log-likelihood in equation (5) is maximized at each site to determine the Koutsoyiannis relationship and GEV marginal parameters for each location $\{\hat{\mu}_i, \hat{\sigma}_i, \hat{\xi}_i, \hat{\delta}_i, \hat{\eta}_i\}$. This yields estimates of five parameters at each site $i = 1,\ldots,N$.

Step 2: Perform spatial interpolation on the independently fitted parameter estimates

The marginal parameters estimated in Step 1 are used to perform a preliminary spatial interpolation. Independent application of thin plate spline regression to each parameter surface yields five response surfaces for the five marginal parameters $\{\tilde{\mu}, \tilde{\sigma}, \tilde{\xi}, \delta, \eta\}$.

Step 3: Analyze spatial dependence across different durations

The five response surfaces from Step 2 are used to transform the extreme rainfall for all durations to a unit Fréchet margin. After that, the observed pairwise extremal coefficients across different durations (e.g., extreme rainfall for 24 and 24 h, 24 and 12 h, 24 and 6 h, 24 and 3 h, 24 and 2 h, 24 and 1 h) are estimated based on the extremal values in the unit Fréchet scale.

Step 4: Fit max-stable process across different durations

The dependence structures of the max-stable process across different durations (i.e., extreme rainfall for 24 and 24 h, 24 and 12 h, 24 and 6 h, 24 and 3 h, 24 and 2 h, 24 and 1 h) were fitted to the data by minimizing the sum of squared errors between the theoretical pairwise extremal coefficient function (calculated from equations (9)–(11)) and the observed pairwise extremal coefficients (calculated from equations (7) and (8)).

Step 5: Implement conditional estimates

Conditional estimates are implemented by calculating conditional probabilities for a unit Fréchet max-stable process based on equation (13) with the dependence parameters from Step 4. The conditional maps of return period and return level are then inferred.

4. Results and Discussion

This section provides results in a stepwise manner that parallels the steps used in the methodology. First, the approach is evaluated for its ability to link extreme rainfall data across multiple durations at individual stations. The spatial patterns of the at-site parameters are then explored. Subsequently, the results of the calibration of the max-stable process across different durations are presented. The final section demonstrates maps of the conditional return periods and return levels.

4.1. Linking Extreme Rainfall for Multiple Durations at Each Site

To evaluate the performance of the re-parameterization, we checked the quantile-quantile plots (QQ plots) to see if the fits are reasonable. Figure 5 provides the QQ plots for the marginal model for one representative station for extreme rainfall of all durations. The QQ plots for all durations indicate that the fitted results for station 20 are reasonable. Similar QQ plots for other stations can be found in the supporting information (supporting information Figures S1–S6), showing that the marginal estimates by using the reparameterization are reasonable for all stations.

4.2. Building the Response Surface for the Reparameterization Model Parameters

The second step in the modeling approach is the development of the spatial model for marginal distribution parameters, which is important for predicting extreme rainfall at unobserved locations. As mentioned

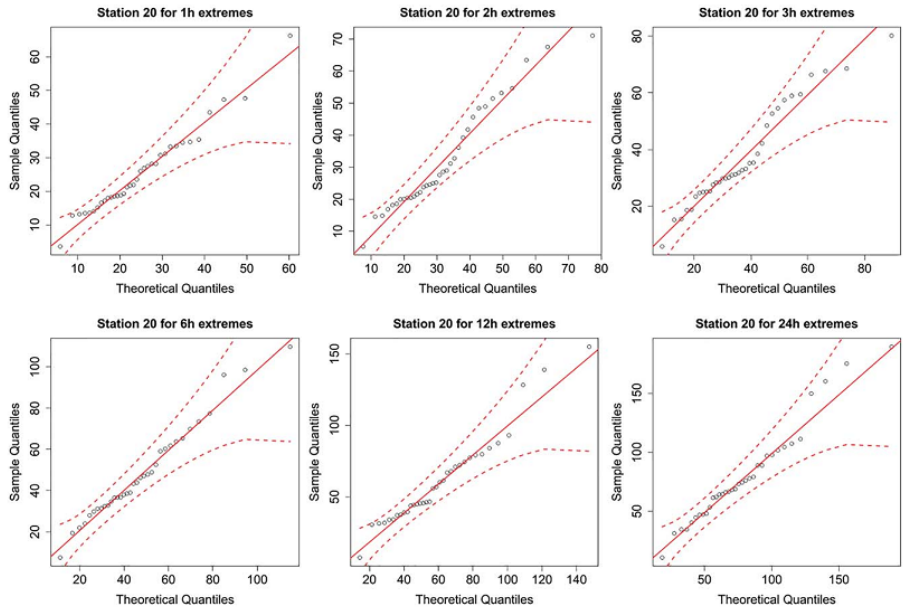

Figure 5. QQ plots for the marginal model based on the reparameterization approach to fit GEV at rain station 20 in the case study. The solid diagonal line indicates a perfect fit, and the dotted lines indicate a 95% confidence interval.

in section 3.4, applying the max-stable process requires transforming extreme data to a unit Fréchet distribution. Marginal distribution parameters are needed to complete this transformation. This section provides the spatial model for the reparameterization of marginal parameters, which can then be used to predict the reparameterized marginal parameters at ungauged locations.

To allow the marginal parameters to vary spatially, the thin plate splines are employed to build the response surface for parameters $\tilde{\mu}$, $\tilde{\sigma}$, ξ, δ, and η based on covariates of longitude and latitude. For this case study, the parameter δ for all stations was found to be in a small range from 0 to 0.03, with δ=0 for most sites. A simplification was therefore made to set δ constant at 0 for the whole domain. Figure 6 shows both the at-site estimates (as colors within each circle) and the response surfaces for $\tilde{\mu}$ and $\tilde{\sigma}$ (on the top) and for ξ and η (on the bottom).

The top-left panel in Figure 6 shows that the range of magnitude for $\tilde{\mu}$ varies from 2.2 to 3.0, with lower magnitude values of $\tilde{\mu}$ at the bottom right of the domain, and higher values at the top left of the domain. The top-right panel shows that the magnitude of $\tilde{\sigma}$ tends to vary from left to right across the domain, with a range from 5 to 11. The modelled surfaces can have discrepancies with some of the at-site estimates due to a large nugget effect.

The response surface for ξ in the bottom-left panel in Figure 6 shows considerable variation over the region, though the range of magnitude is very small, only from −0.05 to 0.1. However, these small variations in values of ξ have a noticeable effect on the shape of the marginal extremal distribution, which then impacts on the predictions, particularly under extrapolation to long recurrence-interval values. The magnitude for ξ is generally higher for the lower portion of the region.

The response surface for η in the bottom-right panel is the most variable surface among the four parameters. This parameter is the power term for the location parameter μ and the scale parameter σ across

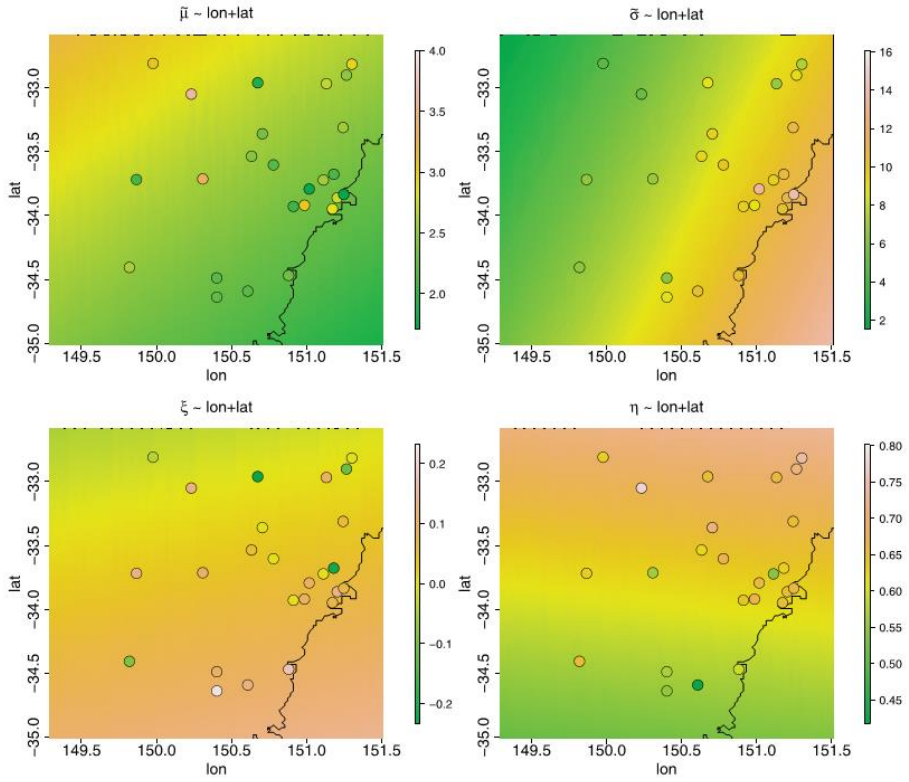

Figure 6. Response surfaces for (top) $\tilde{\mu}$ and $\tilde{\sigma}$ and for (bottom) ξ and η. The circles are at-site parameter estimates of subdaily extremes, matching the domain in Figure 2.

durations, which affects the function's shape. Spatially, it fluctuates with local highs and lows across the region, ranging from 0.45 to 0.75, which indicates that the shape of the relationships between the location parameter μ and durations, and between the scale parameter σ and durations, are different over the domain.

4.3. Calibration of the Max-Stable Process Across Different Durations

The max-stable process across different durations was calibrated to determine the spatial dependence parameters for extreme rainfall. To do this, the theoretical pairwise extremal coefficient function was estimated and compared with the observed pairwise extremal coefficients. The theoretical pairwise extremal coefficient function between two locations (x_1 and x_2) was calculated based on equations (9)–(11), and the observed pairwise extremal coefficient $\hat{\theta}$ was calculated using equations (7) and (8) in section 3.4.

Figure 7 provides the pairwise extremal coefficient estimates for the Brown-Resnick model versus distance h (in km). To reduce the uncertainty of the observed pairwise extremal coefficients, pairs of rain gauges were grouped into distance classes. The black points are observed pairwise extremal coefficients while the red lines are the fitted extremal coefficient functions. A coefficient equal to 1 indicates complete spatial dependence, and a value of 2 indicates complete spatial independence. The top-left panel shows the

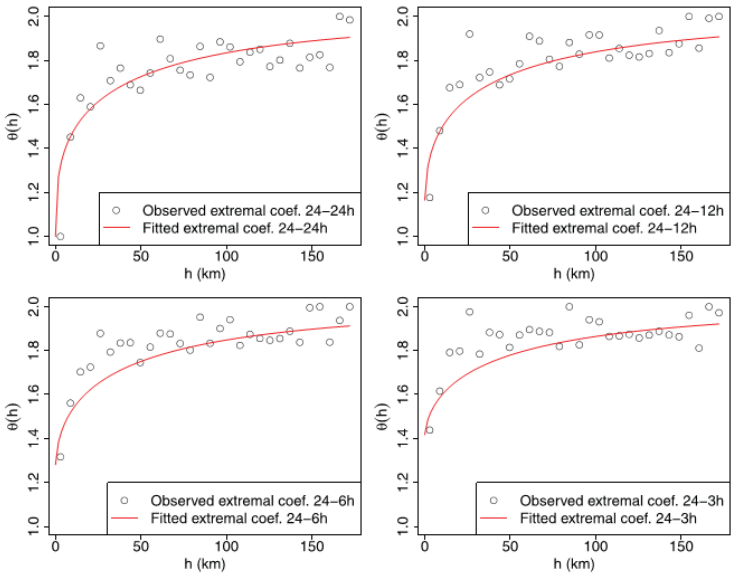

Figure 7. Plot of pairwise extremal coefficient against distance. Pairwise extremal coefficient estimates for Brown-Resnick model between: (top left) 24 h extremes and 24 h extremes; (top right) 24 h extremes and 12 h extremes; (bottom left) 24 h extremes and 6 h extremes; and (bottom right) 24 h extremes and 3 h extremes. The black points are observed extremal coefficients for pairs of subdaily stations grouped into distance classes, and the red lines are fitted extremal coefficient function.

dependence between 24 h extremes across space, with the distance $h = 0$ corresponding to "complete dependence," and with the dependence decreasing for increasing distance.

The remaining panels of Figure 7 show the 24 versus 12 h extremes, 24 versus 6 h extremes, and 24 versus 3 h extremes. As can be seen, the dependence levels are weaker compared with 24 versus 24 h extremes at the same distance, especially at the distance of 0. This is expected, as the dependence at the same site between annual maxima at different durations will be lower than between annual maxima at the same duration. This is because the annual maxima of different durations may arise from different storm events (Zheng et al., 2015). Even though events giving rise to the maxima may be different, there can still be a level of dependence as they can arise from the same generating process (e.g., low-pressure system or a wetter than average season).

4.4. Conditional Modeling Across Durations

The previous sections outlined how to link extremes across multiple durations and how to extend the dependence structure of the extremes to encompass space and duration. Having defined and calibrated this model it is now possible to use it for estimating conditional extremes over a spatial domain. While the model is noticeably idealized when compared to real observations (Figures 5–7), the approach opens up new possibilities for addressing design problems that are not otherwise achievable with the use of typical IDF curves.

Consider the situation where a house at location i has been designed to a 20% annual exceedance probability (AEP; corresponding to a 5 year return period). In other words, this exceedance probability has been used to set the building level for the house. Assuming a one-to-one correspondence between extreme rainfall intensity and flood magnitude, the probability of the house getting flooded is given as:

$$Pr(r_i > u_i) = 0.2 \quad (14)$$

where u_i mm is the minimum water level at which the house would be considered "flooded." Assuming that the residents of the house will need to evacuate to higher ground upon the house flooding, it is desirable to design a route at some other location j with its own corresponding probability of failure. Given that the evacuation route is only needed if location i is flooded, we might specify a design criterion that we are only willing to tolerate a 10% risk of the evacuation route being flooded conditional on it being required. To specify this problem, we can write the conditional probability as follows:

$$Pr(r_j > u_j | r_i > u_i) = 0.1 \quad (15)$$

To calculate the conditional distribution, it is necessary to account for the spatial dependence of flooding at the two locations. Hence, we use spatial dependence of the flood-producing rainfall (assuming a one-to-one correspondence). There are two extreme situations in this scenario:

1. **Very strong spatial dependence between locations *i* and *j*.** This situation might arise if locations i and j are very close together, such that if there is a rainfall event of a given exceedance probability at location i, one can expect a rainfall event of identical exceedance probability at location j. To preserve the conditional probability in equation (15) we would have to design the evacuation route at location j to have marginal probability $Pr(r_j > u_j) = 0.2 * 0.1 = 0.02$, so that the evacuation route can only be flooded once every 50 years on average. In other words, designing the evacuation route to a 2% annual failure probability will ensure that its average failure rate is one in every 10 times that location i is flooded.
2. **Very weak spatial dependence between locations *i* and *j*.** This situation might arise if locations i and j are very far apart, so that a rainfall event at location i provides no information on the likely magnitude of a rainfall event at location j. We would design the evacuation route at location j to have a marginal probability equivalent to the conditional probability, so that $Pr(r_j > u_j) = 0.1$. This is because a flood at location i will have no influence on whether the evacuation route at location j is flooded.

In reality, the marginal probability at location j needed to achieve the conditional probability given in equation (15) will be somewhere between the two extremes specified above. The max-stable process described in the previous sections is capable of providing information to estimate these conditional probabilities, so that it is possible to calculate the appropriate marginal probabilities $Pr(r_i > u_i)$ to be used for design. This is illustrated in Figure 8, which is specified to provide marginal probabilities $Pr(r_j > u_j)$, such that the

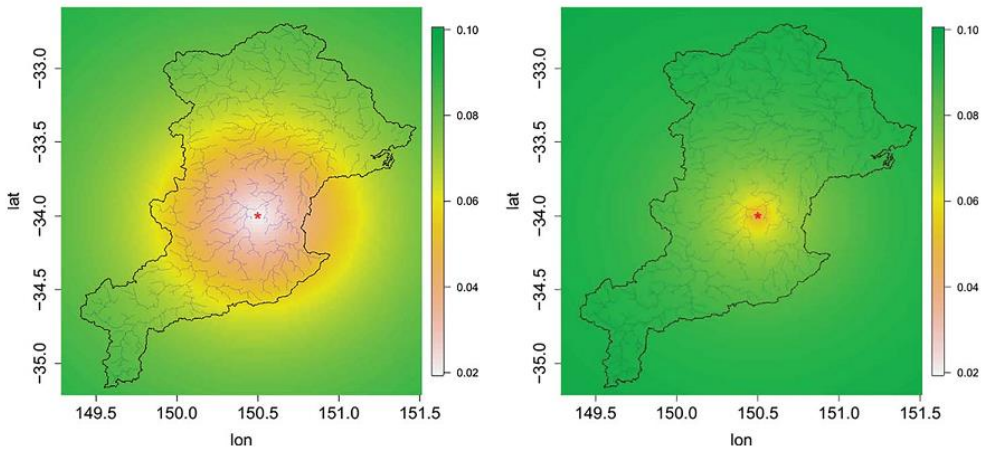

Figure 8. Map of marginal probabilities $Pr(r_j > u_j)$ corresponding to a conditional probabilities $Pr(r_j > u_j | r_i > u_i) = 0.1$, assuming a house at location i (indicated in the center of the domain by the red star) floods with probability $Pr(r_i > u_i) = 0.2$. Plots are presented for (left) 24 h extremes and (right) 1 h extremes at locations j, conditional on a 24 h extreme event at location i. The color scales are the same for comparison.

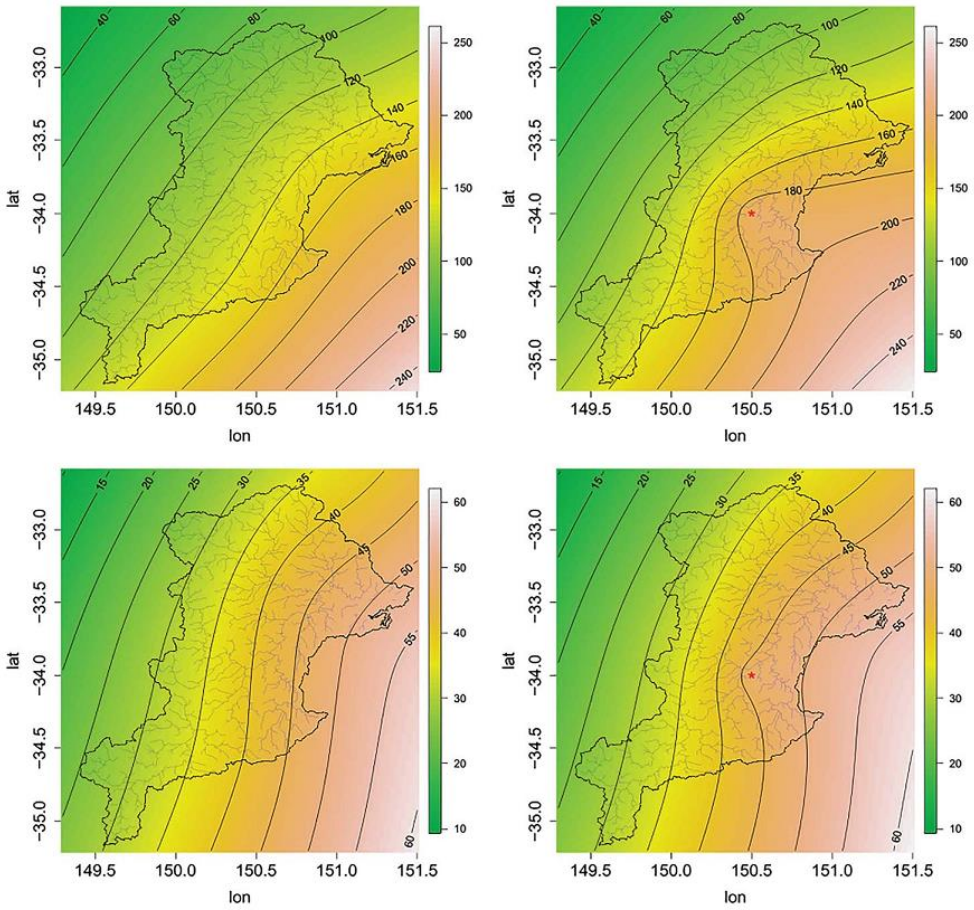

Figure 9. Pointwise 10 year unconditional return level map (mm), and pointwise 10 year conditional return level map (mm) given a 5 year event for 24 h extremes happen at location *i* (the red star). (top) Pointwise unconditional return level map for (left) 24 h extremes, and (right) pointwise conditional return level map for 24 h extremes. (bottom) Pointwise unconditional return level map for (left) 1 h extremes, and (right) pointwise conditional return level map for 1 h extremes.

conditional probability in equation (15) is preserved, assuming the marginal probability at location *i* given in equation (14).

Figure 8 (left panel) illustrates the situation where the critical storm durations for locations *i* and *j* are the same (i.e., both 24 h). Here, the range of annual exceedance probabilities varies from 0.02 when locations *i* and *j* are close together, to 0.1 when locations *i* and *j* are far apart. The shape of the decay is determined by the function $f(s_i, x)$ mentioned in section 3.1. These results show that the design criteria of the evacuation route (in terms of marginal failure criteria) needs to be stronger as the evacuation route is increasingly close to location *i*, as expected from the spatial nature of the storm.

The situation where critical durations at locations *i* and *j* are different (Figure 8, right panel) shows a similar decaying behavior away from the storm, but with lower annual exceedance probabilities required for the evacuation route design close to location *i*. Such a situation might arise in practice if a house is located near a larger river system, but where the evacuation route needs to cross over a smaller tributary into that river system. The lowered dependence can be explained by the fact that a large 24 h storm event does not imply an equally large (in terms of exceedance probabilities) 1h storm event. This is consistent with Zheng et al. (2015) who showed that annual maximum 24h events in Sydney often occur in different seasons from the annual maximum 1h events.

The above results are expressed as exceedance probabilities, but it is also possible to illustrate the results as a return level. The left-hand panel of Figure 9 shows the unconditional return level map for u_j corresponding to $Pr(r_j > u_j)=0.1$. As can be seen, there is a gradient of rainfall intensity from relatively less intense in the top left of the domain to higher intensity in the bottom right of the domain. This feature is a result of the coastal effects that are well-known in the Sydney region, with higher extreme rainfall typically occurring closer to the coastline. These results are presented for both the 24 h rainfall event (top left panel) and 1h event (bottom left panel). They are obtained from the multi-duration surface of the fitted max stable model developed in the previous section.

We now consider the return level given that an event equal to the return periods given in Figure 8 for the 24h rainfall (Figure 9 upper right panel) and 1 h rainfall (Figure 9 lower right panel). The return levels are higher close to the conditional point (*i*) and decrease away from this point, until they become equivalent to the unconditional plots. All the plots in Figure 9 are produced using the same model, thus providing a unifying framework for generating both conditional and unconditional IDF maps.

This above analysis highlights the potential of the spatial max-stable process approach. Not only is it possible to develop spatial maps of return periods and return levels at both gauged and ungauged locations, but it is also possible to use a single model to estimate return periods and levels at all durations from 1 h through to 24 h. Furthermore, it is possible to estimate the conditional return periods given that an extreme rainfall event has occurred at a given location. There are some assumptions using the analysis of extreme rainfall to infer the properties of a flood, which include that there is a one-to-one correspondence between the extreme rainfall and the streamflow derived from a hydrological model of that rainfall, and that the spatial dependence structure of the rainfall is the same as the streamflow. These assumptions are common to most methods that rely on IDF curves.

The substantial differences in return levels for the conditional and unconditional plots highlight the potential for under-designing infrastructure if conditional dependencies are not taken into account. This figure shows that the neighboring region of the location *i* would likely be under-designed if considering only the unconditional extremes. In particular, it is extremely common for infrastructure and engineered systems to fail in multiple places during a single extreme event, because of the substantial conditional storm-level dependencies associated with extremes. Conditional probabilities are not just an issue in spatial extreme rainfall; they can also be found in a wider range of extreme events, such as extreme rainfall together with storm surge in coastal areas (Zheng et al., 2013, 2014). To ensure that critical emergency infrastructure does not fail during a hazardous event, it is necessary to use much higher return levels than if one is merely designing to the marginal distribution of key decision variables such as rainfall or floods.

5. Conclusions

With increasing exposure of the built environment to floods, improving frameworks used to model extreme rainfall is an active and important domain of research. Conditional estimates of extremes such as those described in this paper are useful for the design of complex civil engineering systems, such as road and rail networks, as well as for emergency evacuation planning. Such estimates need to account for the dependence between extreme rainfall not only in space, but also across different durations.

This challenge has been addressed here by exploring the ability to link the max-stable process of extreme rainfall across multiple durations using the reparameterization of Koutsoyiannis et al. (1998). Subdaily rainfall from 25 sites, having at least 19 years of record, were taken from the Hawkesbury-Nepean catchment of New South Wales, Australia. Six durations spanning from 1 to 24 h were considered. Assuming each duration is estimated separately, this would require 450 parameters (i.e., 25 sites × 6 durations × 3 parameters)

in order to represent the marginal distributions at all locations. Due to the linking of durations, the number of parameters needed to estimate the marginal distribution is significantly lower than if independent estimates of the GEV distribution were made (125 parameters, i.e., 25 sites × 5 parameters) followed by spatial interpolation (20 parameters, i.e., 5 parameter surfaces × 4 interpolation parameters per surface). It would be possible to further reduce the number of parameters by implementing a method of jointly fitting the sites so that the 125 at-site parameters did not need to be determined prior to fitting the spatial surface. It is possible that joint fitting of the marginal and dependence components of the model may lead to different outcomes regarding the significance of the covariate terms. Two additional parameters are required for the max-stable dependence structure at a 24 h duration along with one additional parameter that extends the dependence structure across durations (i.e., from 24 h to shorter durations). Given the large number of parameters across the marginal, spatial, and dependence structures of the model it would be useful to further explore the uncertainty contribution of each component (Stephenson et al., 2016).

The reparameterization used in this study, to link together the extremes for multiple durations when fitting the marginal model, works well for the locations analyzed. The proposed adjustment for the variograms helps the max-stable process capture the spatial dependence of rainfall extremes across different durations. A key reason for this proposed method is that it accounts for the dependence between durations, which arises because in some situations long-duration extreme rainfall events will have shorter-duration extremes embedded inside them, but in other situations the extremes at different durations will occur at different times. This is addressed by the pairwise extremal coefficient, which shows complete dependence at a distance of zero for the 24–24 h duration, but shows lesser dependence for other pairs of durations, such as the 24 h extreme event and a 6 h extreme event at the same location. While this paper focused on subdaily durations, application to large catchments may require durations longer than 1 day or take into account the influence of daily rainfall accumulations (Lehmann et al., 2016).

The additional complexity involved in fitting a max-stable process to rainfall extremes across different durations may not be warranted in all cases. For example, where the interest is in developing conditional estimates of rainfall in two neighboring gauges with sufficient at-site rainfall data, it may be sufficient to represent the bivariate dependence in catchment-average rainfall at the relevant critical durations of both catchments, for example using a bivariate extreme value model. However, frameworks of extremes offer numerous advantages over traditional approaches that only have point-wise estimates of extremes; for example by providing consistency between both unconditional and conditional IDF estimates. The development of spatiotemporal models of rainfall is also important for the potential to merge multiple data sources and further improve estimates of extremes, whether conditional or unconditional. For example, the use of ground-based and satellite-based remote sensed data to characterize spatial and spatio-temporal features of storms merged with daily and subdaily gauges across a region that have longer periods of observation. The proposed adjustment in this paper for pairwise distances with three additional parameters enables the model to infer the conditional estimate for any shorter duration extreme given the 24 h extreme. Understanding the storm-level dependence structure of rainfall is important for achieving more realistic representations of flood-generating mechanisms and their role in flood impacts. This allows results to be presented in conditional maps that show exceedance probabilities and return levels across different durations. These maps can then be used to better communicate and account for the complex dependences associated with extreme rainfall for use in a range of planning and engineering design contexts.

Acknowledgments
The lead author was supported by the Australia Awards Scholarships (AAS) from Australia Government. A/Prof Westra was supported by Australian Research Council (ARC) Discovery project DP150100411. We are grateful to the three anonymous reviewers for their detailed constructive comments and helpful insights to improve the paper. We would like to thank Leticia Mooney (editor at the School of Civil, Environmental and Mining Engineering at Adelaide University) for her help in improving this manuscript. The extracted data set used for this study can be directly accessed here https://figshare.com/articles/Data_zip/5923789.

References

Bennett, B., Thyer, Leonard, M., Lambert, M. M., & Bates, B. (2016). A comprehensive and systematic evaluation framework for a parsimonious daily rainfall field model. *Journal of Hydrology*, *556*, 1123–1138.

Boyd, M. J., Rigby, E. H., & VanDrie, R. (1996). WBNM: A computer software package for flood hydrograph studies. *Environmental Software*, *11*(1), 167–172.

Bracken, C., Rajagopalan, B., Cheng, L., Kleiber, W., & Gangopadhyay, S. (2016). Spatial Bayesian hierarchical modeling of precipitation extremes over a large domain. *Water Resources Research*, *52*, 6643–6655. https://doi.org/10.1002/2016WR018768

Brown, B. M., & Resnick, S. I. (1977). Extreme values of independent stochastic processes. *Journal of Applied Probability*, *14*(4), 732–739.

Chow, V. T., Maidment, D. R., & Mays, L. W. (1988). *Applied hydrology*. New York, NY: McGraw-Hill.

Cooley, D., Naveau, P., & Poncet, P. (2006). Variograms for spatial max-stable random fields. In P. Bertail, P. Soulier, & P. Doukhan (Eds.), *Dependence in probability and statistics* (pp. 373–390). New York, NY: Springer.

Cooley, D., Nychka, D., & Naveau, P. (2007). Bayesian spatial modeling of extreme precipitation return levels. *Journal of the American Statistical Association*, *102*(479), 824–840.

Davison, A. C., & Gholamrezaee, M. M. (2012). Geostatistics of extremes. *Proceedings of the Royal Society A: Mathematical, Physical and Engineering Science*, *468*(2138), 581–608.
Davison, A. C., Padoan, S. A., & Ribatet, M. (2012). Statistical modeling of spatial extremes. *Statistical Science*, *27*, 161–186.
de Haan, L. (1984). A spectral representation for max-stable processes. *The Annals of Probability*, *12*(4), 1194–1204.
de Haan, L., & Ferreira, A. (2006). *Extreme value theory an introduction*. New York, NY: Springer.
Genton, M. G., Padoan, S. A., & Sang, H. (2015). Multivariate max-stable spatial processes. *Biometrika*, *102*(1), 215–230.
Huser, R., & Davison, A. C. (2014). Space–time modelling of extreme events. *Journal of the Royal Statistical Society: Series B (Statistical Methodology)*, *76*(2), 439–461.
Kabluchko, Z., Schlather, M., & de Haan, L. (2009). Stationary max-stable fields associated to negative definite functions. *The Annals of Probability*, *37*(5), 2042–2065.
Koutsoyiannis, D., Kozonis, D., & Manetas, A. (1998). A mathematical framework for studying rainfall intensity-duration-frequency relationships. *Journal of Hydrology*, *206*(1–2), 118–135.
Laurenson, E. M., & Mein, R. G. (1997). *RORB version 4 runoff routing program user manual*. Victoria, Australia: Department of Civil Engineering, Monash University.
Lehmann, E. A., Phatak, A., Stephenson, A., & Lau, R. (2016). Spatial modelling framework for the characterisation of rainfall extremes at different durations and under climate change. *Environmetrics*, *27*(4), 239–251.
Mulvaney, T. J. (1851). On the use of self-registering rain and flood gauges in making observation of the relation of rainfall and floods discharges in a given catchment. *Transactions of the Institution of Civil Engineers of Ireland*, *4*, 18–31.
Oesting, M., Schlather, M., & Friederichs, P. (2017). Statistical post-processing of forecasts for extremes using bivariate Brown-Resnick processes with an application to wind gusts. *Extremes*, *20*(2), 309–332.
Opper ESM, S., Cinque Oam, P., & Davies, B. (2010). Timeline modelling of flood evacuation operations, 1st Conference on Evacuation Modeling and Management. *Procedia Engineering*, *3*, 175–187.
Padoan, S. A., Ribatet, M., & Sisson, S. A. (2010). Likelihood-based inference for max-stable processes. *Journal of the American Statistical Association*, *105*(489), 263–277.
Renard, B. (2011). A Bayesian hierarchical approach to regional frequency analysis. *Water Resources Research*, *47*, W11513. https://doi.org/10.1029/2010WR010089
Renard, B., & Lang, M. (2007). Use of a Gaussian copula for multivariate extreme value analysis: Some case studies in hydrology. *Advances in Water Resources*, *30*(4), 897–912.
Ribbons, S. (2015). *Hawkesbury-Nepean valley flood management review: Developing a strategy where flood depth can be nine metres above flood planning level*. Paper presented at 2015 Floodplain Management Association National Conference, Australia.
Schlather, M., & Tawn, J. A. (2003). A dependence measure for multivariate and spatial extreme values: Properties and inference. *Biometrika*, *90*(1), 139–156.
Smith, R. L. (1990). *Max-stable processes and spatial extremes*. University of Surrey. Retrieved from http://www.stat.unc.edu/postscript/rs/spatex.pdf
Stephenson, A. G., Lehmann, E. A., & Phatak, A. (2016). A max-stable process model for rainfall extremes at different accumulation durations. *Weather and Climate Extremes*, *13*(Suppl. C), 44–53.
Thibaud, E., Mutzner, R., & Davison, A. C. (2013). Threshold modeling of extreme spatial rainfall. *Water Resources Research*, *49*, 4633–4644. https://doi.org/10.1002/wrcr.20329
Westra, S., & Sisson, S. A. (2011). Detection of non-stationarity in precipitation extremes using a max-stable process model. *Journal of Hydrology*, *406*(1–2), 119–128.
Zheng, F., Westra, S., & Leonard, M. (2015). Opposing local precipitation extremes. *Nature Climate Change*, *5*(5), 389–390.
Zheng, F., Westra, S., Leonard, M., & Sisson, S. A. (2014). Modeling dependence between extreme rainfall and storm surge to estimate coastal flooding risk. *Water Resources Research*, *50*, 2050–2071. https://doi.org/10.1002/2013WR014616
Zheng, F., Westra, S., & Sisson, S. A. (2013). Quantifying the dependence between extreme rainfall and storm surge in the coastal zone. *Journal of Hydrology*, *505*, 172–187.

References

Alaya, M.B., Ouarda, T., Chebana, F., 2018. Non-Gaussian spatiotemporal simulation of multisite daily precipitation: downscaling framework. Climate Dynamics, 50(1-2): 1-15.

Allen, R.J., DeGaetano, A.T., 2005. Areal Reduction Factors for Two Eastern United StatesRegions with High Rain-Gauge Density. Journal of hydrologic engineering: 327-335. DOI:10.1061/(ASCE)1084-0699(2005)10:4(327)

Asadi, P., Davison, A.C., Engelke, S., 2015. Extremes on river networks. Ann. Appl. Stat., 9(4): 2023-2050. DOI:10.1214/15-AOAS863

Asquith, W.H., Famiglietti, J.S., 2000. Precipitation areal-reduction factor estimation using an annual-maxima centered approach. Journal of Hydrology, 230(1–2): 55-69. DOI:http://dx.doi.org/10.1016/S0022-1694(00)00170-0

Bacchi, B., Ranzi, R., 1996. On the derivation of the areal reduction factor of storms. Atmospheric Research, 42(1): 123-135. DOI:http://dx.doi.org/10.1016/0169-8095(95)00058-5

Ball, J. et al., 2016. Australian Rainfall and Runoff: A Guide to Flood Estimation. © Commonwealth of Australia (Geoscience Australia).

Baxevani, A., Lennartsson, J., 2015. A spatiotemporal precipitation generator based on a censored latent Gaussian field. Water Resources Research, 51(6): 4338-4358. DOI:doi:10.1002/2014WR016455

Bengtsson, L., Niemczynowicz, J., 1986. Areal Reduction Factors from Rain Movement. Hydrology Research, 17(2): 65-82.

Bennett, B., Lambert, M., Thyer, M., Bates, B.C., Leonard, M., 2016a. Estimating Extreme Spatial Rainfall Intensities. Journal of Hydrologic Engineering, 21(3): 04015074. DOI:doi:10.1061/(ASCE)HE.1943-5584.0001316

Bennett, B., Thyer, M., Leonard, M., Lambert, M., Bates, B., 2016b. A comprehensive and systematic evaluation framework for a parsimonious daily rainfall field model. Journal of Hydrology. DOI:https://doi.org/10.1016/j.jhydrol.2016.12.043

Bernard, M.M., 1932. Formulas for rainfall intensities of long duration. Transactions of the American Society of Civil Engineers, 96(1): 592-606.

Beven, K.J., 2002. Rainfall-Runoff Modelling: The Primer. John Wiley, New York, 360 pp.

BITRE, 2008. Analysis of the Emergency Management Australia database. About Australia's Regions. Bureau of Infrastructure, Transport and Regional Economics. Department of Infrastructure, Transport, Regional Development and Local Government, Australian Government, Canberra, Table 30; 44

Blanchet, J., Davison, A.C., 2011. SPATIAL MODELING OF EXTREME SNOW DEPTH. The Annals of Applied Statistics, 5(3): 1699-1725.

Blazkova, S., Beven, K., 2002. Flood frequency estimation by continuous simulation for a catchment treated as ungauged (with uncertainty). Water Resources Research, 38(8): 14-1-14-14. DOI:doi:10.1029/2001WR000500

Blazkova, S., Beven, K., 2009. A limits of acceptability approach to model evaluation and uncertainty estimation in flood frequency estimation by continuous simulation: Skalka catchment, Czech Republic. Water Resources Research, 45(12). DOI:doi:10.1029/2007WR006726

Blume, T., Zehe, E., Bronstert, A., 2007. Rainfall—runoff response, event-based runoff coefficients and hydrograph separation. Hydrological Sciences Journal, 52(5): 843-862. DOI:10.1623/hysj.52.5.843

Boughton, W., Droop, O., 2003. Continuous simulation for design flood estimation—a review. Environmental Modelling & Software, 18(4): 309-318. DOI:https://doi.org/10.1016/S1364-8152(03)00004-5

Boyd, M.J., Rigby, E.H., VanDrie, R., 1996. WBNM — a computer software package for flood hydrograph studies. Environmental Software, 11(1): 167-172. DOI:https://doi.org/10.1016/S0266-9838(96)00042-1

Bracken, C., Rajagopalan, B., Cheng, L., Kleiber, W., Gangopadhyay, S., 2016. Spatial Bayesian hierarchical modeling of precipitation extremes over a large domain. Water Resources Research, 52(8): 6643-6655. DOI:10.1002/2016WR018768

Brath, A., Montanari, A., Moretti, G., 2002. On the use of simulation techniques for the estimation of peak river flows, Proceedings of the International Conference on Flood Estimation, International Commission for the Hydrology of the Rhine Basin, Lelystad, Netherlands, pp. 587-599.

Brown, B.M., Resnick, S.I., 1977. Extreme Values of Independent Stochastic Processes. Journal of Applied Probability, 14(4): 732-739. DOI:10.2307/3213346

Buishand, T.A., de Haan, L., Zhou, C., 2008. On Spatial Extremes: With Application to a Rainfall Problem. The Annals of Applied Statistics, 2(2): 624-642.

Cameron, D.S., Beven, K.J., Tawn, J., Blazkova, S., Naden, P., 1999. Flood frequency estimation by continuous simulation for a gauged upland catchment (with uncertainty). Journal of Hydrology, 219(3): 169-187. DOI:https://doi.org/10.1016/S0022-1694(99)00057-8

Casson, E., Coles, S., 1999. Spatial Regression Models for Extremes. Extremes, 1(4): 449-468. DOI:10.1023/a:1009931222386

Chow, V.T., Maidment, D.R., Mays, L.W., 1988. Applied Hydrology. McGraw-Hill, c1988, New York.

Coles, S., 2001. An Introduction to Statistical Modeling of Extreme Values. Springer Series in Statistics. Springer.

Coles, S., Casson, E., 1998. Extreme value modelling of hurricane wind speeds. Structural Safety, 20(3): 283-296. DOI:https://doi.org/10.1016/S0167-4730(98)00015-0

Coles, S., Heffernan, J., Tawn, J., 1999. Dependence Measures for Extreme Value Analyses. Extremes, 2(4): 339-365. DOI:10.1023/a:1009963131610

Coles, S., Pericchi, L.R., Sisson, S., 2003. A fully probabilistic approach to extreme rainfall modeling. Journal of Hydrology, 273(1–4): 35-50. DOI:http://dx.doi.org/10.1016/S0022-1694(02)00353-0

Coles, S., Tawn, J., 1994. Statistical Methods for Multivariate Extremes: An Application to Structural Design, 43. DOI:10.2307/2986112

Coles, S., Tawn, J., 1996. Modelling Extremes of the Areal Rainfall Process. Journal of the Royal Statistical Society. Series B (Methodological), 58(2): 329-347. DOI:10.2307/2345980

Cooley, D., Naveau, P., Jomelli, V., Rabatel, A., Grancher, D., 2006a. A Bayesian hierarchical extreme value model for lichenometry. Environmetrics, 17(6): 555-574. DOI:doi:10.1002/env.764

Cooley, D., Naveau, P., Poncet, P., 2006b. Variograms for spatial max-stable random fields. In: Bertail, P., Soulier, P., Doukhan, P. (Eds.), Dependence in Probability and Statistics. Springer New York, New York, NY, pp. 373-390. DOI:10.1007/0-387-36062-x_17

Cooley, D., Nychka, D., Naveau, P., 2007. Bayesian Spatial Modeling of Extreme Precipitation Return Levels. Journal of the American Statistical Association, 102(479): 824-840. DOI:10.2307/27639928

Cunderlik, J.M., Ouarda, T.B.M.J., 2006. Regional flood-duration–frequency modeling in the changing environment. Journal of Hydrology, 318(1): 276-291. DOI:https://doi.org/10.1016/j.jhydrol.2005.06.020

Davison, A.C., Gholamrezaee, M.M., 2012. Geostatistics of extremes. Proceedings of the Royal Society A: Mathematical, Physical and Engineering Science, 468(2138): 581-608. DOI:10.1098/rspa.2011.0412

Davison, A.C., Huser, R., Thibaud, E., 2013. Geostatistics of Dependent and Asymptotically Independent Extremes. Mathematical Geosciences, 45(5): 511-529. DOI:10.1007/s11004-013-9469-y

Davison, A.C., Padoan, S.A., Ribatet, M., 2012. Statistical Modeling of Spatial Extremes. Statistical Science: 161-186. DOI:10.1214/11-STS376

Davison, A.C., Smith, R.L., 1990. Models for exceedances over high thresholds. Journal of the Royal Statistical Society. Series B (Methodological): 393-442.

de Haan, L., 1984. A Spectral Representation for Max-stable Processes. The Annals of Probability, 12(4): 1194-1204. DOI:10.2307/2243357

de Haan, L., Ferreira, A., 2006. Extreme Value Theory An Introduction. Springer Series in Operations Research and Financial Engineering. Springer New York. DOI:10.1007/0-387-34471-3

Demarta, S., McNeil, A.J., 2005. The t Copula and Related Copulas. International Statistical Review / Revue Internationale de Statistique, 73(1): 111-129.

Diggle, P.J., Ribeiro, P.J.J., 2007. Model-based Geostatistics. Springer Series in Statistics. Springer New York. DOI:10.1007/978-0-387-48536-2

Diggle, P.J., Tawn, J.A., Moyeed, R.A., 1998. Model-based geostatistics. Journal of the Royal Statistical Society: Series C (Applied Statistics), 47(3): 299-350. DOI:10.1111/1467-9876.00113

Dombry, C., Engelke, S., Oesting, M., 2016. Exact simulation of max-stable processes. Biometrika, 103(2): 303-317.

Durocher, M., Chebana, F., Ouarda, T.B.M.J., 2016. On the prediction of extreme flood quantiles at ungauged locations with spatial copula. Journal of Hydrology, 533: 523-532. DOI:https://doi.org/10.1016/j.jhydrol.2015.12.029

Eagleson, P.S., 1972. Dynamics of flood frequency. Water Resources Research, 8(4): 878-898. DOI:doi:10.1029/WR008i004p00878

El Adlouni, S., Bobée, B., Ouarda, T.B.M.J., 2008. On the tails of extreme event distributions in hydrology. Journal of Hydrology, 355(1): 16-33. DOI:https://doi.org/10.1016/j.jhydrol.2008.02.011

Engelke, S., de Fondeville, R., Oesting, M., 2017. Extremal behavior of aggregated data with an application to downscaling. To appear in Biometrika. DOI:https://arxiv.org/abs/1712.09816

Engelke, S., Malinowski, A., Kabluchko, Z., Schlather, M., 2015. Estimation of Hüsler–Reiss distributions and Brown–Resnick processes. Journal of the Royal Statistical Society: Series B (Statistical Methodology), 77(1): 239-265. DOI:10.1111/rssb.12074

Evin, G., Favre, A.C., Hingray, B., 2018. Stochastic generation of multi-site daily precipitation focusing on extreme events. Hydrol. Earth Syst. Sci., 22(1): 655-672. DOI:10.5194/hess-22-655-2018

Faulkner, D., Wass, P., 2005. FLOOD ESTIMATION BY CONTINUOUS SIMULATION IN THE DON CATCHMENT, SOUTH YORKSHIRE, UK. Water and Environment Journal, 19(2): 78-84. DOI:doi:10.1111/j.1747-6593.2005.tb00554.x

Favre, A.C., Adlouni, S.E., Perreault, L., Thiémonge, N., Bobée, B., 2004. Multivariate hydrological frequency analysis using copulas. Water Resources Research, 40(1). DOI:doi:10.1029/2003WR002456

Fawcett, L., Walshaw, D., 2006. A hierarchical model for extreme wind speeds. Journal of the Royal Statistical Society: Series C (Applied Statistics), 55(5): 631-646. DOI:doi:10.1111/j.1467-9876.2006.00557.x

Ferreira, A., de Haan, L., Zhou, C., 2012. Exceedance probability of the integral of a stochastic process. Journal of Multivariate Analysis, 105(1): 241-257. DOI:http://dx.doi.org/10.1016/j.jmva.2011.08.020

Gaetan, C., Grigoletto, M., 2007. A Hierarchical Model for the Analysis of Spatial Rainfall Extremes. Journal of Agricultural, Biological, and Environmental Statistics, 12(4): 434-449. DOI:10.2307/27595656

Genton, M.G., Padoan, S.A., Sang, H., 2015. Multivariate max-stable spatial processes. Biometrika, 102(1): 215-230. DOI:10.1093/biomet/asu066

He, Y., Bárdossy, A., Zehe, E., 2011. A review of regionalisation for continuous streamflow simulation. Hydrology and Earth System Sciences, 15(11): 3539.

Hosking, J.R.M., 1990. L-Moments: Analysis and Estimation of Distributions Using Linear Combinations of Order Statistics. Journal of the Royal Statistical Society. Series B (Methodological), 52(1): 105-124.

Huser, R., Davison, A.C., 2013. Composite likelihood estimation for the Brown–Resnick process. Biometrika, 100(2): 511-518. DOI:10.1093/biomet/ass089

Huser, R., Davison, A.C., 2014. Space–time modelling of extreme events. Journal of the Royal Statistical Society: Series B (Statistical Methodology), 76(2): 439-461. DOI:10.1111/rssb.12035

Hüsler, J., Reiss, R.-D., 1989. Maxima of normal random vectors: Between independence and complete dependence. Statistics & Probability Letters, 7(4): 283-286. DOI:https://doi.org/10.1016/0167-7152(89)90106-5

Jain, M.K., Kothyari, U.C., Ranga Raju, K.G., 2004. A GIS based distributed rainfall–runoff model. Journal of Hydrology, 299(1): 107-135. DOI:https://doi.org/10.1016/j.jhydrol.2004.04.024

Jenkinson, A.F., 1955. The frequency distribution of the annual maximum (or minimum) values of meteorological elements. Quarterly Journal of the Royal Meteorological Society, 87: 158–171.

Joe, H., 1997. Multivariate models and multivariate dependence concepts. Chapman & Hall, London.

Jordan, P., Weinmann, E., Hill, P., Wiesenfeld, C., 2013. Australian Rainfall & Runoff Revision Project: Project 2-Collation and Review of Areal Reduction Factors from Applications of the CRC-FORGE Method in Australia.

Kabluchko, Z., Schlather, M., de Haan, L., 2009. Stationary Max-Stable Fields Associated to Negative Definite Functions. The Annals of Probability, 37(5): 2042-2065.

Kao, S.-C., Govindaraju, R.S., 2008. Trivariate statistical analysis of extreme rainfall events via the Plackett family of copulas. Water Resources Research, 44(2). DOI:doi:10.1029/2007WR006261

Katz, R.W., Parlange, M.B., Naveau, P., 2002. Statistics of extremes in hydrology. Advances in Water Resources, 25(8): 1287-1304. DOI:https://doi.org/10.1016/S0309-1708(02)00056-8

Khaliq, M.N., Ouarda, T.B.M.J., Ondo, J.C., Gachon, P., Bobée, B., 2006. Frequency analysis of a sequence of dependent and/or non-stationary hydro-meteorological observations: A review. Journal of Hydrology, 329(3): 534-552. DOI:https://doi.org/10.1016/j.jhydrol.2006.03.004

Kleiber, W., Katz, R.W., Rajagopalan, B., 2012. Daily spatiotemporal precipitation simulation using latent and transformed Gaussian processes. Water Resources Research, 48(1). DOI:doi:10.1029/2011WR011105

Klemes, V., 1993. Probability of extreme hydrometeorological events-a different approach, the Yokohama Symposium, Extreme Hydrological Events: Precipitation, Floods and Droughts,. IAHS Publ, Yokohama, Japan, pp. 167-176.

Kotz, S., Nadarajah, S., 2000. Extreme Value Distributions. Imperial College Press, London.

Koutsoyiannis, D., 1994. A stochastic disaggregation method for design storm and flood synthesis. Journal of Hydrology, 156(1–4): 193-225. DOI:http://dx.doi.org/10.1016/0022-1694(94)90078-7

Koutsoyiannis, D., Kozonis, D., Manetas, A., 1998. A mathematical framework for studying rainfall intensity-duration-frequency relationships. Journal of Hydrology, 206(1–2): 118-135. DOI:http://dx.doi.org/10.1016/S0022-1694(98)00097-3

Kuichling, E., 1889. The relation between the rainfall and the discharge of sewers in populous districts. Transactions of the American Society of Civil Engineers, 20(1): 1-56.

Laurenson, E.M., Mein, R.G., 1997. RORB Version 4 Runoff Routing Program User Manual, Monash University Department of Civil Engineering.

Le, P.D., Davison, A.C., Engelke, S., Leonard, M., Westra, S., 2018a. Dependence properties of spatial rainfall extremes and areal reduction factors. Journal of Hydrology, Submitted.

Le, P.D., Leonard, M., Westra, S., 2018b. Modeling Spatial Dependence of Rainfall Extremes Across Multiple Durations. Water Resources Research, 54(3): 2233-2248. DOI:doi:10.1002/2017WR022231

Ledford, A.W., Tawn, J.A., 1996. Statistics for Near Independence in Multivariate Extreme Values. Biometrika, 83(1): 169-187.

Lehmann, E.A., Phatak, A., Stephenson, A., Lau, R., 2016. Spatial modelling framework for the characterisation of rainfall extremes at different durations and under climate change. Environmetrics, 27(4): 239-251. DOI:10.1002/env.2389

Leonard, M., Lambert, M.F., Metcalfe, A.V., Cowpertwait, P.S.P., 2008. A space-time Neyman–Scott rainfall model with defined storm extent. Water Resources Research, 44(9). DOI:doi:10.1029/2007WR006110

Leonard, M. et al., 2014. A compound event framework for understanding extreme impacts. Wiley Interdisciplinary Reviews: Climate Change, 5(1): 113-128. DOI:doi:10.1002/wcc.252

Li, J., Sharma, A., Johnson, F., Evans, J., 2015. Evaluating the effect of climate change on areal reduction factors using regional climate model projections. Journal of Hydrology, 528(Supplement C): 419-434. DOI:https://doi.org/10.1016/j.jhydrol.2015.06.067

Linsley, R.K., 1986. Flood estimates: How good are they? Water Resources Research, 22(9S): 159S-164S. DOI:doi:10.1029/WR022i09Sp0159S

Merz, B., Vorogushyn, S., Lall, U., Viglione, A., Blöschl, G., 2015. Charting unknown waters—On the role of surprise in flood risk assessment and management. Water Resources Research, 51(8): 6399-6416. DOI:10.1002/2015WR017464

Mulvaney, T.J., 1851. On the use of self-registering rain and flood gauges in making observation of the relation of rainfall and floods discharges in a given catchment. Proc. Civ. Eng. Ireland, 4: 18–31.

Myers, V.A., 1980. A methodology for point-to-area rainfall frequency ratios. In: Zehr, R.M. (Ed.). Dept. of Commerce, National Oceanic and Atmospheric Administration, National Weather Service, [Silver Spring, Md.] :.

Nelsen, R.B., 2006. An Introduction to Copulas. Springer, New York. DOI:MR2197664

Nicolet, G., Eckert, N., Morin, S., Blanchet, J., 2017. A multi-criteria leave-two-out cross-validation procedure for max-stable process selection. Spatial Statistics, 22(Part 1): 107-128. DOI:https://doi.org/10.1016/j.spasta.2017.09.004

Oesting, M., Schlather, M., Friederichs, P., 2017. Statistical post-processing of forecasts for extremes using bivariate Brown-Resnick processes with an application to wind gusts. Extremes, 20(2): 309-332. DOI:10.1007/s10687-016-0277-x

Omolayo, A.S., 1993. On the transposition of areal reduction factors for rainfall frequency estimation. Journal of Hydrology, 145(1): 191-205. DOI:http://dx.doi.org/10.1016/0022-1694(93)90227-Z

Opitz, T., 2013. Extremal t processes: Elliptical domain of attraction and a spectral representation. Journal of Multivariate Analysis, 122: 409-413. DOI:https://doi.org/10.1016/j.jmva.2013.08.008

Opper ESM, S., Cinque OAM, P., Davies, B., 2010. Timeline modelling of flood evacuation operations. 1st Conference on Evacuation Modeling and Management, Procedia Engineering, 3: 175-187. DOI:http://dx.doi.org/10.1016/j.proeng.2010.07.017

Over, T.M., Gupta, V.K., 1996. A space-time theory of mesoscale rainfall using random cascades. Journal of Geophysical Research: Atmospheres, 101(D21): 26319-26331. DOI:doi:10.1029/96JD02033

Padoan, S.A., Ribatet, M., Sisson, S.A., 2010. Likelihood-Based Inference for Max-Stable Processes. Journal of the American Statistical Association, 105(489): 263-277. DOI:10.1198/jasa.2009.tm08577

Panthou, G., Vischel, T., Lebel, T., Quantin, G., Molinié, G., 2014. Characterising the space–time structure of rainfall in the Sahel with a view to estimating IDAF curves. Hydrol. Earth Syst. Sci., 18(12): 5093-5107. DOI:10.5194/hess-18-5093-2014

Pathiraja, S., Westra, S., Sharma, A., 2012. Why continuous simulation? The role of antecedent moisture in design flood estimation. Water Resources Research, 48(6). DOI:doi:10.1029/2011WR010997

Pegram, G., Parak, M., 2004. A review of the regional maximum flood and rational formula using geomorphological information and observed floods. water sa, 30(3): 377-392.

Pegram, G.G.S., 2003. Rainfall, rational formula and regional maximum flood - some scaling links. Australasian Journal of Water Resources, 7(1): 29-39. DOI:10.1080/13241583.2003.11465226

Pickands, J., 1975. Statistical Inference Using Extreme Order Statistics. The Annals of Statistics, 3(1): 119-131. DOI:10.2307/2958083

Pilgrim, D.H., 1986. Bridging the gap between flood research and design practice. Water Resources Research, 22(9S): 165S-176S. DOI:doi:10.1029/WR022i09Sp0165S

Pilgrim, D.H., Cordery, I., 1993. Flood runoff. In: Maidment, D.R. (Ed.), Handbook of Hydrology. McGraw-Hill, New York, pp. 9.1–9.42.

Poapongsakorn, N., Meethom, P., 2013. Impact of the 2011 floods, and flood management in Thailand. ERIA Discussion Paper Series, 34: 2013.

Rahman, A., Charron, C., Ouarda, T.B., Chebana, F., 2018. Development of regional flood frequency analysis techniques using generalized additive models for Australia. Stoch Environ Res Risk Assess, 32(1): 123-139.

Rahman, A., Weinmann, P.E., Hoang, T.M.T., Laurenson, E.M., 2002. Monte Carlo simulation of flood frequency curves from rainfall. Journal of Hydrology, 256(3): 196-210. DOI:https://doi.org/10.1016/S0022-1694(01)00533-9

Rasmussen, P.F., 2013. Multisite precipitation generation using a latent autoregressive model. Water Resources Research, 49(4): 1845-1857. DOI:doi:10.1002/wrcr.20164

Reich, B.J., Shaby, B.A., 2011. A hierarchical Bayesian analysis of max-stable spatial processes. Unpublished manuscript.

Renard, B., 2011. A Bayesian hierarchical approach to regional frequency analysis. Water Resources Research, 47(11): W11513. DOI:10.1029/2010WR010089

Renard, B., Lang, M., 2007. Use of a Gaussian copula for multivariate extreme value analysis: Some case studies in hydrology. Advances in Water Resources, 30(4): 897-912. DOI:http://dx.doi.org/10.1016/j.advwatres.2006.08.001

Resnick, S.I., 1987. Extreme Values, Regular Variation, and Point Processes. Springer-Verlag.

Ribatet, M., 2009. A User's Guide to the SpatialExtremes Package. The Comprehensive R Archive Network.

Ribatet, M., Cooley, D., Davison, A.C., 2012. BAYESIAN INFERENCE FROM COMPOSITE LIKELIHOODS, WITH AN APPLICATION TO SPATIAL EXTREMES. Statistica Sinica, 22(2): 813-845.

Ribbons, S., 2015. Hawkesbury-nepean valley flood management review - developing a strategy where flood depth can be nine metres above flood planning level, 2015 Floodplain Management Association National Conference, Australia.

Rodriguez-Iturbe, I., Mejía, J.M., 1974. On the transformation of point rainfall to areal rainfall. Water Resources Research, 10(4): 729-735. DOI:10.1029/WR010i004p00729

Rogger, M. et al., 2012. Runoff models and flood frequency statistics for design flood estimation in Austria – Do they tell a consistent story? Journal of Hydrology, 456-457: 30-43. DOI:https://doi.org/10.1016/j.jhydrol.2012.05.068

Russell, B.T., Cooley, D.S., Porter, W.C., Heald, C.L., 2016. Modeling the spatial behavior of the meteorological drivers' effects on extreme ozone. Environmetrics, 27(6): 334-344. DOI:doi:10.1002/env.2406

Sang, H., Gelfand, A., 2009. Hierarchical modeling for extreme values observed over space and time. Environ Ecol Stat, 16(3): 407-426. DOI:10.1007/s10651-007-0078-0

Sang, H., Gelfand, A., 2010. Continuous Spatial Process Models for Spatial Extreme Values. Journal of Agricultural, Biological, and Environmental Statistics, 15(1): 49-65. DOI:10.1007/s13253-009-0010-1

Schlather, M., 2002. Models for Stationary Max-Stable Random Fields. Extremes, 5(1): 33-44. DOI:10.1023/A:1020977924878

Schlather, M., Tawn, J.A., 2003. A Dependence Measure for Multivariate and Spatial Extreme Values: Properties and Inference. Biometrika, 90(1): 139-156. DOI:10.2307/30042025

Seneviratne, S.I. et al., 2012. Managing the Risks of Extreme Events and Disasters to Advance Climate Change Adaptation: Changes in Climate Extremes and their Impacts on the Natural Physical Environment.

Shaw, S.B., Royem, A.A., Riha, S.J., 2011. The Relationship between Extreme Hourly Precipitation and Surface Temperature in Different Hydroclimatic Regions of the United States. Journal of Hydrometeorology, 12(2): 319-325. DOI:10.1175/2011jhm1364.1

Siriwardena, L., Weinmann, P., 1996. Derivation of areal reduction factors for design rainfalls in Victoria for Rainfall Durations 18–120 hours. Report, 96(4): 60.

Sivapalan, M., Blöschl, G., 1998. Transformation of point rainfall to areal rainfall: Intensity-duration-frequency curves. Journal of Hydrology, 204(1): 150-167. DOI:http://dx.doi.org/10.1016/S0022-1694(97)00117-0

Sivapalan, M., Blöschl, G., Merz, R., Gutknecht, D., 2005. Linking flood frequency to long-term water balance: Incorporating effects of seasonality. Water Resources Research, 41(6). DOI:doi:10.1029/2004WR003439

SKM, 2011. Nambucca Heads Flood Study.

Smith, E.L., Stephenson, A.G., 2009. An extended Gaussian max-stable process model for spatial extremes. Journal of Statistical Planning and Inference, 139(4): 1266-1275. DOI:https://doi.org/10.1016/j.jspi.2008.08.003

Smith, R.L., 1990. Max-stable processes and spatial extremes, Unpublished manuscript.

Srikanthan, R., 1995. A review of the methods for estimating areal reduction factors for design rainfalls / R. Srikanthan. Report (Cooperative Research Centre for Catchment Hydrology) ; 95/3. Cooperative Research Centre for Catchment Hydrology, Clayton, Vic.

Srikanthan, R., Pegram, G.G., 2007. Stochastic generation of multi-site rainfall occurrences, Advances in Geosciences: Volume 6: Hydrological Science (HS). World Scientific, pp. 1-10.

Stedinger, J., Vogel, R., Foufoula-Georgiou, E., 1993. Frequency Analysis of Extreme Events. In: Maidment, D.R. (Ed.), Handbook of Hydrology. McGraw-Hill, New York, pp. 18.1-18.66.

Stephenson, A.G., Lehmann, E.A., Phatak, A., 2016. A max-stable process model for rainfall extremes at different accumulation durations. Weather and Climate Extremes, 13(Supplement C): 44-53. DOI:https://doi.org/10.1016/j.wace.2016.07.002

Svensson, C., Jones, D.A., 2010. Review of methods for deriving areal reduction factors. Journal of Flood Risk Management, 3(3): 232-245. DOI:10.1111/j.1753-318X.2010.01075.x

Talei, A., Chua, L.H.C., 2012. Influence of lag time on event-based rainfall–runoff modeling using the data driven approach. Journal of Hydrology, 438-439: 223-233. DOI:https://doi.org/10.1016/j.jhydrol.2012.03.027

Talei, A., Chua, L.H.C., Quek, C., 2010. A novel application of a neuro-fuzzy computational technique in event-based rainfall–runoff modeling. Expert Systems with Applications, 37(12): 7456-7468. DOI:https://doi.org/10.1016/j.eswa.2010.04.015

Thibaud, E., Mutzner, R., Davison, A.C., 2013. Threshold modeling of extreme spatial rainfall. Water Resources Research, 49(8): 4633-4644. DOI:10.1002/wrcr.20329

Thibaud, E., Opitz, T., 2015. Efficient inference and simulation for elliptical Pareto processes. Biometrika, 102(4): 855-870. DOI:10.1093/biomet/asv045

Tramblay, Y. et al., 2010. Assessment of initial soil moisture conditions for event-based rainfall–runoff modelling. Journal of Hydrology, 387(3): 176-187. DOI:https://doi.org/10.1016/j.jhydrol.2010.04.006

UNDP, 1991. Manual and guidelines for comprehensive flood loss prevenion and management. Economic and social commission for Asia and the Pacific.

van den Honert, R.C., McAneney, J., 2011. The 2011 Brisbane Floods: Causes, Impacts and Implications. Water, 3(4): 1149.

Veneziano, D., Langousis, A., 2005. The areal reduction factor: A multifractal analysis. Water Resources Research, 41(7): n/a-n/a. DOI:10.1029/2004WR003765

von Mises, R., 1954. La Distribution de la Plus Grande de n Valeurs. American Mathematical Society: 271–294.

Wadsworth, J.L., Tawn, J.A., 2012. Dependence modelling for spatial extremes. Biometrika, 99(2): 253-272. DOI:10.1093/biomet/asr080

Wadsworth, J.L., Tawn, J.A., 2014. Efficient inference for spatial extreme value processes associated to log-Gaussian random functions. Biometrika, 101(1): 1-15. DOI:10.1093/biomet/ast042

Wahl, T., Jain, S., Bender, J., Meyers, S.D., Luther, M.E., 2015. Increasing risk of compound flooding from storm surge and rainfall for major US cities. Nature Climate Change, 5: 1093. DOI:10.1038/nclimate2736

https://www.nature.com/articles/nclimate2736#supplementary-information

Wang, Q.J., 2001. A Bayesian Joint Probability Approach for flood record augmentation. Water Resources Research, 37(6): 1707-1712. DOI:10.1029/2000WR900401

Wang, Q.J., Robertson, D.E., Chiew, F.H.S., 2009. A Bayesian joint probability modeling approach for seasonal forecasting of streamflows at multiple sites. Water Resources Research, 45(5). DOI:doi:10.1029/2008WR007355

Wang, X., Gebremichael, M., Yan, J., 2010. Weighted likelihood copula modeling of extreme rainfall events in Connecticut. Journal of Hydrology, 390(1–2): 108-115. DOI:http://dx.doi.org/10.1016/j.jhydrol.2010.06.039

Westra, S., Evans, J.P., Mehrotra, R., Sharma, A., 2013. A conditional disaggregation algorithm for generating fine time-scale rainfall data in a warmer climate. Journal of Hydrology, 479: 86-99. DOI:https://doi.org/10.1016/j.jhydrol.2012.11.033

Westra, S., Sisson, S.A., 2011. Detection of non-stationarity in precipitation extremes using a max-stable process model. Journal of Hydrology, 406(1–2): 119-128. DOI:http://dx.doi.org/10.1016/j.jhydrol.2011.06.014

WMAWater, 2011. Review of Bellinger, Kalang and Nambucca River Catchments Hydrology, Bellingen Shire Council, Nambucca Shire Council, New South Wales Government.

Zhang, L., Singh, V.P., 2007. Gumbel–Hougaard Copula for Trivariate Rainfall Frequency Analysis. Journal of Hydrologic Engineering, 12(4): 409-419. DOI:doi:10.1061/(ASCE)1084-0699(2007)12:4(409)

Zheng, F., Westra, S., Leonard, M., 2015. Opposing local precipitation extremes. Nature Clim. Change, 5(5): 389-390. DOI:10.1038/nclimate2579

http://www.nature.com/nclimate/journal/v5/n5/abs/nclimate2579.html#supplementary-information

Zheng, F., Westra, S., Leonard, M., Sisson, S.A., 2014. Modeling dependence between extreme rainfall and storm surge to estimate coastal flooding risk. Water Resources Research, 50(3): 2050-2071. DOI:10.1002/2013WR014616

Zheng, F., Westra, S., Sisson, S.A., 2013. Quantifying the dependence between extreme rainfall and storm surge in the coastal zone. Journal of Hydrology, 505: 172-187. DOI:http://dx.doi.org/10.1016/j.jhydrol.2013.09.054

Zscheischler, J. et al., 2018. Future climate risk from compound events. Nature Climate Change, 8(6): 469-477. DOI:10.1038/s41558-018-0156-3